PROGRAMA INTERINSTITUCIONAL DE PÓS-GRADUAÇÃO
EM CIÊNCIAS FISIOLÓGICAS
ASSOCIAÇÃO AMPLA UFSCar/UNESP
Via Washington Luiz, km 235 - Caixa Postal 676.
Fone/Fax: (016) 3351 8328 – e-mail: ppgcf@power.ufscar.br
13565-905 - São Carlos, SP – Brasil

UNESP

Estudo do papel da ADAM9 na disseminação tumoral via sistema linfático: Possível alvo farmacológico

SÃO CARLOS - SP
Dezembro 2014

PROGRAMA INTERINSTITUCIONAL DE PÓS-GRADUAÇÃO
EM CIÊNCIAS FISIOLÓGICAS
ASSOCIAÇÃO AMPLA UFSCar/UNESP
Via Washington Luiz, km 235 - Caixa Postal 676.
Fone/Fax: (016) 3351 8328 – e-mail: ppgcf@power.ufscar.br
13565-905 - São Carlos, SP – Brasil

UNESP

Estudo do papel da ADAM9 na disseminação tumoral via sistema linfático: Possível alvo farmacológico

KELLI CRISTINA MICOCCI

Tese apresentada ao Programa de Pós-Graduação em Ciências Fisiológicas, do Centro de Ciências Biológicas e da Saúde da Universidade Federal de São Carlos, como parte dos requisitos para a obtenção do título de Doutora em Ciências Fisiológicas, área de concentração: Ciências Fisiológicas.

Orientadora: Prof. Dra. HELOISA SOBREIRO SELISTRE DE ARAUJO

SÃO CARLOS - SP
Dezembro 2014

Ficha catalográfica elaborada pelo DePT da Biblioteca Comunitária/UFSCar

M626ep

Micocci, Kelli Cristina.
Estudo do papel da ADAM9 na disseminação tumoral via sistema linfático : Possível alvo farmacológico / Kelli Cristina Micocci. -- São Carlos : UFSCar, 2015.
134 f.

Tese (Doutorado) -- Universidade Federal de São Carlos, 2014.

1. Bioquímica. 2. ADAM9. 3. Mamas - câncer. 4. Metástase. 5. RNA interferente. 6. Células - adesão. I. Título.

CDD: 612.015 (20ª)

UNIVERSIDADE FEDERAL DE SÃO CARLOS

Centro de Ciências Biológicas e da Saúde
Programa Interinstitucional de Pós-Graduação em Ciências Fisiológicas

Folha de Aprovação

Assinaturas dos membros da comissão examinadora que avaliou e aprovou a Defesa de Tese de Doutorado da candidata Kelli Cristina Micocci, realizada em 12/12/2014:

Profa. Dra. Heloisa Sobreiro Selistre de Araujo
UFSCar

Profa. Dra. Mônica Rosas da Costa Iemma
UFSCar

Prof. Dr. Alessandro Silva Nascimento
USP

Prof. Dr. Ricardo Della Coletta
UNICAMP

Profa. Dra. Márcia Regina Cominetti
UFSCar

"Só um sentido de invenção e uma necessidade intensa de criar levam o homen a revoltar-se, a descobrir e a descobrir-se com lucidez."

Pablo Picasso

DEDICATÓRIA

Dedico à finalização desse trabalho ao SENHOR DEUS pai todo poderoso.

ELE foi a minha luz, minha salvação e o meu refúgio em todas as etapas de minha vida, e de maneira especial, na conclusão deste trabalho.

"O SENHOR é o meu pastor, nada me faltará.

Deitar-me faz em verdes pastos, guia-me mansamente a águas tranquilas.

Refrigera a minha alma; guia-me pelas veredas da justiça, por amor do seu nome. Ainda que eu andasse pelo vale da sombra da morte, não temeria mal algum, porque tu estás comigo; a tua vara e o teu cajado me consolam.

Preparas uma mesa perante mim na presença dos meus inimigos, unges a minha cabeça com óleo, o meu cálice transborda. Certamente que a bondade e a misericórdia me seguirão todos os dias da minha vida; e habitarei na casa do SENHOR por longos dias."

(Salmo 23)

Aos meus Pais:

.

NATAL E MARIA, pelo apoio, incentivo e amor incondicional.

Meus exemplos de vida e de superação.

Nunca mediram esforços na educação de seus filhos

Muito obrigada pela dedicação e paciência!

Vocês foram e sempre serão meus queridos mestres ... luz da minha vida ...melhores e maiores pais e avós do mundo.

AMO MUITO VOCÊS!

À meu irmão:

CRISTIAN pelos conselhos e ajuda sempre que precisei.

Você é um grande amigo...

A minha cunhada MARCELI e minha sobrinha VALENTINA...

por fazerem parte da minha vida.

À minhas amigas:

Margareth, pela doce infância que passamos juntas.

Graziéle, pelos momentos inesquecíveis em nossas vidas.

Glaussy, por me consolar e segurar em minhas mãos quando mais precisei...do outro lado do mundo.

Obrigada meninas pela amizade sincera!

À minha Filha

"Um anjo do céu
Que trouxe pra mim
É a mais bonita
A jóia perfeita
Que é pra eu cuidar
Que é pra eu amar
Gota cristalina
Tem toda inocência...".

Meu anjo, meu amor, minha vida, meu bem mais precioso...minha filha...MARIA EDUARDA...minha PITUQUINHA...você faz tudo valer a pena.

À meu esposo:

Meu refúgio, minha fortaleza, meu guerreiro, meu melhor amigo e companheiro, lutou comigo até o fim...homen, pai e marido exemplar, ***ADMIRÁVEL.***

ADILSON...muito obrigada por estar ao meu lado e cuidar de mim várias vezes que fraquejei como mãe e pesquisadora. Não tenho palavras para expressar o amor, gratidão e admiração que tenho por você.

Foi por vocês que consegui chegar até o fim deste trabalho...

AMO VOCÊS MINHA AMADA FAMÍLIA...

ADILSON, CRISTIAN, MARIA, MARIA EDUARDA, MARCELI, NATAL E VALENTINA.

V.S.M.V.

AGRADECIMENTO ESPECIAL

À minha orientadora:

Heloisa Sobreiro Selistre de Araújo, pelos preciosos conhecimentos a mim concedidos, pela paciência e pela confiança depositada desde os tempos da iniciação científica, afinal, passaram-se 13 anos de convivência e durante todo este período aprendi muito. Exemplo de competência e profissionalismo.

MULHER forte, segura e admirável, simplesmente não tenho palavras para agradecê-la por tudo de bom que fez para mim, por mim e em mim!

Ao meu supervisor:

Normand Pouliot por ter me recebido em seu laboratório: Laboratório de Metástase no Peter MacCallum Cancer Centre Hospital – Melbourne- Austrália. Pessoa e orientador admirável. Muito obrigada por ter tido paciência com minha adaptação à língua e cultura inglesa.

Às professoras Marcia Cominetti e Angela Leal (UFSCar):

Pela parceria com o laboratório de Biologia do Envelhecimento (LABEN) e laboratório de Cultura Celular do Departamento de Medicina que contribuiram para a realização da pesquisa, sempre me abrindo as portas.

AGRADECIMENTOS

<u>Aos colegas do Laboratório de Bioquímica e Biologia Molecular</u>:

Pela compreensão, carinho, auxílio e troca de experiências. Agradeço a todos que de uma forma ou de outra participaram dessa etapa de minha vida, entre eles, Carol, Leonardo, Matheus, Patty, Sabrina, Taís, Uliana e Vinícius.

Agradeço também os colegas que já encontraram seus caminhos, mas fizeram parte dessa estória, entre eles, Araceli, Camila, Fernanda Duarte, Juliana, Natália (técnica), Patrícia Bueno, Rita, Sarinha (IC) e Tamires.

Agradeço em especial, a Mônica, Carmen Lúcia, Lívia e Cyntia pelas contribuições e troca de experiências durante todo o trabalho. Ao Rafael, meu ajudante. Á Beth, pelo auxílio técnico.

Milene pelas contribuições e troca de experiências no final deste trabalho e pelo nascimento de uma nova amizade.

A amiga/irmã Graziéle pelo empréstimo da sua sala de cultura celular e de seu ombro amigo. Por nossa convivência e verdadeira amizade nas horas felizes e triste...obrigada minha amiga, por sempre me ouvir...

***Aos colegas do Laboratório de Biologia do Envelhecimento (LABEN)**:*

Em especial a Patrícia Manzine, Amanda, Júlio (Djava) e Angelina por estarem sempre dispostos a me ajudar.

Às professoras da Universidade do Estado do Rio de Janeiro (UERJ):

Verônica Morandi e Camila Castro Figueiredo pelo estágio realizado em seu laboratório. E aos alunos: Laila, Antonio, Viviane e Fernanda pela ajuda nos ensaios e pelo turismo na cidade maravilhosa: Rio de Janeiro.

A todos os professores e colegas do Departamento de Ciências Fisiológicas e também ao secretário do programa de Pós-Graduação em Ciências Fisiológicas, Alexandre, muito obrigada pela atenção, respeito e conhecimento transmitido.

***À FAPESP**:*

Pelo suporte financeiro e pela bolsa de doutorado.

Enfim, a todos que me auxiliaram direta ou indiretamente para que este trabalho pudesse ser finalizado com êxito.

Muito obrigada...

RESUMO

A disseminação tumoral ocorre principalmente por duas vias: por vasos sanguíneos e por vasos linfáticos, sendo esta última preferida pelos tumores mamários. Algumas proteínas estão envolvidas na proteólise e na adesão celular, ocasionando metástase, tais como as ADAMs, uma família de proteínas multi-domínios e multi-funcionais que contribuem nesses processos. A ADAM9, um membro desta família, apresenta expressão aumentada em um grande número de carcinomas humanos, entre eles, mama. Nesse contexto, o objetivo desse estudo foi avaliar o papel da ADAM9 na disseminação tumoral via sistema sanguíneo e linfático, visando o desenvolvimento de novas ferramentas terapêuticas. Para tanto, células de tumor de mama MDA-MB-231 foram silenciadas para a ADAM9 e testadas com relação às suas atividades adesivas e invasivas frente ao endotélio sanguíneo e linfático. Nossos resultados mostraram que o siADAM9 inibiu a invasão das células de câncer de mama MDA-MB-231 em matrigel (71,51 ± 8,02%) quando comparado com os controles, sem afetar a adesão celular, proliferação, migração, e expressão gênica da ADAM10, ADAM12, ADAM17, cMYC, MMP9, VEGF-A, VEGF-C, Osteopontina e Colágeno XVII, entretanto houve uma diminuição da expressão da ADAM15 e um aumento da expressão da MMP2 quando comparado com as controles: meio e negativo. O siADAM9 nas células MDA-MB-231 não afetou sua adesão sob fluxo às endoteliais vasculares (HMEC-1 e HUVEC) e linfáticas (HMVEC-dLyNeo-Der). Entretanto, houve uma diminuição na taxa de transmigração através da monocamada das células endoteliais (HUVEC, HMEC-1 e HMVEC-dLyNeo-Der) em aproximadamente 50%, 40% e 32%, respectivamente. Assim, conclui-se que a ADAM9 mostrou-se essencial no processo de invasão e extravasamento das células de câncer de mama MDA-MB-231 pelos vasos sanguíneos e linfáticos *in vitro*.

Palavras chaves: ADAM9, câncer de mama, metástase, RNAi (RNA de interferência), transmigração endotelial e adesão celular.

ABSTRACT

Tumor spreading occurs mainly by two pathways: through blood vessels and by lymphatic vessels, but the last is preferred by breast tumor cells. Some proteins are involved in cell adhesion and proteolysis, causing metastasis, such as ADAMs, a family of multi-domain and multi-functional proteins that contribute in these processes. ADAM9, a member of this family, has been increased in a large number of human carcinomas, including, breast cancer. In this context, the aim of this study was to evaluate the role of ADAM9 in tumor spreading via blood and lymphatic systems, in the search for new targets and focusing the development of new therapeutical tools. Therefore, MDA-MB-231 breast tumor cells were silenced for ADAM9 and tested with respect to their adhesive and invasive activity against blood and lymphatic endothelium. Our results showed that ADAM9 silencing in MDA-MB-231 breast cancer cells inhibited the invasion of this cells in matrigel (71.51 ± 8.02%) when compared to control cells, without affecting cell adhesion, proliferation, migration, and gene expression of the ADAM10, ADAM12, ADAM-17, cMyc, MMP9, VEGF-A, VEGF-C, Osteopontin and Collagen XVII, however, there was a decrease in the expression of the ADAM15 and increased expression of MMP2 when compared to controls. Furthermore, ADAM9 silencing did not affect the adhesion under flow to these vascular endothelial cells (HMEC-1 and HUVEC) and lymphatic (HMVEC-dLyNeo-Der). However, there was a decrease in the rate of trans-endothelial migration through the monolayer endothelial cells (HUVEC, HMEC-1 and HMVEC-dLyNeo-Der) by approximately 50%, 40% and 32%, respectively. In conclusion, ADAM9 showed to be essential in invasion and extravasation of MDA-MB-231 breast cancer cells through the blood and lymphatic vessels in vitro.

Key words: ADAM9, breast cancer, metastasis, interference RNA (iRNA), Trans-Endothelial Migration, and cell adhesion.

LISTA DE FIGURAS

LISTA DE ABREVIATURAS

Abreviação e Sigla	Descrição

ADAM: Proteína modular com domínios metaloprotease e desintegrina

BMDCs: Células dendríticas derivadas da medulla óssea

BSA: Albumina de soro bovino

BVI: Invasão de vasos sangüíneos

CAFs: Fibroblastos Associados a Carcinomas

cDNA: Ácido Desoxirribonucléico complementar

c-MYC: oncogene homólogo à mielocitomatose viral aviária

CTCs: Células de tumor circulantes

CTMS: Células tronco mesenquimais

DMEM: Meio de culutra dulbecco's modified eagle

DTC: Células de tumor disseminadas

ECD: Ácido glutâmico - Cisteína - Ácido aspártico

EGF: Fator de crescimento epitelial

EGFR: Receptor do Fator de crescimento epitelial

EMT: Transição epitélio-mesenquimal

FBS: Soro fetal bovino

GAGs: Glicosaminoglicanas

HIF-1: Fator-1 de indução de hipóxia

HMEC-1: Célula endotelial microvascular humana

HMVEC-dLyAd-Der: Célula endotelial microvascular linfática da derme de humano adulto

HMVEC-dLyNeo-Der: Célula endotelial microvascular linfática da derme de neonato humano

HUVECs: Células endoteliais de veia de cordão umbilical humano

LOX*:* Lisil Oxidase

LVI: Invasão de vasos linfáticos

MATs: Macrófagos Associados ao Tumor

MEC: Matriz Extracelular

MET: Transição mesenquimal-epitelial

MMP: Metalopeptidases de Matriz

mRNA: ácido ribonucléico mensageiro

NF-κB: Factor Nuclear Kappa B

NO: Óxido Nítrico

NOTCH: Sinalização na diferenciação de células neuronais

PBS: Tampão fosfato salino

PIGF: Fator de crescimento placentário

PROK2: Procineticina **2**

RGD: Arginina - Glicina - Ácido aspártico

RTKS: Receptores Tirosina Quinase

SDF1*α*: Fator 1 α derivado de célula estromal

SDS: Dodecil sulfato de sódio

SH3GL2: Endofilina 2

SVMP: Metaloprotease de veneno de serpente

TEMED: Tetrametiletilenodiamina

TGF-β: Fator de crescimento tumoral β

TIMPs: Inibidor tecidual de metaloproteinases

TMAs: Tumour-Associated Macrophages

TNF-α: Fator de necrose tumoral α

VEGF: Fator de crescimento vascular endotelial

VEGF-A: Fator de crescimento vascular endotelial A

VEGFR1: Receptor do fator de crescimento vascular endotelial 1

SUMARIO

1. INTRODUÇÃO

1.1. Câncer

A proliferação, a diferenciação e a sobrevivência das células em organismos pluricelulares são precisamente reguladas por mecanismos intrínscecos, sendo que raramente ocorrem erros nesses controles (DE MATOS *et al.*, 2005; EVAN & VOUSDEN, 2001; LOPES *et al.,* 2002). Caso ocorram, estas células começam a crescer e a se dividir de maneira irregular, indepedente das necessidades específicas do tipo celular. Quando essas células têm descendentes que herdam a propensão para proliferar sem responder à regulação, o resultado é um clone de células capaz de expandir-se indefinidamente, formando uma massa chamada de tumor (DE MATOS *et al.*, 2005; EVAN & VOUSDEN, 2001). Esta regulação é perdida nas células cancerosas que crescem e se dividem de uma maneira descontrolada, fazendo com que elas espalhem-se por todo o corpo (metástases), interferindo nas funções dos tecidos e órgãos normais (BAU *et al.*, 2006; DE MATOS *et al.*, 2005; VIDEIRA *et al.*, 2002).

O câncer é uma doença multifatorial crônica caracterizada por uma série de alterações genéticas e epigenéticas que desregulam os mecanismos de controle dos processos celulares resultando na quebra da homeostase celular. A resposta da célula aos danos no seu material genético e sua capacidade de manter a estabilidade genética através da maquinaria de reparo do DNA é essencial na prevenção, iniciação e progressão tumoral (BAU *et al.*, 2006).

É uma doença associada a fatores alimentares, obesidade, tabaco, sedentarismo, exposição a fatores de risco decorrentes da urbanização e industrialização, como por exemplo, a exposição a pesticidas, ou adquiridas de forma hereditária, que podem estimular a proliferação celular e adaptação ao microambiente, levando assim a invasão de

tecidos vizinhos, promovendo a formação de uma massa tumoral em crescimento contínuo (COCO 2002; STRATTON *et al,*. 2009).

"Câncer é o nome dado a um conjunto de mais de 100 doenças que têm em comum o crescimento desordenado de células, que invadem tecidos e órgãos".

(Texto extraído do site: www.inca.gov.br)

Apesar de grandes esforços mundiais para desvendar os mecanismos celulares e moleculares que envolvem a tumorigênese, esta doença ainda é uma das maiores causas de mortes no mundo (PAVELIC *et al.*, 2011; YAN & HUANG, 2012).

No Brasil, a estimativa para o ano de 2014 (válida também para 2015) aponta para a ocorrência de aproximadamente 576 mil novos casos de câncer, incluindo os casos de pele não melanoma. O câncer de pele do tipo não melanoma (182 mil novos casos) será o mais incidente na população brasileira, seguido pelos tumores de próstata (69 mil), mama feminina (57 mil), cólon e reto (33 mil), pulmão (27 mil), estômago (20 mil) e colo de útero (15 mil). Não considerando os casos de câncer de pele não melanoma, estima-se 395 mil novos casos de câncer, sendo 204 mil para o sexo masculino e 190 mil para o feminino. Em homens os mais incidentes serão: próstata, pulmão, cólon e reto, estômago e cavidade oral; e nas mulheres: mama, cólon e reto, colo de útero, pulmão e glândula tireóide (INCA, 2014).

O número de mortes por câncer na Europa em 2013 foi de 1.314.296 (737.747 para o sexo masculino e 576.489 para o feminino). Sendo o câncer de pulmão o de maior incidência nos homens, com cerca de 187.000 mortes (25% do total). E nas mulheres, o câncer de mama representa o maior número de mortes, com aproximadamente 88.886 (15% do total) (MALVEZZI *et al.*, 2013).

Entretanto, progressos nas pesquisas científicas e melhora nos prognósticos têm aumentado a sobrevida de pacientes com câncer. Pesquisa realizada pela Associação Americana para Pesquisa em Câncer realizada em 2013, demonstrou que de 1971 a 2012 houve uma grande melhora da sobrevida de americanos com câncer, pois em 1971, 1 em cada 69 americanos conseguia sobreviver ao câncer, e em 2012, essa relação passou para 1 em cada 23 americanos (AACR, 2013).

A progressão do câncer é um processo complexo e com muitas etapas, que inclui o crescimento tumoral, a migração, invasão, angiogênese e metástase, sendo a metástase a principal causa de morbidade e mortalidade em pacientes com câncer (YAN & HUANG, 2012). Em países desenvolvidos, como por exemplo, a Europa, uma em cada dez mulheres apresenta o diagnóstico de câncer de mama, sendo que, a taxa de mortalidade é de 90% quando ocorre metástase para tecidos distantes do foco primário (SLOAN *et al.*, 2006).

1.2. Metástase

HANAHAN & WEINBERG (2000) caracterizaram o câncer como uma doença neoplásica compreendida por seis capacidades biológicas adquiridas durante as múltiplas etapas do desenvolvimento do tumor humano, entre elas, sinalização da proliferação, escape de supressores de crescimento, ativação da invasão e metástase, proliferação ilimitada, indução à angiogênese e resistência à morte celular. Entretanto, o avanço do conhecimento na última década levou esses autores a adicionarem características emergentes a essa lista, entre elas, o metabolismo energético e escape das células tumorais do sistema imune (HANAHAN & WEINBERG, 2011).

Figura 1 – Caracterização do câncer por capacidades biológicas adquiridas durante o desenvolvimento tumoral. Extraído e modificado de HANAHAN & WEINBERG 2011.

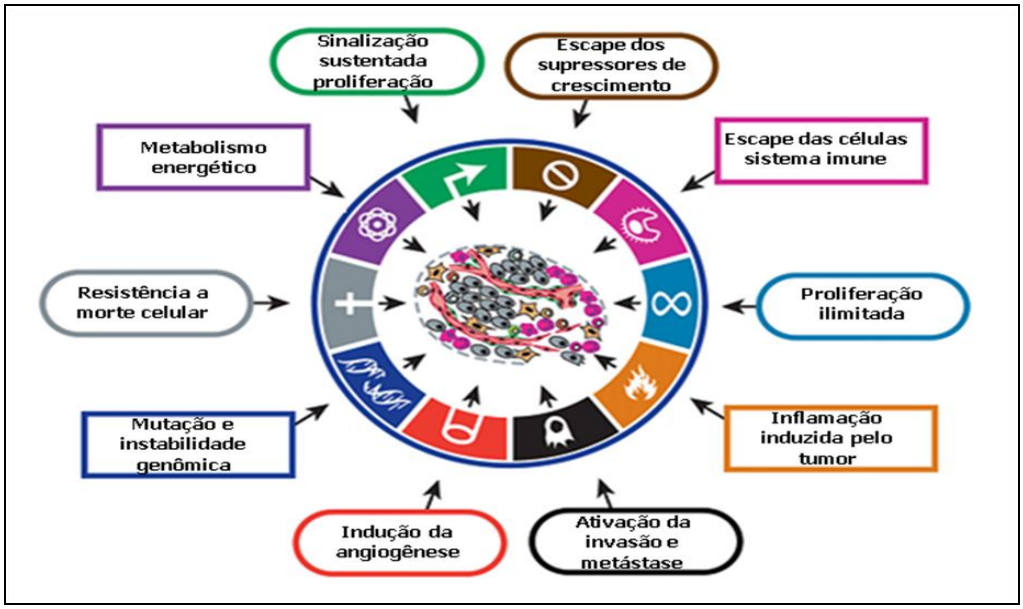

A metástase resulta de uma complexa cascata molecular na qual as células tumorais deixam o sítio tumoral primário e disseminam para sítios distantes, e nestes novos sítios essas células proliferaram dando origem ao foco de tumor secundário (BROOKS *et al.*, 2008). Desta forma, invasão e metástase de tumores humanos são processos compostos por muitas etapas e que exigem interações célula-célula e célula-matriz extracelular dentro do tecido hospedeiro. Os resultados dessas interações levam a produção, liberação e ativação de uma variedade de citocinas e fatores de crescimento, gerando sinais que diretamente ou indiretamente promovem o crescimento e sobrevivência tumoral (ZIGRINO *et al.*, 2005).

Essas etapas envolvidas na cascata metastática podem ser resumidas da seguinte forma: separação de algumas células do tumor primário, penetração destas através da membrana basal, migração das células para dentro da matriz extracelular (MEC), extravasamento para os vasos sanguíneos ou linfáticos, sobrevivência dentro dos vasos, adesão das células tumorais ao endotélio dos vasos, extravasamento das células pelos capilares de órgãos ou tecidos alvos, adesão ao novo sítio e, formação dos tumores secundários. Uma vez no tecido secundário essas células podem morrer, tornarem-se células

dormentes ou iniciar a proliferação em focos avasculares ou micrometástases. Esses focos podem permancer durante um período em latência e em estado indetectável, até que consigam o recrutamento adequado de fatores angiogênicos (HOOD & CHERESH, 2002; PONTIER & MULLER, 2008) (ver Figura 2).

Figura 2 - Principais etapas da metástase. Transformação nas células epiteliais normais leva ao carcinoma *in situ*, o qual perde as conexões de adesão e evolui para o carcinoma invasivo. Após a degradação da membrana basal, as células tumorais invadem o estroma circundante, migram e intravasam para os vasos sanguíneos e linfáticos, e são transportadas até aderirem em capilares de órgãos distantes (Extraído e modificado de BACAC & STAMENKOVIC, 2007).

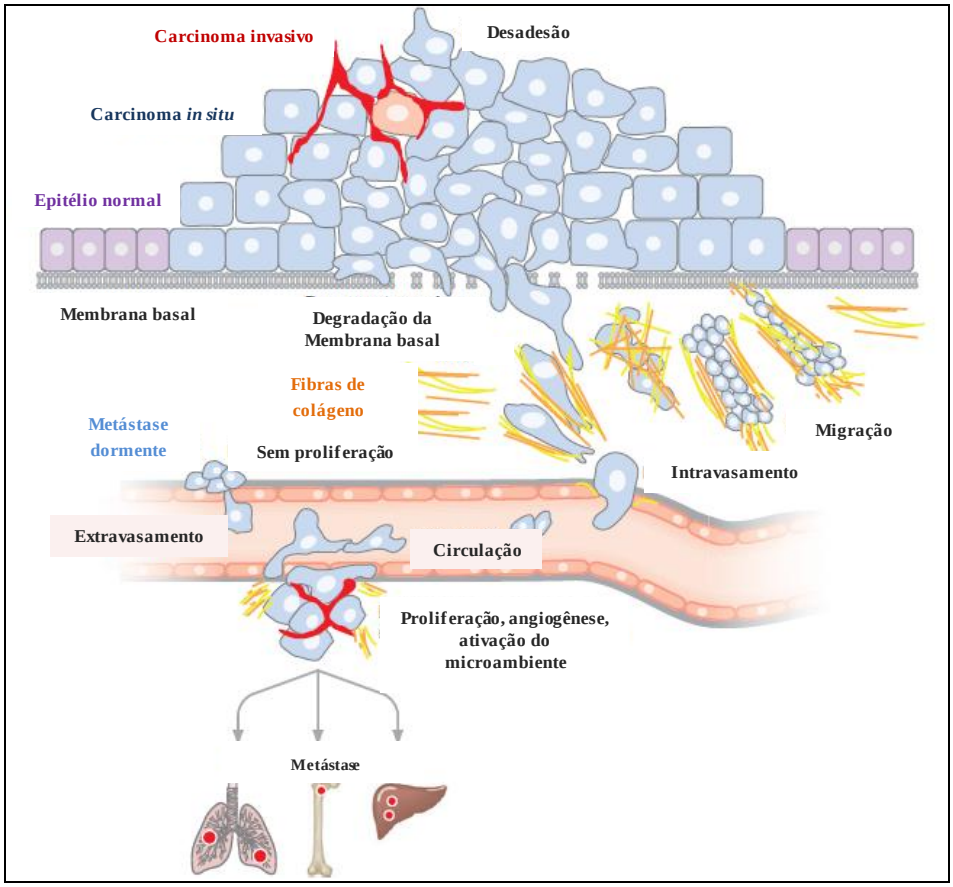

Segundo GEIGER & PEEPER (2009) as etapas apresentadas acima sobre a metástase representam uma visão clássica da cascata metastática. Recentes estudos sugerem uma nova etapa, ou seja, a etapa "0": a criação do nicho pré-metastático no tecido alvo antes mesmo das primeiras células de câncer alcançar este local distante (Figura 3).

A metástase de tumores de mama é a principal causa de morte por câncer em mulheres. Pacientes com câncer de mama em estágio avançado apresentam metástases em diversos tecidos, incluindo osso, pulmão, fígado e nodos linfáticos (ECKHARDT *et al.*, 2005; KUSUMA *et al.*, 2011; SLOAN *et al.*, 2006). Além disso, numerosos estudos sugerem que os vasos linfáticos facilitam a metástase, fornecendo um portal de disseminação das células tumorais (BANDO *et al.*, 2006; SCHOPPMANN, 2005).

A distribuição seletiva da metástase é ditada por diversos fatores, entre eles, padrão do fluxo vascular do foco primário, contatos adesivos complementares e interações moleculares entre a célula de tumor e estroma no sítio secundário (ECKHARDT *et al.*, 2005; KUSUMA *et al.*, 2011; SLOAN *et al.*, 2006).

Figura 3 – A cascata metastática. 0) Nicho pré-metastático; 1) Células no sítio primário sob transição epitélio-mesenquimal e com propriedades invasivas; 2) Degradação da membrana basal e matriz extracelular (MEC); 3) Invasão de células individuais (3a) ou em grupo (3b); 4) Intravasamento de células tumorais nos vasos próximos ao tumor; 5) Células tumorais são transportadas na circulação e aderem nos capilares (6); 7) As células extravasam e podem ficar dormentes por anos; 8) Algumas células disseminadas podem proliferam no novo sítio requerendo assim remodelamento da MEC e angiogênese; 9) Neste novo sítio, há o requerimento de angiogênese e remodelamento da MEC, e as células fora de seu microambiente normal sofrem *Anoikis*. Extraído e modificado de GEIGER & PEEPER, 2009.

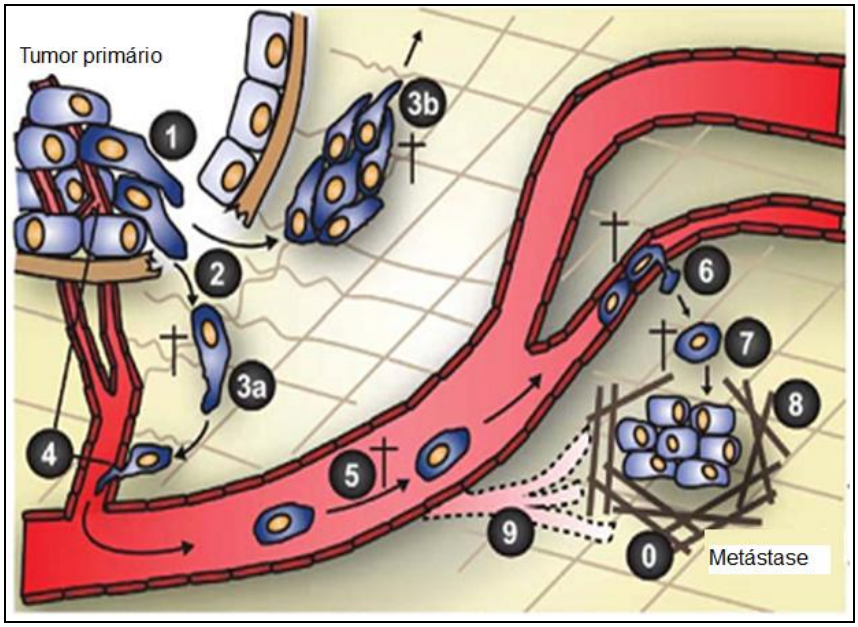

1.2.1. Disseminação Metastática e Epithelial Mesenchymal Transition (EMT).

Após a separação de algumas células do tumor primário e entrada nos vasos sanguíneos ou linfáticos, as células podem em princípio ser transportadas por todo o organismo. Uma etapa importante na formação da metástase é à saída das **células de tumor circulantes** (**CTCs**) do sistema circulatório, e sua chegada no foco secundário tornando-se **células de tumor disseminadas** (**DTCs**) (SLEEMAN 2012).

Para que ocorra o desprendimento das células do tumor primário muitas vezes as células necessitam passar pela Transição Epitélio-Mesenquimal (**EMT**). Essa mudança pode ser descrita como a perda da morfologia epitelial e o ganho da mesenquimal, fornecendo mecanismos para as células epiteliais superarem as limitações físicas impostas pelas junções intercelulares e adotarem um fenótipo móvel (CHRISTIANSEN & RAJASEKARAN 2006; YILMAZ *et al.*, 2007). Essa transição é caracterizada pela perda de polaridade celular, diminuição da expressão de proteínas epiteliais, tais como, E-caderina, ocludina, claudina, citoqueratinas, e catenina (CHRISTIANSEN & RAJASEKARAN 2006; GEIGER & PEEPER, 2009), e aumento da expressão de proteínas mesenquimais como, N-caderina, vimentina, tenascina-C, laminina β_1, e colágeno VI, bem como várias proteases (GEIGER & PEEPER, 2009).

A regulação da adesão célula-célula é realizada principalmente pelas caderinas e cateninas. Durante a EMT essa regulação é perdida e algumas células perdem a capacidade de se aderirem às suas vizinhas. Além disso, as células adquirem uma morfologia fusiforme a qual exacerba características migratórias e invasivas necessárias para ultrapassarem barreiras físicas e atingirem o foco secundário (CHRISTIANSEN & RAJASEKARAN 2006; GEIGER & PEEPER, 2009). SCHEEL *et al.* (2011) descreveram três vias de sinalizações que colaboram para a ativação e manutenção do estado mesenquimal na EMT, sendo elas,

superfamília dos TGF-β, canonical e não-canonical Wnt. Outras vias ou moléculas também consideradas chaves na indução da EMT são, receptores tirosina quinase (RTKs), NOTCH, NF-kB, e Hedgehog (CHRISTIANSEN & RAJASEKARAN 2006; GEIGER & PEEPER, 2009).

Segundo GEIGER & PEEPER (2009) a EMT pode promover metástase de diferentes maneiras. Primeiramente pela perda da adesão célula-célula permitida às células tumorais invasoras. A invasão de tecidos ou do sistema circulatório (vasos sanguíneos ou linfáticos) pode ser auxiliada por uma segunda propriedade das células em EMT, a de secretarem enzimas que degradam proteínas da MEC, como por exemplo, as MMPs. As metaloproteinases de matrix (MMPs) apresentam sua expressão aumentada nos tumores, e especialmente em tumores estromais, além disso, são moléculas capazes de remodelar a MEC dentro do microambiente tumoral clivando componentes como, laminina 5 e colágeno IV, auxiliando a migração ou induzindo a angiogênese (CHRISTIANSEN & RAJASEKARAN 2006; GEIGER & PEEPER, 2009). Outra maneira é através da redução na expressão das caderinas, pois essas moléculas promovem não somente a adesão, mas também participam da sinalização intracelular interagindo com a δ-catenina, ou ainda podem agir estimulando ou reprimindo os receptores do fator de crescimento epidérmico (EGFR) (LOWERY & DIHUA 2012). A indução de proteínas mesenquimais durante a EMT também promove os processos invasivos e metastáticos, por exemplo, o aumento da expressão da N-caderina induz a migração celular, invasão e metástase. E por último, membros da família SNAIL e TWIST, mediadores da EMT, inibem a apoptose durante o processo metastático, afetando assim a proliferação e disseminação tumoral (GEIGER & PEEPER, 2009).

Após migrarem para novos territórios as células que passaram pela EMT podem recuperar a morfologia epitelial através de um fenômeno conhecido como Transição Mesenquimal Epitelial (MET). Essas células voltam a exibir a morfologia epitelial e

restabelecem a expressão de E-caderinas e junções celulares, para assim ocuparem o novo sítio metastático (CHRISTIANSEN & RAJASEKARAN 2006).

1.2.2. Microambiente tumoral

O microambiente tumoral é constituído por diferentes componentes que incluem a MEC, fatores de crescimento e citocinas, e por uma população heterogênea de células estromais, tais como, fibroblastos, células endoteliais e macrófagos (ALPHONSO & ALAHARI, 2009).

A MEC é formada por macromoléculas que são produzidas localmente pelas células da matriz, principalmente por fibroblastos. Estas células auxiliam na organização da MEC, e a orientação do citoesqueleto no interior da célula pode controlar a produção dos componentes da MEC (GEIGER, *et al.*, 2001). Existem duas classes principais de macromoléculas que constituem a matriz: glicosaminoglicanos (GAGs), cadeia de polissacarídeos, as quais estão normalmente ligadas covalentemente a proteínas na forma de proteoglicanos; e as proteínas fibrosas, incluindo colágeno, elastina, a fibronectina e a laminina, que promovem funções estruturais e adesivas (ALPHONSO & ALAHARI, 2009). Desta forma, a MEC confere estrutura para a adesão celular e desenvolvimento dos tecidos. As células têm vias de comunicação bem desenvolvidas entre as superfícies celulares e a MEC (TANZER, 2006).

Figura 4 - Microambiente tumoral. Extraído e modificado de JOYCE & POLLARD, 2009.

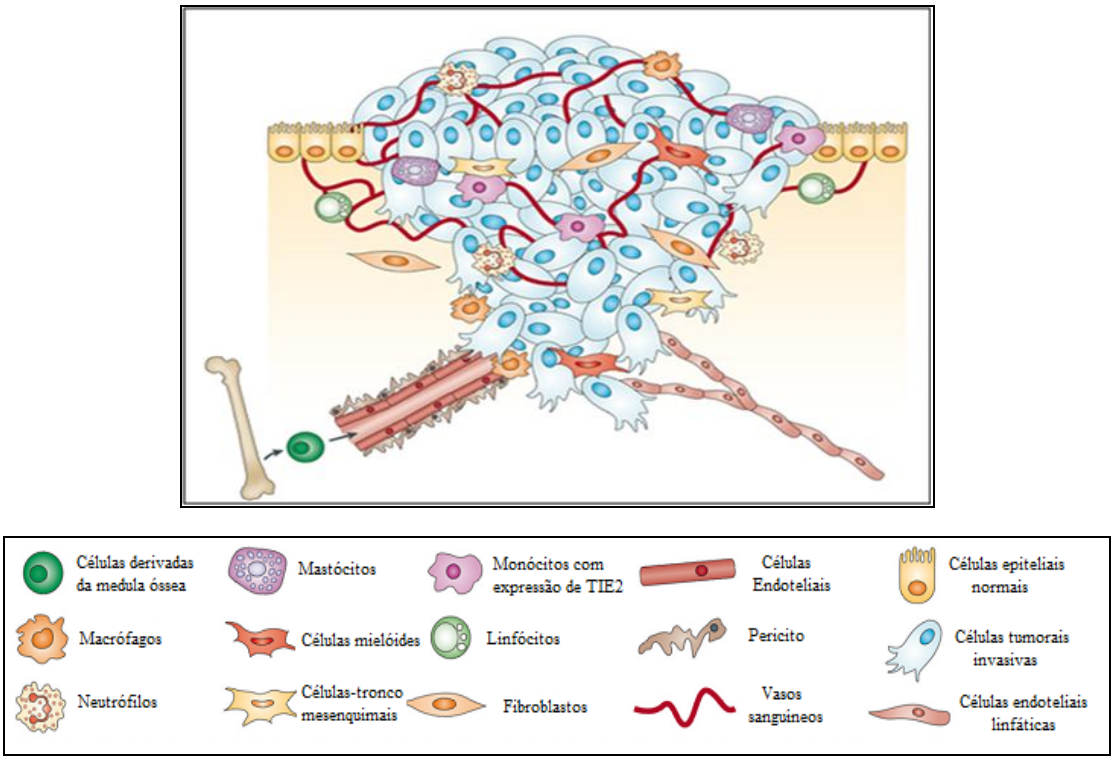

A figura acima representa o microambiente tumoral (Figura 4). As células tumorais estão circundadas por um microambiente complexo formado por diferentes tipos celulares, tais como, células endoteliais (vasos sanguíneos ou linfáticos), fibroblastos, e uma variedade de células derivadas da medula óssea (BMDCs), incluindo macrófagos, células supressoras derivadas das células mielóides (MDSCs), monócitos que expressam TIE-2 (TEMs), e células-tronco mesenquimais (CTMs) (JOYCE & POLLARD, 2009).

Um dos maiores componentes que constitui o estroma tumoral são os fibroblastos ativados. Os fibroblastos normais são responsáveis pela síntese, deposição e remodelamento da MEC, bem como, produção de fatores de crescimento. Em contraste com os fibroblastos normais, os fibroblastos associados ao câncer (CAFs ou miofibroblastos) expressam actina de músculo liso (GEIGER & PEEPER, 2009). No experimento realizado por ORIMO e colaboradores utilizando co-injeção de células epiteliais fracamente ou não-tumorigênicas, os CAFs estimularam a transformação celular epitelial, proliferação tumoral, e

angiogênese (ORIMO *et al.*, 2005). Os CAFs podem ser derivados de fibroblastos normais de tumor ou células epiteliais normais que sofreram EMT, ou ainda das células tronco mesenquimais derivadas da medula óssea (MSCs), as quais se apresentam em número elevado em tumores (GEIGER & PEEPER, 2009; JOYCE & POLLARD, 2009). Os miofibroblastos produzem uma variedade de fatores de crescimento e citocinas, tais como, S100A4, TGF-β, e SDF1a, além disso, são importantes fonte de fibronectina e tenascina-C (SLEEMAN 2012).

Outros componentes cruciais do estroma tumoral são representados por células e mediadores do sistema imune, entre elas, macrófagos, neutrófilos, monócitos que expressam TIE-2 (TEMs) e mastócitos. Essas células mielóides derivadas da medula óssea contribuem com a angiogênese tumoral através da produção de fatores de crescimento, citocinas, proteases, fator de crescimento endotelial A (VEGFA), PROK2 (também chamada de BV8), e MMPs (JOYCE & POLLARD, 2009).

Os macrófagos podem ser considerados um protótipo de células derivadas da medula óssea (BMDC) capazes de modificar o comportamento de células e promover angiogênese, invasão, intravasamento, e metástase em modelos animais (POLLARD 2004; CONDEELIS & POLLARD, 2006). Macrófagos assim como os fibroblastos, são células altamente plásticas o que faz com que eles tenham funções distintas e podendo agir como supressores ou indutores em diferentes momentos da progressão tumoral (ALPHONSO & ALAHARI, 2009; JOYCE & POLLARD, 2009).

Os macrófagos associados ao tumor (TAMs) produzem pequenas quantidades de citocinas pró-inflamatórias e NO (óxido nítrico), possuem fraca capacidade de apresentar antígenos, e suprimem efetivamente a ativação das células T. Desta forma, os macrófagos de fenótipo M2 efetivamente promovem a proliferação das células tumorais e metástases, através da secreção de metaloproteases, uma ampla variedade fatores de crescimento e pró-

angiogênicos por seu envolvimento nos circuitos de sinalização que regulam a função do fibroblasto no estroma tumoral (LUO *et al.*, 2006; ALPHONSO & ALAHARI 2009).

Além disso, condições de hipóxia no microambiente tumoral induzem a expressão gênica de HIF-1 (*hypoxia-inducing factor 1*). HIF-1, por sua vez, aumenta a expressão de VEGF, resultando no aumento da permeabilidade vascular e da degradação de MEC, para a formação de novos vasos (ALPHONSO & ALAHARI 2009; SLEEMAN 2012). Segundo SLEEMAN (2012), a hipóxia tem papel importante no tumor primário induzindo a expressão de fatores, como por exemplo, VEGF-A (fator de crescimento endotelial de vasos – A), PIGF (fator de crescimento placentário), e LOX (lisil oxidases) que iniciam e regulam a formação do nicho metastático. No entanto, é provável que a hipóxia desempenhe importante papel também na promoção de metástases, pois propicia um microambiente inflamatório para a metástase, além de aumentar a expressão de SDF1α (fator α derivado de células estromais), e também recrutar VEGFR1 (receptor 1 do fator de crescimento endotelial de vasos), CD11b, e BMDCs.

1.2.3. Invasão e Migração Celular

O processo normal de migração/invasão ocorre em diferentes processos, entre eles, morfogênese da ramificação mamária, desenvolvimento do sistema nervoso, brotamento/surgimento de novos vasos, desenvolvimento placentário, cicatrização de feridas, tráfego de células do sistema imune e gastrulação embrionária. Entretanto, existem situações patológicas que alteram esse movimento celular de maneira altamente significante, sendo a migração e a invasão das células tumorais o exemplo clinicamente mais relevante (KRAMER *et al.*, 2012). A migração e invasão de células de câncer é o passo inicial da metástase (YAMAGUCHI *et al.*, 2005; TOCHHAWNG *et al.*, 2012).

Migração e invasão são termos distintos dentro da Biologia Celular. Migração é definida como o movimento das células em um substrato como, por exemplo, membrana basal, MEC, ou placas de plástico. A migração ocorre em superfícies bidimensionais (2D) sem redes de fibras obstrutivas. Já a invasão é definida como o movimento celular através de uma matriz tridimensional (3D) a qual é acompanhada por uma reestruturação do ambiente 3D (KRAMER *et al.*, 2012). As células, para mover-se através da matriz, necessitam modificar sua morfologia e interagir com componentes da MEC, a qual por um lado fornece substratos para a adesão celular e por outro lado representa uma barreira para o movimento das células (CHRISTIANSEN & RAJASEKARAN 2006; GEIGER & PEEPER, 2009; KRAMER *et al.*, 2012). Invasão de carcinomas é definida como a penetração através de barreiras teciduais, tais como, passagem pela membrana basal e infiltração por entre tecidos intersticiais subjacentes por células de tumor maligno (KRAMER *et al.*, 2012).

Dependendo do tipo celular e tecido, as células podem migrar de duas formas: individualmente, quando as junções célula-célula são ausentes, ou coletivamente como grupos multicelulares, quando as adesões célula-célula são mantidas. A migração individual pode ser subdividida em movimento do tipo amebóide ou mesenquimal, sendo considerado o mais simples tipo de migração celular (FRIEDL & ALEXANDER 2011; KRAMER *et al.*, 2012). Independente do tipo de migração, todas as células precisam modificar sua morfologia para interagirem com a MEC a sua volta e se locomoverem (SCHMIDT & FRIEDL 2010). Essa interação das células com a matriz ocorre principamente através das integrinas.

1.3. Integrinas

A ligação da célula à MEC requer proteínas de adesão transmembrana, que atuam como receptores da matriz e a conectam ao citoesqueleto celular. Os principais

receptores das células animais para a ligação com a maioria das proteínas da matriz extracelular, incluindo os colágenos, a fibronectina e as lamininas, são as integrinas. Essas moléculas de adesão são receptores de membrana e sua estrutura é caracterizada pela presença de duas cadeias heterodiméricas, uma cadeia α e uma cadeia β. Atualmente são conhecidas 18 cadeias α e 8 cadeias β, que podem se combinar e formar 24 diferentes receptores, apresentando propriedades de ligação distintas (Figura 5) (HYNES, 1987; PLOW *et al.*, 2000; BERMAN *et al.*, 2003; BERRIER & YAMADA, 2007). A maioria das interações adesivas dessas moléculas ocorre através da ligação da integrina a um sítio de ligação celular formado por três peptídeos, arginina-glicina-ácido aspártico (RGD), um motivo encontrado em muitas proteínas da MEC, tais como, fibrinogênio, vitronectina e fibronectina (YAMADA, 1991; SELISTRE-DE-ARAUJO *et al.*, 2005). Entretanto, outros ligantes não-RGD podem interagir com as integrinas, entre eles, os ligantes ECD (ácido glutâmico, cisteína, acido aspártico) (BERMAN *et al.*, 2003; BERRIER & YAMADA, 2007). Portanto, as integrinas funcionam como conectores entre a MEC e o citoesqueleto, e apresentam papéis cruciais em diversos processos biológicos, tais como, na organogênese, remodelamento de tecidos, trombose, migração de leucócito, adesão, sinalização e proliferação celular (PETRUZZELLI *et al.*, 1999). Desta forma, esta classe de moléculas pode influenciar o desenvolvimento celular em diversas condições biológicas e patológicas, tais como, embriogênese, diferenciação, morfogênese, crescimento tumoral, metástase, apoptose e cicatrização de ferimentos (BERMAM *et al.*, 2003; YAMADA *et. al.*, 2003).

Figura 5 – Esquema da estrutura de uma integrina e das diferentes associações entre as subunidades α e β e a divisão dos heterodímeros em subgrupos. Extraído e modificado de TAKADA *et al.*, 2007 e do site: www.the-scientist.com/article/display/15706/. Acesso: 18/08/2014.

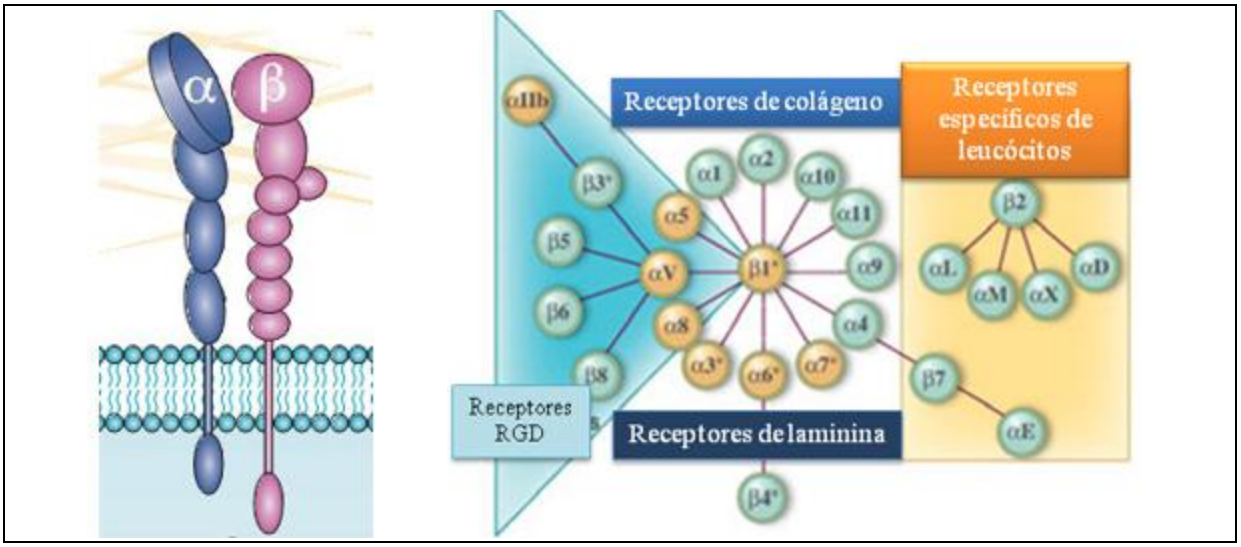

As integrinas são expressas em padrões que podem ser alterados nos tumores, participando da adesão e migração celular, processos envolvidos na metástase (HOOD & CHERESH, 2002). Estudos exemplificam o envolvimento dessa classe de receptor de adesão na progressão tumoral, por exemplo, as integrinas $\alpha_V\beta_3$ e $\alpha_V\beta_5$ apresentam perfil de expressão alterada nas células de câncer de mama, contribuindo na adesão e migração celular. Estudos histopatológicos correlacionam a expressão da integrina $\alpha_6\beta_4$ com a progressão tumoral (BARTSCH *et al.*, 2003; PETRUZZELLI *et al.*, 1999). Além disso, segundo BARTSCH *et al.* (2003), a expressão alterada de diversas integrinas nas células de câncer de mama está associada com as diferenças no comportamento metastático. ZUTTER *et al.* (1990), encontraram que o aumento na expressão da integrina $\alpha_2\beta_1$ esta associada com o fenótipo de câncer de mama com maior malignidade. Altos níveis de expressão da integrina α_6 foram identificados em mais de 50% dos cânceres de mama estudados e inversamente correlacionados a sobrevida dos pacientes. MUKHOPADHYAY *et al.* (1999) observaram que a expressão da subunidade α_6 está correlacionada com o potencial metastático em diferentes linhagens de células tumorais. Já em melanomas a expressão das integrinas $\alpha_v\beta_3$ e $\alpha_5\beta_1$ leva a

um fenótipo de metástase para linfonodos, além disso, à integrina $\alpha_v\beta_3$ aumenta a metástase óssea em tumores de próstata (HOOD & CHERESH, 2002; DESGROSELLIER & CHERESH, 2010).

Estudos de YAO e colaboradores (2007) correlacionaram o aumento da expressão da subunidade β_1 e seu ligante (fibronectina) com diminuição da sobrevida de pacientes com câncer de mama (YAO *et al.*, 2007). Além disso, a proteína ADAM9 e a ADAM9S (isoforma secretada) podem ligar-se à integrina β_1, e essa combinação pode induzir a expressão de MMP9 (via Ras-Raf-Erk) facilitando assim, a migração celular em diversas linhagens de tumor humano (KOHN *et al.*, 2012).

1.4. ADAMs

A modulação do microambiente tecidual através da degradação da MEC, o processamento de fatores de crescimento e ativação de moléculas de adesão celular são essenciais para a proliferação e progressão das células de câncer (MOCHIZUKI & OKADA, 2007). Além disso, a degradação da matriz extracelular é um pré-requisito para o reparo tecidual, migração celular e para liberação de fatores de crescimento e peptídeos bioativos (ZIGRINO *et al.*, 2007). Diferentes proteases têm sido implicadas nesses processos, tais como metalopeptidases de matriz (MMPs), outras famílias de proteases (serino, cisteína e aspártica), as ADAMs (***A*** ***D****isintegrin* ***A****nd* ***M****etalloprotease*) e as ADAMTSs (que apresentam o domínio trombospondina adicional) (MOCHIZUKI & OKADA, 2007; ROCKS *et al.*, 2008; ZIGRINO *et al.*, 2007).

As ADAMs, também chamadas de MDCs (*Metalloprotease/Disintegrin/Cystein-rich*), recebem um número seguido ao nome, que representa a ordem de sua descoberta. Elas são glicoproteínas de membrana que contém multidomínios, com funções e estruturas

específicas. Todas as ADAMs possuem alguns ou todos os seguintes domínios: um peptídeo sinal, um pró-domínio, e os domínios, metaloprotease, desintegrina ou desintegrina-*like*, rico em cisteína, EGF-*like* (*Epidermal Growth Factor-like*), transmembrana e citoplasmático (Figura 6) (BLOBEL, 1997; SEALS & COURTNEIDGE, 2003; WHITE, 2003).

Figura 6 – Desenho esquemático representando a estrutura de uma ADAM com seus diferentes domínios e diferentes funções. EGF-*like*: domínio *Epidermal Growth Factor-like*, TM: domínio transmembrana. Os números acima representam a quantidade de resíduos de aminoácidos na proteína. N-term. = região amino-terminal, C-term. = região carboxi-terminal. Extraído e modificado de BLACK & WHITE, 1998; ROCKS *et. al.*, 2008; SEALS & COURTNEIDGE, 2003.

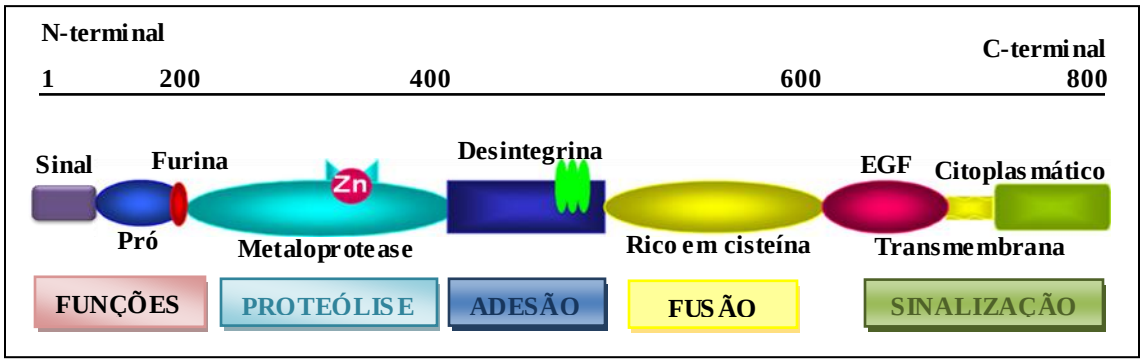

As ADAMs têm papel fundamental nas interações entre células ou entre células e a MEC, sendo tais interações de fundamental importância em processos de adesão, migração, proliferação, desenvolvimento, diferenciação, transdução de sinais, resposta imunológica, manutenção da estrutura tecidual, cicatrização de ferimentos, angiogênese, desenvolvimento do coração, interação entre o espermatozóide e óvulo, determinação do destino celular. Estas moléculas estão envolvidas também em situações patológicas, como por exemplo, câncer e formação de metástases (BLOBEL, 1997; BLACK & WHITE, 1998; MAUCH *et al.*, 2010; REISS & SAFTIG, 2009). Além disso, essas proteínas transmembrana tipo I têm se destacado como a principal família de proteases que participa de clivagem de ectodomínios (REISS & SAFTIG, 2009) (Figura 7).

Já foram identificados 20 genes que codificam para ADAMs e mais de 30 membros protéicos desta família foram descritos (DUFFY *et al.*, 2003; PRIMAKOFF & MYLES, 2000; STONE *et al.*, 1999). Os genes para esta família de proteínas são classificados em dois grupos: o primeiro é o grupo de metaloproteases ativas ou potencialmente ativas, as quais possuem sequência consenso para a ligação do zinco no domínio catalítico; o outro grupo corresponde as ADAMs com o domínio metaloprotease proteoliticamente inativo, devido a ausência de motivos íntegros para a ligação de zinco envolvido na catálise enzimática (EMI *et al.*, 1993; WOLFSBERG *et al.*, 1993; WOLFSBERG & WHITE, 1996). Além do *Homo sapiens*, as ADAMs podem ser encontradas em outras espécies, incluindo *C. elegans*, *Drosophila*, *Xenopus* e camundongos, mas não estão presentes em *E. coli*, *S. cerevisiae*, ou em plantas (BLOBEL, 1997; FAMBROUGH *et al.*, 1996; SEALS & COURTNEIDGE, 2003).

1.4.1. ADAM9

A ADAM9 (MDC9 ou meltrin γ) é um importante membro da família de glicoproteínas ancoradas na membrana (FRITZSCHE *et al.*, 2008[a]; FRITZSCHE *et al.*, 2008[b]; ZUBEL *et al.*, 2009), sendo uma molécula de adesão que interage com a integrina $\alpha_V\beta_5$ e está envolvida no processamento proteolítico (clivagem de ectodomínio) do fator de crescimento tipo epidérmico ligado à heparina (HB-EGF) e ancorado à membrana (FRITZSCHE *et al.*, 2008[b]; FRITZSCHE *et al.*, 2008[a]; GRÜTZMANN *et al.*, 2004). Além disso, essa proteína está envolvida em processos celulares, tais como adesão celular, migração e sinalização (ZUBEL *et al.*, 2009).

A ADAM9 também pode estar essencialmente envolvida na carcinogênese e progressão tumoral, pois participa da ativação do receptor de EGF e promove a invasão das

células de câncer via regulação de E-caderina e diversos tipos de integrinas (FRITZSCHE *et al.*, 2008[b]). Estudos mostram que o domínio metaloprotease da ADAM9 pode clivar a cadeia β da insulina, fator de necrose tumoral α, gelatina, caseína-β e fibronectina, e induzir a liberação do EGF, do receptor do fator de crescimento fibroblástico 2IIIB ou do fator de crescimento tipo EGF que se liga à heparina. Além disso, o domínio desintegrina da ADAM9 contém o motivo ECD (Glu-Cys-Asp), que pode participar da adesão celular via integrinas $\alpha_6\beta_1$ e $\alpha_V\beta_5$. A cauda citoplasmática da ADAM9 apresenta um motivo de ligação a SH3, o qual interage com importantes proteínas regulatórias, tais como endofilina 1 (SH3GL2) e SH3PX1 (SUNG *et al.*, 2006).

Embora a ADAM9 seja considerada uma proteína transmembrana, uma forma solúvel ADAM9-S foi descrita (HOTODA *et al.*, 2002). A ADAM9-S é derivada de um *splicing* alternativo do gene que codifica para a ADAM9. Essa proteína solúvel promove o fenótipo invasivo em linhagens celulares de carcinoma. Um modelo proposto para metástase hepática por MAZZOCCA *et al.* (2005), mostrou que a ADAM9-S liberada pelas células hepáticas ativadas se liga às integrinas $\alpha_6\beta_4$ e $\alpha_2\beta_1$ na superfície do tumor, e, através de sua atividade proteolítica, ADAM9-S promove a invasão pela degradação dos componentes da membrana basal, incluindo laminina-1, e, desta forma, permite que células tumorais invadam a matriz ao seu redor (MAZZOCCA *et al.*, 2005).

FRY & TOKER (2010), utilizando anticorpos específicos para ADAM9-L e ADAM9-S detectaram a expressão de ambas isoformas em tecidos e células de câncer de mama, entre elas, na linhagem MDA-MB-231. Além disso, esses dois autores utilizando a técnica de RNAi puderam identificar que essas isoformas funcionam de maneira oposta na regulação da migração celular, ou seja, a ADAM9-S promove e a ADAM9-L atenua a migração, sendo assim, este estudo foi o primeiro a identificar uma ADAM como um supressor de migração celular.

Figura 7 – Postulado dos domínios estruturais das ADAMs. Clivagem de proteínas transmembrana mediada pelas ADAMs leva à liberação de domínios extracelulares solúveis e fornece mecanismo para a regulação das proteínas da superfície celular, e também para sinalização extracelular. Extraído e modificado de REISS & SAFTIG *et. al*, 2009.

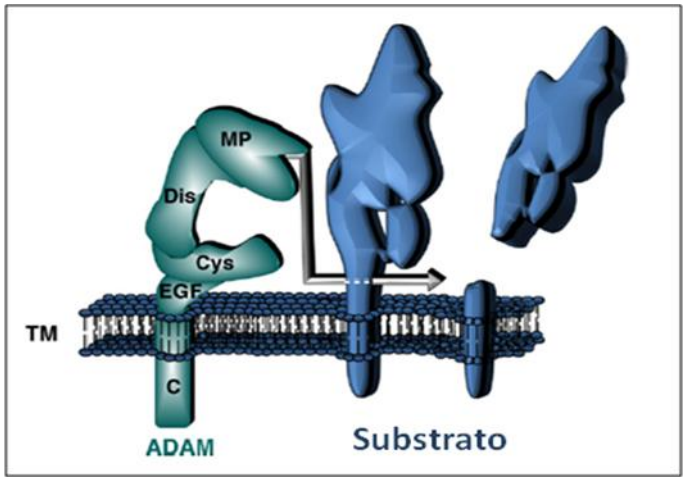

A expressão aumentada da ADAM9 tem sido descrita em diversos carcinomas humanos, tais como, renal (FRITZSCHE *et al.*, 2008[a]), próstata (FRITZSCHE *et al.*, 2008[b]), mama (O'SHEA *et al.*, 2003), fígado (TANNAPFEL *et al.*, 2003), pâncreas (GRÜTZMANN *et al.*, 2004; MOCHIZUKI & OKADA, 2007), estômago (CARL-McGRATH *et al.*, 2005; MOCHIZUKI & OKADA, 2007) e intestino (PEDUTO *et al.*, 2005). Um estudo experimental utilizando um modelo de metástase em ratos demonstrou que ADAM9 contribui para a carcinogênese prostática por clivagem de ligantes do receptor EGF e do receptor do fator de crescimento fibroblástico (FGFR) (PEDUTO *et al.*, 2005). Além disso, a ADAM9 secretada por células estromais ativadas, parece induzir invasão celular de carcinoma de cólon (*in vitro*) através da ligação às integrinas $\alpha_6\beta_4$ e $\alpha_2\beta_1$ (MAZZOCCA *et al.*, 2005). A ADAM9 aumenta a adesão e invasão de células de carcinoma de pulmão através da modulação de moléculas de adesão, tal como a integrina $\alpha_3\beta_1$, e sensibilidade a fatores de crescimento e, desta forma, promove a capacidade de metástase para o cérebro. Sendo assim, a ADAM9 desempenha um papel importante na tumorigênese, invasão e metástases através da modulação da função da

atividade de fatores de crescimento e de integrinas (MAZZOCCA *et al.*, 2005; SHINTANI *et al.*, 2004).

Nosso laboratório vem produzindo com sucesso o domínio desintegrina da ADAM9 humana (ADAM9D) em sistema bacteriano, através do vetor pGEX-4T-1. A produção deste domínio ocorreu na sua forma solúvel e ativa, e a ADAM9D foi capaz de promover a adesão de células da linhagem K562 (eritroleucemia humana), DU-145 (câncer de próstata) e MDA-MB-231 (câncer de mama), de forma dose-dependente, mostrando que este domínio se comporta como um domínio adesivo. Além disso, ensaios de competição com anticorpos e de citometria de fluxo, mostraram que a ADAM9D se liga às integrinas β_1, α_3, $\alpha_V\beta_3$, $\alpha_V\beta_5$ e α_2 em diferentes linhagens celulares, e pela primeira vez, mostrou-se a interação do domínio desintegrina da ADAM9 humana com a integrina $\alpha_V\beta_3$. Por fim, a ADAM9D inibiu em 75% a adesão das células MDA-MB-231 e em 65% das plaquetas ao colágeno tipo I em condições dinâmicas de fluxo, e também inibiu a invasão destas células ao matrigel, de forma semelhante aos anticorpos bloqueadores anti-$\alpha_V\beta_3$ e $\alpha_V\beta_5$ (COMINETTI *et al.*, 2009).

Estudo realizado por ZIGRINO e colaboradores mostrou que a ADAM9 participa de interações diretas entre células de melanoma e fibroblasto, pois a incubação das células MV3 (melanoma) com domínio DC-9 (domínio recombinante da ADAM9) resultou em diminuição da adesão dessas células ao fibroblasto. Além disso, o número de células de melanoma aderidas aos fibroblastos diminuiu consideravelmente quando a ADAM9 foi silenciada nas células de melanoma. E essa redução foi adicional quando utilizado fibroblastos de camundongo com deficiência de ADAM9. Esses autores ainda mostraram que a ADAM9 é uma proteína adesiva, que induz a sinalização celular levando a um aumento de atividade proteolítica, ou seja, a adesão de células de fibroblastos ao domínio DC-9 aumentou a síntese de MMP-1 e MMP-2, e a ativação de pró-MMP-2. Entretanto, quando usadas células de melanoma com maior e menor capacidade de invasão notou-se que a expressão de MMP-2

foi apenas um pouco maior nas células de melanoma mais invasivas (ZIGRINO *et al.*, 2011). TAKEDA *et al.* (2006) descreveram no domínio rico em cisteína da ADAM9 a presença de uma região altamente variável (HVR), a qual seria a responsável pela interação com ligantes, uma vez que o *loop* do domínio desintegrina apresenta-se escondido e inacessível para a interação com ligantes.

Estudo realizado por XU e colaboradores mostrou que o silenciamento da ADAM9 reduziu a proliferação e a invasão de células de carcinoma de adenóide cístico (SACC-LM) (XU *et al.*, 2010). Entretanto, experimentos realizados em nosso laboratório utilizando a técnica do RNAi mostraram que a ADAM9 não está envolvida na proliferação das células MDA-MB-231. Porém, esta proteína mostrou-se essencial para a invasão dessas células em matrigel (MICOCCI *et al.*, 2013).

Resultados obtidos por MONGARET *et al.* (2010) mostraram que a exposição das células A549 (carcinoma de pulmão) ao peróxido de hidrogênio (H_2O_2) induziu a expressão da ADAM9, tanto da forma ancorada à membrana quanto da secretada. Além disso, quando a ADAM9 foi silenciada nesta linhagem celular houve a diminuição da capacidade de invasão e adesão celular, mesmo quando estas células foram induzidas pelo H_2O_2, sugerindo assim que a ADAM9 pode ser um determinante importante na disseminação das células de câncer.

A proteína ADAM9 também tem mostrado sua importância no processo de cicatrização de feridas. MAUCH e colaboradores mostraram em seus experimentos que o aumento na cicatrização utilizando animais sem a expressão da ADAM9 é resultante de uma menor indução da clivagem de colágeno XVII, sendo assim, a expressão aumentada da ADAM9 durante a cicatrização resulta em uma regulação negativa da re-epitelização (MAUCH *et al.*, 2010).

1.5. Vasos linfáticos e metástase

Durante a metástase tumoral, algumas células tumorais separam-se do tumor primário e dispersam através dos sistemas sanguíneo e linfático. Essas células utilizam-se destes sistemas, e por fim, invadem e crescem nos sítios secundários (WOODWARD *et al.*, 2005; HE *et al.*, 2002). Metástase tumorais para os linfonodos sentinelas representam o primeiro passo da disseminação tumoral na maioria dos cânceres humanos, incluindo carcinoma de mama, pescoço e cabeça, servindo assim como um importante indicador prognóstico para progressão da doença (CUENI *et al.*, 2010; ECCLES *et al.*, 2007; WISSMANN & DETMAR, 2006).

Estudos sugerem que os vasos linfáticos facilitam a metástase, fornecendo um portal de disseminação das células tumorais (BANDO *et al.*, 2006; SCHOPPMANN, 2005). Os vasos linfáticos oferecem vantagens para a invasão e transporte de células pré-metastáticas em relação aos vasos sanguíneos, tais como: (1) membrana basal descontínua e junções célula-célula mais frouxas; (2) taxa de fluxo menor que aumenta a sobrevida por minimizar o estresse de cisalhamento; e (3) concentração 1000 vezes maior de ácido hialurônico (na linfa), uma molécula com potentes propriedades de pró-sobrevivência (LAURENT *et al.*, 1992; RAN *et al.*, 2009). O sistema linfático é naturalmente equipado para transportar células pelo corpo, garantindo simultaneamente a sua sobrevivência e atividade. Tumores epiteliais, incluindo câncer de mama (SCHOPPMANN *et al.*, 2002; SKOBE *et al.*, 2001), melanoma (DADRAS *et al.*, 2005), próstata (JENNBACKEN *et al.*, 2005), cabeça e pescoço (BEASLEY *et al.*, 2002), tiram proveito da capacidade do sistema linfático de transportar células e, preferencialmente, disseminam-se através dos vasos linfáticos ao invés da rota hematogênica (RAN *et al.*, 2009). Além disso, o sistema linfático é composto por uma rede de capilares de parede fina e baixa pressão, que se estendem por todo o corpo coletando líquido

intersticial, macromoléculas e células do sistema imune, retornando-os à circulação sanguínea. Esses capilares são altamente permeáveis e revestidos por apenas uma única camada de células endoteliais, facilitando assim o seu acesso por células do sistema imune e tumorais (VANTYGHEM *et al.*, 2005), sendo assim, as células tumorais de mama utilizam esta rota como sua principal via de propagação precoce (RAN *et al.*, 2009).

A propagação preferencial através dos vasos linfáticos pode derivar da alta frequência de invasão de vasos linfáticos (LVI) por células de câncer de mama, em comparação com a invasão de vasos sanguíneos (BVI). Isto fica bem ilustrado por estudos independentes envolvendo um número considerável de pacientes. Estudo realizado com um n=1408 mostrou a presença de LVI em 34,2% dos casos, enquanto BVI foi detectado em apenas 4,2% (LAURIA *et al.*, 1995). Outro estudo utilizando 177 carcinomas de mama invasivos detectou a invasão linfática em 96,4% de todos os espécimes analisados, enquanto BVI foi detectada em apenas 3,5% (MOHAMMED *et al.*, 2007).

Devido aos recentes progressos conquistados com o emprego da técnica do RNAi em tumorigênese e o grande envolvimento da ADAM9 em diversos carcinomas humanos, entre eles o de mama, o presente trabalho estudou o papel da ADAM9 na disseminação tumoral via sistema linfático, visto que mais de 90% das mortes por câncer são consequências da propagação metastática, preferencialmente disseminada por vasos linfáticos. Desta forma, é de grande importância o estudo detalhado da função desta proteína na disseminação tumoral via sistema linfático, visando o emprego de novas ferramentas terapêuticas que possam atuar nas terapias antimetastáticas, emergindo assim como uma nova esperança para um tratamento específico do câncer.

2. OBJETIVOS

2.1. Objetivo geral

Estudar o papel da ADAM9 na disseminação tumoral via sistema linfático, visando o desenvolvimento de novas ferramentas terapêuticas. Para tanto, células de tumor de mama MDA-MB-231 silenciadas para a ADAM9 foram testadas com relação às suas atividades adesivas e invasivas frente ao endotélio vascular e linfático.

Hipótese inicial: A ADAM9 presente nas células tumorais é importante para a adesão ao endotélio vascular sanguíneo e linfático, contribuindo para a disseminação metastática.

2.2. Objetivos específicos

Verificar o efeito do silenciamento da ADAM9 nas células MDA-MB-231 em diferentes ensaios biológicos. Para a execução dos mesmos foram utilizadas também as células endoteliais: HUVEC, HMEC-1 e HMVEC-dLy:

- Proliferação Celular;
- Adesão Celular Estática;
- Migração Celular*: Wound Healing*;
- Migração Celular: *Transwell*;
- Invasão Celular;
- Adesão Celular Estática e Sob Fluxo;
- Transmigração Endotelial.

REFERÊNCIAS BIBLIOGRÁFICAS

3. REFERÊNCIAS BIBLIOGRÁFICAS

ALPHONSO, A.; ALAHARI, S. K. (2009). Stromal cells and integrins: conforming to the needs of the tumor microenvironment. *Neoplasia,* **11** (12): 1264-1271.

AMERICAN ASSOCIATION FOR CANCER RESEARCH (AACR), 2013.

BACAC, M.; STAMENKOVIC, I. Metastic Cancer Cell. (2008). *Annu. Rev. Pathol. Mech. Dis.*, **3**: 221-247.

BANDO, H.; WEICH, H. A.; HORIGUCHI, S.; FUNATA, N.; OGAWA, T.; TOI, M. (2006). The association between vascular endothelial growth factor-C, its corresponding receptor, VEGFR-3, and prognosis in primary breast cancer: a study with 193 cases, *Oncol. Rep.*, **15**: 653–659.

BARTSCH, J. E.; STAREN, E. D.; APPERT, H. E. (2003). Adhesion and migration of extracellular matrix-stimulated breast cancer. *Journal of Surgical Research,* **110:** 287–294.

BAU, DA-T.; MAUA, YI-C.; SHEN, C.-Y. (2006). The role of BRCA1 in non-homologous end-joining. *Cancer Letters*, **240**: 1–8.

BEASLEY, N. J.; PREVO, R.; BANERJI, S.; LEEK, R. D.; MOORE, J.; VAN TRAPPEN, P.; COX, G.; HARRIS, A. L.; JACKSON, D. G. (2002). Intratumoral lymphangiogenesis and lymph node metastasis in head and neck câncer. *Cancer Res.* **62**: 1315–1320.

BERMAN, A. E.; KOZLOVA, N. I.; MOROZEVICH, G. E. (2003). Integrins: structure and signaling. *Biochemistry,* **68** (12): 1284-99.

BERRIER, A.L.; YAMADA, K. M. (2007). Cell–Matrix Adhesion. *J. Cell. Physiol.*, **213**: 565–573.

BLACK, R. A.; WHITE, J. M. (1998). ADAMs: focus on the protease domain. *Curr. Opin. Cell Biol.*, **10**: 654-659.

BLOBEL, C. P. (1997). Metalloprotease-disintegrins: links to cell adhesion and cleavage of TNFα and Notch. *Cell,* **90**: 589-592.

BROOKS, S. A; LOMAX-BROWNE, H. J.; CARTER, T. M.; KINCH, C. E.; HALL, D. M. (2000). Molecular interactions in cancer cell metastasis. *Acta Histochem.,* **112** (1): 3-25.

CARL-McGRATH, S.; LENDECKEL, U.; EBERT, M.; ROESSNER, A.; ROCKEN, C. (2005). The disintegrin and metalloproteinases ADAM9, ADAM12, and ADAM15 are upregulated in gastric cancer. *Int. J. Oncol.*, **26**: 17–24.

CHRISTIANSEN, J. J.; RAJASEKARAN, A. K. (2006). Reassessing epithelial to mesenchymal transition as a prerequisite for carcinoma invasion and metastasis. *Cancer Res.*, **66** (17): 8319-8326.

COCCO, P. (2002). On the rumors about the silent spring. Review of the scientific evidence linking occupational and environmental pesticide exposure to endocrine disruption health effects. *Cad. Saúde Pública, Rio de Janeiro*, **18** (2): 379-402.

COMINETTI, M. R.; MARTIN, A. C.; RIBEIRO, J. U.; DJAAFRI, I.; FAUVEL-LAFÈVE, F.; CRÉPIN, M.; SELISTRE-DE-ARAUJO, H. S. (2009). Inhibition of platelets and tumor cell adhesion by the disintegrin domain of human ADAM9 to collagen I under dynamic flow conditions. *Biochimie.*, **91** (8): 1045-1052.

CONDEELIS, J.; POLLARD, J. W. (2006). Macrophages: obligate partners for tumor cell migration, invasion, and metastasis. *Cell,* **124** (2): 263-266.

CUENI, L.N.; HEGYI, I.; SHIN, J. W.; ALBINGER-HEGYI, A.; GRUBER, S.; KUNSTFELD, R.; MOCH, H.; DETMAR, M. (2010). Tumor Lymphangiogenesis and Metastasis to Lymph Nodes Induced by Cancer Cell Expression of Podoplanin. *The American Journal of Pathology*, **177** (2).

DADRAS, S. S.; LANGE-ASSCHENFELDT, B.; VELASCO, P.; NGUYEN, L.; VORA, A.; MUZIKANSKY, A.; JAHNKE, K.; HAUSCHILD, A.; HIRAKAWA, S.; MIHM, M. C.; DETMAR, M. (2005). Tumor lymphangiogenesis predicts melanoma metastasis to sentinel lymph nodes. *Mod. Pathol.*, **18**: 1232–1242.

DE MATOS, L. L.; MACHADO, L. N.; SUGIYAMA, M. M.; BOZZETTI, R. M.; DA SILVA PINHAL, M. A. (2005). Tecnology applied in the detection of tumor markers. *Arq. Med. ABC*, **30** (1): 19-25.

DESGROSELLIER, J. S.; CHERESH, D. A. (2010). Integrins in cancer: biological implications and therapeutic opportunities. *Nat Rev Cancer*, **10** (1): 9-22.

DUFFY, M. J.; MCKIERNAN, E.; O'DONOVAN, N.; MCGOWAN, P. M. (2009). Role of ADAMs in cancer formation and progression. *Clin Cancer Res*, **15**: 1140–1144.

ECCLES, S.; PAON, L.; SLEEMAN, J. (2007). Lymphatic metastasis in breast cancer: importance and new insights into cellular and molecular mechanisms. *Clin Exp Metastasis.,* **24** (8): 619-636.

ECKHARDT, B. L.; PARKER, B. S.; VAN LAAR, R. K.; RESTALL, C. M.; NATOLI, A. L.; TAVARIA, M. D.; STANLEY, K. L.; SLOAN, E. K.; MOSEL, J. M.; ANDERSON, R. L. (2005). Genomic analysis of a spontaneous model of breast cancer metastasis to bone reveals a role for the extracellular matrix. *Mol. Cancer Res.*, **3** (1): 1-13.

EVAN, G. I.; VOUSDEN, K. H. (2001). Proliferation, cell cycle and apoptosis in câncer. *Nature*, **411**: 342-348.

FAMBROUGH, D.; PAN, D.; RUBIN, G.M.; GOODMAN, C.S. (1996). The cell surface metalloprotease/disintegrin Kuzbanian is required for axonal extension in *Drosophila*. *Proc. Natl. Acad. Sci. USA*, ***93*:** 13233–13238.

FRIEDL, P.; ALEXANDER, S. (2011). Cancer invasion and the microenvironment: plasticity and reciprocity. *Cell*, **147** (5): 992-1009.

FRITZSCHE, F .R.; JUNG, M.; TÖLLE, A.; WILD, P.; HARTMANN, A.; WASSERMANN, K.; RABIEN, A.; LEIN, M.; DIETEL M.; PILARSKY, C.; CALVANO, D.; GRUTZMANN, R.; JUNG, K.; KRISTIANSEN, G. (2008[a]). ADAM9 Expression is a Significant and Independent Prognostic Marker of PSA Relapse in Prostate Cancer. *European Urology*, **54**: 1097–11082.

FRITZSCHE, F. R.; WASSERMANN, K.; JUNG, M.; TÖLLE, A.; KRISTIANSEN, I.; LEIN, M.; JOHANNSEN,M.; DIETEL, M.; JUNG, K.; KRISTIANSEN, G. (2008[b]). ADAM9 is highly expressed in renal cell cancer and is associated with tumour progression. *BMC Cancer*, **8** (179): 1-9.

FRY, J. L.; TOKER, A. (2010). Secreted and Membrane-Bound Isoforms of Protease ADAM9 Have Opposing Effects on Breast Cancer Cell Migration. *Cancer Res*., **70** (20): 8187-8198.

GEIGER, B.; BERSHADSKY, A.; PANKOV, R.; YAMADA, K. M. (2001). Transmembrane crosstalk between the extracellular matrix and the cytoskeleton. *Nat. Rev. Cell Biol*., **2**: 793-805.

GEIGER, T. R.; PEEPER D. S. (2009). Metastasis mechanisms. *Biochim. Biophys. Acta*, **1796** (2): 293-308.

GRÜTZMANN, R.; LÜTTGES, J.; SIPOS, B.; AMMERPOHL, O.; DOBROWOLSKI, F.; ALLDINGER, I.; KERSTING, S.; OCKERT, D.; KOCH, R.; KALTHOFF, H.; SCHACKERT, H. K.; SAEGER, H. D.; KLÖPPE, G.; PILARSKY, C.(2004). ADAM9 expression in pancreatic cancer is associated with tumour type and is a prognostic factor in ductal adenocarcinoma. *Br. J. Cancer*, **90** (5): 1053-1058.

HANAHAN, D.; WEINBERG R. A. (2000). Hallmarks of cancer. *Cell*, **100**: 57-70.

HANAHAN, D.; WEINBERG R. A. (2011). Hallmarks of cancer: the next generation. *Cell*, **144** (5): 646-674.

HE, Y.; KOZAKI, K.; KARPANEN, T.; KOSHIKAWA, K.; YLA-HERTTUALA, S.; TAKAHASHI, T.; ALITALO, K. (2002). Suppression of tumor lymphangiogenesis and lymph node metastasis by blocking vascular endothelial growth factor receptor 3 signaling. *J. Natl. Cancer Inst*. **94** (11): 819-825.

HOOD, J. D.; CHERESH, D. A. (2002). Role of integrins in cell invasion and migration. *Nature Reviews*, **2**: 91-100.

HOTODA, N.; KOIKE, H.; SASAGAWA, N.; ISHIURA, S. (2002). A secreted form of ADAM9 has an alpha-secretase activity for APP. *Biochem Biophys. Res.Commun*., **293** (2): 800-805.

HYNES, R. O. Integrins: a family of cell surface receptors. (1987). *Cell*, **48** (4): 549-554.

JENNBACKEN, K.; VALLBO, C.; WANG, W.; DAMBER, J. E. (2005). Expression of vascular endothelial growth factor C (VEGF-C) and VEGF receptor-3 in human prostate cancer is associated with regional lymph node metastasis. *Prostate*, 110–116.

JOYCE, J. A.; POLLARD, J. W. (2009). Microenvironmental regulation of metastasis. *Nat. Rev. Cancer*, **9** (4): 239-252.

KRAMER, N.; WALZL, A.; UNGER, C.; ROSNER, M.; KRUPITZA, G.; HENGSTSCHLÄGER, M.; DOLZNIG, H. (2012). In vitro cell migration and invasion assays. *Mutat. Res.*, **752** (1):10-24.

KOHN, K. W.; ZEEBERG, B. R.; REINHOLD, W. C.; SUNSHINE, M.; LUNA, A.; POMMIER, Y. (2012). Gene expression profiles of the NCI-60 human tumor cell lines define molecular interaction networks governing cell migration processes. *PLoS One*. **7** (5).

KUSUMA, N.; DENOYER, D.; EBLE, J. A.; REDVERS, R. P.; PARKER, B. S,; PELZER, R.; ANDERSON, R. L.; POULIOT, N. (2011). Integrin-dependent response to laminin-511 regulates breast tumor cell invasion and metastasis. *Int J Cancer*., **130** (3): 555-566.

LAURENT, T. C.; FRASER, J. R.; HYALURONAN. (1992). *FASEB J.* **6:** 2397–2404.

LAURIA, R.; PERRONE, F.; CARLOMAGNO, C.; DE LAURENTIIS, M.; MORABITO, A.; GALLO, C.; VARRIALE, E.; PETTINATO, G.; PANICO, L.; PETRELLA, G. (1995). The prognostic value of lymphatic and blood vessel invasion in operable breast câncer. *Cancer*, **76:** 1772–1778.

LOPES, A. A.; OLIVEIRA, A. M.; PRADO, C. B. C. (2002). Principais genes que participam da formação de tumores. *Revista de biologia e ciências da terra*, **2** (2): 1-7.

LOWERY, F. J.; DIHUA, Y. U. (2012). Growth factor signaling in metastasis: current understanding and future opportunities. *Cancer Metastasis Rev*.

LUO, Y., *et al.* (2006). Targeting tumor-associated macrophages as a novel strategy against breast cancer. *J. Clin. Invest.*, **116** (8): 2132-2141.

MALVEZZI M.; BERTUCCIO, P.; LEVI, F. L. A.; VECCHIA, C.; NEGRI, E. (2013). European cancer mortality predictions for the year. *Ann Oncol.* **24** (3).

MAUCH, C.; ZAMEK, J.; ABETY, A.N.; GRIMBERG, G.; FOX, J.W.; ZIGRINO, P. (2010). Accelerated wound repair in ADAM-9 knockout animals, J Invest Dermatol, 130 2120-2130.

MAZZOCCA A.; COPPARI R.; DE FRANCO R.; CHO J.Y.; LIBERMANN T.A.; PINZANI M., Toker A. (2005). A secreted form of ADAM9 promotes carcinoma invasion through tumor-stromal interactions, *Cancer Res*. **65**: 4728-4738.

MICOCCI, K. C.; MARTIN, A. C.; MONTENEGRO, C. D.; DURANTE, A. C.; POULIOT, N.; COMINETTI, M. R.; SELISTRE-DE-ARAUJO, H. S. (2013). ADAM9 silencing inhibits breast tumor cell invasion in vitro. *Biochimie*.

MOCHIZUKI, S.; OKADA, Y. (2007). ADAMs in cancer cell proliferation and progression. *Cancer Sci.*, **98** (5): 621-628.

MONGARET, C.; ALEXANDRE, J.; THOMAS-SCHOEMANN, A.; BERMUDEZ, E.; CHÉREAU, C.; NICCO, C.; GOLDWASSER, F.; WEILL, B.; BATTEUX, F.; LEMARE, F. (2010). Tumor invasion induced by oxidative stress is dependent on membrane ADAM 9 protein and its secreted form, *Int. J. Cancer.*, **129**: 791-798.

MOHAMMED, R. A.; MARTIN, S. G.; GILL, M. S.; GREEN, A. R.; PAISH, E. C.; ELLIS, I. O. (2007). Improved methods of detection of lymphovascular invasion demonstrate that it is the predominant method of vascular invasion in breast cancer and has important clinical consequences. *Am. J. Surg. Pathol.*, **31:** 1825–1833.

MUKHOPADHYAY, R.; THERIAULT, R. L.; PRICE, J. E. (1999). Increased levels of α_6 integrins are associated with the metastatic phenotype of human breast cancer cells. *Clin. Exp. Metastasis*, **17:** 325-332.

ORIMO, A *et al.* (2005). Stromal Fibroblasts Present in Invasive Human Breast Carcinomas Promote Tumor Growth and Angiogenesis through Elevated SDF-1/CXCL12 Secretion. *Cell*, **121**: 335–348.

O'SHEA, C.; McKIE, N.; BUGGY, Y.; DUGGAN, C.; HILL, A.D.; McDERMOTT, E.; O'HIGGINS, N.; DUFFY, M.J. (2003). Expression of ADAM9 mRNA and protein in human breast cancer. *Int. J. Cancer.*, **105**: 754–761.

PAVELIC KRALJEVIC, S.; SEDIC, M.; BOSNJAK, H.; SPAVENTI, S.; PAVELIC, K. (2011). Metastasis: new perspectives on an old problem. *Mol. Cancer*.

PEDUTO, L.; REUTER, V. E.; SHAFFER, D. R.; SCHER, H. I.; BLOBEL, C. P. (2005). Critical Function for ADAM9 in Mouse Prostate Cancer. *Cancer Research*, **65**: 9312-9319.

PERRET, G. Y.; CRÉPIN, M. (2008). New pharmacological strategies against metastatic spread. *Fundam Clin Pharmacol*, **22** (5): 465-492.

PETRUZZELLI, L.; TAKAMI, M.; HUMES, H. D. (1999). Structure and function of cell adhesion molecules. *Am. J. Med.*, **106** (4): 67-476.

POLLARD, J. W. (2004). Tumour-educated macrophages promote tumour progression and metastasis. *Nature Reviews*, **4**: 71-78.

PLOW, E. F.; HAAS, T. A.; ZHANG, L.; LOFTUSI, J.; SMITH, J. W. (2000). Ligand Binding to Integrins**.** *The Journal of Biological Chemistry*, **275** (29): 21785–21788.

PONTIER, S. M.; MULLER, W. J. (2008). Integrins in breast cancer dormancy. *APMIS*, **116:** 677–694.

PRIMAKOFF, P.; MYLES, D. G. (2000). The ADAM gene family: surface proteins with adhesion and protease activity. *Trends Genet*., **16**: 82-87.

RAN, S.; VOLK, L.; HALL, K.; FLISTER, M. J. (2009). Lymphangiogenesis and lymphatic metastasis in breast cancer. Pathophysiology. 2009.

REISS. K,; SAFTIG, P. (2009). The "a disintegrin and metalloprotease" (ADAM) family of sheddases: physiological and cellular functions. *Semin. Cell Dev. Biol.*, **20** (2): 126-137.

ROCKS, N.; PAULISSEN, G.; EL HOUR, M.; QUESADA, F.; CRAHAY, C.; GUEDERS, M.; FOIDART, J. M.; NOEL, A.; CATALDO, D. (2008). Emerging roles of ADAM and ADAMTS metalloproteinases in cancer. *Biochimie*, **90** (2): 369-79.

SCHEEL, C.; EATON, E. N., LI, S. H.; CHAFFER, C. L.; REINHARDT, F.; KAH, K. J.; BELL, G.; GUO, W.; RUBI,N J.; RICHARDSON, A. L.; WEINBERG, R. A. (2011). Paracrine and autocrine signals induce and maintain mesenchymal and stem cell states in the breast. *Cell*, **145** (6): 926-40.

SCHOPPMANN, S. F.; HORVAT, R.; BIRNER, P. (2002). Lymphatic vessels and lymphangiogenesis in female cancer: mechanisms, clinical impact and possible implications for anti-lymphangiogenic therapies. *Oncol. Rep*., **9**: 455–460.

SCHMIDT, S.; FRIEDL, P. (2010). Interstitial cell migration: integrin-dependent and alternative adhesion mechanisms. *Cell Tissue Res*, **339** (1): 83-92.

SEALS, D. F.; COURTNEIDGE, S. S. (2003). The ADAMs family of metalloproteases: multidomain proteins with multiple functions. *Gen. Dev*., **17:** 7-30.

SELISTRE-DE-ARAÚJO, H. S; COMINETTI, M. R.; TERRUGGI, C. H. B.; MARIANO-OLIVEIRA, A.; FREITAS, M. S.; CREPIN, M.; FIQUEIREDO, C. C.; MORANDI, V. (2005). Alternagin-C a disintegrin-like protein from the venom of Bothrops alternatus, modulates α2β1 integrin-mediated cell adesion, migration and proliferation. *Braz. J. Med. Biol. Res*., **38** (10): 1505-1511.

SHINTANI, Y.; HIGASHIYAMA, S.; OHTA, M.; HIRABAYASHI, H.; YAMAMOTO, S.; YOSHIMASU, T.; MATSUDA, H.; MATSUURA, N. (2004). Overexpression of ADAM9 in Non-Small Cell Lung Cancer Correlates with Brain Metastasis. *Cancer Research*, **64**: 4190–4196.

SKOBE, M.; HAWIGHORST, T.; JACKSON, D. G.; PREVO, R.; JANES, L.; VELASCO, P.; RICCARDI, L.; ALITALO, K.; CLAFFEY, K.; DETMAR, M. (2001). Induction of tumor lymphangiogenesis by VEGF-C promotes breast cancer metastasis. *Nat. Med*., **7:** 192–198.

SLEEMAN, J. P. (2012). The metastatic niche and stromal progression. *Cancer Metastasis Rev*.

SLOAN, E. K.; POULIOT, N.; STANLEY, K. L.; CHIA, J.; MOSELEY, J. M.; HARDS, D. K.; ANDERSON, R. L. (2006). Tumor-specific expression of alphavbeta3 integrin

promotes spontaneous metastasis of breast cancer to bone. *Breast Cancer Res*., **8** (2): 1-14.

STONE, A. L.; KROEGER, M.; SANG, Q. X. (1999). Structure-function analysis of the ADAM family of disintegrin-like and metalloproteinase-containing Proteins (Review). J. *Protein Chem*., **18**: 447-465.

SUNG, S.Y.; KUBO, H.; SHIGEMURA, K.; ARNOLD, R. S.; LOGANI, S.; WANG, R.; KONAKA, H.; NAKAGAWA, M.; MOUSSES, S.; AMIN, M.; ANDERSON, C.; JOHNSTONE, P.; PETROS, J.A.; MARSHALL, F.F.; ZHAU, H.E.; CHUNG, L.W. (2006). Oxidative stress induces ADAM9 protein expression in human prostate cancer cells. *Cancer Res*., **66** (19): 9519-9526.

STRATTON, M. R.; CAMPBELL P. J.; FUTREAL, P. A. (2009). The cancer genome. *Nature*, **458** (7239): 719-724.

TAKADA, Y.; YE, X.; SIMON, S. (2007). The integrins. *Genome Biology*, **8 (**215): 1-9.

TAKEDA, S.; IGARASHI, T.; MORI, H.; ARAKI, S. (2006). Crystal structures of VAP1 reveal ADAMs MDC domain architecture and its unique C-shaped scaffold. Embo J, **25** (11): 2388-2396.

TANNAPFEL, A.; ANHALT, K.; HAUSERMANN, P.; SOMMERER, F.; BENICKE, M.; UHLMANN, D.; WITZIGMANN, H.; HAUSS, J.; WITTEKIND, C. (2003). Identification of novel proteins associated with hepattocellular carcinomas using protein microarrays. *J. Pathol*., **201:** 238–249.

TANZER, M. L. (2006). Current concepts of extracellular matrix. *J. Orthop. Sci*., **11**: 326-331.

TOCHHAWNG, L.; DENG, S.; PERVAIZ, S.; YAP, C. T. (2012). Redox regulation of cancer cell migration and invasion. *Mitochondrion*.

VANTYGHEM, S. A.; ALLAN, A. L.; POSTENKA, C. O.; AL-KATIB, W.; KEENEY, M.; TUCK, A. B.; CHAMBERS, A. F. (2005). A new model for lymphatic metastasis: Development of a variant of the MDA-MB-468 human breast cancer cell line that aggressively metastasizes to lymph nodes. *Clinical & Experimental Metastasis*, **22**: 351–361.

VIDEIRA, R, S.; DEBONI, M. C. Z.; ARAÚJO, C. A. S.; OKAMOTO, A. C.; MELHADO, A. M. (2002). Oncogenes e desenvolvimento do câncer. *Arq. Ciênc. Saúde Unipar*, **6** (1): 71-76.

WHITE, J. M. (2003). ADAMs: modulators of cell–cell and cell–matrix interactions. *Current Opinion in Cell Biology*, **15**: 598-606.

WISSMANN, C.; DETMAR, M. (2006). Pathways TargetingTumor Lymphangiogenesis. *Clin Cancer Res*., **12** (23).

WOLFSBERG, T. G.; BAZAN, J. J.; BLOBEL, C. P.; MYLES, D. G.; PRIMAKOFF, P.; WHITE, J. M. (1993). The precursor region of a protein active in sperm-egg fusion contains a metalloprotease and a disintegrin domain: Structural, functional, and evolutionary implications. *Proc. Natl. Acad. Sci. U.S.A.*, **90** (22): 10783-10787.

WOLFSBERG, T. G.; WHITE, J. M. (1996). ADAMs in fertilization and development. *Developmental Biology*, **180**: 389-401.

WOODWARD, J. K.; RENNIE, I. G.; BURN, J. L.; SISLEY, K. (2005). A potential role for TGFbeta in the **r**egulation of uveal melanoma adhesive interactions with the hepatic endothelium. *Nature*, **(19),** 342–348.

www.inca.gov.br. Acesso: 15/03/2013.

YAMADA, K. (1991). Adhesive recognition sequences. *J. Biol. Chem.*, **266**: 12809-12812.

YAMADA, K. M.; PANKOV, R.; CUKIERMAN, E. (2003). Dimensions and dynamics in integrin function. Braz. *J. Med. Biol. Res.*, **36**: 959-966.

YAMAGUCHI, H.; WYCKOFF, J.; CONDEELIS, J. (2005). Cell migration in tumors. *Curr. Opin. Cell Biol*, **17** (5): 559-564.

YAN, J., HUANG, Q. (2012). Genomics screens for metastasis genes. *Cancer Metastasis Rev.*, **31** (3-4): 419-428.

YAO, E. S; ZHANG, H.; CHEN, Y. Y.; LEE, B.; CHEW, K.; MOORE, D.; PARK, C. (2007). Increased β_1 integrin is associated with decreased survival in invasive breast cancer. *Cancer Research*, **67**: 659–664.

YILMAZ, M.; CHRISTOFORI, G.; LEHEMBRE, F. (2007). Distinct mechanisms of tumor invasion and metastasis. *Trends Mol. Med.*, **13** (12): 535-541.

XU, Q.; LIU, X.; CAI, Y.; YU, Y.; CHEN, W. (2010). RNAi-mediated ADAM9 gene silencing inhibits metastasis of adenoid cystic carcinoma cells. *Tumour Biol.*, **31** (3): 217-224.

ZIGRINO, P.; MAUCH, C.; FOX, J. W.; NISCHT, R. (2005). ADAM-9 expression and regulation in human skin melanoma and melanoma cell lines. *Int. J. Cancer*, **116:** 853–859.

ZIGRINO, P.; STEIGER, J.; FOX, J. W.; LOFFEK, S.; SCHILD, A.; NISCHT, R.; MAUCH, C. (2007). Role of ADAM-9 Disintegrin-Cysteine-rich Domains in Human Keratinocyte Migration. *The Journal of Biological Chemistry*, **282** (42): 30785–30793.

ZIGRINO, P.; NISCHT, R.; MAUCH, C. (2011). The disintegrin-like and cysteine-rich domains of ADAM-9 mediate interactions between melanoma cells and fibroblasts, J Biol Chem., **286**: 6801-6807.

ZUBEL, A.; FLECHTENMACHER, C.; EDLER, L.; ALONSO, A. (2009). Expression of ADAM9 in CIN3 lesions and squamous cell carcinomas of the cervix. *Gynecologic Oncology*.

ZUO, Y.; WU, Y.; CHAKRABORTY, C. (2012). Cdc42 Negatively Regulates Intrinsic Migration of Highly Aggressive Breast Cancer Cells. *J. Cell Physiol.*, **227** (4): 1399-1407.

ZUTTER, M. M.; MAZOUJIAN, G.; SANTORO, S. A. (1990). Decreased expression of integrin adhesive protein receptors in adenocarcinoma of the breast. *Am. J. Pathol.,* **137:** 863-870.

4. MANUSCRITOS

4.1. MANUSCRITO I – Em fase de redação

Proteína ADAM9: papel na progressão tumoral via vasos linfáticos e sanguíneos

Kelli Cristina Micocci[a*], Milene Nóbrega de Oliveira Moritz[a], Rafael Luis Bressani Lino[a], Laila Riveiro Fernandes[b], Antonio Gilclêr Ferreira Lima[b], Camila Castro Figueiredo, Verônica Morandi, Heloisa Sobreiro Selistre-de-Araujo[a].

[a] Departamento de Ciências Fisiológicas, Rodovia Washington Luís, Km 235, CEP 13565-905, São Carlos, SP, Brasil. Fax: +55-16-33518328; Fone: +55-16-33518333.

[b] Departamento de Biologia Celular, Rua São Francisco Xavier, 524, Pavilhão Haroldo Lisboa da Cunha – 2º Andar, Rio de Janeiro, RJ, Brasil. Fone: +55-21-2334-0499.

*Autor correspondente: kelli_micocci@hotmail.com

RESUMO

ADAMs é o termo usado para descrever a presença dos domínios desintegrina e metaloprotease (A Disintegrin And Metalloprotease) em uma determinada classe de proteínas de membrana, multimodulares e multifuncionais. Elas exercem funções importantes em processos fisiológicos como na fertilização, fusão de mioblastos, migração, proliferação e sobrevivência celular, resposta inflamatória, clivagem de ectodomínios de proteínas de membrana, e também em processos patológicos, incluindo câncer e formação de metástases. Um representante das ADAMs envolvida em neoplasias é a meltrina γ (ADAM9), cuja expressão está aumentada em um grande número de carcinomas humanos. O objetivo desse trabalho foi estudar o papel da ADAM9 na disseminação tumoral via sistemas sanguíneo e linfático, visando o desenvolvimento de novas ferramentas terapêuticas. O papel da ADAM9 na interação de células tumorais de mama MDA-MB-231 com células endoteliais *in vitro* foi estudado utlizando-se silenciamento gênico por RNA de interferência. Os resultados mostraram que o siADAM9 nas células MDA-MB-231 não afetou a expressão da ADAM10, ADAM12, ADAM17, cMYC, MMP9, VEGF-A, VEGF-C, Osteopontina e Colágeno XVII, entretanto houve uma diminuição da expressão da ADAM15 e um aumento da expressão da MMP2 quando comparado com as controles: meio e negativo. O siADAM9 nas células MDA-MB-231 não afetou a adesão sob fluxo das células às endoteliais vasculares (HMEC-1 e HUVEC) e linfáticas (HMVEC-dLyNeo). Entretanto, houve uma dimuição na taxa de transmigração através da monocamada das células endoteliais (HUVEC, HMEC-1 e HMVEC-dLyNeo) em aproximadamente 50%, 40% e 32%, respectivamente. Dessa forma, sugere-se o envolvimento da ADAM9 no processo de invasão, extravasamento pelos vasos sanguíneos e linfáticos, e formação de metástase.

Palavras chaves: ADAM9, câncer de mama, células endoteliais sanguíneas e linfáticas.

1. INTRODUÇÃO

O câncer é uma doença de ocorrência mundial considerada atualmente como um dos maiores problemas de saúde pública [1-2]. Também conhecido como tumores malignos, o câncer é um termo genérico para um grande grupo de doenças que pode afetar qualquer parte do corpo. O desenvolvimento do tumor é iniciado por um acúmulo de alterações genéticas e epigenéticas que promovem a iniciação, invasão e metástase tumoral [3-4-5]. Durante o desenvolvimento das neoplasias humanas algumas características são adquiridas, incluindo a sustentação da sinalização proliferativa, a evasão de supressores de crescimento, a resistência à morte celular, a habilidade de imortalidade replicativa, a indução da angiogênese, a ativação da invasão e metástase, a instabilidade genômica e mutações, a promoção tumoral da inflamação, a falta de regulação do metabolismo energértico celular e a proteção contra a destruição imune [5-6]. Os tipos de câncer mais comuns que causam mortes no mundo são: pulmão (1,59 milhões), fígado (745 mil), estômago (723 mil), colorretal (694 mil), mama (521 mil) e esôfago (400 mil) [2].

O câncer de mama é o tipo de câncer que mais acomete as mulheres tanto em países desenvolvidos quanto em países em desenvolvimento. As taxas de incidência em 2012 foram maiores na Europa Ocidental (96 casos para 100 mil mulheres) e menores na África Central e Ásia Oriental (27/100 mil). No Brasil, em 2014, são esperados 57.120 novos casos de câncer de mama, com um risco estimado de 56 casos para cada 100 mil mulheres [1].

A disseminação das células tumorais para fora do sítio primário, estabelecendo novas colônias em orgãos distantes é definida como metástase, sendo esta a maior causa de morbidade e mortalidade em pacientes com câncer de mama [7-8]. O processo metastático é composto por uma complexa cascata de eventos que se inicia com as células se desprendendo do tumor primário. Para que este evento ocorra, as células tumorais necessitam modificar sua

morfologia para facilitar a sua dispersão e motilidade, processo chamado de transição epitélio-mesenquimal (EMT). Esse processo causa a desadesão das células do tumor primário que perdem a capacidade de se aderirem às suas vizinhas e adquirem características migratórias e invasivas necessárias para transpor barreiras físicas e atingir seu sítio metastático. O processo de migração nas células tumorais pode ocorrer sob duas formas, individual e coletiva. Após atingirem o seu sítio metastático, as células cancerígenas que passaram pelo EMT têm o processo revertido voltando a expressar sua morfologia epitelial, processo chamado de transição mesenquimal-epitelial (MET) [9].

Segundo Bacac and Stamenkovic [10] existem três rotas principais para a disseminação tumoral: vasos linfáticos, sanguíneos e superfícies serosas. Entretanto, apesar da presença de uma rica rede vascular sanguínea no câncer de mama, a invasão vascular ocorre predominantemente via vasos linfáticos (96,4%) em oposição aos sanguíneos (3,5%) [7]. Resultados similares também foram encontrados em melanoma, no qual, 85,5% do total da invasão ocorre via sistema linfático [11]. Além disso, em relação aos critérios clínico-patológicos e de sobrevivência, a invasão vascular linfática foi significativamente associada com maior tamanho do tumor, presença de metástase nos linfonodos, desenvolvimento de recidiva regional e metástases para outros órgãos ou tecidos, bem como pior sobrevida global [12-13, 7].

A modulação do microambiente tecidual através da degradação da matriz extracelular (MEC), o processamento de fatores de crescimento e ativação de moléculas de adesão celular são essenciais para a proliferação e progressão das células de câncer [14-15]. Além disso, a degradação da matriz extracelular é um pré-requisito para o reparo tecidual, migração celular e liberação de fatores de crescimento e peptídeos bioativos [16]. Diferentes proteases têm sido coadjuvantes nesses processos, tais como, as metalopeptidases de matriz (MMPs), outras famílias de proteases (serino, cisteína e aspártica), as ADAMs (***A D****isintegrin*

***A**nd **M**etalloprotease*) e as ADAMTSs (que apresentam o domínio trombospondina adicional) [14, 16-17].

Membros da família das ADAMs estão associados com metástases de cânceres humanos, e diversas ADAMs estão superexpressas em tecidos de câncer metastático comparado com tecidos normais ou tumores benignos do mesmo órgão. Além disso, parametros de formação, progressão e agressividade tumoral tem sido correlacionado com o nível de expressão de algumas dessas proteínas, entre elas, ADAM9, ADAM12, ADAM15 e ADAM17 [17-18-19].

A ADAM9 (MDC9 ou meltrin γ) é um importante membro desta grande família de glicoproteínas que, além de mediar respostas celulares em ambientes de estresse e regular diversos processos celulares, tais como, adesão celular, migração, invasão, proliferação, ligação a MEC e clivagem de ectodomínios [20-21], também tem sido correlacionada com tumorigênese e metástase tumoral [22]. Prévios estudos do nosso laboratório mostraram que a ADAM9 tem um papel importante na invasão das células de tumor de mama MDA-MB-231, porém sem afetar a migração dessas células [23]. Entretanto, FRY e TOKER [24] utilizando RNAi e diferentes células de tumor de mama verificaram que a ADAM9-S (secretada) e ADAM9-L (transmembrana) funcionam de forma opostas na regulação da migração celular, ou seja, a ADAM9-S promove e a ADAM9-L atenua a migração. PEDUTO e colaboradores [25] reportaram que, em modelos de carcinoma em camundongos, entre eles, próstata, mama e intestinal, a expressão da ADAM9 foi maior nas regiões dos tumores quando comparada com tecidos adjacentes normais.

Procurando contribuir para a compreensão dos mecanismos de disseminação tumoral, o presente estudo buscou avaliar o papel da ADAM9 na interação de células de tumor de mama com células endoteliais linfáticas e sanguíneas, na busca de novos alvos e o desenvolvimento de novas ferramentas terapêuticas antimetastáticas.

2. MATERIAIS E MÉTODOS

2.1. Cultura celular

As linhagens de tumor de mama (MDA-MB-231) foram gentilmente cedidas pelo Dr. Michel Crépin (INSERM, Paris, França) e as endoteliais vasculares de cordão umbilical humano (HUVEC) foram doadas pelo Dr. Gerson Jhonatan Rodrigues (UFSCar, São Carlos, SP). Ambas as linhagens foram cultivadas em meio DMEM (*Dulbecco's Modified Eagle Medium* – Vitrocell Embriolife), contendo 10% de soro fetal bovino (FBS), L-glutamina (2 mM), penicilina (100 U/mL - Vitrocell Embriolife), estreptomicina (100 µg/mL - Vitrocell Embriolife) e anfotericina B (250 UG/mL - Gibco). As células primárias HUVEC foram cedidas gentilmente pela Dra. Verônica Morandi (UERJ, Rio de Janeiro, RJ) e isoladas através de digestão do interior da veia umbilical por colagenase 0,2% e mantidas em meio 199 (M-199) com HEPES (Sigma), suplementado com penicilina 100 Ul/mL, estreptomicina 100 µg/mL, anfotericina-B 5 µg/mL, L-glutamina 2 mM e 20% soro fetal bovino (Gibco). As células da linhagem HMEC-1 foram também cedidas pela Dra. Verônica Morandi (UERJ, Rio de Janeiro, RJ) e foram cultivadas em meio MCDB–131 (Gibco) suplementado com 10% de soro fetal bovino (Gibco), L-glutamina 2 mM, hidrocortisona 1 mg/mL, fator de crescimento epidérmico (EGF) 10 µg/mL (Gibco) e antibióticos. As células HMVEC-dLyAd-Der (n° catálogo 2810) ou HMVEC-dLyNeo-Der (n° catálogo 2812) foram compradas da empresa Lonza e cultivadas em meio de cultura EBM-2 (n° catálogo CC-3156) suplementado com o kit EGM-2 MV SingleQuots (n° catálogo CC-4147). Todas as culturas celulares foram mantidas em estufa com 5% de CO_2 a 37ºC. As células da linhagem MDA-MB-231, HUVEC e HMEC-1 foram utilizadas da passagem 15 a 35. As células de cultura primárias HUVEC, HMVEC-dLyAd-Der e HMVEC-dLyNeo-Der foram usadas somente até a passagem 5.

Para os ensaios de *Western Blotting* foram utilizados os seguintes anticorpos: anti-camundongo ADAM9 (1:1000) (Ectodomínio – R&D Systems - n° catálogo AF949) e anti-βeta Actina conjugado com HRP (1:200) (Santa Cruz - n° catálogo sc1616).

2.2. Silenciamento de RNA (RNAi)

Para esta técnica foi utilizado um *kit* (*Silencer® siRNA Starter Kit* – Ambion). O protocolo foi realizado de acordo com a metodologia já padronizada e descrita por Micocci *et al.* [23]. Após 72 horas da transfecção, as células foram lavadas com tampão fosfato-salino - PBS (1X) e retiradas das placas para ensaios de expressão gênica (utilizando o reagente TRizol – Life Technologies). A eficiência do silenciamento com esiRNAADAM9 (2,5 nM) em função do tempo foi verificada pela análise do transcrito ADAM9 por PCR em tempo real.

2.2.1. Desenho dos Primers de Silenciamento de RNA

Foram utilizados *primers* do domínio desintegrina (#104056) para ligação ao éxon 13 (*Silencer*® Pre-designed siRNA, Ambion). As sequencias dos *primers* foram: senso (5'-rCrCrArGrArGrUrArCrUrGrCrArArUrGrGrUrUrCrUrUrCTC-3') e anti-senso (5'-rGrArGrArArGrArArCrCrArUrUrGrCrArGrUrArCrUrCrUrGrGrArA-3'). O controle negativo (*scrambled*) usado foi Silencer Select Negative Control No. 1 siRNA (Ambion). Também testou-se novo *primer* para o silenciamento da ADAM9, o esiRNA *human* ADAM9 (Sigma-Aldrich, n° cat. EHU020151) e o controle negativo de silenciamento chamado de esiRNA *targeting* EGFP (Sigma-Aldrich, n° cat. EHUEGFP). O esiRNA é uma mistura de siRNA tendo como alvo a mesma sequência do mRNA, sendo assim, esses múltiplos *primers* de siRNA levam a um silenciamento altamente específico e eficaz.

2.2.2. Extração de RNA e Síntese de cDNA

O RNA total foi extraído das células usando o reagente TRIzol (Invitrogen) seguindo as intruções do fabricante. Todas as amostras foram tratadas com DNAse I (*Deoxyribonuclease I, Amplification Grade* – Invitrogen). Após a quantificação em NanoDrop 2000 (Thermo Scientific), um total de 1 µg RNA foi misturado com água livre de RNAse e DNAse para um volume final de 8 µL. Cerca de 0,5 µL de *primer* oligo-DT (0,5 µg/µL, Promega) foi adicionado a essa mistura e incubado a 70°C por 5 minutos, seguido de um resfriamento rápido por 5 minutos. Em seguida, foram adicionados 0,5 µL de *Moloney Monkey Leukemia vírus reverse transcriptase* (200 U/µL - M-MLV, Promega), 2,5 µL de tampão MMLV 5X (Promega), 2,5 µL de dNTP mix (10 nM). A mistura foi incubada por 1 hora a 37°C e, em seguida, utilizada em qPCR.

2.2.3. Desenho dos primers para o RT-qPCR

Os oligonucleotídeos para a análise da expressão gênica da ADAM9 e de outros genes de interesse para a técnica do RT-qPCR foram desenhados utilizando o site *http://www.ncbi.nlm.nih.gov/tools/primer-blast/*. As sequências dos *primers* foram checadas pelo Blast (http://blast.ncbi.nlm.nih.gov/Blast.cgi). Abaixo estão representadas as sequências de *primers*:

Tabela 1. *Primers Forward e Reverse* utilizados.

Gene	*Primer Forward*	*Primer Reverse*	Produto amplificado (pb)
ADAM9	CTTGCTGCGAAGGAAGTACC	AACATCTGGCTGACAGAACTGA	173
ADAM10	ACCTTCAGGAAGCTCTGGAGGAAT	CTGGTGTGCACTCTGTTCCAGAAT	200
ADAM12	AGCCACACCAGGATAGAGAC	CGCCTTGAGTGACACTACAG	105
ADAM15	CAAATATAGGTGGCACTGAGGAG	TAGCAGCAGTTCTCCAAAGTGTG	286
ADAM17	GATCTACAGACTTCAACACAT	AGTGTACTCGCTTTCGTT	150
MMP2	AGGACCGGTTCATTTGGCGG	TGGCTTGGGGTACCCTCGCT	200
MMP9	CGCTACCACCTCGAACTTTG	GCCATTCACGTCGTCCTTAT	196
cMYC	CCTTCTCTCCGTCCTCGGAT	TTCTTGTTCCTCCTCAGAGTCG	128
OSTEOPONTINA (OPN)	CTGACATCCAGTACCCTGATGC	GGCCTTGTATGCACCATTCA	83
COLÁGENO	GCTACTTACGGACTTCGGGG	AGACAGGAGGGACCCATCTC	176

XVII (COL XVII)			
VEGF-A	CACATTGTTGGAAGAAGCAGCCCA	ACTCACACACACACAACCAGGTCT	165
VEGF-C	GCCACGGCTTATGCAAGCAAAGAT	AGTTGAGGTTGGCCTGTTCTCTGT	160
VEGF-D	CGATGTGGTGGCTGTTGCAATGAA	GCTGTTGGCAAGCACTTACAACCT	164
VEFGR1	CGACGTGTGGTCTTACGGAGTA	CTTCCCTCAGGCGACTGC	107
HPRT	TGACACTGGCAAAACAATGCA	GGTCCTTTTCACCAGCAAGCT	97
GAPDH	GATGCTGGTGCTGAGTATGTCG	GTGGTGCAGGATGCATTGCTGA	197

2.2.4. PCR em Tempo Real

A expressão do mRNA dos diferentes genes foi analisada utilizando o Corbett Rotor Gene 3000 (Corbett Research). As reações de RT-qPCR foram padronizadas com volume final de 25 µL e com as proporções apresentadas nos materiais e métodos suplementares 1 e 2.

2.3. Caracterização da expressão de integrinas por citometria de fluxo

A expressão de algumas integrinas na superfície das células HMEC-1, HUVEC (linhagem) e HMVEC-dLy foram analisadas utilizando o citômetro de fluxo FACscalibur ou Accuri C6 (BD Biosciences). As células ($1x10^6$) foram incubadas em gelo com 10 µg/mL de anticorpo primário para diferentes integrinas [β_1, β_4, α_v, α_2, α_4, α_5, α_6, $\alpha_v\beta_5$, e $\alpha_v\beta_3$ (Santa Cruz e BD Biosciences)]. Após 45 minutos, as células foram lavadas 2 vezes com PBS e incubadas por 45 minutos em gelo com 5 µg/mL de anti-IgG marcado com isotiocianato de fluoresceína (FITC) (Santa Cruz - SC-2010). As células foram novamente lavadas com PBS (1X) e analisadas em um citômetro de fluxo. Para a linhagem MDA-MB-231, foi analisada a expressão da ADAM9 utilizado o anticorpo *Mouse ADAM9 Ectodomain Affinity Purified Polyclonal Ab* (1:1000) (R&D Systems - n˚ catálogo AF949) e o anticorpo secundário *Donkey anti-Goat* Alexa Fluor 488 (n° catálago A-11055 – Life Technologies).

2.4. Transmigração Endotelial

As células endoteliais (HUVEC, HMEC-1 e HMVEC-dlyNeo-Der) foram semeadas ($7x10^4$) em insertos com poros de 8 μm (24 poços) (BD Biosciences) recobertos com gelatina 2% e/ou fibronectina (20 μg/mL), para a formação da monocamada. Após 48 h, as células MDA-MB-231 (controle, controle negativo e siADAM9) foram marcadas com *PKH26 Red Fluorescent Cell Linker* (Sigma) seguindo as instruções do fabricante. Após a marcação, as células tumorais foram contadas ($5x10^4$) e semeadas na porção superior dos insertos previamente recobertos pela monocamada em meio DMEM sem FBS e na face inferior foi adicionado meio DMEM com FBS (quimioatraente). Após 16 horas, as células tumorais que permaneceram na face superior da câmera foram removidas e as células que transmigraram foram lavadas com meio de cultura DMEM sem soro e fixadas com formaldeído 3,7%. Um total de 15 campos aleatoriamente foram fotografados (Carl Zeiss GmbH, Jena, German - Objetiva de 20x) e contados com auxílio do programa *Image J*.

2.5. Inibição da Adesão Celular

Para o ensaio de inibição da adesão, colágeno tipo I, colágeno tipo IV, laminina e fibronectina (1-10 μg/100μl/poço) foram imobilizados em placas de 96 poços por 12 horas a 4ºC. Todos os poços foram bloqueados com solução de soroalbumina bovina (solução de BSA 1% solubilizada em tampão de adesão: HEPES 20 mM acrescido de NaCl 150 mM, $MgCl_2$ 5 mM e $MnCl_2$ 0,25 mM, pH 7,4 – 200 μL/poço) por 1 hora. BSA 2% foi adicionada aos poços dos controles negativos. Após o bloqueio, as células HMVEC-dLyAd-Der ($1x10^5$/tubo) foram previamente incubadas a 37°C durante 30 minutos com os anticorpos bloqueadores anti-β_1 (Santa Cruz - SC-13590), anti-β_3 (BD Biosciences- 555753), anti-β_4 (Santa Cruz - SC-13543), anti-α_V (Santa Cruz - SC-9969), anti-α_2 (R&D Systems - MAB1233), anti-α_4 (Santa Cruz - SC-23933), anti-α_5 (Santa Cruz - SC-71419), anti-α_6 (Santa

Cruz - SC-71426), anti-$\alpha_V\beta_5$ (Santa Cruz - SC-71450), anti- $\alpha_V\beta_3$ (Santa Cruz - SC-7312). Para o ensaio de adesão celular as células HMVEC-dLyAd-Der foram plaqueadas sem a incubação com os anticorpos. As células foram transferidas para placas de 96 poços e incubadas por 45 minutos. Os poços foram lavados 3 vezes com meio de cultura sem soro e as células aderidas foram fixadas com etanol 70% por 10 minutos. As células foram coradas com Cristal Violeta 0,5% por 20 minutos e os poços foram lavados com PBS (1X) diversas vezes para retirada do excesso de corante e as células coradas foram solubilizadas em SDS 1% (30 minutos). A leitura da placa foi feita a 540 nm em leitor da absorbância Dynex.

2.6. Adesão Celular Estática e Sob Fluxo

Para o ensaio de adesão estática e sob fluxo as células endoteliais foram previamente semeadas em placas de 24 poços ou 3 cm previamente recobertas com gelatina 2% e/ou fibronectina (20 µg/mL) 48 horas antes do ensaio propriamente dito. No ensaio de adesão sob fluxo as células MDA-MB-231 foram marcadas com *Cell Tracker Green CFSE* (Life Technologies) seguindo as instruções do fabricante. As células misturadas ao meio de cultura DMEM sem soro ($1x10^6$ células em 4 mL) foram perfundidas com o auxílio de uma bomba peristáltica sob condições dinâmicas de fluxo com uma taxa de cisalhamento de 5 *dynes*/cm^2 em uma câmara de perfusão durante 10 minutos.

Para o ensaio de adesão estática as células endoteliais foram semeadas em placas de 24 poços ($1x10^5$ células/mL; $1,1x10^5$ células/mL e $1,2x10^5$ células/mL de HUVEC, HMEC-1 e HMVEC-dlyAd-Der, respectivamente) e mantidas até atingirem a confluência. Os poços foram lavados com meio sem FBS e adicionado TNF-α (2,5 ng/mL; 5,0 ng/mL e 10 ng/mL, 1mL/poço) diluído em meio sem FBS e suplementado com 0,1% BSA, por 5 horas. Após ativação das células endoteliais, os poços foram lavados 2 vezes com meio sem FBS e foram adicionados à eles as células tumorais MDA-MB-231 marcadas com CFSE ($3x10^4$

células/poço em 500 µL/poço) diluídas em seu próprio meio de cultura sem FBS suplementado com 0,1% BSA, por 1 hora. Após a perfusão e adesão, as células tumorais aderidas às células endoteliais foram lavadas com meio de cultura DMEM sem FBS e fixadas com formaldeído 3,7%. Foi usado o DAPI para marcação dos núcleos celulares. Foram fotografados 15 campos aleatoriamente (Carl Zeiss GmbH, Jena, German- Objetiva de 20x) e as células foram contadas com auxílio do programa *Image J*.

2.7. Análise dos Resultados

Os ensaios foram analisados quanto a sua significância estatística utilizando o programa de estatística GraphPad Prism 5. Cada experimento foi repetido no mínimo três vezes em triplicata. Todos os valores apresentaram distribuição normal, por isso foi utilizada a análise de variância ANOVA one-way e os testes Tukey ou Dunnett para múltiplas comparações. Em todos os cálculos foram fixados o nível crítico 5% ($p \leq 0,05$), ou seja, *$p<0,05$, **$p<0,01$ e ***$p<0,001$ foram utilizados como critério de significância.

3. RESULTADOS

3.1. Silenciamento da ADAM9 detectado pelo nível de mRNA e proteína

Após o silenciamento da ADAM9 sua expressão foi reduzida nas células MDA-MB-231 tanto em nível proteico quanto ao nível de mRNA (Figura 1A e C, respectivamente) quando comparado com as células controles (sem tratamento e tratadas com esiRNAEGFP = Controle Negativo).

O esiRNA são endoribonucleases preparadas de siRNAs que possuem o mesmo alvo, em nosso estudo, a ADAM9, e desta forma, levando a um silenciamento altamente eficaz e específico, porém transiente. O silenciamento da ADAM9 ocorreu do 3°

ao 5° dia, entretanto, no 7° dia de silenciamento (P7) a expressão aumentou de forma exponencial atingindo valores semelhantes aos obtidos pelas células controle. Sendo assim, conclui-se que o silenciamento perdeu sua eficiência após o 7º dia (Figura 1B).

3.2. Silenciamento da ADAM9 afeta a expressão gênica da ADAM15 sem afetar os transcritos da ADAM10, ADAM12, ADAM17

A expressão gênica da ADAM9 foi reduzida nas células MDA-MB-231 tratadas com o *primer* de siRNA (siADAM9D) (Figura 2A) comprovando assim a eficiência da técnica, além disso, o silenciamento da ADAM9 não foi capaz de afetar a expressão gênica da ADAM10, ADAM12, ADAM17 (Figura 2B, C e D, respectivamente), porém reduziu de maneira significante a expressão da ADAM15 (Figura 2E) em aproximadamente 33,3%.

3.3. Silenciamento da ADAM9 afeta a expressão gênica da MMP2, mas não afeta a expressão de c-MYC, OPN, MMP9, VEGF-A, VEGF-C e COL XVII

Observou-se que o siADAM9 nas células MDA-MB-231 não afetou o nível de expressão dos diferentes genes analisados, entre eles, c-MYC, OPN, MMP9, VEGF-A, VEGF-C e COL XVII (Figura 3A, B, C, E, F e G, respectivamente), entretanto, houve um aumento significativo de aproximadamente 90% na expressão da MMP2 nas células siADAM9D (Figura 3D).

3.4. Caracterização da expressão gênica nas células HMVEC-dLyAd-Der por RT-qPCR

Para análise da expressão de diferentes genes nas células HMVEC-dLyAd-Der foi utilizada a quantificação absoluta de transcritos descrita por Allen *et al.* [26]. Na figura 4 estão representados os valores de expressão de cada gene analisado em ng/µL. Os níveis de expressão de mRNA de ADAMs, c-MYC, MMP2, VEGF-A, VEGF-C, VEGF-D, e

VEGFR1 foram normalizados pelos níveis de mRNA para HPRT e GAPDH, entretanto na figura estão apresentados apenas os valores obtidos para GAPDH, pois esse gene foi melhor relacionado com a célula testada. Nota-se que praticamente todos os genes analisados apresentaram concentrações em ng/µL similares de 0,05 – 0,07 ng/µL, entretanto, apenas a MMP2 apresentou uma expressão maior nesta linhagem de aproximadamente 0,1 ng/µL, ou seja, em torno de 40% maior que os demais genes analisados.

3.5. Caracterização da expressão de integrinas nas células MDA-MB-231, HMEC-1, HUVEC e HMVEC-dLyAd-Der por citometria de fluxo

A expressão de algumas integrinas foi analisada por citometria de fluxo nas células utilizadas neste trabalho. Nossos resultados mostraram que as células apresentaram diferentes perfis de integrinas (Figura 5), ou seja, as células MDA-MB-231 expressam mais de 80% de cada subunidade de integrinas α_5, α_6, α_V e β_1. As células HMEC-1 apresentam uma alta expressão das integrinas α_5, α_V e β_1. As células HMVEC-dLyAd-Der expressam mais de 80% os receptores α_5, α_6, α_V, β_1, β_3, β_4 e $\alpha_V\beta_5$. As células HUVEC apresentam um perfil de expressão semelhante ao da HMVEC-dLyAd-Der, entrentanto essas células apresentam uma expressão mais baixa da subunidade β_3 (25%; ++) (Figuras Suplementares 1, 2 e 3).

3.6. Adesão das células HMVEC-dLyAd-Der a diferentes componentes da MEC

Na figura 6 estão representadas imagens das monocamadas das células HMVEC-dLyAd-Der fotografadas na passagem 2. Em (A) a monocamanda das células HMVEC-dLyAd-Der foi fotografada com aumento de 4X e em (B) com aumento de 10X. Essas células foram utilizadas somente até a passagem 5 (seguindo o manual de instruções da empresa Lonza).

As células HMVEC-dLyAd-Der foram adicionadas sobre diversos componentes da MEC (1-10 µg/poço), entre eles, colágeno tipo I (Col I), colágeno tipo IV (Col IV), Fibronectina (FN) e Laminina (LA). Todas as proteínas da MEC testadas promoveram a adesão das células linfáticas significativamente quando comparadas com o controle negativo (BSA 2%) (Figura 7).

3.7. Inibição da adesão das células HMVEC-dLyAd-Der a diferentes componentes da MEC

Nos ensaios de inibição da adesão as células HMVEC-dLyAd-Der foram primeiramente incubadas com diferentes anticorpos anti-integrinas (α_2, α_4, α_5, α_6, β_1, β_3, β_4, $\alpha_V\beta_3$ e $\alpha_V\beta_5$), anti-ADAM9 e anti-IgG. Após a incubação, essas células foram adicionadas sobre componentes da MEC imobilizados em placas de 96 poços, entre eles, LA, FN e Col. IV (1-10 µg/poço). Observa-se que as células HMVEC-dLyAd-Der não foram capazes de se ligarem à LA apenas quando incubadas com o anticorpo anti-β_1 (Figura 8A). Quando utilizado a FN como proteína da MEC imobilizada, as células HMVEC-dLyAd-Der não foram capazes de se ligar a esta proteína significativamente apenas quando incubada com o anticorpo anti-$\alpha_V\beta_5$ (Figura 8B). As HMVEC-dLyAd-Der incubadas com o anticorpo anti-β_1 não foram capazes de se ligar significativamente ao Col IV (Figura 8C), evento também observado quando usado a LA como proteína imobilizada.

3.8. Efeito da pré-estimulação das células endoteliais com TNF-α na adesão das células MDA-MB-231

O efeito da pré-estimulação das células endoteliais HUVEC, HMEC-1 e HMVEC-dLyAd-Der com diferentes concentrações de TNF-α [0 (não tratada); 2,5; 5,0 e 10 ng/mL] foi testado na adesão das células de tumor de mama MDA-MB-231. A pré-

estimulação das células endoteliais com TNF-α por 5 horas não causou alterações na adesão das MDA-MB-231 à monocamada de HUVEC (9A) e HMEC-1 (9B), entretanto, houve um aumento significativo quando comparado com as células HMVEC-dLyAd-Der (9C) não estimuladas com as tratadas com 10 ng/mL de TNF-α.

3.9. Efeito do silenciamento da ADAM9 na adesão das células de tumor de mama MDA-MB-231 em condições dinâmicas de fluxo

O efeito do siADAM9 nas células MDA-MB-231 foi testado em condições dinâmicas de fluxo na tentativa de simular as etapas necessárias para a cascata metastática que ocorre *in vivo*. As células MDA-MB-231 foram silenciadas utilizando o *primer* de silenciamento esiRNAADAM9 e esiRNAEGFP foi utilizado como controle negativo.

As células tumorais silenciadas ou não para a proteína ADAM9 foram perfundidas com o auxílio de uma bomba peristáltica sob condições dinâmicas de fluxo com uma taxa de cisalhamento de 5 *dynes*/cm^2 e durante 10 minutos. Os resultados sugerem que o siADAM9 não afetou a adesão das células tumorais MDA-MB-231 à células endoteliais HUVEC (Figura 10A), HMEC-1 (Figura 10B) e HMVEC-dLyNeo-Der (Figura 10C), entretanto, nota-se que nas últimas células testadas há uma tendência em diminuição da adesão à MDA-MB-231 silenciadas para ADAM9, porém não significativa.

3.10. Efeito do silenciamento da ADAM9 na transmigração das células de tumor de mama MDA-MB-231 em diferentes células endoteliais: HMEC-1, HUVEC e HMVEC-dLyNeo-Der

O siADAM9 nas células tumorais MDA-MB-231 inibiu significativamente a transmigração dessas células às endoteliais HUVEC (Figura 11A), HMEC-1 (Figura 11B) e HMVEC-dLyNeo-Der (Figura 11C). Nota-se que essa inibição foi mais acentuada quando

utilizadas as células HUVEC como monocamada, ou seja, cerca de 50 % quando comparada com as células controle e controle negativo. Quando utilizadas as células HMEC-1 e HMVEC-dLy Neo a redução da taxa de transmigração das células tumorais siADAM9 foi de 40% e 32%, respectivamente.

4. DISCUSSÃO

A principal causa de morte de pacientes com câncer é devido ao desprendimento das células tumorais do foco primário para órgãos distantes [27-28]. A disseminação metastática é dependente da característica do microambiente tumoral [29]. Interações complexas entre células do tumor e o micorambiente tumoral medeiam os principais passos da cascata metastática que envolve: EMT e passagem através da membrana basal; disseminação das células da massa tumoral para fora do sítio primário; invasão do tecido vizinho; entrada nos vasos linfáticos ou sanguíneos, onde terão que sobreviver ao ataque do sistema imune; saída dos vasos e extravasamento para um novo sítio, onde as células terão que se estabelecerem no sítio secundário [9, 30-31].

Parâmetros da disseminação tumoral e doenças agressivas foram correlacionados com os níveis de expressão de algumas ADAMs. Resultados obtidos utilizando modelos animais de metástase demonstraram que as ADAMs, incluindo a ADAM9, ADAM12, ADAM15 e ADAM17, estão envolvidas na formação e progressão tumoral. Algumas evidências implicam essas ADAMs na malignidade tumoral, entre elas, a inibição da expressão da ADAM17 diminui o crescimento de células de câncer da mama (T4-2) *in vitro* e reverte sua aparência morfológica para células normais. A deficiência de algumas ADAMs, tais como, ADAM9, ADAM15 e ADAM17, resulta na diminuição do crescimento de células de tumor em modelos de metástase em ratos [18]. Além disso, estudo recente em

nosso laboratório demonstrou que o silenciamento da ADAM9 inibiu a invasão em matrigel das células tumorais MDA-MB-231 (altamente metastática) cerca de 70% quando comparado com o controle de silenciamento (*scrambled*) [23].

Para comprovar a eficiência do silenciamento da glicoproteína ADAM9 nas células MDA-MB-231 foram realizadas análises por RT-qPCR, *Western Blotting* e citometria de fluxo (dados não mostrados), utilizando o *primer* esiRNADAM9. Notamos que nas amostras silenciadas a expressão gênica e protéica da ADAM9 foi reduzida drasticamente quando comparada com os dois controles: meio e negativo. Além disso, verificamos com a curva de silenciameno que o tempo eficiência deste *primer* é do 3° ao 6° dia, desta forma, todos experiementos foram realizados neste período.

Em seguida, foi analisada a expressão de algumas ADAMs nas células de tumor de mama MDA-MB-231 e nas células endoteliais HMVEC-dLyAd-Der, pois não foram encontrados dados da expressão de ADAMs nestas células linfáticas. Nas células MDA-MB-231 o silenciamento da ADAM9 foi verificado em relação à sua influência na expressão gênica de outras ADAMs também envolvidas na progressão tumoral, entre elas, ADAM10, -12, -15 e -17. Os resultados obtidos mostram que a ADAM10, -12 e -17 não tiveram alteração na expressão gênica quando a ADAM9 foi silenciada, entretanto a expressão da ADAM15 sofreu uma redução significativa de aproximadamente 40%.

MAUCH *et al.* [32] observaram um aumento na expressão da ADAM10 e -17 durante o reparo da pele em camundongos *knockout* para a ADAM9. Os resultados de MOSS *et al.* [33] sugerem que a inibição da ADAM9 controla a atividade da ADAM10 transmembrana, pois a inibição da ADAM9 levou a ativação da ADAM10 em células BT474. Desta forma, os resultados obtidos neste trabalho diferem dos encontrados por MAUCH e MOSS [32-33], porém as células analisadas são diferentes nos três trabalhos podendo este ser o diferencial para os resultados divergentes.

cMYC é um proto oncogene que pode promover a tumorigênese em vasta gama de tecidos e a sua expressão aumentada inibe significativamente a migração e a capacidade de invasão de células de câncer de mama MDA-MB-231, *in vitro* [34]. MMP-9 é uma metalopeptidase de matriz que pode estar envolvida na invasão de células tumorais, além disso, estudos relacionam o aumento dos níveis de MMP9 e MMP2 com o potencial de invasão neoplásico geral, aumento da angiogênese e metástase tumoral [35].

Neste trabalho também testamos se o silenciamento da ADAM9 poderia afetar a expressão do cMYC, MMP-2 e MMP-9. Os resultados mostram que o siADAM9 não afetou a expressão do cMYC e MMP9, entretanto houve um aumento de aproximadamente 90% na expressão da MMP-2 nas células MDA-MB-231 silenciadas. A MMP-2 é uma gelatinase A que pode ser encontrada numa variedade de células normais, bem como, em algumas células que sofreram transformações, incluindo fibroblastos, queratinócitos, células endoteliais e condrócitos [35]. Segundo JEZIERSKA & MOTYL [36] a MMP-2 degrada a matriz extracelular levando à invasão e metástase de células de câncer de mama, entre elas, a linhagem MDA-MB-231. Além disso, a taxa de ativação de pró-MMP-2 para MMP-2 ativa é usado como um indicador de metástase tumoral e diminuição da sobrevida do paciente [36-37].

Desta forma, o resultado obtido neste trabalho com siADAM9 afetando positivamente a expressão da MMP-2 mostrou a estratégia de silenciamento para ADAM9 desfavorável para o tratamento do câncer de mama, entretando, observando os resultados obtidos por MICOCCI *et al.* [23], comprovou-se que o siADAM9 inibiu em aproximadamente 70% a invasão das célula tumorais de mama MDA-MB-231 em matrigel. Dessa forma, sugere-se que o aumento da expressão de MMP-2 sozinha não é suficiente para desencadear invasão. Observamos também que o siADAM9 não afetou a expressão gênica da Osteopontina, Colágeno XVII, VEGF-A e VEGF-C.

Nas células HMVEC-dLyAd-Der os níveis de expressão de mRNA para as ADAMs, cMYC, VEGF-A, VEGF-C e VEGFR1 em ng/µL foram praticamente semelhantes, ou seja, aproximadamente 0,05 - 0,07 ng/µL. Já o VEGF-D apresentou expressão praticamente nula e a expressão da MMP-2 foi a maior, ou seja, aproximadamente 0,1 ng/µL. Em relação à expressão do VEGF nessas células, PRANGSAENGTONG e colaboradores encontraram uma expressão maior de VEGF-C quando comparado com o VEGF-A e –D [38], porém, em nossos experimentos encontramos uma maior expressão de VEGF-A quando comparado com o VEGF-C, e praticamente nula do VEGF-D.

Em condições normais, o cMYC está envolvido em diversos processos celulares, entre eles, crescimento celular e proliferação. Além disso, é um gene também expresso em células endoteliais, sendo assim, o resultado obtido vai ao encontro dos resultados encontrados nos artigos pesquisados [34; 39-40]. Nosso estudo é pioneiro na avaliação da expressão de ADAMs nas células HMVEC-dLyAd-Der.

As células endoteliais que revestem as paredes internas dos vasos estão continuamente expostas a estímulos mecânicos, tais como, estresse de cisalhamento e tensão de estiramento gerado pelo fluxo sanguíneo e pressão arterial, respectivamente. Tal estresse desempenha um papel importante na regulação de vários aspectos da função das células endoteliais, incluindo proliferação, mudanças na motilidade e migração celular, bem como, mudanças na morfologia das células [41]. Além disso, o estresse de cisalhamento gerado pelo fluxo sanguíneo nas paredes internas dos vasos afeta as características dos receptores de adesão celular [42-43].

O processo metastático é compreendido por etapas nas quais a adesão celular é de essencial importância, pois as células cancerígenas interagem com as células adjacentes, entre elas, as endoteliais, e com componentes da membrana extracelular e basal para desencadear sinalizações mediadas por integrinas e assim disseminar o tumor [44-45]. Para

verificar a necessidade de pré-estimulação com TNF-α nas células endoteliais sanguíneas e linfáticas realizou-se ensaios de adesão estática. Os nossos resultados mostraram que as células HMVEC-dLyAd ou Neo-Der requerem pré-estimulação com TNF-α (10 ng/mL por 5 horas), diferentemente dos resultados obtidos com as células HUVEC e HMEC-1

Investigando a participação da ADAM9 na adesão das células tumorais de mama às endoteliais, observamos que o siADAM9 não inibiu a adesão dessas células tumorais em condições dinâmicas de fluxo às endoteliais vasculares HUVEC e HMEC-1, bem como, as linfáticas HMVEC-dLyNeo-Der. Esse resultado corrobora com o obtido por nosso grupo em trabalho prévio, no qual, observamos que o siADAM9 não afetou a adesão estática das células MDA-MB-231 a diferentes componentes da MEC, entre eles, colágeno tipo I, fibronectina e laminina [23]. Sendo assim, apesar do envolvimento dessa proteína na adesão de diversos tipos de câncer, entre eles, carcinoma de pulmão e melanoma [46-47-48], a ADAM9 parece não participar da adesão das células tumorais de mama às endoteliais sanguíneas e linfáticas utilizadas neste trabalho, podendo ser esta a função de outra classe de receptores de adesão presentes nas superfícies das células MDA-MB-231.

Durante a disseminação metastática as células tumorais ficam expostas a forças mecânicas que podem afetar a sua sobrevivência. Para povoar um novo sítio essas células precisam interagir com as paredes dos vasos e atravessá-los, sendo que nesta fase a adesão entre as células é de suma importância, e são as integrinas os principais mediadores deste processo [27; 49]. ORR *et al.* [50] observaram que o fluxo é capaz de ativar nas células endoteliais aórtica bovina as integrinas $\alpha_V\beta_3$, $\alpha_2\beta_1$ e $\alpha_5\beta_1$. Além disso, GOMES *et al.* [27] mostraram que ocorre uma cooperação entre as integrinas $\alpha_{IIb}\beta_3$ plaquetária e $\alpha_V\beta_3$ tumoral para promover a adesão a matriz subendotelial em condições dinânicas de fluxo, entretanto, as células MDA-MB-231 não expressam a integrina $\alpha_{IIb}\beta_3$, sendo assim, essa função principal seria dada a integrina $\alpha_V\beta_3$, porém, a inibição da integrina $\alpha_V\beta_3$ não foi suficiente para abolir a

adesão da célula MDA-MB-231 à MEC, ou seja, ocorreu uma redução de somente 45%. Desta forma, os autores sugerem a participação de outros receptores no processo de adesão sob fluxo, tais como, $\alpha_2\beta_1$ e $\alpha_5\beta_1$. Segundo Gomes *et al.* [49] a expressão de integrinas está relacionada com a progressão tumoral, e, em especial a $\alpha_V\beta_3$ que é altamente expressa nas células MDA-MB-231. Esses autores observaram que a modificação aguda no estresse de cisalhamento induz a liberação de trombospondina-1 (TSP-1) e fator de Willebrand (vWF) endotelial na MEC contribuindo assim para o aumento da adesão da células MDA-MB-231 à MEC, principalmente via integrina $\alpha_V\beta_3$ na célula tumoral.

Os nossos resultados sugerem que possivelmente essas integrinas estejam sendo ativadas nas três linhagens de células endoteliais e/ou células tumorais durante o processo de fluxo, reforçando assim a adesão entre elas, e desfavorecendo a função da ADAM9 como molécula adesiva.

A primeira etapa do processo de extravasamento na progressão metastática é similar ao observado durante a diapedese de leucócitos: células de câncer começam rolando sobre a superfície do endotélio de maneira dependente de selectina e então se aderem firmemente através de integrinas. Esta primeira etapa é seguida pela transmigração endotelial por meio da rota transcelular ou paracelular [44]. Conhecendo a importância desta etapa no processo de metástase, procuramos testar também se o siADAM9 poderia influenciar a transmigração de células de tumor de mama por entre as células endoteliais.

Os resultados obtidos sugerem que o siADAM9 pode modular a transmigração das células tumorais MDA-MB-231 à células endoteliais HUVEC, HMEC-1 e HMVEC-dLy, ou seja, a transmigração das células MDA-MB-231 siADAM9 diminuiu significativamente em 50%, 40% e 32%, respectivamente. Além disso, essa interação entre a ADAM9 das células tumorais e ligantes das células endoteliais parece ser mais efetiva nas células sanguíneas em relação às linfáticas. COMINETTI *et al.* [51] mostraram que a ADAM9D

recombinante se liga às integrinas β_1, α_3, $\alpha_V\beta_3$, $\alpha_V\beta_5$ e α_2 em diferentes linhagens celulares, e pela primeira vez, mostrou-se a interação do domínio desintegrina da ADAM9 humana com a integrina $\alpha_V\beta_3$. Entretanto, SAFUAN *et al.* [8] demonstraram que as células MDA-MB-231 apresentam maior afinidade pelas células endoteliais sanguíneas em relação às células linfáticas.

Em síntese, nós demonstramos que a ADAM9 parece não participar da adesão estática e sob fluxo das células tumorais MDA-MB-231 às endoteliais sanguíneas (HUVEC e HMEC-1) e linfáticas (HMVEC-dLy), entretanto, parece ter um papel importante na transmigração dessas células às endoteliais. Sendo a invasão uma etapa fundamental para a ocorrência de metástase, nossos resultados apontam o silenciamento da ADAM9 como estratégia para minimizar o processo de extravasamento na progressão metastática.

Agradecimentos

Este trabalho foi financiado pela FAPESP (Fundação de Amparo à Pesquisa do Estado de São Paulo, Brasil), CNPQ (Conselho Nacional de Desenvolvimento Científico e Tecnológico) e CAPES (Coordenação de Aperfeiçoamento de Pessoal de Nível Superior).

6. REFERÊNCIAS

[1] http://www2.inca.gov.br/
[2] http://www.who.int/en/
[3] D. Hanahan and R.A Weinberg, The hallmarks of cancer, Cell 100 (2000) 57-70.
[4] G.P. Gupta and J. Massague, Cancer metastasis: building a framework, Cell 127 (2006) 679-695.
[5] Y. Huang and L-P. Li, Progress of cancer research on astrocyte elevated gene-1/Metadherin (Review), Oncol Lett 8 (2014) 493-501.
[6] D. Hanahan and R.A Weinberg, Hallmarks of cancer: the next generation, Cell 144 (2011) 646-674.
[7] R.A. Mohammed, S.G. Martin, M.S. Gill, A.R. Green, E.C. Paish, I.O. Ellis, Improved methods of detection of lymphovascular invasion demonstrate that it is the predominant method of vascular invasion in breast cancer and has important clinical consequences, Am J Surg Pathol, 31 (2007) 1825-1833.

[8] S. Safuan, S.J. Storr, P.M. Patel, S.G. Martin, A comparative study of adhesion of melanoma and breast cancer cells to blood and lymphatic endothelium, Lymphat Res Biol, 10 (2012) 173-181.
[9] T.R. Geiger and D.S. Peeper, Metastasis mechanisms. Biochim. Biophys. Acta, 1796 (2009) 293-308.
[10] M. Bacac and I. Stamenkovic, Metastic Cancer Cell, Annu. Rev. Pathol. Mech. Dis., 3 (2008) 221-247.
[11] S.J. Storr, S. Safuan, A. Mitra, F. Elliott, C. Walker, M.J. Vasko, B. Ho, M. Cook, R.A. Mohammed, P.M. Patel, I.O. Ellis, J.A. Newton-Bishop, S.G. Martin, Objective assessment of blood and lymphatic vessel invasion and association with acrophage infiltration in cutaneous melanoma, Mod. Pathol., 25 (2012) 493-504.
[12] J.S. Wong, A. O'Neill, A. Recht, S.J. Schnitt, J.L. Connolly, B. Silver, J.R. Harris. The relationship between lymphatic vessell invasion, tumor size, and pathologic nodal status: can we predict who can avoid a third field in the absence of axillary dissection? Int J Radiat Oncol. Biol. Phys. 48 (2000).
[13] S.F. Schoppmann, R. Horvat, P. Birner, P, Lymphatic vessels and lymphangiogenesis in female cancer: mechanisms, clinical impact and possible implications for anti-lymphangiogenic therapies, Oncol. Rep. 9 (2002) 455–460.
[14] S. Mochizuki, Y. Okada, ADAMs in cancer cell proliferation and progression, Cancer Sci. (2007) 98 621-628.
[15] T.H. Lee, H.K. Avraham, S. Jiang, S. Avraham, Vascular Endothelial Growth Factor Modulates the Transendothelial Migration of MDA-MB-231 Breast Cancer Cells through Regulation of Brain Microvascular Endothelial Cell Permeability, J. Biol. Chem. (2003) 278 5277-5284.
[16] P. Zigrino, J. Steiger, J.W. Fox, S. Loffek, A. Schild, R. Nischt, C. Mauch, Role of ADAM-9 Disintegrin-Cysteine-rich Domains in Human Keratinocyte Migration, The Journal of Biological Chemistry (2007) 282 30785–30793.
[17] N. Rocks, G. Paulissen, M. El Hour, F. Quesada, C. Crahay, M. Gueders, J.M. A. Noel, D. Cataldo, Emerging roles of ADAM and ADAMTS metalloproteinases in cancer, Biochimie (2008) 90 369-379.
[18] M.J. Duffy, E. Mckiernan, N. O'Donovan, P.M. Mcgowan, Role of ADAMs in cancer formation and progression, Clin Cancer Res. (2009) 15: 1140–1144.
[19] M.J. Duffy, M. Mullooly, N. O'Donovan, S. Sukor, J. Crown, A. Pierce, P.M. Mcgowan, The ADAMs family of proteases: new biomarkers and therapeutic targets for cancer? Clin Proteomics (2011) 8 1-13.
[20] A. Zubel, C. Flechtenmacher, L. Edler, A. Alonso, Expression of ADAM9 in CIN3 lesions and squamous cell carcinomas of the cervix, Gynecologic Oncology (2009).
[21] C.M. Liu, C.L. Hsieh, Y.C. He, S.J. Lo, J.A. Liang, T.F. Hsieh, S. Josson, L.W. Chung, M.C. Hung, S.Y. Sung. In vivo targeting of ADAM9 gene expression using lentivirus-delivered shRNA suppresses prostate cancer growth by regulating REG4 dependent cell cycle progression, PLoS One. 8 (2013).
[22] Q. Xu, X. Liu, Y. Cai, Y. Yu, W. Chen, RNAi-mediated ADAM9 gene silencing inhibits metastasis of adenoid cystic carcinoma cells, Tumour Biol. (2010) 31 217-224.
[23] K.C. Micocci, A.C. Martin, C.D. Montenegro, A.C. Durante, N. Pouliot, M.R. Cominetti, H.S. Selistre-de-Araujo, ADAM9 silencing inhibits breast tumor cell invasion in vitro. Biochimie (2013).
[24] L. Peduto, V.E. Reuter, D.R. Shaffer, H.I. Scher, C.P. Blobel, Critical function for ADAM9 in mouse prostate cancer, Cancer Res. 65 (2005) 9312-9319.
[25] J.L. Fry, A. Toker, Secreted and membrane-bound isoforms of protease ADAM9 have opposing effects on breast cancer cell migration, Cancer Res. 70 (2010) 8187-8198.

[26] D.L. Allen, A.S. Cleary, K.J. Speaker, S.F. Jlindsay, J. Uyenishi, J.M. Reed, M.C. Madden, R.S. Mehan, Myostatin, activin receptorIIb, and follistatin-like-3 gene expression are altered in adipose tissue and skeletal muscle of obese mice. Am J Physiol Endocrinol Metab, 294 (2008) 918-927.
[27] N. Gomes, J. Vassy, C. Lebos, B. Arbeille, C. Legrand, F. Fauvel-Lafeve, Breast adenocarcinoma cell adhesion to the vascular subendothelium in whole blood and under flow conditions: effects of alphavbeta3 and alphaIIbbeta3 antagonists, Clin. Exp. Metastasis, 21 (2004) 553-561.
[28] C. Mongaret, J. Alexandre, A. Thomas-Schoemann, E. Bermudez, C. Chéreau, C. Nicco, F. Goldwasser, B. Weill, F. Batteux, F. Lemare, Tumor invasion induced by oxidative stress is dependent on membrane ADAM 9 protein and its secreted form, Int. J. Cancer., 129 (2010) 791-798.
[29] J.A. Joyce, AND J.W. Pollard, Microenvironmental regulation of metastasis, 9 (2012), 239–252.
[30] C.L. Chaffer, R.A. Weinberg, A perspective on cancer cell metastasis, Science, 331 (2011) 1559-1564.
[31] C.F. Montenegro, C.L. Salla-Pontes, J.U. Ribeiro, A.Z. Machado, R.F. Ramos, C.C. Figueiredo, V. Morandi, H.S. Selistre-de-Araujo, Blocking αvβ3 integrin by a recombinant RGD disintegrin impairs VEGF signaling in endothelial cells, Biochimie, 94 (2012) 1812-1820.
[32] C. Mauch, J. Zamek, A.N. Abety, G. Grimberg, J.W. Fox, P. Zigrino, Accelerated wound repair in ADAM-9 knockout animals, J Invest Dermatol, 130 (2010) 2120-2130.
[33] M.L. Moss, G. Powell, M.A. Miller, L. Edwards, B. Qi, Q.X. Sang, B. De Strooper, I. Tesseur, S.F. Lichtenthaler, M. Taverna, J.L. Zhong, C. Dingwall, T. Ferdous, U. Schlomann, P. Zhou, L.G. Griffith, D.A. Lauffenburger, R. Petrovich, J.W. Bartsch, ADAM9 inhibition increases membrane activity of ADAM10 and controls α-secretase processing of amyloid precursor protein, J Biol Chem., 286 (2011) 40443-40451.
[34] C.Y. Lin, J. Lovén, P.B. Rahl, R.M. Paranal, C.B. Burge, J.E. Bradner, T.I. Lee, R.A. YOUNG, Transcriptional amplification in tumor cells with elevated c-Myc, Cell, 151 (2012) 56-67.
[35] A.B.P. Carpena, A.A.M. Francisco, R.R. Bonamigo, As metaloproteinases-2 e -9 da matriz e o carcinoma espinocelular: uma análise da literatura, Med. Cutan. Iber. Lat. Am., 36 (2008) 285-290.
[36] A. Jezierska, T. Motyl, Matrix Metalloproteinase-2 involvement in breast cancer progression: A mini-review, Med. Sci. Monit., 15 (2009) 32-40.
[37] M.R. Roh, Z. Zheng, H.S. Kim, J.E. Kwon, H.-C Jeung, S.Y. Rha, K.Y. Chung, Differential expression patterns of MMPs and their role in the invasion of epithelial premalignant tumors and invasive cutaneous squamous cell carcinoma, Experimental and molecular pathology, 92 (2012) 236-242.
[38] O. Prangsaengtong, J.Y. Park, A. Inujima, Y. Igarashi, N. Shibahara, K. Koizumi, Enhancement of Lymphangiogenesis In Vitro via the Regulations of HIF-1α Expression and Nuclear Translocation by Deoxyshikonin. Evid Based Complement Alternat Med, (2013).
[39] C.A. Thibodeaux, X. Liu, G.L. Disbrow, Y. Zhang, J.D. Rone, B.R. Haddad, R. Schlegel, Immortalization and transformation of human mammary epithelial cells by a tumor-derived Myc mutant, Breast Cancer Res Treat, 116 (2009) 281-294.
[40] C.E. Kan, R. Cipriano, M.W.V. Jackson, c-MYC functions as Molecular switch to alter the response of human mammary epithelial cells to oncostatin M, Cancer Res, 71 (2011) 6930-6939.
[41] K.I. Mantilidewi, Y. Murata, M. Mori, C. Otsubo,T. Kotani, S. Kusakari, H. Ohnishi, T. Matozaki, Shear stress-induced redistribution of vascular endothelial-protein-tyrosine

phosphatase (VE-PTP) in endothelial cells and its role in cell elongation. J Biol Chem. 289 (2014) 645164.
[42] J. Pilch, R. Habermann, B. Felding-Habermann, Unique ability of integrin alpha(v)beta 3 to support tumor cell arrest under dynamic flow conditions, J Biol Chem, 277 (2002) 21930-21938.
[43] R.S. Dua, G.P. Gui, C.M. Isacke, Endothelial adhesion molecules in breast cancer invasion into the vascular and lymphatic systems, Eur J Surg Oncol., 31 (2005) 824-832
[44] G.Y. Perret, M. Crépin, New pharmacological strategies against metastatic spread. Fundam Clin Pharmacol, 22 (2008) 465-492.
[45] SLEEMAN, J. P. The metastatic niche and stromal progression. Cancer Metastasis Rev., 2012.
[46] A. Mazzoca, R. Coppari, R. De Franco, J-Y. Cho, T.A. Libermann, M. Pinzani, A. TOKER, A secreted form of ADAM 9 promotes carcinoma invasion through tumor-stromal interactions, Cancer Res., 65 (2005) 4728-4738.
[47] Y. Shintani, S. Higashiyama, M. Ohta, H. Hirabayashi, S. Yamamoto, T. Yoshimasu, H. Matsuda, N. Matsuura, Overexpression of ADAM9 in Non-Small Cell Lung Cancer Correlates with Brain Metastasis. Cancer Research, 64 (2004) 4190–4196.
[48] P. Zigrino, R. Nischt, C. Mauch, The disintegrin-like and cysteine-rich domains of ADAM-9 mediate interactions between melanoma cells and fibroblasts, J Biol Chem., 286 (2011) 6801-6807.
[49] N. Gomes, C. Legrand, F. Fauvel-Lafeve, Shear stress induced release of von Willebrand factor and thrombospondin-1 in HUVEC extracellular matrix enhances breast tumour cell adhesion, Clin Exp Metastasis, 22 (2005) 215-223.
[50] A.W. Orr, M.H. Ginsberg, S.J Shattil, H. Deckmyn, M.A. Schwartz, Matrix-specific suppression of integrin activation in shear stress signaling, Mol Biol Cell, 17 (2006) 4686-4697.
[51] M.R. Cominetti, A.C. Martin, J.U. Ribeiro, I. Djaafri, F. Fauvel-Lafève, M. Crépin, H.S. Selistre-de-Araujo, Inhibition of platelets and tumor cell adhesion by the disintegrin domain of human ADAM9 to collagen I under dynamic flow conditions. Biochimie, 91 (2009) 1045-1052.

Figura 1

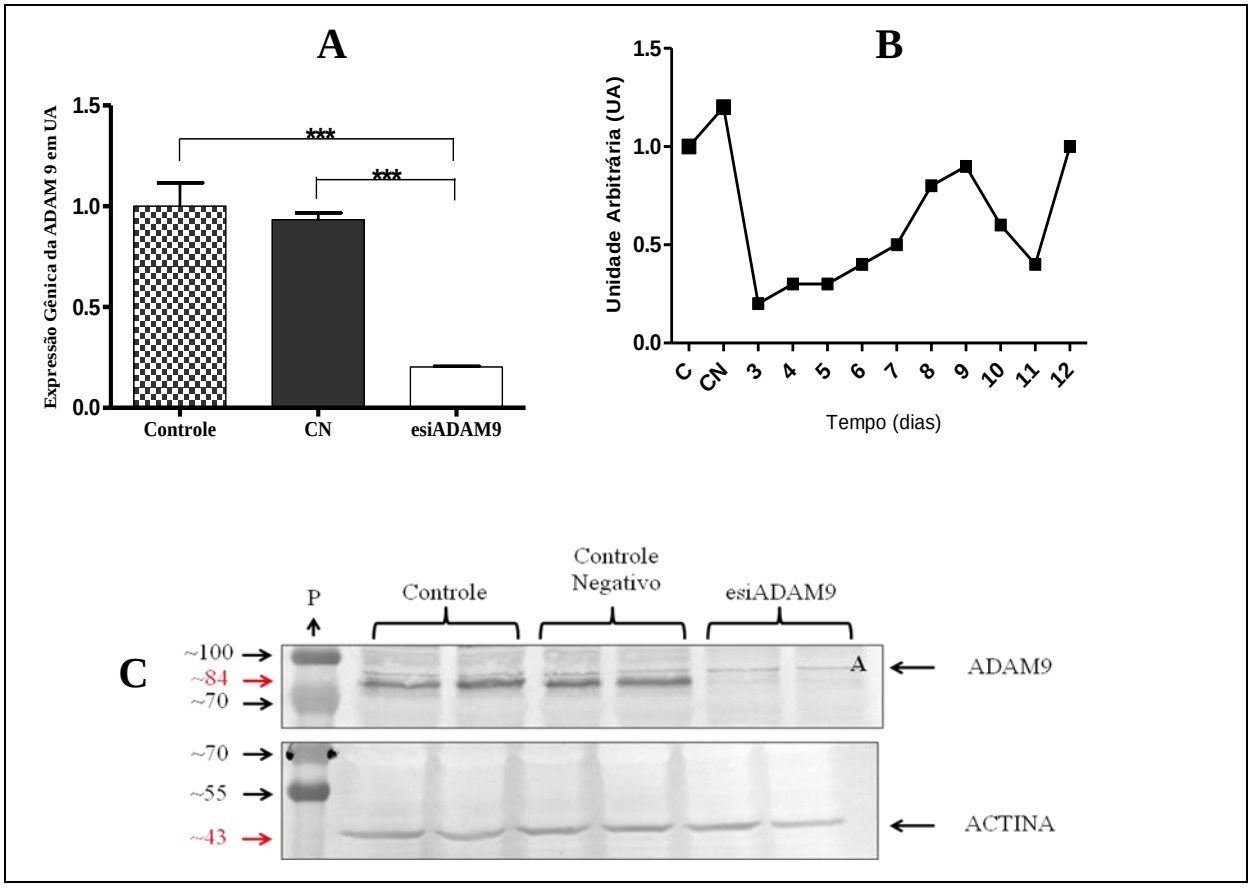

Figura 1 – Silenciamento da ADAM9. **(A)** Expressão do mRNA da ADAM9 nas células MDA-MB-231 analisada por RT-qPCR. Os valores estão em unidades arbitrárias (UA) e o valor de *P* foi determinado usando ANOVA seguido do teste Tukey comparando controle, controle negativo (CN) e células tratadas com esiRNAADAM9 (*** $p<0.001$). **(B)** Curva de silenciamento: O silenciamento da ADAM9 usando esiRNAs é transiente sendo eficaz somente do terceiro ao sexto dia. Os valores estão representados em unidades arbitrárias (UA). **(C)** Análise da expressão protéica da ADAM9 por *Western blotting* em lisados extraídas das células MDA-MB-231: Controle, Controle Negativo e silenciadas para a ADAM9 usando anticorpo primário anti-ADAM9. O anticorpo anti-βeta actina foi usado como controle endógeno.

Figura 2

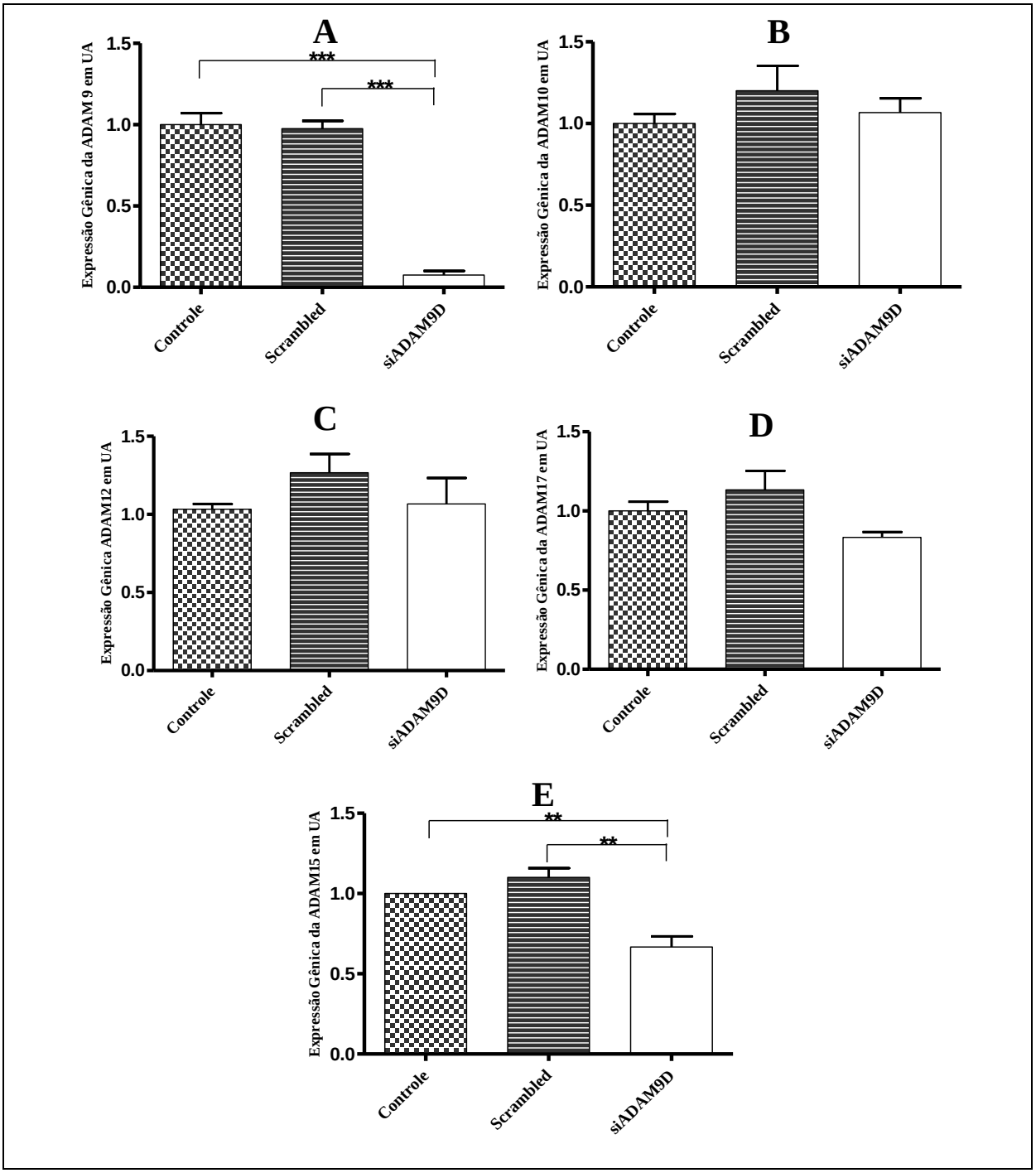

Figura 2 – Expressão do mRNA da ADAM9 **(A)**, ADAM10 (**B**), ADAM12 (**C**) e ADAM17 (**D**) e ADAM15 (**E**) analisada por RT-qPCR nas células MDA-MB-231. Os valores estão em unidades arbitrárias (UA) e o valor de *P* foi determinado usando ANOVA com o teste Tukey comparando controle, *scrambled* e células tratadas com siADAM9D (**p<0,01). Os Genes normalizadores utilizados foram HPRT e GAPDH.

Figura 3

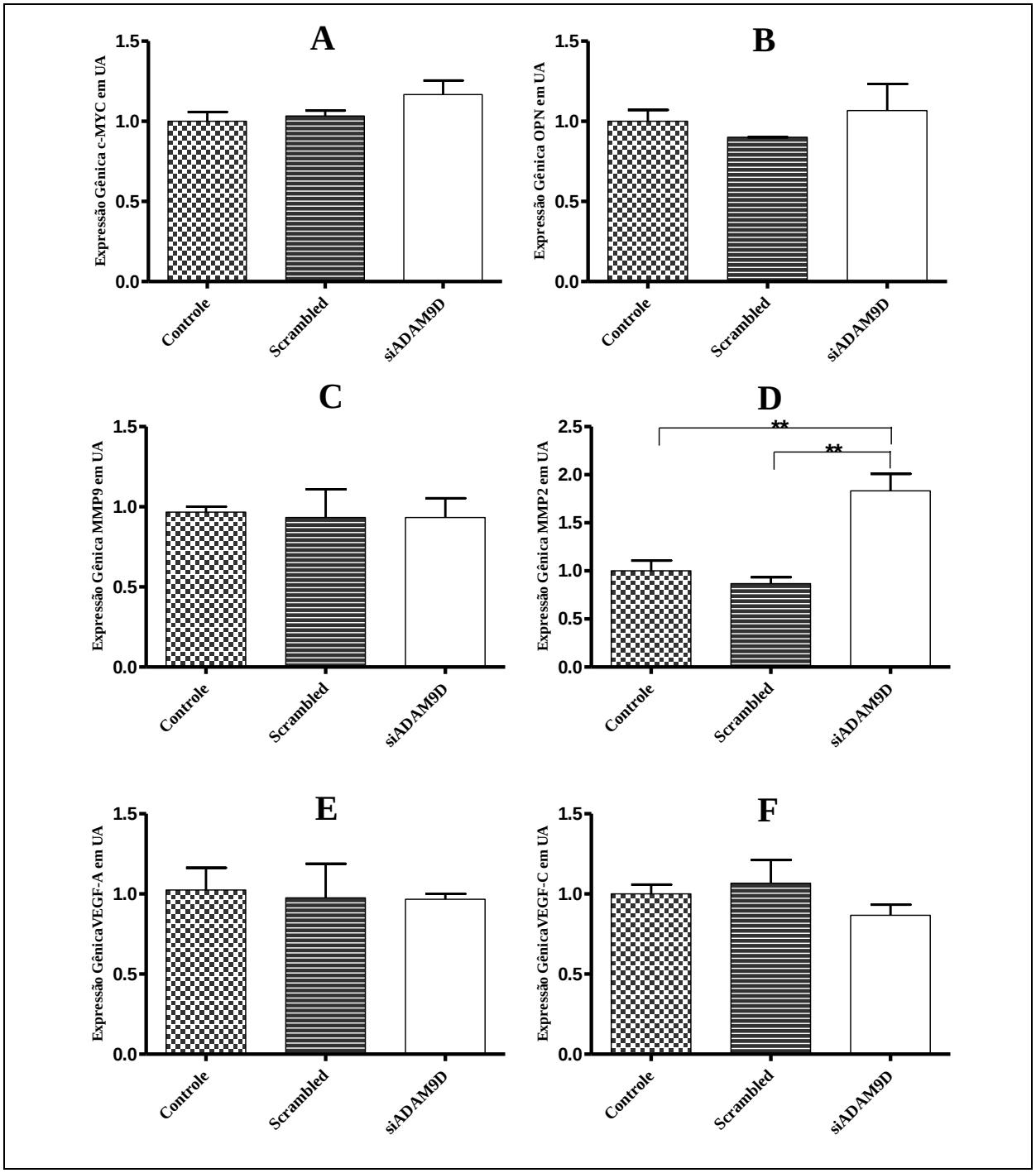
A
Expressão Gênica c-MYC em UA
1.5
1.0
0.5
0.0
Controle
Scrambled
siADAM9D
B
Expressão Gênica OPN em UA
1.5
1.0
0.5
0.0
Controle
Scrambled
siADAM9D
C
Expressão Gênica MMP9 em UA
1.5
1.0
0.5
0.0
Controle
Scrambled
siADAM9D
D
Expressão Gênica MMP2 em UA
2.5
2.0
1.5
1.0
0.5
0.0
**
**
Controle
Scrambled
siADAM9D
E
Expressão GênicaVEGF-A em UA
1.5
1.0
0.5
0.0
Controle
Scrambled
siADAM9D
F
Expressão GênicaVEGF-C em UA
1.5
1.0
0.5
0.0
Controle
Scrambled
siADAM9D

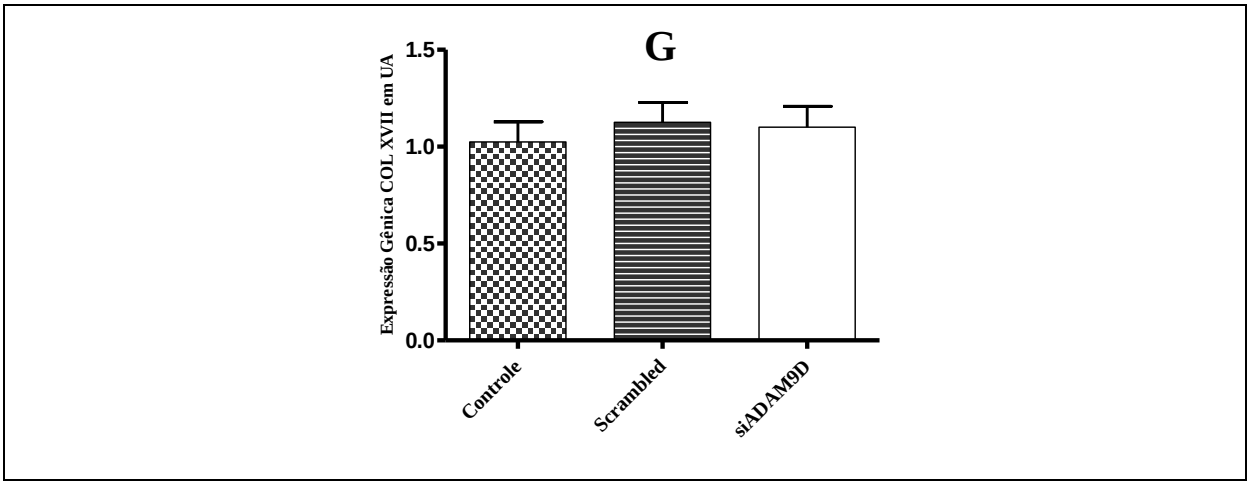

Figura 3 – Expressão do mRNA da c-MYC **(A)**, OPN (**B**), MMP9 (**C**), MMP2(**D**), VEGF-A (**E**), VEGF-C (**F**) e COL XVII (**G**) analisada por RT-qPCR nas células MDA-MB-231 (controle, *scrambled* e tratadas com siADAM9D). Os valores estão em unidades arbitrárias (UA) e o valor de *P* foi determinado usando ANOVA com o teste Tukey comparando controle, *scrambled* e células tratadas com siADAM9D (**p<0,01). Os Genes normalizadores utilizados foram HPRT e GAPDH.

Figura 4

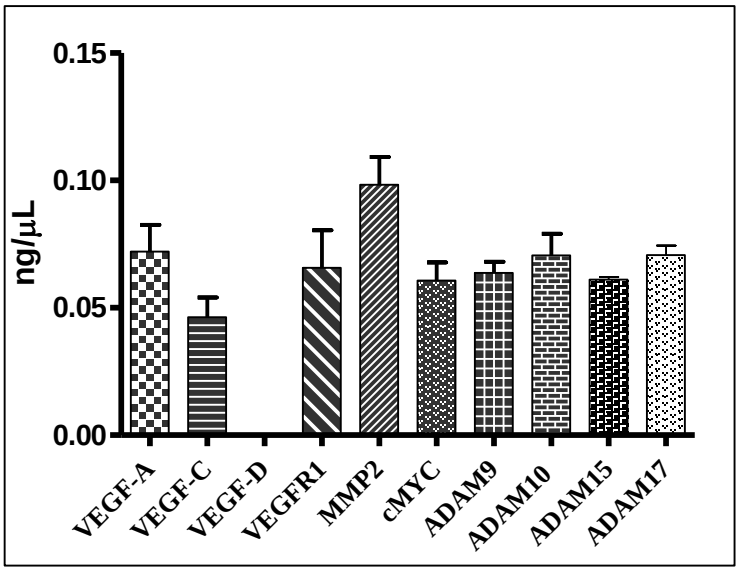

Figura 4 – Expressão do mRNA da ADAM9, ADAM10, ADAM15, ADAM17, c-MYC, MMP2, VEGF-A, VEGF-C, VEGF-D e VEGFR1 analisada por RT-qPCR utilizando a quantificação absoluta nas células HMVEC-dLyAd-Der. Os genes normalizadores utilizados foram HPRT e GAPDH.

Figura 5

Linhagem Celular	**Integrinas**									
	α_2	**α_4**	**α_5**	**α_6**	**α_v**	**$\alpha_V\beta_3$**	**$\alpha_V\beta_5$**	**β_1**	**β_3**	**β_4**
MDA-MB-231	+	+	+++	+	+	+	+	+++	+	++
HMVEC-dLy	+++	+	+++	+++	+++	+++	+++	+++	+++	+++
HMEC-1	++	++	+++	++	+++	+	+	+++	++	+++
HUVEC	+++	+	+++	+++	+++	+	+++	+++	++	+++

Figura 5 – Análise de integrinas por citometria de fluxo nas células MDA-MB-231, HMEC-1, HUVEC e HMVEC-dLyAd-Der. +: 1% a 10%, + +: 11% a 50%, + + +: 51% a 100%.

Figura 6

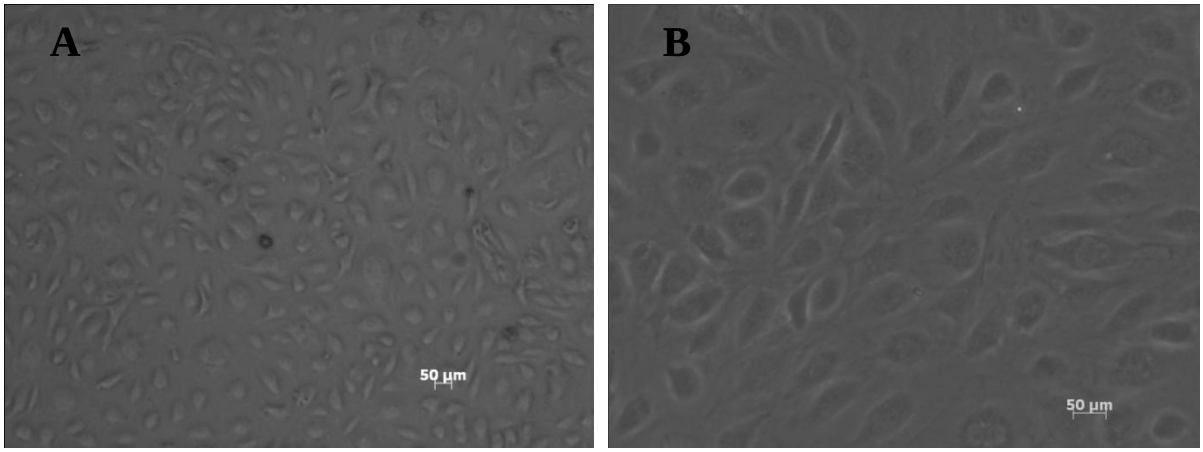

Figura 6 – Monocamada das células HMVEC-dLyAd-Der. **(A)** Fotografadas na passagem 2 e com objetiva de 4X; **(B)** Fotografadas na passagem 2 e com objetiva de 10X. Escala de 50 µm.

Figura 7

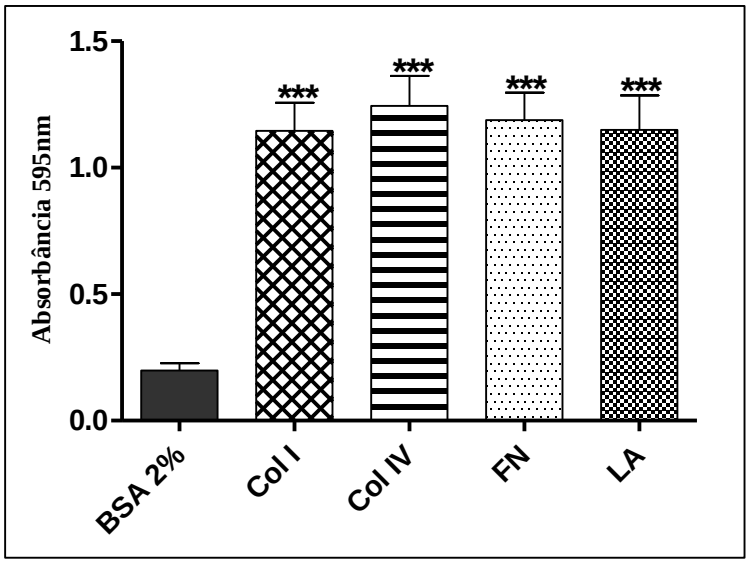

Figura 7 – Ensaio de adesão das células HMVEC-dLyAd-Der a componentes da MEC. As células foram adicionadas sobre diversas proteínas da MEC: colágeno tipo I (Col I), colágeno tipo IV (Col IV), Fibronectina (FN) e Laminina (LA). Os valores de absorbância para o cristal de violeta com significância estatística foram atribuídos para $p<0,05$, sendo ***$p<0,001$ (ANOVA/DUNNETT).

Figura 8

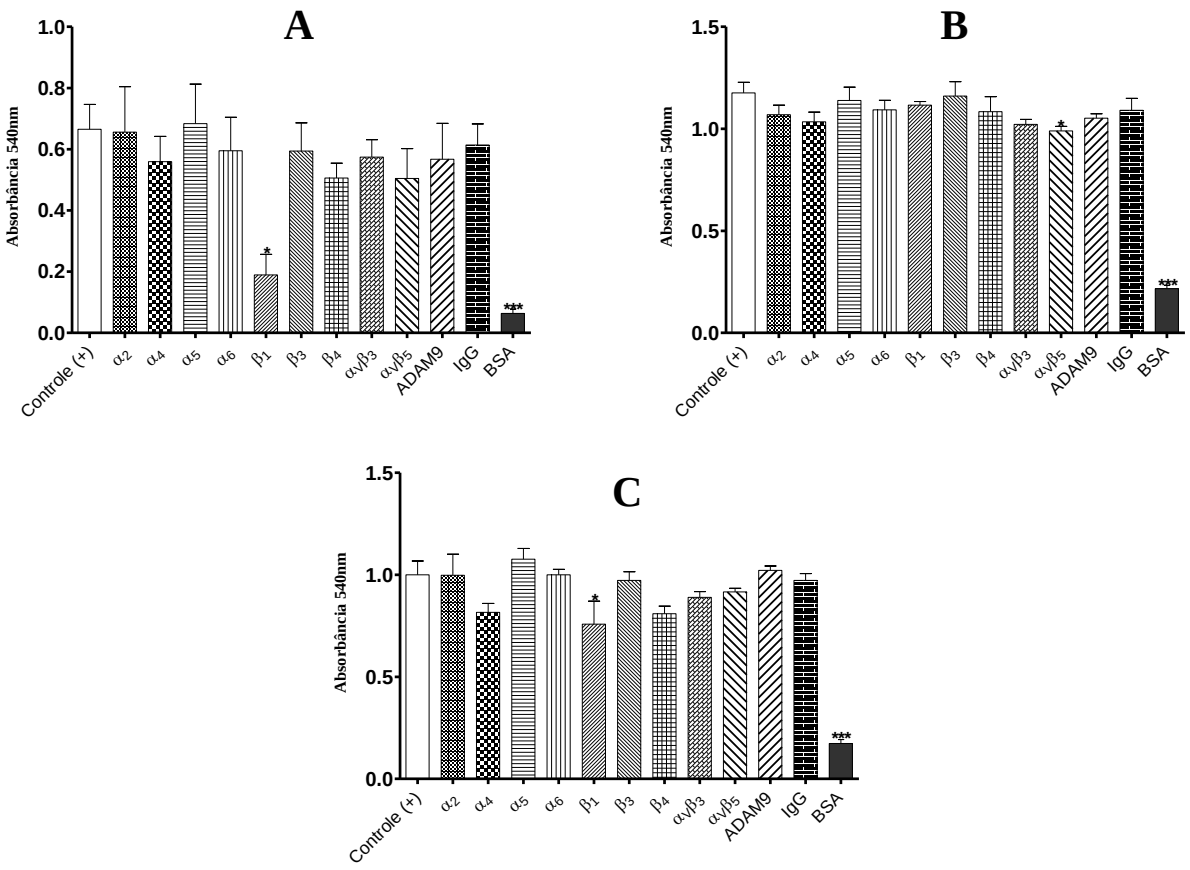

Figura 8 - Ensaio de inibição da adesão das células HMVEC-dLyAd-Der. As células foram previamente incubadas com diferentes anticorpos (10 µg/mL) e posteriormente adicionadas sobre proteínas da MEC imobilizadas em placas de 96 poços, Laminina (LA - 1µg/poço) (**A**), Fibronectina (FN - 10µg/poço) (**B**), e Colágeno tipo IV (Col. IV - 10µg/poço) (**C**). Os valores de absorbância para o cristal de violeta com significância estatística foram atribuídos para $p<0,05$, sendo *$p<0,05$; ***$p<0,001$ (ANOVA/DUNNETT).

Figura 9

(A)

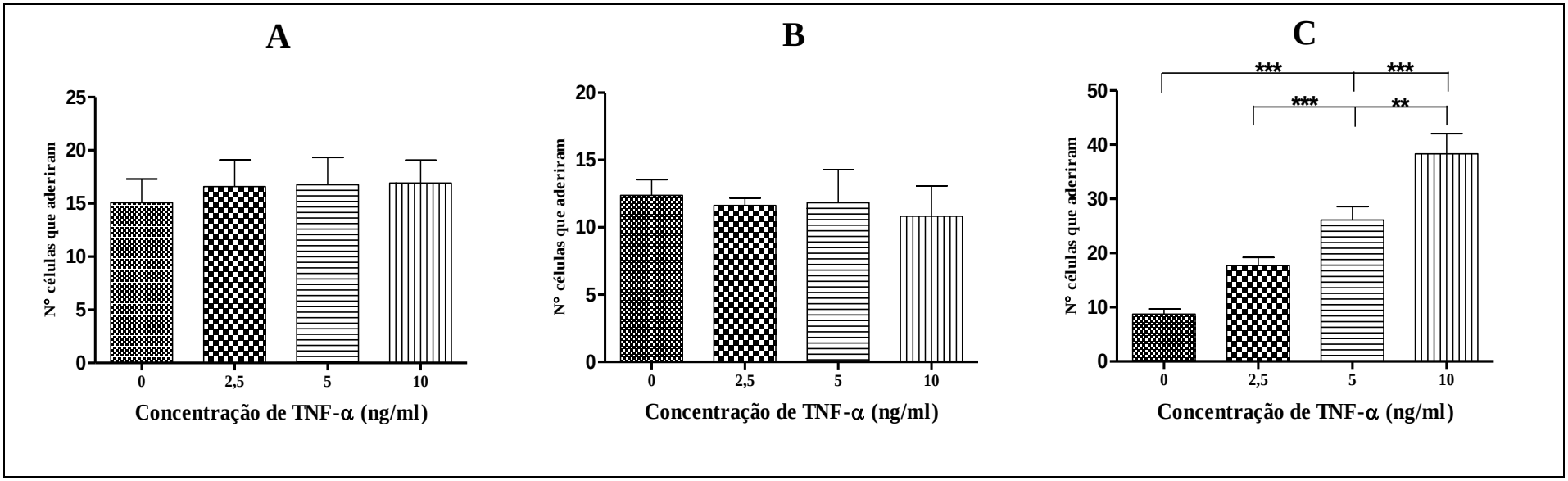

Figura 9 – Efeito da pré-estimulação das células endoteliais HUVEC (**A**), HMEC-1 (**B**) e HMVEC-dLyAd-Der (**C**) com diferentes concentrações de TNF-α na adesão das células de tumor de mama MDA-MB-231. As células endoteliais foram tratadas com diferentes concentrações de TNF-α: 0 (não tratada); 2,5; 5,0 e 10 ng/mL por 5 horas. Em seguida, as células MDA-MB-231 foram marcadas com CFSE e semeadas sobre a monocamada das células endoteliais para aderirem. Após 40-45 minutos as células foram fixadas com formaldeído 3,7% e 15 campos aleatórios foram fotografados como o axílio do microscópio da Carl ZEISS (Axio Vision - Objetiva de 20x) e a Camera (Axio Vision CAM) para posteriores análises. Os valores com significância estatística foram atribuídos para $p<0,05$, sendo $^{**}p<0,01$; $^{***}p<0,001$ (ANOVA/TUKEY'S) **(A)**. Imagens representativas da pré-estimulação com diferentes concentrações de TNF-α. Escala de 50 μm (**B**).

(B)

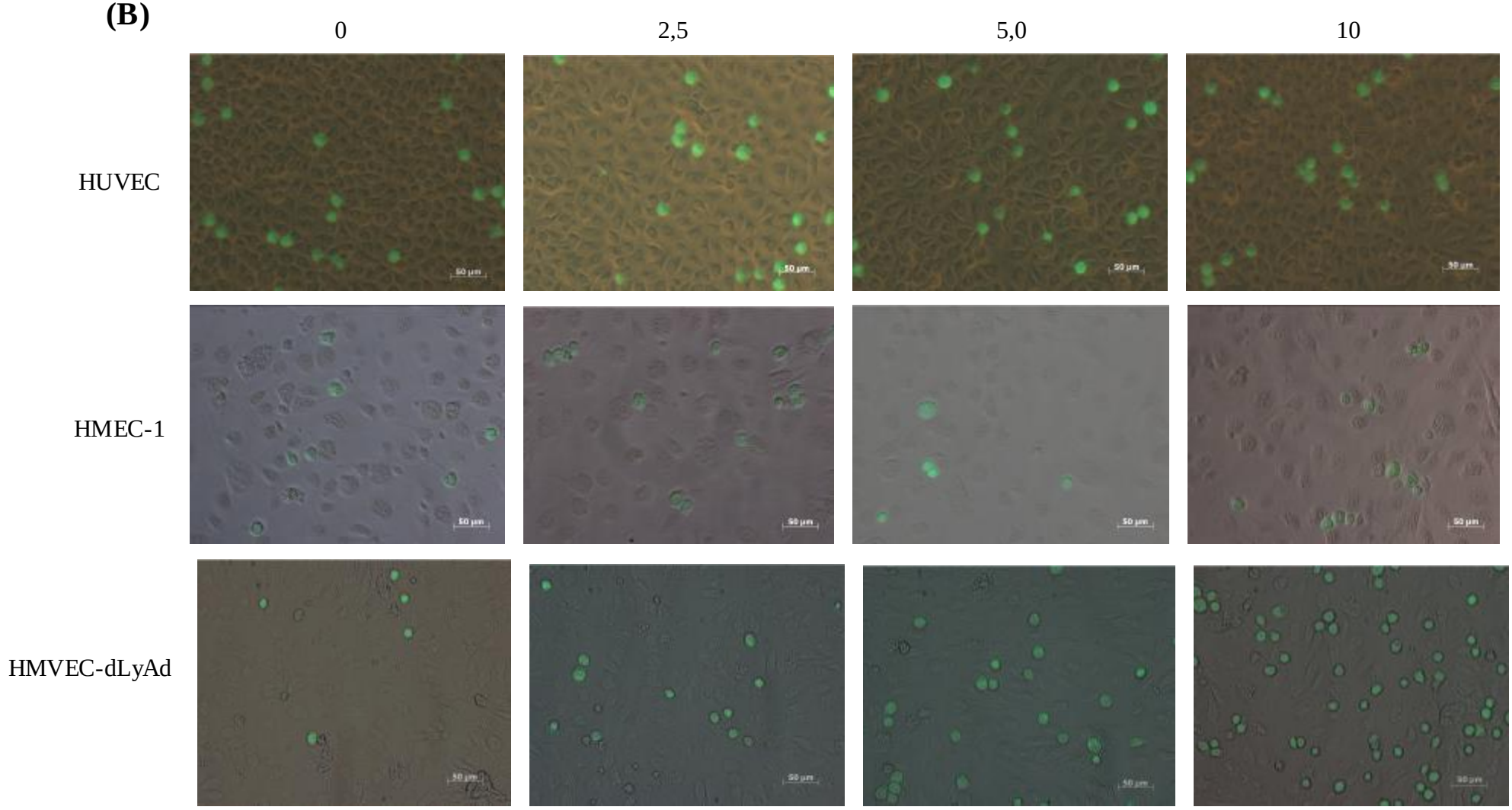

Figura 10

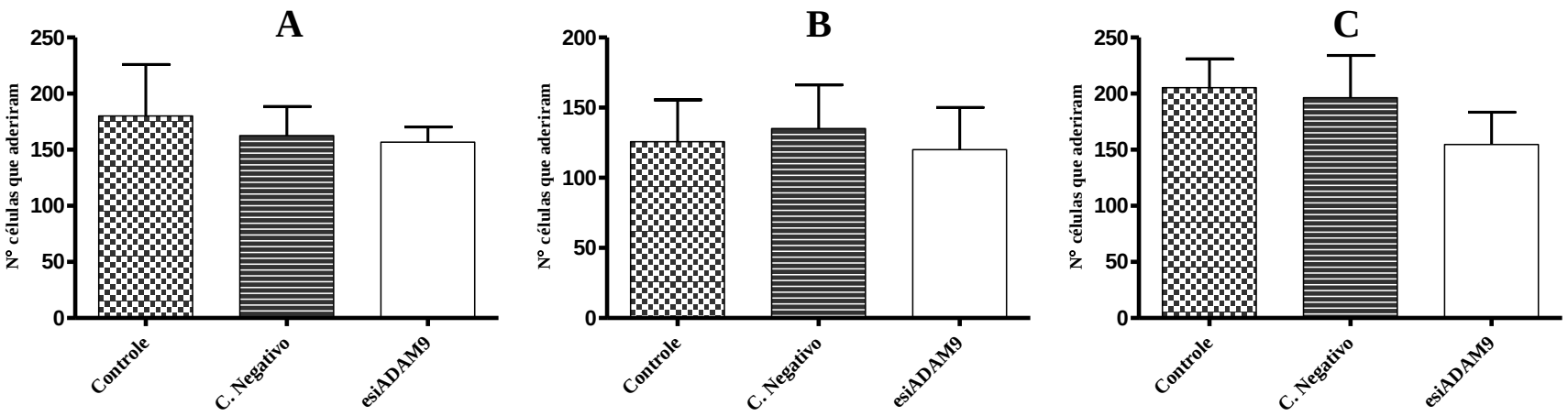

Figura 10 – Efeito do silenciamento da ADAM9 na adesão das células MDA-MB-231 através da monocamanda das células endoteliais HUVEC (**A**), HMEC-1 (**B**) e HMVEC-dLyNeo-Der (**C**) em condições de fluxo. As células tumorais silenciadas ou não foram misturadas ao meio de cultura DMEM sem soro. As células MDA-MB-231 foram marcadas com CFSE e submetidas à perfusão sobre placas de Petri (3 cm) recobertas com células endoteliais. O tempo de perfusão foi de 10 minutos a um fluxo de 5 *dynes/cm*^{2}, e logo após a perfusão as células foram fixadas com formaldeído 3,7% para posteriores análises. As células HMVEC-dLyNeo-Der foram pré-estimuladas com TNF-α (10 ng/mL) por 5 horas.

Figura 11

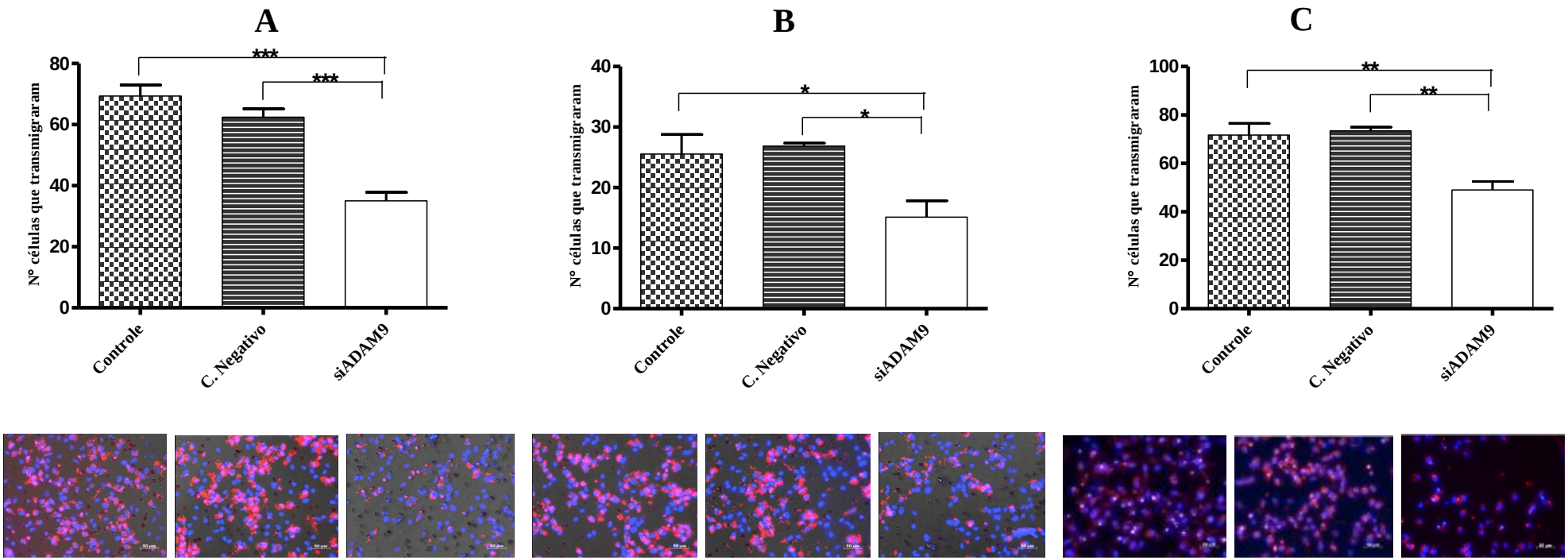

Figura 11 – Efeito do silenciamento da ADAM9 na transmigração das células MDA-MB-231 através das células endoteliais HUVEC (**A**), HMEC-1 (**B**) e HMVEC-dLyNeo-Der (**C**). As células tumorais silenciadas ou não e foram plaqueadas na parte superior dos insertos previamente recobertos com uma monocamada de células endoteliais e deixadas por 16 horas em estufa 37°C e 5% de CO_2 para transmigrarem. Em vermelho = células MDA-MB-231 coradas com *PKH26 Red Fluorescent Cell Linker* (Sigma); Azul = núcleos das células tumorais ou endoteliais corados com DAPI. As células HMVEC-dLyNeo-Der foram pré-estimuladas com TNF-α (10 ng/mL) por 5 horas. Os valores com significância estatística foram atribuídos para $p<0,05$, sendo *$p<0,05$; **$p<0,01$ e ***$p<0,001$ (ANOVA/TUKEY'S).(Objetiva de 20x - Escala de 50 µm)

MATERIAIS E MÉTODOS SUPLEMENTARES

Suplementar 1 – Padronizações do volume final das reações.

REAÇÃO ADAM9, ADAM10, ADAM12, ADAM17, MMP2, MMP9, cMYC, Colágeno XVII, Osteopontina (OPN), VEGF-C, VEGF-D, HPRT, GAPDH: 10,0 µL água DEPC, 12,5 µL SYBR Green, 0,5 µL cDNA, 2,0 µL *Primers Forward e Reverse*. **TOTAL DA REAÇÃO** = 25 µL.

REAÇÃO ADAM15 : 11,0 µL água DEPC, 12,5 µL SYBR Green, 0,5 µL cDNA, 1,0 µL *Primers Forward e Reverse*. **TOTAL DA REAÇÃO** = 25 µL.

REAÇÃO VEGF-A E VEGFR1: 9,5 µL água DEPC, 12,5 µL SYBR Green, 0,5 µL cDNA, 2,5 µL *Primers Forward e Reverse*. **TOTAL DA REAÇÃO** = 25 µL

Suplementar 2 – Padronizações do ciclo de amplificação e temperatura de *Melting* de cada gene testado.

ADAM9	
95 °C, 10 minutos	
Ciclos (40 repetições)	Etapa 1: 95 °C, 15 segundos
	Etapa 2: 55 °C, 5 segundos
	Etapa 3: 72 °C, 20 segundos
Melt (72-95 °C), 45 segundos na etapa 1, 5 segundos nas etapas seguintes	

ADAM10	
95 °C, 10 minutos	
Ciclos (40 repetições)	Etapa 1: 95 °C, 15 segundos
	Etapa 2: 66 °C, 60 segundos
	Etapa 3: 72 °C, 20 segundos
Melt (72-95 °C), 45 segundos na etapa 1, 5 segundos nas etapas seguintes	

MMP9, ADAM12, COL XVII	
95 °C, 10 minutos	

Ciclos (45 repetições)	Etapa 1: 95 °C, 15 segundos
	Etapa 2: 59 °C, 30 segundos
	Etapa 3: 72 °C, 30 segundos
Melt (72-95 °C), 45 segundos na etapa 1, 5 segundos nas etapas seguintes	

ADAM15	
95 °C, 10 minutos	
Ciclos (40 repetições)	Etapa 1: 95 °C, 15 segundos
	Etapa 2: 61 °C, 30 segundos
	Etapa 3: 72 °C, 30 segundos
Melt (72-95 °C), 45 segundos na etapa 1, 5 segundos nas etapas seguintes	

ADAM17	
95 °C, 10 minutos	
Ciclos (40 repetições)	Etapa 1: 95 °C, 15 segundos
	Etapa 2: 57 °C, 30 segundos
	Etapa 3: 72 °C, 30 segundos
Melt (72-95 °C), 45 segundos na etapa 1, 5 segundos nas etapas seguintes	

cMYC	
95 °C, 10 minutos	
Ciclos (46 repetições)	Etapa 1: 95 °C, 15 segundos
	Etapa 2: 64 °C, 30 segundos
Melt (72-95 °C), 45 segundos na etapa 1, 5 segundos nas etapas seguintes	Etapa 3: 72 °C, 30 segundos

MMP2	
95 °C, 10 minutos	
Ciclos (40 repetições)	Etapa 1: 95 °C, 15 segundos
	Etapa 2: 68 °C, 30 segundos
	Etapa 3: 72 °C, 30 segundos
Melt (72-95 °C), 45 segundos na etapa 1, 5 segundos nas etapas seguintes	

VEGF-A	
95 °C, 10 minutos	

Ciclos (40 repetições)	Etapa 1: 95 °C, 15 segundos
	Etapa 2: 57 °C, 30 segundos
	Etapa 3: 72 °C, 20 segundos
Melt (72-95 °C), 45 segundos na etapa 1, 5 segundos nas etapas seguintes	

VEGF-C	
95 °C, 10 minutos	
Ciclos (40 repetições)	Etapa 1: 95 °C, 15 segundos
	Etapa 2: 63 °C, 30 segundos
	Etapa 3: 72 °C, 20 segundos
Melt (72-95 °C), 45 segundos na etapa 1, 5 segundos nas etapas seguintes	

VEGF-D e OPN	
95 °C, 10 minutos	
Ciclos (45 repetições) – VEGF-D	Etapa 1: 95 °C, 15 segundos
Ciclos (40 repetições) – OPN	Etapa 2: 65 °C, 30 segundos
	Etapa 3: 72 °C, 20 segundos
Melt (72-95 °C), 45 segundos na etapa 1, 5 segundos nas etapas seguintes	

VEGFR1	
95 °C, 10 minutos	
Ciclos (40 repetições)	Etapa 1: 95 °C, 15 segundos
	Etapa 2: 55 °C, 30 segundos
	Etapa 3: 72 °C, 20 segundos
Melt (72-95 °C), 45 segundos na etapa 1, 5 segundos nas etapas seguintes	

HPRT	
95 °C, 10 minutos	
Ciclos (40 repetições)	Etapa 1: 95 °C, 15 segundos
	Etapa 2: 58 °C, 15 segundos
	Etapa 3: 72 °C, 20 segundos
Melt (72-95 °C), 45 segundos na etapa 1, 5 segundos nas etapas seguintes	

GAPDH	
95 °C, 10 minutos	

Ciclos (40 repetições)	Etapa 1: 95 °C, 15 segundos
	Etapa 2: 56 °C, 15 segundos
	Etapa 3: 72 °C, 20 segundos
Melt (72-95 °C), 45 segundos na etapa 1, 5 segundos nas etapas seguintes	

FIGURAS SUPLEMENTARES

Figura Suplementar 1 - Análise da expressão de diferentes integrinas nas células HUVEC por citometria de fluxo.

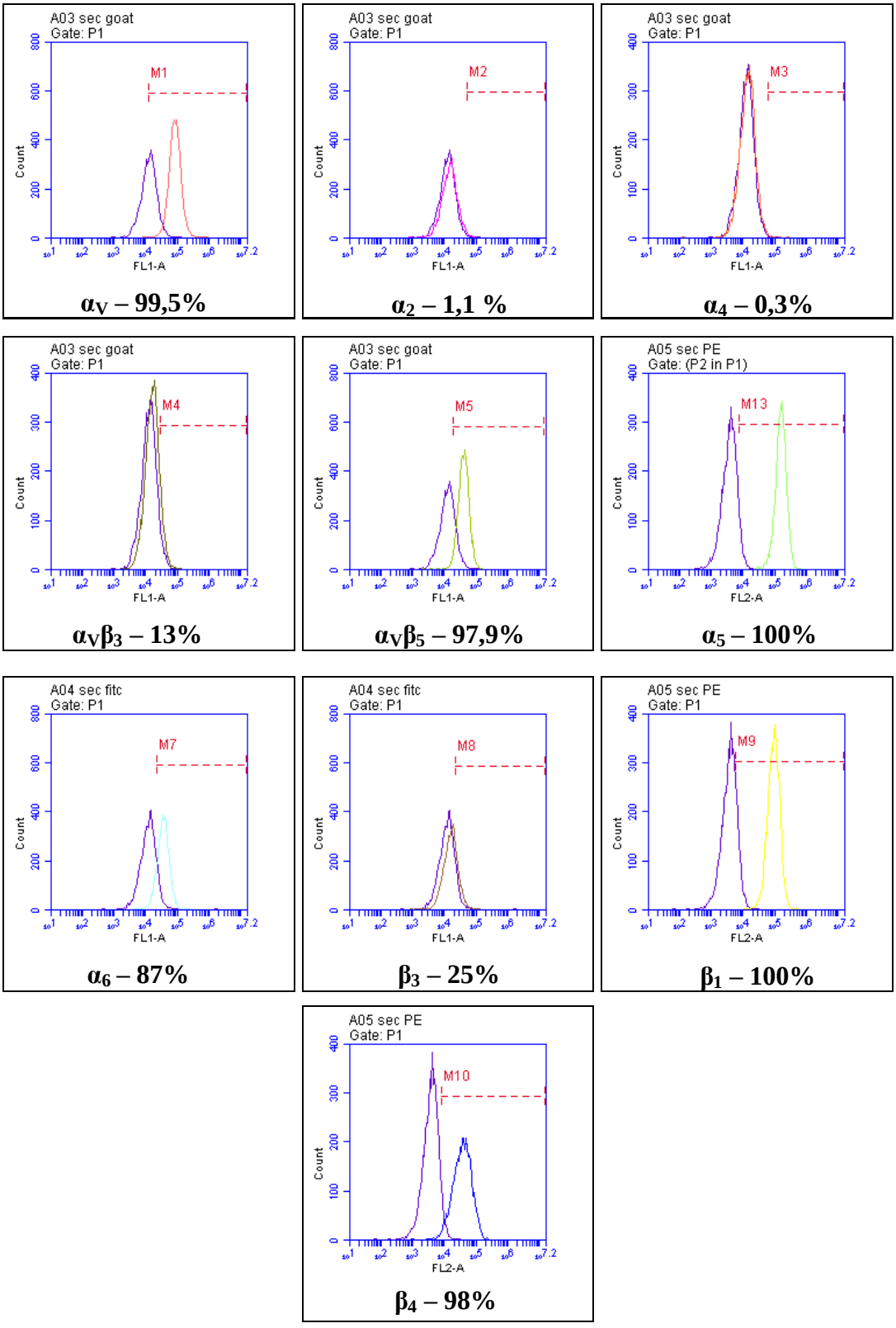

Figura Suplementar 2 - Análise da expressão de diferentes integrinas nas células HMEC-1 por citometria de fluxo.

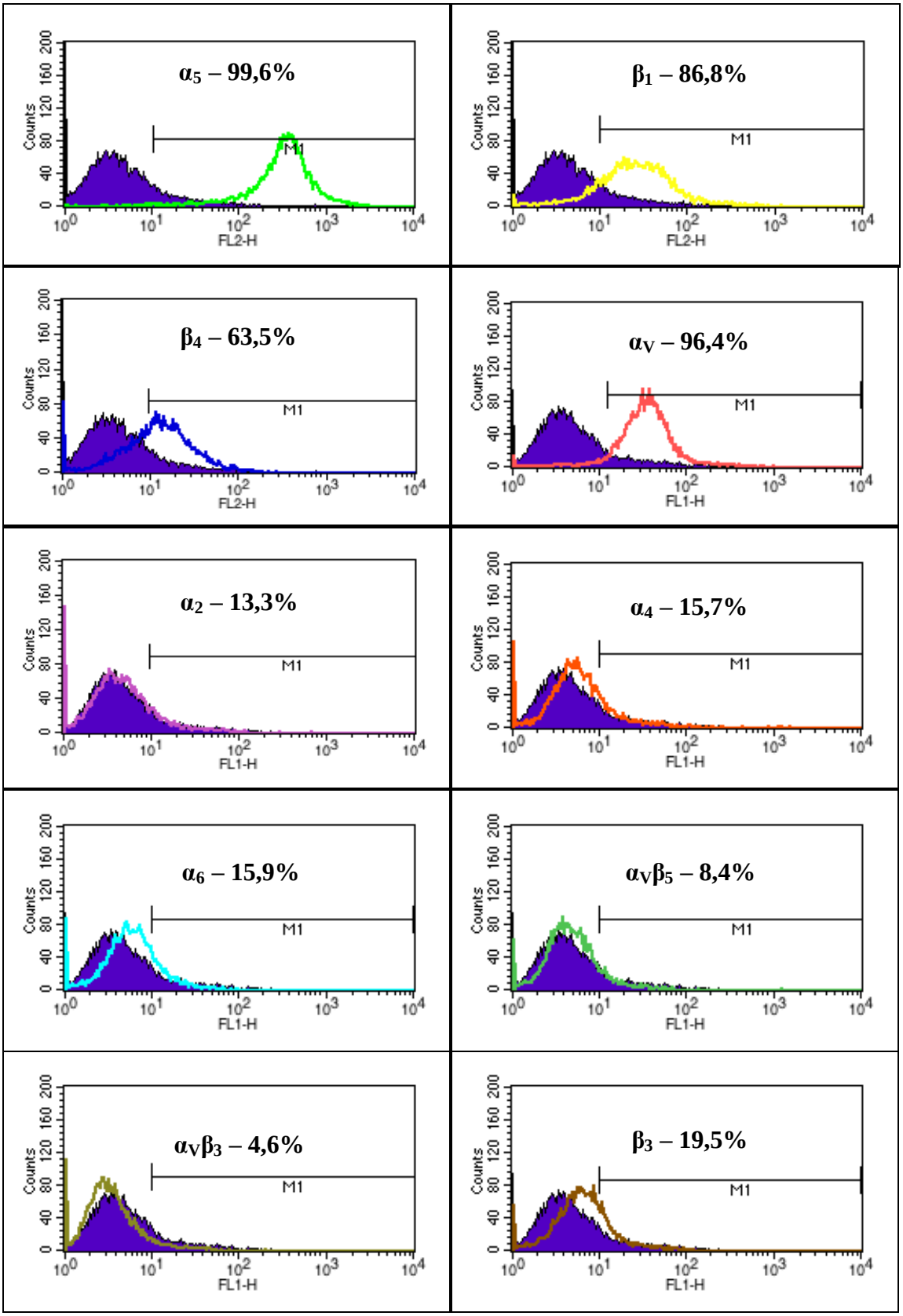

Figura Suplementar 3 - Análise da expressão de diferentes integrinas nas células HMVEC-dLyAd-Der por citometria de fluxo.

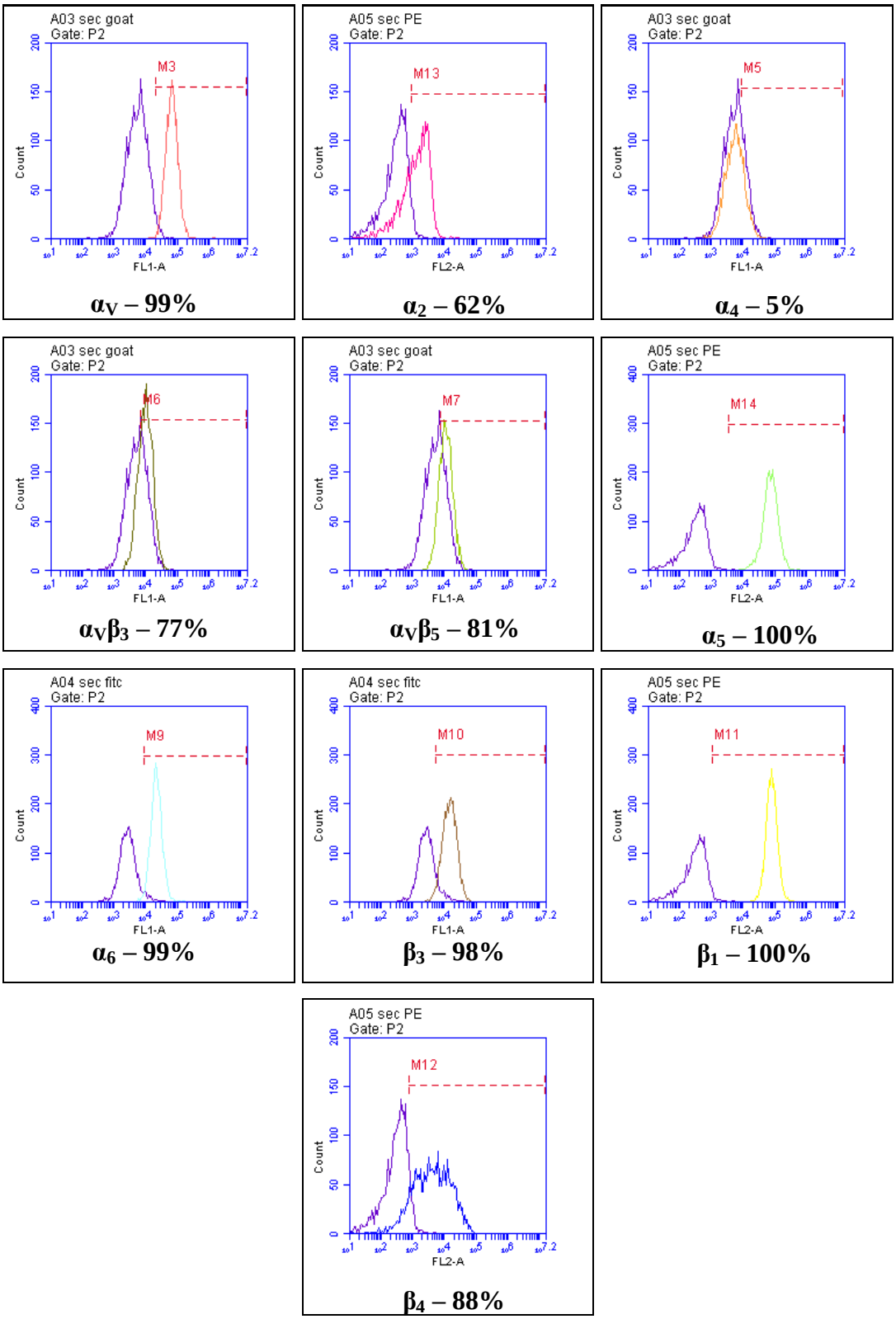

4.2. MANUSCRITO II – Publicado

ADAM9 SILENCING INHIBITS BREAST TUMOR CELL INVASION IN VITRO

Kelli Cristina Micocci[a], Ana Carolina Baptista Moreno Martin[a], Cyntia de Freitas Montenegro[a], Araceli Cristina Durante[a], Normand Pouliot[b,c,d], Márcia Regina Cominetti[a 1*], Heloisa Sobreiro Selistre-de-Araujo[a]. ***Biochimie,*** vol. 95, n° 7, pp. 1371–1378, 2013.

[a]Departamento de Ciências Fisiológicas, Rodovia Washington Luís, Km 235, CEP 13565-905, São Carlos, SP, Brazil. Fax: +55-16-33518328; Phone: +55-16-33518333.

[b]Metastasis Research Laboratory, Peter MacCallum Cancer Centre and [c]Sir Peter MacCallum Department of Oncology/[d]Pathology Department, The University of Melbourne, Melbourne, VIC Australia. Fax: +61-3-96561411; Phone +61-3-96561285.

*corresponding author: mcominetti@ufscar.br

Running title: ADAM9 SILENCING INHIBITS CELL INVASION

[1]Present address: Departamento de Gerontologia, Rodovia Washington Luís, Km 235, CEP 13565-905, São Carlos, SP, Brazil. Fax: +55-16-33519628; Tel: +55-16-33066663.

ABSTRACT

ADAM9 (*A D*isintegrin *A*nd *M*etalloproteinase 9) is a member of the ADAM protein family which contains a disintegrin domain. This protein family plays key roles in many physiological processes, including fertilization, migration, and cell survival. The ADAM proteins have also been implicated in various diseases, including cancer. Specifically, ADAM9 has been suggested to be involved in metastasis. To address this question, we generated ADAM9 knockdown clones of MDA-MB-231 breast tumor cells using silencing RNAs that were tested for cell adhesion, proliferation, migration and invasion assays. In RNAi-mediated ADAM9 silenced MDA-MB-231 cells, the expression of ADAM9 was lower from the third to the sixth day after silencing and inhibited tumor cell invasion in matrigel by approximately 72% when compared to control cells, without affecting cell adhesion, proliferation or migration. In conclusion, the generation of MDA-MB-231 knockdown clones lacking ADAM9 expression inhibited tumor cell invasion *in vitro*, suggesting that ADAM9 is an important molecule in the processes of invasion and metastasis.

Key words: ADAM9, integrin, RNA silencing, disintegrin, cell adhesion, cancer, metastasis.

Research Highlights

▶ RNAi-mediated ADAM9 silencing inhibits MDA-MB-231 cell invasion ▶ADAM9 silencing had no effect on the migration or proliferation of MDA-MB-231 cells ▶ ADAM9 can be a target for the design of drugs against breast cancer

1. INTRODUCTION

Attachment of cells to the extracellular matrix (ECM) depends mainly on a family of glycoproteins known as integrins [1], which are expressed on the cell surfaces of many cultured cell types at specialized adhesion sites known as focal contacts [2]. A number of structural and signaling proteins, such as integrins, cytoskeletal proteins, and kinases are concentrated at these sites and are known to initiate signal transduction pathways [3-4]. The aggregation of integrin receptors, ligand occupancy and tyrosine kinase-mediated phosphorylation are the key events that result in different processes, including cell migration, differentiation, tissue remodeling, cell proliferation, angiogenesis, tumor cell invasion and metastasis [1, 5].

Members of the ADAM (an acronym for *A* *D*isintegrin *A*nd *M*etalloprotease) protein family are involved in several human diseases such as inflammatory disorders, neurological diseases, asthma and cancer metastasis [6-7]. ADAM9 is a transmembrane protein with a number of characteristic domains, including a pro-domain, a metalloproteinase domain, a disintegrin-like domain, a cysteine-rich region, a transmembrane domain, and a short cytoplasmic tail [8]. The ADAM9 disintegrin domain binds to numerous integrins, such as $\alpha_6\beta_1$ integrins in fibroblasts [9], $\alpha_V\beta_5$ in myeloma cells [10] and $\alpha_V\beta_3$ in MDA-MB-231 breast tumor cells [11]. Mahimkar et al. [12] and Zigrino et al. [13] have demonstrated that the recombinant disintegrin and cysteine-rich domains from human ADAM9 mediate cellular adhesion through β_1 integrins. Furthermore, the disintegrin-like and cysteine-rich domains of ADAM-9 mediate interactions between melanoma cells and fibroblasts [14].

Over-expression of ADAM9 has been reported in several human carcinomas, including kidney [15], prostate [16], breast [17], liver [18-19], pancreatic [20], gastric [21], cervix [22] and oral [23]. Expression of ADAM9 is elevated in skin melanoma but is

restricted to the invading front [24]. Peduto et al. [25] found a correlation between ADAM9 titer and cancerous changes in mouse models of prostate cancer, especially in well-differentiated tumors. Increased expression of ADAM9 led to increased structural abnormalities and growth of early-stage tumors compared to controls.

The ADAM9 protein also appears to interfere with various cell signaling systems. In prostate cancers, the fibroblast growth factor (FGF) signaling pathway is believed to be particularly important [26], with down-regulation of the fibroblast growth factor receptor 2 isoform IIIb (FGFR2IIIb) being a feature of prostrate tumor progression [27]. Transfection of FGFR2IIIb into malignant tumors is enough to inhibit their growth [28]. Therefore, it is potentially significant that over-expression of ADAM9 increases shedding of FGFR2IIIb from cells, which is expected to disrupt FGFR2IIIb signaling and reduce its function [25]. Additionally, over-expression of ADAM9 leads to increased release of epidermal growth factor (EGF) [25], a factor known to induce prostate cancer growth in rat pups [29].

Although ADAM9 is normally considered a transmembrane protein, a soluble form ADAM9-S has been described [30], which is derived from alternative splicing of the gene [31]. The ADAM9-S protein promotes the invasive phenotype of carcinoma cell lines, and ADAM9 is strongly expressed at the invading front of hepatic metastases, although the authors did not distinguish ADAM9 and ADAM9-S [31]. Taken together, these studies suggest that ADAM9 has a significant role in tumorigenesis and metastasis.

To better understand the role of ADAM9 in breast cancer progression, we generated knockdown clones lacking ADAM9 using RNAi in the MDA-MB-231 human breast tumor cell line. As far as we know, this is the first demonstration that decreased ADAM9 expression impaired the invasiveness of this cell line. In addition, the present work demonstrated, for the first time, ADAM9 silencing in a breast tumor cell line and provided

evidence that ADAM9 may play an important role in the metastatic progression of human breast cancer.

2. MATERIAL AND METHODS

2.1. Cell culture

MDA-MB-231 breast tumor cells were cultivated in DMEM medium (Invitrogen) containing 10% bovine fetal serum (FBS), L-glutamine (2 mM), penicillin (100 U/ml), streptomycin (100 µg/ml) and amphotericin B (250 µg/ml) (Invitrogen) in 5% CO_2 at 37˚C. The anti-ADAM9 antibody was from Abcam (anti-RP2ADAM9) and the anti-β-actin antibody was from Santa Cruz Biotech (sc-1616).

2.2. Design of siRNA primers

Primer set #104056, which targets exon 13 (disintegrin domain) (Silencer® Pre-designed siRNA, Ambion), was selected to ensure that other ADAMs would not be silenced simultaneously. The primer sequences were: sense (5'-rCrCrArGrArGrUrArCrUrGrCrArArUrGrGrUrUrCrUrUrCTC-3') and antisense (5'-rGrArGrArArGrArArCrCrArUrUrGrCrArGrUrArCrUrCrUrGrGrArA-3'). The negative control (scrambled) used in the assays was *Silencer*® Select Negative Control No. 1 siRNA (Ambion). This sequence does not target any gene product and have no significant sequence similarity to human gene sequences, being essential for determining the effects of siRNA delivery.

2.3. ADAM9 RNA silencing

On the day before transfection, $2x10^5$ MDA-MB-231 cells were plated in 5 ml of DMEM medium supplemented with 10% FBS without antibiotics. Ten microliters of lipofectamine were mixed with 490 µl OPTI-MEM serum-free medium (Invitrogen) and incubated at room temperature for 5 minutes. A total of 10 nM of RNA silencing primer was diluted in OPTI-MEM, added to the Lipofectamine/OPTI-MEM mixture and incubated for 20 minutes at room temperature. This mixture was then added to the cells. The medium was changed 24 hours after transfection. Controls comprised non-treated cells, cells treated with transfection reagent only (lipofectamine), and cells treated with a scrambled primer. Cells were washed in phosphate buffered saline, harvested with Trizol reagent (Invitrogen) according to the manufacturer's protocol, and frozen immediately. For western blotting assays, cells were lysed with Triton X-100 in Hepes buffer [150 mM NaCl, 50 mM Hepes, 1.5 mM $MgCl_2$, 1% Triton X-100, 0.1% SDS, protease inhibitor cocktail (Sigma), 100 mM NaF and 100 mM Na_3VO_4]. Protein concentrations in the lysed samples were determined by the BCA method (Pierce), and 30 µg of each sample was resolved by SDS-PAGE [32]. Protein bands were transferred to nitrocellulose membranes and probed with anti-RP2ADAM9 and anti-β-actin antibodies. Western blots were scanned on an Image Scanner (GE - General Electric). All the assays using ADAM9 knockdown MDA-MB-231 cells were performed after the third day of siRNA transfections.

2.4. Extraction of RNA and synthesis of cDNA

Total RNA was extracted from cells using Trizol reagent (Invitrogen) following the manufacturer's instructions. All samples were treated with DNase I (Deoxyribonuclease I, Amplification Grade, Invitrogen). After quantification, a total of 1 µg of RNA was mixed with 0.5 µl of oligo dT (0.5 µg/µl) (Promega) and nuclease-free water to a

volume of 7 µl and incubated at 70°C for 5 minutes, followed by 5 minutes on ice. Next, 0.5 µl of 200 units/µl of Moloney Monkey Leukemia virus (MMLV) reverse transcriptase (Promega), 2.5 µl of 5x MMLV buffer (Promega), and 2.5 µl of 10 mM dNTP mix was added to the reaction. The whole mixture was incubated at 37°C for 1 hour, and was used posteriorly for qPCR.

2.5. Design of qPCR primers

ADAM9 primers targeting the disintegrin domain were designed using Primer3Plus software (http://www.bioinformatics.nl/cgi-bin/primer3plus/primer3plus.cgi). Primers spanned exon boundaries so that only mRNA sequences would be amplified. The primers were ADAM9DF1 (5'CTT GCT GCG AAG GAA GTA CC); and ADAM9DR1 (5'AAC ATC TGG CTG ACA GAA CTG A). Primers targeting HPRT1F1 (5'TGA CAC TGG CAA AAC AAT GCA), HPRT1R1 (5'GGT CCT TTT CAC CAG CAA GCT), GAPDHF1 (5'GAT GCT GGT GCT GAG TAT GT) and GAPDHR1 (5'GTG GTG CAG GAT GCA TTG CT) were used as endogen controls.

2.6. Gene expression

ADAM9 mRNA expression was measured in a Corbett Rotor-gene RG 3000 (Corbett Research) using the following thermocycling conditions: 95°C for 10 minutes, followed by 40 cycles of amplification at 95°C for 15 seconds, 55°C for 5 seconds and 72°C for 20 seconds. The master mix in each well consisted of 12.5 µl ABsoluteTM QPCR SYBR Green mix (6 mM $MgCl_2$, reaction buffer, DNA polymerase and SYBR green dye) (Advanced Biotechnologies), 1.25 µl each of 5 µM forward and reverse primer and 10.5 µl of nuclease-free water in a total volume of 25 µl.

2.7. Proliferation assays

To measure the effect of RNAi-mediated ADAM9 silencing on cell proliferation the transition of 3-(4,5-Dimethylthiazol-2-yl)-2,5-diphenyltetrazolium bromide (MTT) to formazan was used [33]. Cells without any treatment, cells treated only with lipofectamine, and cells transfected with siRNAs were seeded in 96-well plates and left at 37°C for 24 and 48 hours. The cells were then washed with PBS and incubated in 50 µl of 0.5 mg/ml MTT in culture medium at 37°C for 4 hours. Following the addition of 100 µl of isopropanol, the absorbance was read at 595 nm in an ELISA plate reader. The mean proliferation of cells without any treatment was expressed as 100%.

2.8. Adhesion assays

The effect of RNAi-mediated ADAM9 silencing on the adhesion of MDA-MB-231 cells was analyzed in 96-well plates (Corning). A solution of type I collagen (10 µg) was immobilized on the plates in 0.1% acetic acid. Fibronectin and laminin (10 µg) were dissolved in adhesion buffer (20 mM HEPES, 150 mM NaCl, 5 mM KCl, 1 mM $MgSO_4$ and 1 mM $MnCl_2$ pH 7.35), overnight at 4°C. On the next day, the wells were blocked with a solution of 1% BSA diluted in adhesion buffer for 1 hour. Cells were counted and their concentration was adjusted in proportion to $5x10^6$/ml. The blocking solution was removed from the wells and they were washed twice with adhesion buffer (100 µl). After this period the cells were incubated for 45 minutes on the coatings and subsequently wells were washed in order to remove non-adherent cells. A solution of 70% ethanol (100 µl) was added to the wells and the plate was incubated for 10 minutes at room temperature. Subsequently, the ethanol was removed and 60 µl of crystal violet (0.5%) was added and incubated for 20 minutes at room temperature. After this time, the solution containing the crystal was removed and the wells were washed with PBS to remove excess. Finally 100 µL of 1% SDS was added

and incubated for 30 minutes at room temperature. The reading of absorbance was performed at a wavelength of 595nm, and three treatments were compared, including cells without any treatment, cells treated only with lipofectamine, and cells transfected with siRNAs. The adhesion of control cells to each substrate was determined as 100%.

2.9. Wound healing assay

Wound-healing migration assay is based on the repopulation of wounded cultures. The cells were seeded into 24-well culture plates at $1x10^5$ cells/well and the cell monolayer were cultured in medium containing 10% FBS until reach 100% of confluence. The monolayers were carefully wounded using a yellow pipette tip, and any cellular debris present was removed by washing twice with DMEM medium. The wounded monolayers were then incubated in DMEM medium containing 10% FBS. Photographs of the exact wound areas taken initially (0h) were again taken after 16 and 24h. The images were compared between three treatments, including cells without any treatment, cells treated only with lipofectamine, and cells transfected with siRNAs, and with or without incubation with the ADAM9D protein [11]. Photographs were analyzed using ImageJ software and the formula of % of wound closure [34].

2.10. Cell migration

Cell migration was assessed in 24 well Boyden chambers (BD Biosciences). MDA-MB-231 (5×10^4) cells were seeded on the upper chamber in FBS-free DMEM medium. DMEM containing FBS (10%) was added to the bottom chamber and acted as a chemoattractant. Tumor cells were allowed to migrate for 22 hours at 37ºC and 5% CO_2 in a humidified environment. Then, the cells that remained in the upper chamber were removed using a cotton swab. The cells that migrated to the other side of the upper chamber membrane

were fixed with methanol and stained with 1% toluidine blue in 1% borax. Cells were counted using the Image J software (public domain software) in 5 fields (100× magnification) per well that essentially covered 80% of the well surface. The average number of cells from each of the triplicates represents the average number of cells that migrated in the different groups. Each experiment had triplicate wells for every treatment group and we repeated each experiment three times. The mean of all results from controls was considered as 100%. After that, the images were compared among three treatments, including cells without any treatment, cells treated only with lipofectamine, and cells transfected with siRNAs.

2.11. Matrigel invasion assay

Cellular invasion assays were carried out using BioCoat Matrigel Invasion Chambers (BD Biosciences) with 8-µm pores in 6-well plates. A total of $2.5x10^4$ cells were added to each chamber. Complete medium was used as a chemoattractant in the lower chamber. After incubation for 22 hours at 37°C and 5% CO_2, cell invasion was measured in the same way as performed for migration assay (item 2.10). The invasion of cells without any treatment was determined as 100%.

2.12. Gelatin zymography

The effect of ADAM9 silencing on the proteolytic activity of MDA-MB-231 cells was determined by zymography [35]. MDA-MB-231 cells ($2x10^6$) in FBS-free DMEM medium were seeded in 6-cm dishes. After incubation for 24 h at 37°C and 5% CO_2, cells were lysed with a buffer containing Tris-HCl (0.2 M) (pH 7.4) and Triton X-100 (0.2%). The cell lysates were centrifuged (10 minutes at 13,000 x *g* and 4ºC), and the supernatants were separated. The total protein concentration in each sample was measured using the BCA colorimetric detection kit (BCA Protein Assay, Pierce). Protein samples (20 µg) were

subjected to electrophoresis under non-reducing conditions in 10% SDS polyacrylamide gels containing 1 mg/ml gelatin. After electrophoresis, gels were washed twice in 2.5% of Triton X-100 to remove SDS and incubated in substrate buffer [50 mM Tris-HCl (pH 8.0); 5 mM of $CaCl_2$ and 0.02% NaN_3] at 37ºC for 20 hours. To confirm the metalloproteinase activity, EDTA in a final concentration of 15mM was added to the samples and substrate buffer. Proteins were stained with Coomassie brilliant blue for 1.5 hours and destained with an acetic acid, methanol and water mixture (in a 1:4:5 v:v:v ratio). Gels were photographed with a Canon G6 Power Shot 7.1 machine. Gelatinase activity was visualized as clear bands in the stained gels, and the average band intensities was measured using the Gene Tools v3.06 software (Syngene). MMP-2 and MMP-9 activity were quantified as arbitrary units and compared between three treatments, including cells without any treatment, cells treated only with lipofectamine, and cells transfected with siRNAs.

2.13. Statistical Analysis

For all assays, each experiment was repeated three times in triplicate (independent experiments), and standard errors of the mean were calculated. The results were compared statistically using a one-way analysis of variance (ANOVA) and Tukey's test was applied for multiple comparisons. All statistical tests used $p \leq 0.05$ as a cut-off for significance. Cases where $p < 0.05$ were marked as follows: * $p < 0.05$, ** $p < 0.01$ and *** $p < 0.001$.

3. RESULTS

3.1. ADAM9 silencing is detected at the mRNA and protein levels.

ADAM9 gene expression was dramatically decreased in MDA-MB-231 cells treated with siRNAs at both the mRNA and protein (Fig. 1A and B, respectively) levels when compared to the controls (MDA-MB-231 cells without treatment and lipofectamine or scrambled-treated cells). qPCR analysis showed a down regulation of 91.35 ± 6.32% of ADAM9 expression in RNAi-mediated knockdown MDA-MB-231 cells when compared to control cells (Fig. 1A). At the protein level, western blotting analysis using anti-ADAM9 antibody presented similar results (Fig. 1B).

Gene silencing using synthetic duplexes siRNA is transient. As a result, 10 plates (6-cm) containing $2x10^5$ MDA-MB-231 cells were silenced. One plate was removed randomly each day to determine the efficiency of ADAM9 silencing over time. RNA knockdown was measured from the third to the eleventh day after transfection and the kinetics of ADAM9 silencing in MDA-MB-231 cells is shown in Figure 1C. The highest efficiency of ADAM9 silencing was observed from the third to the sixth days, although on the seventh and eighth days, the gene expression still remained low. From the ninth and tenth days onwards, the expression of ADAM9 expression increased exponentially and reached similar levels to those obtained by control cells (Fig. 1C).

3.2. ADAM9 silencing does not affect MDA-MB-231 cell proliferation or adhesion

ADAM9 silencing had no effect on the proliferation of MDA-MB-231 cells on the third (Fig. 2A) or sixth (Fig. 2B) days after silencing in 24 or 48 hours of incubation. No significant differences were observed among the groups. ADAM9 silencing also had no effect on the adhesion of MDA-MB-231 cells to different ECM proteins, such as collagen type I, fibronectin or laminin (Fig. 3).

3.3. ADAM9 silencing strongly inhibits MDA-MB-231 cell invasion without affecting cell migration

RNAi-mediated ADAM9 silencing was not able to significantly inhibit the migration of MDA-MB-231 human breast tumor cells when compared with non-transfected cells or with lipofectamine-transfected cells after 16 (Fig. 4A) or 24 hours that the wounds were made (Fig. 4B). ADAM9 knockdown cells were incubated with different concentrations of ADAM9D, the disintegrin domain of ADAM9 [11]. ADAM9D in concentrations of 500, 1000 and 2000 nM had no effects in inhibiting ADAM9 knockdown MDA-MB-231 cell migration after 16 (Fig. 4A) or 24 (Fig. 4B) hours of incubation. Photographs were taken after 0, 16 or 24 hours after wound (Fig. 4C).

To ensure these results we also performed migration assays using Boyden chambers. RNAi-mediated ADAM9 silencing had had no effect on MDA-MB-231 cell migration when compared with control cells or lipofectamine-treated cells after 22 hours of incubation (Fig. 5AB).

On the other hand, RNAi-mediated ADAM9 knockdown MDA-MB-231 cells strongly inhibited the invasion in an *in vitro* matrigel assay by 71.51 ± 8.02% when compared to control untransfected cells (Fig. 6A). Lipofectamine and negative control-transfected cells (scrambled) remained invasive and no statistically significant differences were observed when compared to untrasfected cells (Fig. 6A). Photographs were taken after 22 hours of incubation (Fig. 6B).

3.4. MMP-2 and MMP-9 concentration and activity

In order to investigate the mechanisms involved in the inhibition of the invasion ability of RNAi-mediated ADAM9 silencing of MDA-MB-231 cells, we performed zymography assays to evaluate the activity of MMP-2 and MMP-9. There was no variation in

the total concentration of MMP-2 or MMP-9 among the three treatment types analyzed in this study, as demonstrated by 1% gelatin-SDS-PAGE (Fig. 7A). The incubation with EDTA resulted in the inhibition of MMP-2 and 9 activities confirming the nature of metalloprotease activity (Fig. 7B). The average activity of MMP-2 and MMP-9 was measured as indicated in section 2.12 and plotted on a graph (Fig. 7C and D, respectively). This result suggests that RNAi-mediated ADAM9 silencing does not affect the activity of MMP-2 or MMP-9.

4. DISCUSSION

The progression of malignant tumors results from the invasion of the primary tumor to a secondary site, causing metastasis in a multi-step process that requires cell-cell and cell-matrix interactions within the host tissue. These steps can be summarized as follows: cell detachment from the primary tumor, migration into the ECM, intravasation into a blood or lymphatic vessel, survival within the vasculature, adherence of these tumor cells in the endothelium, extravasation, and formation of secondary tumors [36-37]. These interactions lead to the production, release and activation of a variety of cytokines and growth factors and subsequent generation of signals to directly or indirectly promote tumor growth and survival [24]. Different proteases have been implicated in these processes, such as MMPs, ADAMs and ADAMTSs [7, 24, 38].

Due to the strong involvement of ADAM9 in the metastatic process, in this study we have generated knockdown clones of MDA-MB-231 human breast tumor cells that lack ADAM9 expression and then tested these clones to their ability to adhere, migrate, proliferate and invade through ECM using in vitro assays. The RNAi-mediated silencing in MDA-MB-231 cells was very successful, with more than 90% of ADAM9 knocked down, as estimated by quantitative PCR and western blotting analysis. The expression of ADAM9 was easily silenced using a relatively small (10 nM) concentration of ADAM9 siRNAs. A similar result

was obtained by other investigators in highly invasive SCC68 cells, a squamous cell carcinoma cell line, but with tenfold higher concentration of siRNAs (100 nM) [39].

Using a matrigel invasion assay, we showed that the ADAM9 silencing significantly inhibited the invasion capacity of MDA-MB-231 human breast cancer cells, which suggests that this protein plays an important role in cell invasion. However, the silencing of ADAM9 had no effect on MDA-MB-231 cell adhesion, migration, proliferation, or MMP-2 and 9 activities. Our results showed that ADAM9 silencing had no impact on MMP-2 and MMP-9 expression or gelatinase activity indicating that reduced invasion in cells expression ADAM9 siRNA is unlikely to be due to indirect inhibition of MMP-2/9. We propose that ADAM9 proteolytic activity may directly contribute to matrigel invasion by MDA-MB-231 cells since ADAM9 has been reported to cleave laminin [31], a major constituent of matrigel.

Shintani et al. [40] showed that the overexpression of ADAM9 enhances adhesion and cell invasion in lung cancers, via modulation of other adhesion molecules and changes in sensitivity to growth factors. According to this study, ADAM9 may either directly degrade the ECM or induce the activation of other proteases in the ECM, such as matrix MMPs, thereby allowing tumor cell penetration into the brain matrix.

Our results are in agreement with Mazzocca et al. [31] who showed that ADAM9-S, an alternatively spliced variant secreted by activated hepatic stellate cells, induces colon carcinoma cell invasion *in vitro* and that this process requires both protease activity and binding to the $\alpha_6\beta_4$ and $\alpha_2\beta_1$ integrins.

Contradictorily to our results, Fry & Toker [41] demonstrated that the silencing of both soluble (ADAM9-S) and transmembrane (ADAM9-L) isoforms, increased the migration of BT549 breast cancer cells. In this work, they also showed that the overexpression of ADAM9-S is responsible for increasing cell migration in BT549 cells

through its metallopeptidase domain. Moreover, they also showed that ADAM9-L is responsible for inhibiting cell migration through its disintegrin domain. Thus, both isoforms have different and opposite responses during cancer progression. Whether MDA-MB-231 cells have ADAM9-S and L isoforms and the effects of isoform silencing in this cell line will be further investigated.

Some ADAMs may induce proliferation by catalyzing the cleavage of growth factors, such as HB-EGF, and its membrane anchored form (proHB-EGF) can act as a negative regulator of proliferation [42-43]. Izumi et al. [44] showed that after induction with TPA (an activator of protein kinase C), ADAM9 interacted with PKCδ and cleaved proHB-EGF; however, we have demonstrated here that ADAM9 is not involved in the proliferation of MDA-MB-231 cells. In another work, RNAi-mediated ADAM9 silencing was responsible by a reduction in adenoid cystic carcinoma metastasis both *in vitro* and *in vivo* [19]. In this work, the authors also demonstrated that ADAM9 is essential for cancer cell proliferation and invasion and that its expression could be used as a prognostic of metastatic risk, since it was elevated in a high metastatic potential cell line (SACC-LM) when compared to a low metastatic potential cell line (SACC-83) [19].

Klessner et al. [39] demonstrated that ADAM9 participates in the shedding of desmoglein 2 (Dsg2), resulting in stronger cell-cell adhesion, which could, in turn, reduce the rate of migration and cell invasion. The ADAMs can also interact with β_1 integrins, and this association facilitates the recognition and location of their substrates for proteolytic shedding [45-46], as reported by Mahimkar et al. [47].

In a recent work, Hamada et al. [48] reported that miR-126 was found to target ADAM9 and that siRNA-based knockdown of ADAM9 in pancreatic cancer cells resulted in reduced cellular migration, invasion, and induction of epithelial marker E-cadherin.

Taken together, the literature results and the data found in the present study suggest that ADAM9 participates in the invasion of tumor cells by either directly degrading the ECM, by inducing activation of other proteases, such as MMPs, by co-localizing with other molecules, such as β_1 integrin, present on the surface of MDA-MB-231 cells (data not shown) or by interacting with other regulators such as miRNAs. A more conclusive demonstration that ADAM9 is a suitable target for metastatic breast cancer will require the use of a stable expression vector in vivo and/or inhibitors of this protein alone or in combination with conventional clinical therapies.

5. CONCLUSIONS

The results presented in this study reinforce the importance of the ADAM9 role in the invasion of breast tumor cells. Considering the significance of cell invasion in metastatic progression, ADAM9 can be pointed as an interesting target for the design of drugs involved in the treatment or prevention of breast cancers. We conclude that ADAM9 has an essential role in cell invasion and may be involved in metastatic spread. Therefore, it may be an interesting target for anti-metastatic therapy.

Acknowledgements

This work was supported by CAPES (Coordenação de Aperfeiçoamento de Pessoal de Nível Superior), CNPQ (Conselho Nacional de Desenvolvimento Científico e Tecnológico), and FAPESP (Fundação de Amparo à Pesquisa do Estado de São Paulo, Brazil).

6. REFERENCES

[1] R.O. Hynes, Integrins: versatility, modulation, and signaling in cell adhesion, Cell 69 (1992) 11-25.
[2] S.H. Lo, L.B. Chen, Focal adhesion as a signal transduction organelle, Cancer Metastasis Rev. 13 (1994) 9-24.
[3] S.E. LaFlamme, K.L. Auer, Integrin signaling, Semin. Cancer Biol. 7 (1996) 111-118.
[4] I.D. Campbell, M.J. Humphries, Integrin structure, activation, and interactions, Cold Spring Harb. Perspect. Biol. 3 (2011) 1-14.
[5] R.L. Juliano, J.A. Varner, Adhesion molecules in cancer: the role of integrins, Curr. Opin. Cell Biol. 5 (1993) 812-818.
[6] T. Klein, R. Bischoff, Active metalloproteases of the A Disintegrin and Metalloprotease (ADAM) family: biological function and structure, J. Proteome Res. 10 (2011) 17-33.
[7] N. Rocks, G. Paulissen, M. El Hour, F. Quesada, C. Crahay, M. Gueders, J.M. Foidart, A. Noel, D. Cataldo, Emerging roles of ADAM and ADAMTS metalloproteinases in cancer, Biochimie 90 (2008) 369-379.
[8] T.G. Wolfsberg, P. Primakoff, D.G. Myles, J.M. White, ADAM, a novel family of membrane proteins containing A Disintegrin And Metalloprotease domain: multipotential functions in cell-cell and cell-matrix interactions, J. Cell Biol. 131 (1995) 275-278.
[9] D. Nath, P.M. Slocombe, A. Webster, P.E. Stephens, A.J. Docherty, G. Murphy, Meltrin gamma (ADAM-9) mediates cellular adhesion through alpha(6)beta(1)integrin, leading to a marked induction of fibroblast cell motility, J. Cell Sci. 113 (2000) 2319-2328.
[10] M. Zhou, R. Graham, G. Russell, P.I. Croucher, MDC-9 (ADAM-9/Meltrin gamma) functions as an adhesion molecule by binding the alpha(v)beta(5) integrin, Biochem. Biophys. Res. Commun. 280 (2001) 574-580.
[11] M.R. Cominetti, A.C. Martin, J.U. Ribeiro, I. Djaafri, F. Fauvel-Lafeve, M. Crepin, H.S. Selistre-de-Araujo, Inhibition of platelets and tumor cell adhesion by the disintegrin domain of human ADAM9 to collagen I under dynamic flow conditions, Biochimie 91 (2009) 1045-1052.
[12] R.M. Mahimkar, O. Visaya, A.S. Pollock, D.H. Lovett, The disintegrin domain of ADAM9: a ligand for multiple beta1 renal integrins, Biochem J 385 (2005) 461-468.
[13] P. Zigrino, J. Steiger, J.W. Fox, S. Loffek, A. Schild, R. Nischt, C. Mauch, Role of ADAM-9 disintegrin-cysteine-rich domains in human keratinocyte migration, J. Biol. Chem. 282 (2007) 30785-30793.
[14] P. Zigrino, R. Nischt, C. Mauch, The disintegrin-like and cysteine-rich domains of ADAM-9 mediate interactions between melanoma cells and fibroblasts, J. Biol. Chem. 286 (2010) 6801-6807.
[15] F.R. Fritzsche, K. Wassermann, M. Jung, A. Tolle, I. Kristiansen, M. Lein, M. Johannsen, M. Dietel, K. Jung, G. Kristiansen, ADAM9 is highly expressed in renal cell cancer and is associated with tumour progression, BMC Cancer 8 (2008) 179.
[16] F.R. Fritzsche, M. Jung, A. Tolle, P. Wild, A. Hartmann, K. Wassermann, A. Rabien, M. Lein, M. Dietel, C. Pilarsky, D. Calvano, R. Grutzmann, K. Jung, G. Kristiansen, ADAM9 Expression is a Significant and Independent Prognostic Marker of PSA Relapse in Prostate Cancer, Eur. Urol. (2007).
[17] C. O'Shea, N. McKie, Y. Buggy, C. Duggan, A.D. Hill, E. McDermott, N. O'Higgins, M.J. Duffy, Expression of ADAM-9 mRNA and protein in human breast cancer, Int. J. Cancer 105 (2003) 754-761.

[18] A. Tannapfel, K. Anhalt, P. Hausermann, F. Sommerer, M. Benicke, D. Uhlmann, H. Witzigmann, J. Hauss, C. Wittekind, Identification of novel proteins associated with hepatocellular carcinomas using protein microarrays, J. Pathol. 201 (2003) 238-249.
[19] K. Tao, N. Qian, Y. Tang, Z. Ti, W. Song, D. Cao, K. Dou, Increased expression of a disintegrin and metalloprotease-9 in hepatocellular carcinoma: implications for tumor progression and prognosis, Jpn J. Clin. Oncol. 40 (2010) 645-651.
[20] R. Grutzmann, J. Luttges, B. Sipos, O. Ammerpohl, F. Dobrowolski, I. Alldinger, S. Kersting, D. Ockert, R. Koch, H. Kalthoff, H.K. Schackert, H.D. Saeger, G. Kloppel, C. Pilarsky, ADAM9 expression in pancreatic cancer is associated with tumour type and is a prognostic factor in ductal adenocarcinoma, Br. J. Cancer 90 (2004) 1053-1058.
[21] S. Carl-McGrath, U. Lendeckel, M. Ebert, A. Roessner, C. Rocken, The disintegrin-metalloproteinases ADAM9, ADAM12, and ADAM15 are upregulated in gastric cancer, Int. J. Oncol. 26 (2005) 17-24.
[22] A. Zubel, C. Flechtenmacher, L. Edler, A. Alonso, Expression of ADAM9 in CIN3 lesions and squamous cell carcinomas of the cervix, Gynecol. Oncol. 114 (2009) 332-336.
[23] Q. Xu, X. Liu, Y. Cai, Y. Yu, W. Chen, RNAi-mediated ADAM9 gene silencing inhibits metastasis of adenoid cystic carcinoma cells, Tumour Biol 31 (2010) 217-224.
[24] P. Zigrino, C. Mauch, J.W. Fox, R. Nischt, Adam-9 expression and regulation in human skin melanoma and melanoma cell lines, Int. J. Cancer 116 (2005) 853-859.
[25] L. Peduto, V.E. Reuter, D.R. Shaffer, H.I. Scher, C.P. Blobel, Critical function for ADAM9 in mouse prostate cancer, Cancer Res. 65 (2005) 9312-9319.
[26] A.I. Evangelou, S.F. Winter, W.J. Huss, R.A. Bok, N.M. Greenberg, Steroid hormones, polypeptide growth factors, hormone refractory prostate cancer, and the neuroendocrine phenotype, J. Cell. Biochem. 91 (2004) 671-683.
[27] B. Naimi, A. Latil, G. Fournier, P. Mangin, O. Cussenot, P. Berthon, Down-regulation of (IIIb) and (IIIc) isoforms of fibroblast growth factor receptor 2 (FGFR2) is associated with malignant progression in human prostate, Prostate 52 (2002) 245-252.
[28] A. Matsubara, M. Kan, S. Feng, W.L. McKeehan, Inhibition of growth of malignant rat prostate tumor cells by restoration of fibroblast growth factor receptor 2, Cancer Res. 58 (1998) 1509-1514.
[29] N. Torring, L.V. Jensen, J.G. Wen, F.B. Sorensen, J.C. Djurhuus, E. Nexo, Chronic treatment with epidermal growth factor induces growth of the rat ventral prostate, Scand. J. Urol. Nephrol. 35 (2001) 339-344.
[30] N. Hotoda, H. Koike, N. Sasagawa, S. Ishiura, A secreted form of human ADAM9 has an alpha-secretase activity for APP, Biochem. Biophys. Res. Commun. 293 (2002) 800-805.
[31] A. Mazzocca, R. Coppari, R. De Franco, J.Y. Cho, T.A. Libermann, M. Pinzani, A. Toker, A secreted form of ADAM9 promotes carcinoma invasion through tumor-stromal interactions, Cancer Res. 65 (2005) 4728-4738.
[32] U.K. Laemmli, Cleavage of structural proteins during the assembly of the head of bacteriophage T4, Nature 227 (1970) 680-685.
[33] T. Mosmann, Rapid colorimetric assay for cellular growth and survival: application to proliferation and cytotoxicity assays, J. Immunol. Methods 65 (1983) 55-63.
[34] P.Y. Yue, E.P. Leung, N.K. Mak, R.N. Wong, A simplified method for quantifying cell migration/wound healing in 96-well plates, J. Biomol. Screen. 15 (2010) 427-433.
[35] J.P. Cleutjens, J.C. Kandala, E. Guarda, R.V. Guntaka, K.T. Weber, Regulation of collagen degradation in the rat myocardium after infarction, J. Mol. Cell. Cardiol. 27 (1995) 1281-1292.
[36] J.D. Hood, D.A. Cheresh, Role of integrins in cell invasion and migration, Nat. Rev. Cancer 2 (2002) 91-100.

[37] S.M. Pontier, W.J. Muller, Integrins in breast cancer dormancy, APMIS 116 (2008) 677-684.
[38] S. Mochizuki, Y. Okada, ADAMs in cancer cell proliferation and progression, Cancer Sci. 98 (2007) 621-628.
[39] J.L. Klessner, B.V. Desai, E.V. Amargo, S. Getsios, K.J. Green, EGFR and ADAMs cooperate to regulate shedding and endocytic trafficking of the desmosomal cadherin desmoglein 2, Mol. Biol. Cell 20 (2009) 328-337.
[40] Y. Shintani, S. Higashiyama, M. Ohta, H. Hirabayashi, S. Yamamoto, T. Yoshimasu, H. Matsuda, N. Matsuura, Overexpression of ADAM9 in non-small cell lung cancer correlates with brain metastasis, Cancer Res. 64 (2004) 4190-4196.
[41] J.L. Fry, A. Toker, Secreted and membrane-bound isoforms of protease ADAM9 have opposing effects on breast cancer cell migration, Cancer Res. 70 (2010) 8187-8198.
[42] A. Gschwind, S. Hart, O.M. Fischer, A. Ullrich, TACE cleavage of proamphiregulin regulates GPCR-induced proliferation and motility of cancer cells, Embo J. 22 (2003) 2411-2421.
[43] Q. Zhang, S.M. Thomas, V.W. Lui, S. Xi, J.M. Siegfried, H. Fan, T.E. Smithgall, G.B. Mills, J.R. Grandis, Phosphorylation of TNF-alpha converting enzyme by gastrin-releasing peptide induces amphiregulin release and EGF receptor activation, Proc. Natl. Acad. Sci. USA 103 (2006) 6901-6906.
[44] Y. Izumi, M. Hirata, H. Hasuwa, R. Iwamoto, T. Umata, K. Miyado, Y. Tamai, T. Kurisaki, A. Sehara-Fujisawa, S. Ohno, E. Mekada, A metalloprotease-disintegrin, MDC9/meltrin-gamma/ADAM9 and PKCdelta are involved in TPA-induced ectodomain shedding of membrane-anchored heparin-binding EGF-like growth factor, Embo J. 17 (1998) 7260-7272.
[45] L.C. Bridges, R.D. Bowditch, ADAM-Integrin Interactions: potential integrin regulated ectodomain shedding activity, Curr. Pharm. Des. 11 (2005) 837-847.
[46] J.M. White, Bridges, L.C., Desimone, D.W., Tomczuk, M., Wolfsberg, T.G., , The ADAM Family of Proteases: Proteases in Biology and Disease, Springer, The Netherlands, Vol. 4, 2005.
[47] R.M. Mahimkar, W.H. Baricos, O. Visaya, A.S. Pollock, D.H. Lovett, Identification, cellular distribution and potential function of the metalloprotease-disintegrin MDC9 in the kidney, J. Am. Soc. Nephrol. 11 (2000) 595-603.
[48] S. Hamada, K. Satoh, W. Fujibuchi, M. Hirota, A. Kanno, J. Unno, A. Masamune, K. Kikuta, K. Kume, T. Shimosegawa, MiR-126 acts as a tumor suppressor in pancreatic cancer cells via the regulation of ADAM9, Mol. Cancer Res. 10 (2012) 3-10.

Figure 1

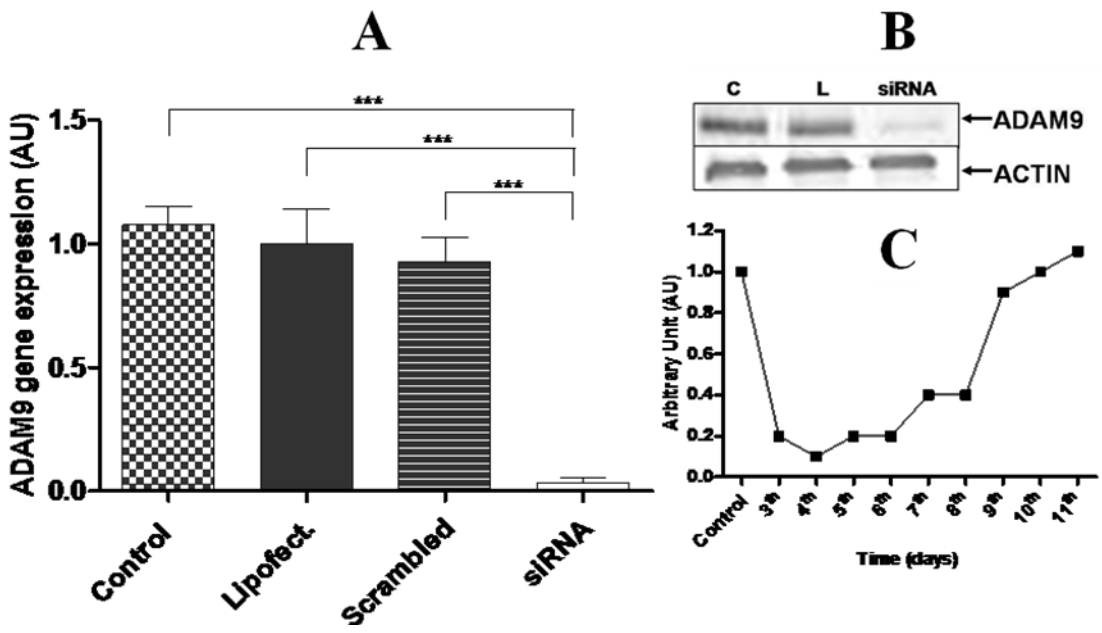

Figure 1 – Silencing of ADAM9. **(A)** Expression of ADAM9 mRNA in RNAi-mediated ADAM9 silenced MDA-MB-231 cells was analysed by qPCR. The values are in arbitrary units (AU) and the *P* value was determined using ANOVA with a Tukey's test comparing control, cells treated with lipofectamine, negative control (scrambled) and cells treated with ADAM9 siRNAs (*** $p < 0.001$). **(B)** Western blotting analysis of MDA-MB-231 cell lysates, with three treatments: cells alone (C), lipofectamine alone (L), and ADAM9 siRNAs using anti-ADAM9RP2 primary antibody and goat anti-rabbit IgG as a secondary antibody. β-actin was used as endogen control. **(C)** The silencing of ADAM9 using siRNAs is transient because it is effective only from the third to the sixth day. The values are in arbitrary units (AU).

Figure 2

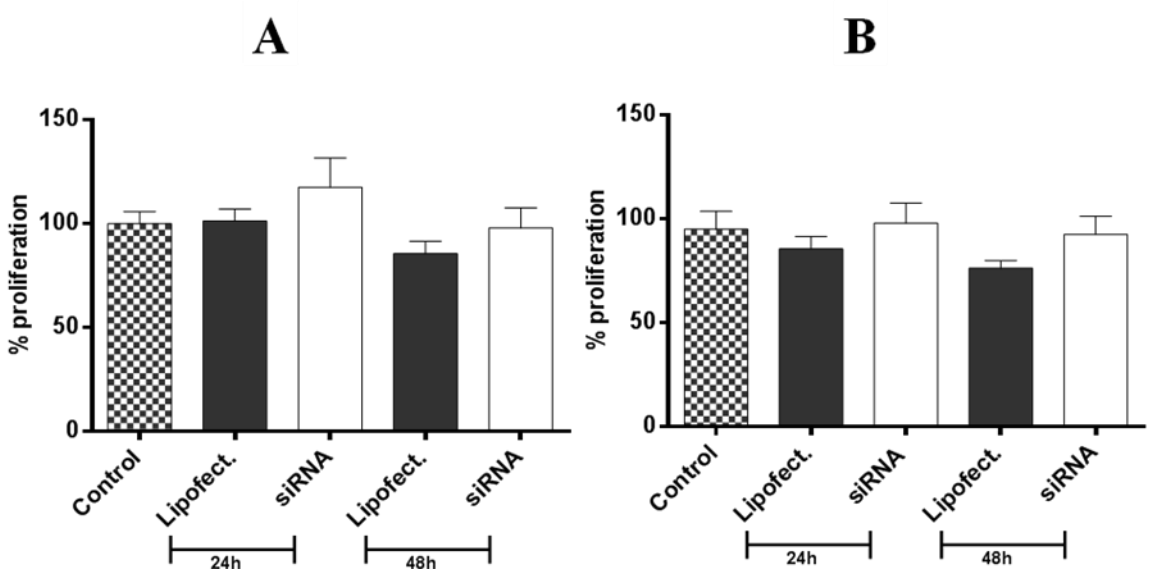

Figure 2 – Proliferation assay. Silencing of ADAM9 had no effect on the proliferation of the MDA-MB-231 cells after three **(A)** or six days **(B)** of transfection. After the different times, the cells were incubated with MTT for 24 hours or 48 hours and compared with control cells or with lipofectamine-treated cells. The absorbance of the samples was measured at 595 nm and the proliferation of control cells was determined as 100%.

Figure 3

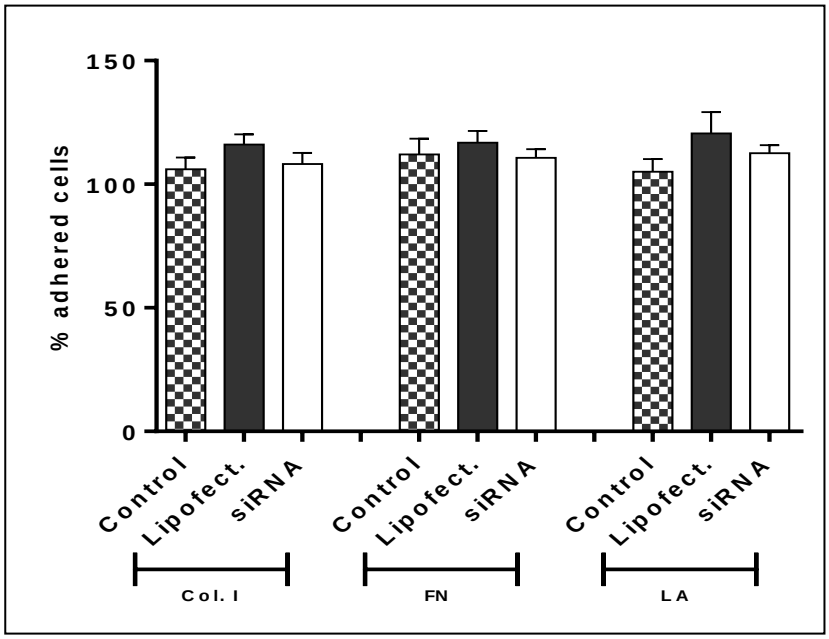

Figure 3 – Adhesion assay. RNAi-mediated ADAM9 silencing had no effect on the adhesion of the MDA-MB-231 under different extracellular matrix proteins, such as Collagen I (Col. I), Fibronectin (FN) and Laminin (LA). The extracellular matrix proteins were coated on the wells of the plate, and on the following day, after the blocking of wells, the cells were allowed to adhere for 45 minutes. The percentage adhesion was determined as described in the materials and methods. The results were compared using a one-way analysis of variance (ANOVA), followed by a Tukey's post-hoc analysis.

Figure 4

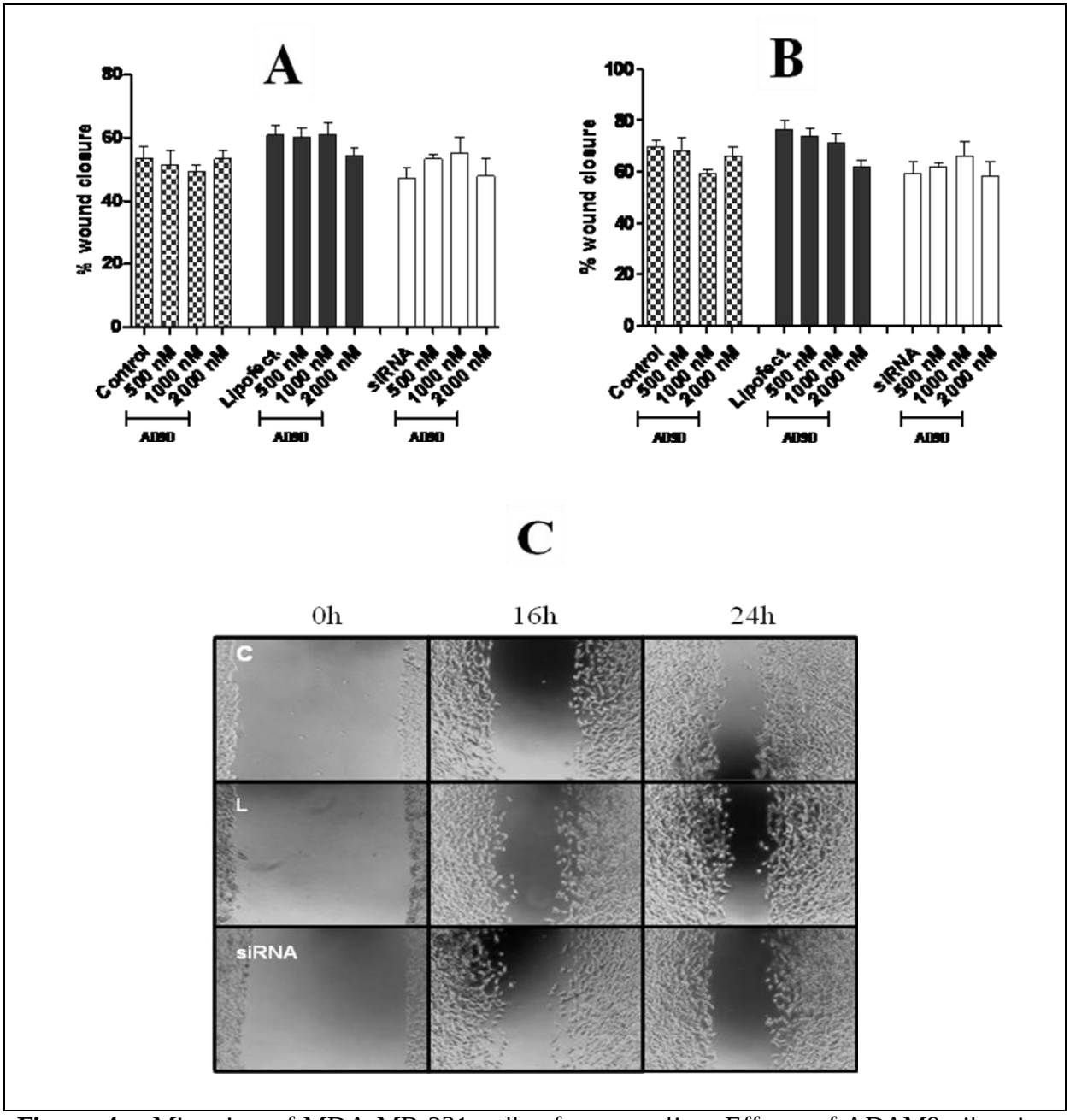

Figure 4 – Migration of MDA-MB-231 cells after wounding. Effects of ADAM9 silencing and ADAM9D recombinant protein on MDA-MB-231cells migration were plotted as a percentage of wound closure in 16 **(A)** or 24 hours **(B)** after wounding. Representative photos of wounds were taken at time zero, 16 h, and 24 hours after wounding **(C)**. In these photos we show pictures representing Control (C), Lipofectamine (L) and siRNA-ADAM9 (siRNA) cells without previous treatment with ADAM9D recombinant protein.

Figure 5

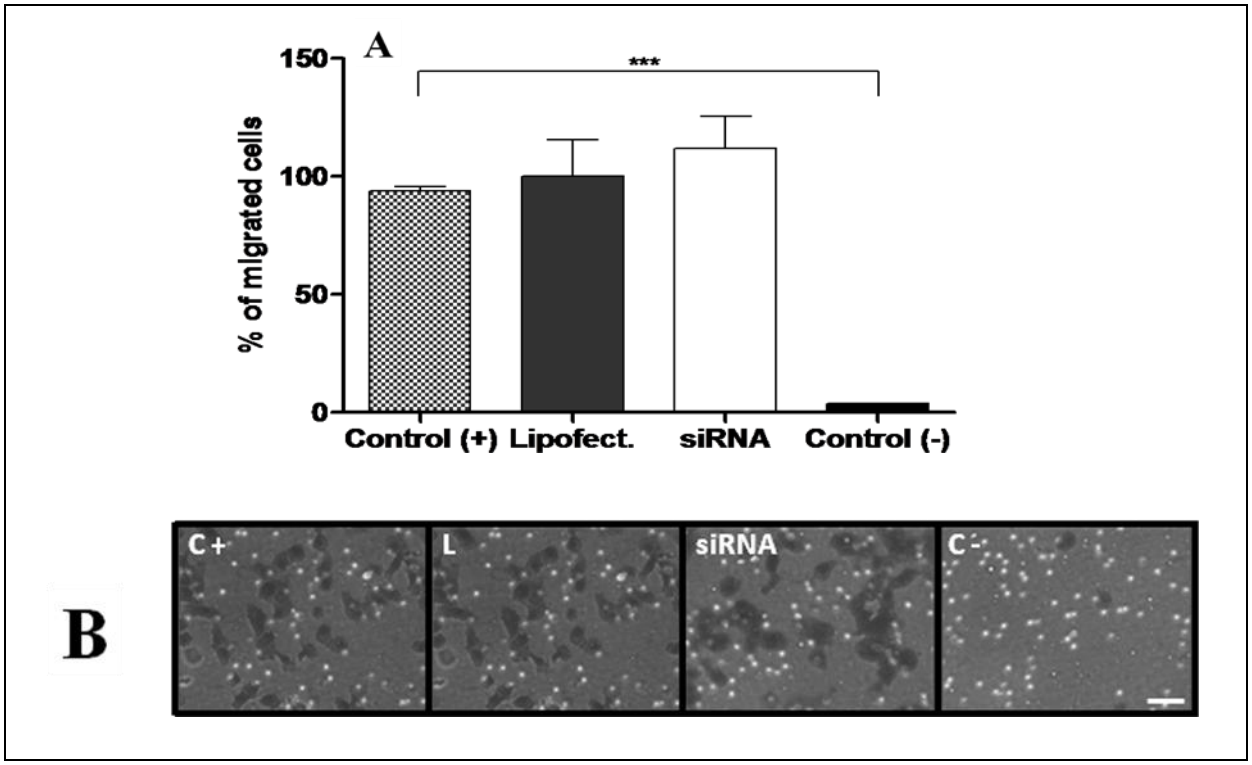

Figure 5 – Effect of RNAi-mediated ADAM9 silencing on migration of MDA-MB-231 cells. **(A)** A transwell migration assay was used to determine the effect of ADAM9 silencing migration of MDA-MB-231 cells. Control cells, lipofectamine-treated cells or siRNA-ADAM9 cells were allowed to migrate towards medium containing 10% FBS for 22 hours. Graphs are representative of three independent experiments. The results were compared using a one-way analysis of variance (ANOVA), followed by a Tukey's post-hoc analysis (*** $p < 0.001$). **(B)** Morphology of cells in the three different treatments: control cells (C+), lipofectamine-treated cells (L), and siRNA-ADAM9 treated cells (siRNA) migrating toward a 10% FBS containing medium. The negative control (C-) was control cells migrating toward a FBS-free medium. Bar represents 10 µm.

Figure 6

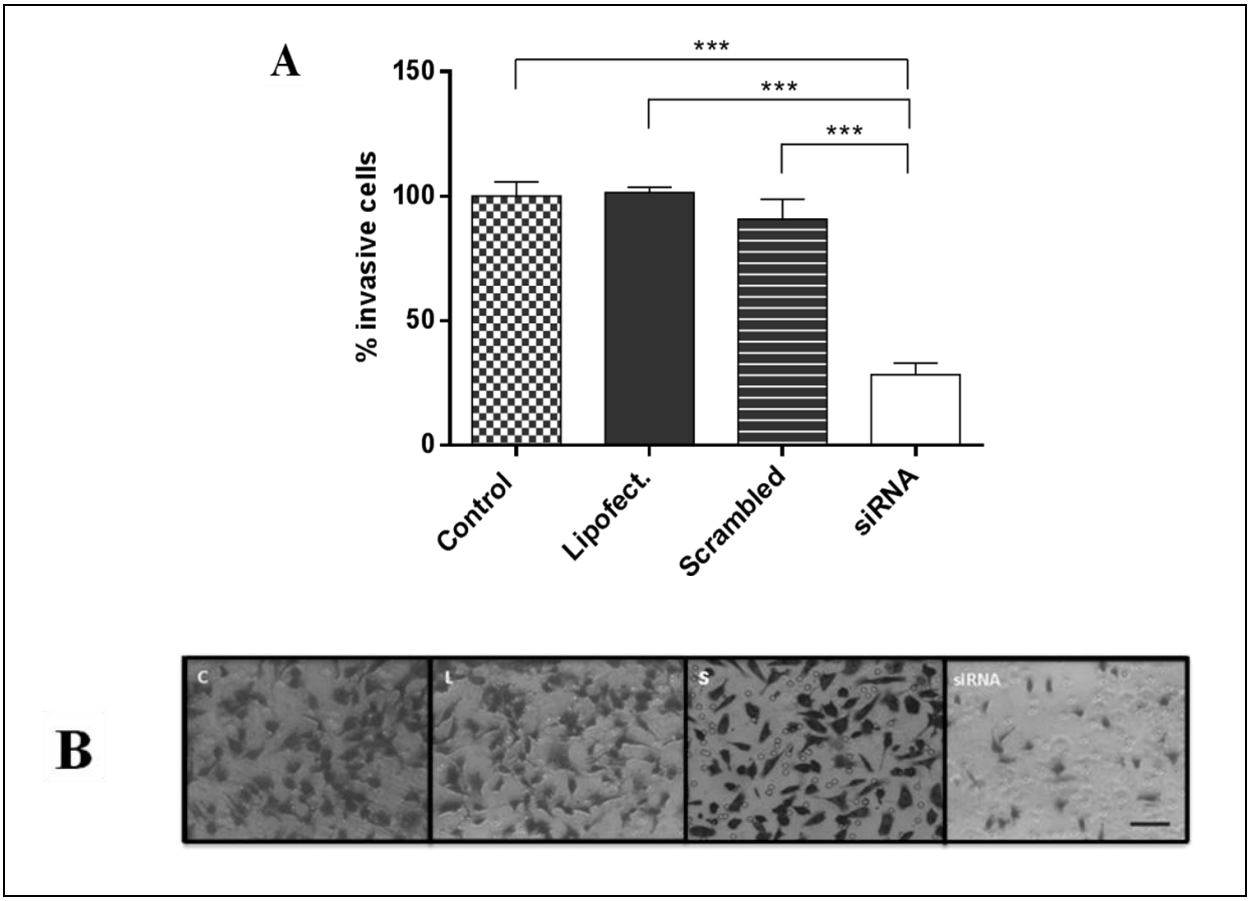

Figure 6 – Effect of RNAi-mediated ADAM9 silencing on the invasion of MDA-MB-231 cells. ADAM9 silencing significantly inhibits the invasion of MDA-MB-231 human breast tumor cells through matrigel compared to the invasion of control cells (A). The cells were plated in wells containing matrigel and FBS was used as a chemoattractant in the lower chamber. The invasive cells were fixed and counted (an average of eight fields from each treatment). The assay was performed in triplicate. The results were compared using a one-way analysis of variance (ANOVA), followed by a Tukey's post-hoc analysis (***$p<0.001$). (B) Cell morphology in the four different treatments: untreated control (C), lipofectamine-treated cells (L), scrambled siRNA-treated control (S), and siRNA-ADAM9 treated cells (siRNA). Bar represents 10 µm.

Figure 7

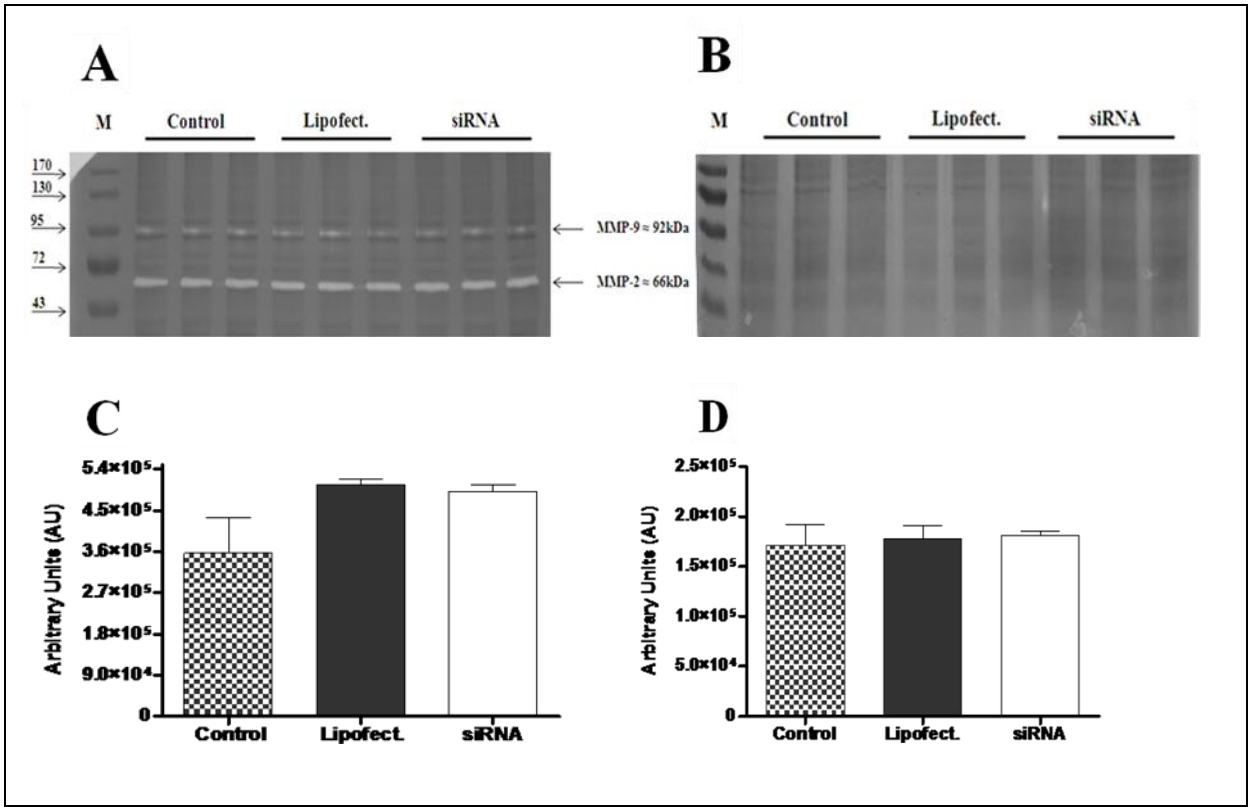

Figure 7 – Analysis of concentration and activity of MMP-2 and MMP-9 in the MDA-MB-231 breast tumor cells. **(A)** Zymography in 1% gelatin-SDS-PAGE or **(B)** EDTA-treated samples. Lane 1: molecular mass marker; lanes 2-4: control cells; lanes 5-7: cells treated with lipofectamine; and lanes 8-10: cells treated with ADAM9 siRNAs (n = 3; 20 µg of total protein was loaded in each lane). **(C)** MMP-2 and **(D)** MMP-9 concentrations were determined by the sum of integrated optical density (IOD) obtained for the intermediate bands. Gels were analyzed by densitometry, and activity was expressed as arbitrary units.

CONSIDERAÇÕES FINAIS

5. CONSIDERAÇÕES FINAIS

Com base nos resultados do presente estudo, foi possível concluir que:

- siADAM9 das células MDA-MB-231 foi eficaz, pois houve o silenciamento gênico e protéico da proteína.
- siADAM9 nas células MDA-MB-231 não provocou mudanças no padrão de adesão dessas células a proteínas da MEC testadas e também não afetou a taxa de proliferação das mesmas, sugerindo o não envolvimento dessa proteína em ambos processos celulares na linhagem testada.
- siADAM9 não foi capaz de inibir a migração *transwell* das células MDAMB-231. Resultado também observado quando realizado o ensaio de *wound healing*, sugerindo que a ADAM9 não participe da migração dessas células. Entretanto, A ADAM9 é essencial para a invasão das células MDA-MB-231 em matrigel.
- siADAM9 alterou a expressão gênica da ADAM15 e MMP2, mas não teve efeito sobre a expressão da ADAM10, ADAM12, ADAM17, VEGF-A, VEGF-C, MMP9, cMYC, Osteopontina e Colágeno XVII.
- A expressão de diferentes genes foi analisada nas células HMVEC-dLyAd-Der e praticamente todos os genes testados apresentaram concentrações em ng/µL similares, com excessão da MMP2 que teve uma maior expressão nessa célula.
- Células endoteliais linfáticas (HMVEC-dLyAd-Der) foram capazes de aderirem a todas as proteínas da MEC testadas.
- As células HMVEC-dLyAd-Der incubadas com o anticorpo anti-β_1 não foram capazes de se ligarem ao Col. IV e LA. Entretanto, quando utilizado FN como proteína imobilizada, essas células não foram capazes a se ligarem a esta proteína quando incubadas com o anticorpo anti-$\alpha_v\beta_5$.

- siADAM9 nas células MDA-MB-231 não provocou mudanças no padrão de adesão das células MDA-MB-231 em condições dinâmicas de fluxo às endoteliais vasculares (HUVEC e HMEC-1) e linfáticas (HMVEC-dLyNeo-Der).
- siADAM9 inibiu a transmigração das células tumorais MDA-MB-231 às células endoteliais vasculares (HUVEC e HMEC-1) e linfáticas (HMVEC-dLyNeo-Der).

Desta forma, conclui-se que o siADAM9 pode ser utilizado como uma estratégia para minimizar o processo de invasão e extravasamento durante a progressão metastática.

6. ANEXOS

6.1. MANUSCRITO III – Publicado em colaboração

Marqueti RC, ***Micocci KC****, Leite RD, Selistre-de-Araujo HS. Nandrolone Inhibits MMP-2 in the Left Ventricle of Rats. Int J Sports Med. 33 (3): 181-185, 2012.* Fator de Impacto 2.374.

Nandrolone Inhibits MMP-2 in the Left Ventricle of Rats

Authors R. C. Marqueti, K. C. Micocci, R. D. Leite, H. S. Selistre-de-Araujo

Affiliation Physiological Sciences, Federal University of São Carlos, Brazil

Key words
- androgenic-anabolic steroid
- left ventricle
- matrix metallopeptidases
- mechanical load exercise

Abstract

The indiscriminate use of anabolic-androgenic steroids has been shown to induce left ventricular dysfunctions. The main objective of the present study was to investigate the effects of nandrolone decanoate on matrix metalloprotease (MMP-2) activity and protein level in the left ventricle (LV) of rats after 7 weeks of mechanical load exercise. Wistar rats were grouped into: sedentary (S); nandrolone decanoate-treated sedentary (AAS); trained without AAS (T) and trained and treated with AAS (AAST). Exercised groups performed a 7-weeks water-jumping program. Training significantly increased the MMP-2 activity by zymography and the protein level by Western blotting analysis. However, the AAS treatment abolished both the increase in MMP activity and protein level induced by exercise. These results suggest that AAS may impair cardiac tissue remodeling which may lead to the heart malfunction.

Introduction

The illicit use of anabolic androgenic steroids (aas) has been associated with cardiovascular diseases [3]. The most widespread cardiovascular consequences of AAS include atherosclerosis (secondary to changes in cholesterol metabolism and platelet function), atrial fibrillation, hypertension, stroke, cardiac hypertrophy, myocardial infarction, ventricular thrombosis, impaired cardiac function, disorders of the haemostatic system and sudden death [1,3,5,10,13,15,21,23,36]. Impaired heart remodeling can lead to myocardial ischemia and cardiomyopathy [35]. Studies using current imaging techniques have supported a left ventricular (LV) diastolic dysfunction [19] and subclinical LV systolic impairment including reduced systolic strain with normal LV ejection fraction in AAS users [9].

Moreover, rocha et al. [34] have evaluated the effects of swimming and anabolic steroids on ventricular function, collagen synthesis, and the local renin-angiotensin system in rats. The AAS exacerbated the cardiac hypertrophy in exercise trained rats and induced defective adaptive remodeling and further deterioration of the cardiac performance. Additionally, the aerobic exercise combined with AAS treatment increased cardiac collagen content associated with activation of the local renin-angiotensin system.

The cardiac remodeling is accompanied by increases in the synthesis and deposition of extracellular matrix (ECM) components as well as increases in extracellular protease activity, especially of matrix metalloproteinases (MMPs) which break down ECM components [20]. However, a decrease in MMP-2 activity in the diabetic heart can contribute to the increased collagen accumulation [37]. Additionally, Linthout and colleagues [37] have reported that the cardiac fibrosis is associated with a dysregulation in extracellular matrix degradation. According to these authors, this condition is attributed to reduced MMP-2 activity, concomitant with Smad 7 and TIMP-2 protein increases and decreased MT1-MMP protein expression.

MMP-2 has been reported to be a direct mediator of ventricular remodeling as well as systolic dysfunction [4]. Previous studies supported by our research group have shown that AAS administration or the association of AAS with load exercise inhibits the activity of MMP-2 impairing tendon [24,27] and skeletal muscle remodeling [25,30]. Several previous papers have demonstrated the negative effects of AAS on the cardiovascular system, however, the effects of AAS on cardiac remodeling, especially on the activity and protein content of MMP-2 has not been previously investigated and it is poorly understood. Accordingly to these findings, the

accepted after revision
September 20, 2011

Bibliography
DOI http://dx.doi.org/10.1055/s-0031-1291252
Published online: January 30, 2012
Int J Sports Med 2012; 33: 181–185 © Georg Thieme Verlag KG Stuttgart · New York
ISSN 0172-4622

Correspondence
Prof. Rita de Cássia Marqueti
Universidade Federal de São Carlos
Ciências Fisiológicas
Washington Luiz
Km 235
Monjolinho
São Carlos
Brazil
13565905
Tel.: +55/163/3518 333
Fax: +55/163/3518 327
marqueti@gmail.com

Downloaded by: Koebenhavns Universitetsbibliotek. Copyrighted material.

hypothesis of this study was that AAS treatment or the combination of ASS and mechanical load exercise can decrease the activity and protein levels of MMP-2 in LV which would impair ECM remodeling while the load exercise could minimize these harmful effects improving the ECM turnover. Therefore, this study focused the presence and activity of MMP-2 in the LV after 7 weeks of mechanical load exercise and aas administration.

Materials and Methods

Animals

20 male rats (Wistar, *Rattus norvegicus albinus*; approximately 200 ± 17 g) were housed at room temperature with access to food and water *ad libitum*. All animal procedures were performed in accordance with the U.S.A. National Research Council's Guide for the Care and Use of Laboratory Animals. The authors also confirmed that the present study meets the ethical standards of the International Journal of Sports Medicine [14]. The experimental procedures of this study were approved by the institutional Ethics Committee in Animal Research of the University (Protocol no. 004/2006).

Experimental groups

Rats were randomly distributed into 4 experimental groups (5 animals/group): sedentary without AAS administration (S); sedentary with AAS administration (AAS); trained (T); and trained with AAS administration (AAST). Animals in the sedentary groups were not submitted to any type of physical activity. Animals in trained groups were exposed to jump training in a plastic tube of 25 cm in diameter filled with water at constant temperature of 30 ± 2 °C to a height of 30 cm. After a pre-training week, the animals started the experimental training protocol, which consisted of 7 weeks of training with 5 training days (1 session per day) per week.

AAS administration

Rats received 5 mg/kg of body mass (supraphysiological dose) of Deca-Durabolin (nandrolone decanoate; Organon do Brasil, São Paulo, Brazil) administered subcutaneously in their backs, twice a week. This dosage is comparable to the dosage frequently used by athletes [32]. The experimental groups with no AAS treatment (S and T) received the vehicle only (peanut oil with benzyl alcohol). The treatment started in the first training week, and continued for 7 weeks.

Training protocol

To reduce stress, the animals were adapted to water in the pre-training week. This adaptation consisted of sessions of weight lifting (50% body weight load), once a day for 5 days in water at 30 ± 2 °C. The jump training was induced by the instinctive reactions of rats: when animals are underwater they make an effort to jump for breathing. The overload was attached to the animal's chest by means of a vest fitted to its body. The numbers of sets (2–4) and repetitions (5–10) were adjusted daily and gradually increased. All sessions were performed in the afternoon after 4 p.m. After the pre-training week, animals were exposed to the experimental training protocol, which consisted of jumps in water at 30 ° ± 2 °C, with the overload adjusted according to the animal's body weight, as previously described [8, 24]. Briefly, the training protocol consisted of a first training week, in which the animal performed 4 sets of 10 jumps with a rest period of 30 s between sets and overload at 50% of body weight. In the next 6 weeks, the training protocol consisted of the same number of sets (4), jumps (10), and resting intervals (30 s between sets), but with increased overload (5% increase per wk), so that in the last week it was 80% of body weight. An observer was present during all the training sessions. All animals were weighed 3 times/wk. The depth of the water column and the overload constituted barriers to avoid the rats to rest on their tails.

Tissue preparation

After 7 experimental weeks, animals were euthanized by decapitation immediately after the last training session. Next, the hearts were removed and left ventricle was isolated, frozen in liquid nitrogen and stored at −80 °C for analysis.

Gelatin zymography

Gelatin zymography of MMP-2 was performed as previously described for cardiac muscle extracts [8]. Frozen LV were washed 3 times with cold saline and then 25 mg of LV were incubated in 2 mL of extraction buffer (10 mM cacodylic acid [pH 5.0]; 0.15 M NaCl; 1 µM $ZnCl_2$; 20 mM $CaCl_2$; 1.5 mM NaN_3; 0.01% Triton X-100 [v/v]), at 4 °C for 24 h. After this period, the solution was centrifuged for 10 min (13 000 x g at 4 °C). 20 µg of total protein measured with the BCA Protein Assay Kit (Pierce, Rockford, IL, USA) were loaded and applied in each lane of sodium dodecyl sulfate (SDS)–10% polyacrylamide gels prepared with 1 mg/mL gelatin. After electrophoresis, the gels were washed twice for 20 min in 2.5% Triton X-100 to remove the SDS. Gels were rinsed and incubated in buffer substrate (50 mM Tris-HCl (pH 8.0); 5 mM $CaCl_2$; 0.02% NaN_3) at 37 °C for 20 h. Gels were stained with Coomassie brilliant blue for 1.5 h and destained with acetic acid:methanol:water (1:4:5) for visualization of the activity bands. The gels were photographed with a Canon G6 Power Shot 7.1 mega pixels camera.

Densitometric quantitative analysis of the MMP-2 protein bands seen in the zymography gels were performed using the Gene Tools version 3.06. software (Syngene, Cambridge, UK).

Western blotting

MMP-2 protein content was determined by Western blotting. The cardiac tissue was homogenized in lysis buffer as previously described by Marsolais and colleagues [28]. 100 µg of protein from the LV homogenate were separated on a 12% SDS-polyacrylamide gel electrophoresis (SDS-PAGE). MMP-2 (2C1: sc-13594; Santa Cruz) and anti-α-actin (sc-1616, Santa Cruz) were detected with each specific antibody. The α -Actin expression levels were used to normalize the results. The bands were analyzed using the Gene Tools version 3.06 software (Syngene, Cambridge, UK).

Statistical analysis

Data were presented as mean ± SEM. The statistical analysis was initially performed by the Shapiro-Wilk test for normality and the homoscedasticity test (Bartlett criterion). All variables showed normal distribution and homoscedasticity and the 2-way ANOVA was used (taking into consideration the intervening variables T vs. AAS) followed by the Tukey post hoc test for multiple comparisons. In all calculations, a critical significance level of 5% ($P < 0.05$) was fixed. All data were analysed using the Statistica 7.0 software package (Stat. Soft. Tusa Inc., OK, USA).

Downloaded by: Koebenhavns Universitetsbibliotek. Copyrighted material.

Results

Gelatinolytic activities in ventricles were detected by zymography in 3 well-defined bands (75 kDa pro-MMP-2, 72 kDa intermediate-MMP-2 and 62 kDa active-MMP-2 [6] in all evaluated groups (**Fig. 1a**). This activity was probably due to the action of matrix metallopeptidases (MMPs) because it was inhibited by ethylenediamine tetraacetic acid (EDTA; not shown). The pro and intermediate-MMP-2 did not change significantly in any group ($p > 0.05$) (**Fig. 1b**). However, the training significantly increased the band of active-MMP-2 in zymography (S, $p = 0.008$; AAS, $p = 0.001$; and AAST, $p = 0.003$) as well as its protein content by Western blotting analysis (**Fig. 2**) ($p < 0.001$, in all groups). Taken together, these results suggest that AAS treatment abolished the increase in MMP-2 activity and protein level induced by exercise.

Discussion

The present study provides new information regarding the negative effects of AAS on the heart. We identified for the first time that the AAS associated with exercise induce an inappropriate cardiac remodeling by restraining the increase in MMP-2 activ-

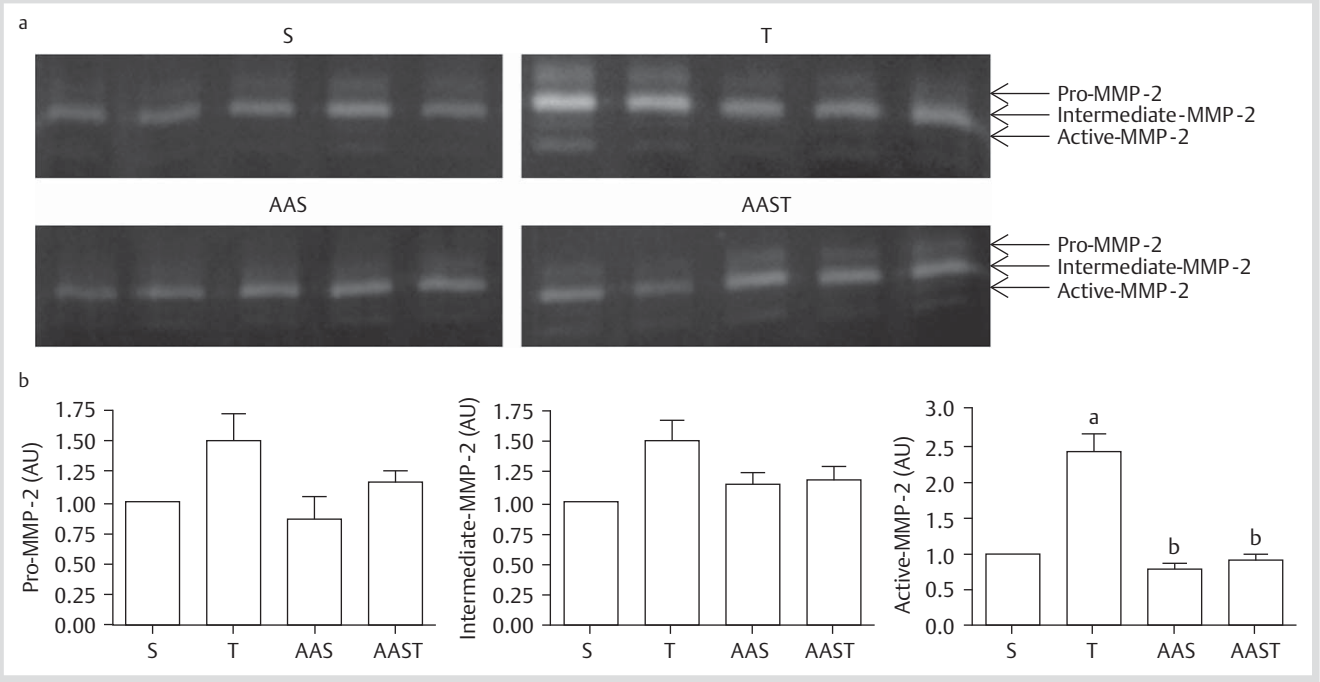

Fig. 1 Effect of training and AAS treatment on pro-(latent), intermediate and active MMP-2 bands by zymography in 1 % gelatin-SDS-PAGE on LV. Before Coomassie staining, the gel was incubated for 20 h in substrate buffer at 37 °C. **a** Bands of MMP activity in gelatin zymograms; **b** Gels were analyzed by densitometry and the activity (62 kDa) was expressed as arbitrary units. Data are reported as mean ± SEM ($P < 0.05$). a = different from sedentary and b = different from trained group.

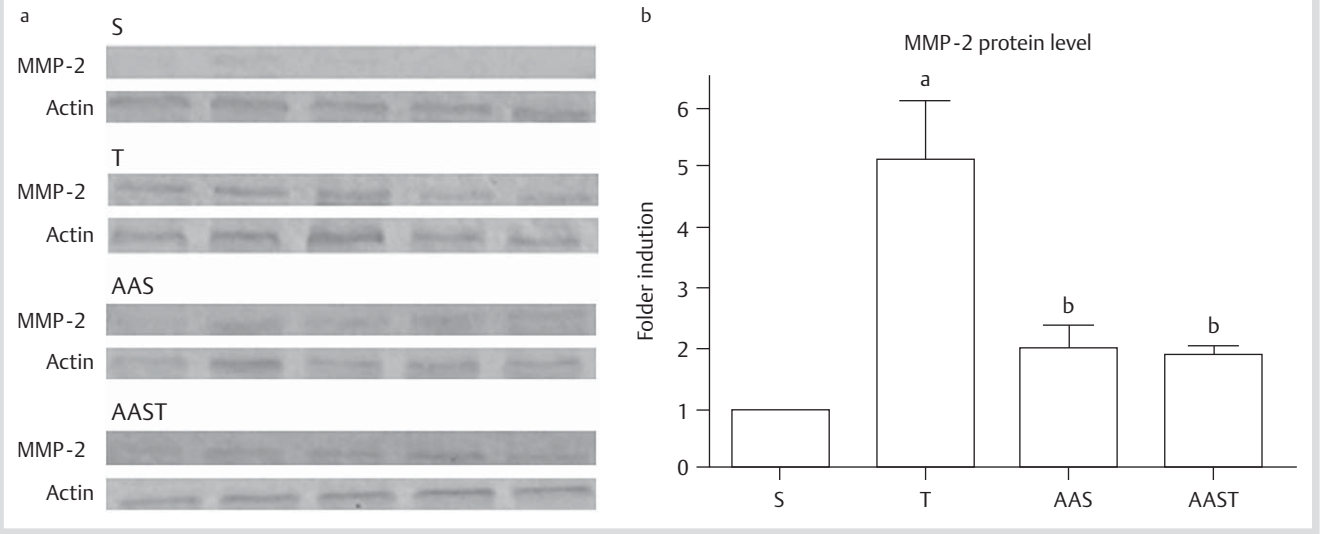

Fig. 2 **a** Western blotting analysis of MMP-2 content in extracts of LV. **b** Quantitative assessment of MMP-2 levels by densitometry. Data are reported as mean ± SEM ($P < 0.05$). a = different from sedentary and b = different from trained group.

Downloaded by: Koebenhavns Universitetsbibliotek. Copyrighted material.

ity and protein level in the LV. These findings have clinical relevance since they indicate further risk factors to cardiac events for AAS users in sports field.

The direction and extent of cardiovascular remodeling is determined by an active and dynamic process in the extracellular matrix including the role of MMPs [17,18]. Numerous studies have shown that alteration in the degradation of extracellular matrix (ECM) by MMPs, especially the MMP-2, is involved in cardiovascular disorders, including atherosclerosis, congestive heart failure, myocardial infarction and cardiomyopathy [2,11].

Additionally, studies have reported that adverse cardiac events and AAS abuse are linked in many case reports of young athletes including acute myocardial infarction [12,13,23], sudden cardiac death [16], ventricular fibrillation with exercise [29], atrial fibrillation and development of dilative cardiomyopathy [21]. Chronic treatment with anabolic steroids in rats, impairs tonic cardiac autonomic regulation, which may induce arrhythmia and sudden cardiac death [31]. Interestingly, heavy resistance exercise can expose AAS users to highly increased pressure loads and lead to a state of systolic failure [1] and cardiac ischemia by exaggerated oxygen demand at peak exercise [35]. Moreover, in AAS users an enlarged interventricular septal wall thickness on echocardiography was observed compared to nonusers and controls [19]. We speculate that these changes may be associated to poor cardiac remodeling.

Our results clearly demonstrated that AAS combined with exercise inhibit the increase of both MMP protein levels and activity and thus impair tissue remodeling. Increased MMP-2 activity is important to maintain tissue turnover and normal cardiac function after exercise training as a physiological mechanism to adaptation [38]. In the same way, our data showed that exercise training increased MMP-2 activity and protein level on LV. However, the combination of AAS and exercise impair the ECM cardiac remodeling and this fact could be related to cardiac dysfunction events as intensively described in the literature.

Previous studies using the same experimental model of this current work showed that the combination of 2 types of AAS caused changes in morphology, as peripheral fibrosis, and decreases in the activity of MMP-2 impairing calcaneal tendon remodeling [24]. Only nandrolone treatment not only caused a reduction in MMP-2 but also inhibited the effect of training thus impairing calcaneal tendon (CT), superficial flexor tendon (SFT), deep flexor tendon (DFT) [27] and skeletal muscle remodeling [25]. Finally, the biomechanical analysis showed that the combination of AAS and training led to greater stiffness in all 3 tendons evaluated which may weaken tendons and predispose to future injuries and ruptures [26]. These data taken together suggest that not only tendon and skeletal muscle but also LV, as focused on in this work, are negatively affected by AAS especially when these drugs are combined with exercise.

Interestingly, training associated with the AAS negatively affected the vascularization of CT, SFT and DFT (data not published). Although the effect of AAS on the blood vessels is still unclear, the training alone increased the mRNA of VEGF mRNA expression in the soleus muscle in rats, the combination of training and AAS administration inhibited this effect [30]. Since VEGF plays a critical role in endothelial cell proliferation and angiogenesis which is strongly needed to respond to the increased oxygen demand induced by the exercise [33], these findings are suggestive of impaired neovascularization in AAS users. It is possible to speculate that AAS could reduce the VEGF expression on LV impairing the cardiac circulation. However, more studies are necessary to clarify this hypothesis.

In summary, our data have shown that the AAS treatment in association with training suppressed the training-induced increase of MMP-2 activity and protein level, which may compromise the cardiac tissue turnover and may lead to the failure of heart functionality, possibly in order to increase the ECM stiffness. We suggest that several cardiac problems linked to misuse of AAS can occur in response to poor remodeling related to reduced MMP-2 function. However, these mechanisms are unclear up to now and this hypothesis needs to be better studied.

Acknowledgements

The authors also acknowledge the financial support from the State of São Paulo Funding Agency (FAPESP). RCM was a recipient of a PhD FAPESP fellowship (no. 06/50986-6).

References

1 *Ahlgrim C*, *Guglin M*. Anabolics and cardiomyopathy in a bodybuilder: case report and literature review. J Card Fail 2009; 15: 496–500
2 *Ahmed SH*, *Clark LL*, *Pennington WR*, *Webb CS*, *Bonnema DD*, *Leonardi AH*, *McClure CD*, *Spinale FG*, *Zile MR*. Matrix metalloproteinases/tissue inhibitors of metalloproteinases: relationship between changes in proteolytic determinants of matrix composition and structural, functional, and clinical manifestations of hypertensive heart disease. Circulation 2006; 113: 2089–2096
3 *Baggish AL*, *Weiner RB*, *Kanayama G*, *Hudson JI*, *Picard MH*, *Hutter AM Jr*, *Pope HG Jr*. Long-term anabolic-androgenic steroid use is associated with left ventricular dysfunction. Circ Heart Fail 2010; 3: 472–476
4 *Bergman MR*, *Teerlink JR*, *Mahimkar R*, *Li L*, *Zhu BQ*, *Nguyen A*, *Dahi S*, *Karliner JS*, *Lovett DH*. Cardiac matrix metalloproteinase-2 expression independently induces marked ventricular remodeling and systolic dysfunction. Am J Physiol 2007; 292: H1847–H1860
5 *Casavant MJ*, *Blake J*, *Griffith A*, *Yates A*, *Copley LM*. Consequences of use on anabolic androgenic steroids. Pediatric Clin North Am 2007; 54: 677–690
6 *Cheung PY*, *Sawicki G*, *Wozniak M*, *Wang W*, *Radomski MW*, *Schulz R*. Matrix metalloproteinase-2 contributes to ischemia-reperfusion injury in the heart. Circulation 18 2000; 101: 1833–1839
7 *Cleutjens JPM*, *Kandala JC*, *Guarda E*, *Guntaka RV*, *Weber KT*. Regulation of collagen degradation in rat myocardium after infartion. J Mol Cell Cardiol 1995; 27: 1281–1292
8 *Cunha TS*, *Tanno AP*, *Costa Sampaio Moura MJ*, *Marcondes FK*. Influence of high intensity training and anabolic steroids treatment on rat tissue glycogen content. Life Sci 2005; 77: 1030–1043
9 *D'Andrea A*, *Caso P*, *Salerno G*, *Scarafile R*, *De Corato G*, *Mita C*, *Di Salvo G*, *Severino S*, *Cuomo S*, *Liccardo B*, *Esposito N*, *Calabro R*. Left ventricular early myocardial dysfunction after chronic misuse of anabolic androgenic steroids: a Doppler myocardial and strain imaging analysis. Br J Sports Med 2007; 41: 149–155
10 *Dhar R*, *Stout CW*, *Link MS*, *Homoud MK*, *Weinstock J*, *Estes NA 3rd*. Cardiovascular toxicities of performance-enhancing substances in sports. Mayo Clin Proc 2005; 80: 1307–1315
11 *Dollery CM*, *McEwan JR*, *Henney AM*. Matrix metalloproteinases and cardiovascular disease. Circ Res 1995; 77: 863–868
12 *Godon P*, *Bonnefoy E*, *Guérard S*, *Munet M*, *Velon S*, *Brion R*, *Touboul P*. Myocardial infarction and anabolic steroid use. A case report. Arch Mal Coeur Vaiss 2000; 93: 879–883
13 *Halvorsen S*, *Thorsby PM*, *Haug E*. Acute myocardial infarction in a young man who had been using androgenic anabolic steroids. Tidsskr Nor Laegeforen 2004; 124: 170–172
14 *Harriss DJ*, *Atkinson G*. Update – Ethical Standards in Sport and Exercise Science Research. Int J Sports Med 2011; 32: 819–821
15 *Hartgens F*, *Kuipers H*. Effects of androgenic-anabolic steroids in athletes. Sports Med 2004; 34: 513–554
16 *Hausmann R*, *Hammer S*, *Betz P*. Performance enhancing drugs (doping agents) and sudden death - a case report and review of the literature. Int J Legal Med 1998; 111: 261–264

Downloaded by: Koebenhavns Universitetsbibliotek. Copyrighted material.

17 *Herity NA*, *Ward MR*, *Lo S*, *Yeung AC*. Review: clinical aspects of vascular remodeling. J Cardiovasc Electrophysiol 1999; 10: 1016–1024
18 *Janssens S*, *Lijnen HR*. What has been learned about the cardiovascular effects of matrix mettaloproteinases from mouse models? Cardiovasc Res 2006; 69: 585–594
19 *Krieg A*, *Scharhag J*, *Albers T*, *Kindermann W*, *Urhausen A*. Cardiac tissue Doppler in steroid users. Int J Sports Med 2007; 28: 638–643
20 *Kukacka J*, *Průsa R*, *Kotaska K*, *Pelouch V*. Matrix metalloproteinases and their function in myocardium. Biomed Pap Med Fac Univ Palacky Olomouc Czech Repub 2005; 149: 225–236
21 *Lau DH*, *Stiles MK*, *John B*, Shashidhar *Young GD*, *Sanders P*. Atrial fibrillation and anabolic steroid abuse. Int J Cardiol 2007; 117: 86–87
22 *Liu PY*, *Death AK*, *Handelsman DJ*. Androgens and cardiovascular disease. Endocr Rev 2003; 24: 313–340
23 *Lyngberg KK*. Myocardial infarction and death of a body builder after using anabolic steroids. Ugeskr Laeger 1991; 153: 587–588
24 *Marqueti RC*, *Parizotto NA*, *Chriguer RS*, *Perez SEA*, *Selistre-de-Araujo HS*. Androgenic-anabolic steroids associated with mechanical loading inhibit matrix metallopeptidase activity and affect the remodeling of the achilles tendon in rats. Am J Sport Med 2006; 34: 1274–1280
25 *Marqueti RC*, *Prestes J*, *Stotzer US*, *Paschoal M*, *Leite RD*, *Perez SE*, *Selistre de Araujo HS*. MMP-2 jumping exercise and nandrolone in skeletal muscle. Int J Sports Med 2007; 29: 559–563
26 *Marqueti RC*, *Prestes J*, *Wang CC*, *Ramos OH*, *Perez SE*, *Nakagaki WR*, *Carvalho HF*, *Selistre-de-Araujo HS*. Biomechanical responses of different rat tendons to nandrolone decanoate and load exercise. Scand J Med Sci Sports 2010 Jul 29. [Epub ahead of print]. PMID: 20673248
27 *Marqueti RC*, *Prestes J*, *Paschoal M*, *Ramos OH*, *Perez SE*, *Carvalho HF*, *Selistre-de-Araujo HS*. Matrix metallopeptidase 2 activity in tendon regions: effects of mechanical loading exercise associated to anabolic-androgenic steroids. Eur J Appl Physiol 2008; 104: 1087–1093
28 *Marsolais D*, *Duchesne E*, *Côté CH*, *Frenette J*. Inflammatory cells do not decrease the ultimate tensile strength of intact tendons in vivo and in vitro: protective role of mechanical loading. J Appl Physiol 2007; 102: 11–17
29 *Nieminen MS*, *Rämö MP*, *Viitasalo M*, *Heikkilä P*, *Karjalainen J*, *Mäntysaari M*, *Heikkilä J*. Serious cardiovascular side effects of large doses of anabolic steroids in weight lifters. Eur Heart J 1996; 17: 1576–1583
30 *Paschoal M*, *de Cássia Marqueti R*, *Perez S*, *Selistre-de-Araujo HS*. Nandrolone inhibits VEGF mRNA in rat muscle. Int J Sports Med 2009; 30: 775–778
31 *Pereira-Junior PP*, *Chaves EA*, *Costa-E-Sousa RH*, *Masuda MO*, *de Carvalho AC*, *Nascimento JH*. Cardiac autonomic dysfunction in rats chronically treated with anabolic steroid. Eur J Appl Physiol 2006; 96: 487–494
32 *Pope HG Jr*, *Katz DL*. Affective and psychotic symptoms associated with anabolic steroids use. Am J Psychiat 1988; 145: 487–490
33 *Prior BM*, *Lloyd PG*, *Yang HT*, *Terjung RL*. Exercise-induced vascular remodeling. Exerc Sport Sci Rev 2003; 31: 26–33
34 *Rocha FL*, *Carmo EC*, *Roque FR*, *Hashimoto NY*, *Rossoni LV*, *Frimm C*, *Anéas I*, *Negrão CE*, *Krieger JE*, *Oliveira EM*. Anabolic steroids induce cardiac renin-angiotensin system and impair the beneficial effects of aerobic training in rats. Am J Physiol Heart Circ Physiol 2007; 293: 3575–3583
35 *Sullivan ML*, *Martinez CM*, *Gennis P*, *Gallagher EJ*. The cardiac toxicity of anabolic steroids. Prog Cardiovasc Dis 1998; 41: 1–15
36 *Thiblin I*, *Petersson A*. Pharmacoepidemiology of anabolic androgenic steroids: a review. Fundam Clin Pharmacol 2005; 19: 27–44
37 *Van Linthout S*, *Seeland U*, *Riad A*, *Eckhardt O*, *Hohl M*, *Dhayat N*, *Richter U*, *Fischer JW*, *Böhm M*, *Pauschinger M*, *Schultheiss HP*, *Tschöpe C*. Reduced MMP-2 activity contributes to cardiac fibrosis in experimental diabetic cardiomyopathy. Basic Res Cardiol 2008; 103: 319–327
38 *Xu X*, *Wan W*, *Powers AS*, *Li J*, *Ji LL*, *Lao S*, *Wilson B*, *Erikson JM*, *Zhang JQ*. Effects of exercise training on cardiac function and myocardial remodeling in post myocardial infarction rats. J Mol Cell Cardiol 2008; 44: 114–122

Downloaded by: Koebenhavns Universitetsbibliotek. Copyrighted material.

6.2. MANUSCRITO IV – Publicado em colaboração

Cancino J, Paino IM, ***Micocci KC****, Selistre-de-Araujo HS, Zucolotto V. In vitro nanotoxicity of single-walled carbon nanotube-dendrimer nanocomplexes against murine myoblast cells. Toxicol Lett. 219 (1): 18-25, 2013.* Fator de Impacto 3.706.

Toxicology Letters 219 (2013) 18–25

Contents lists available at SciVerse ScienceDirect

Toxicology Letters

journal homepage: www.elsevier.com/locate/toxlet

In vitro nanotoxicity of single-walled carbon nanotube–dendrimer nanocomplexes against murine myoblast cells

J. Cancino[a,*], I.M.M. Paino[a], K.C. Micocci[b], H.S. Selistre-de-Araujo[b], V. Zucolotto[a]

[a] Physics Institute of São Carlos, University of São Paulo (IFSC-USP), São Carlos, São Paulo, Brazil
[b] Department of Physiology, Federal University of São Carlos, São Carlos, São Paulo, Brazil

HIGHLIGHTS

- Effects of SWCNT and PAMAM nanomaterials on the C2C12 murine cell line.
- The toxicity of SWCNT and PAMAM in C2C12 cells was correlated with the charge.
- PAMAM inhibited proliferation and cell adhesion more pronouncedly than SWCNT.
- First nanotoxicological study with C2C12 cells and SWCNT and PAMAM nanomaterials.

ARTICLE INFO

Article history:
Received 6 November 2012
Received in revised form 18 February 2013
Accepted 19 February 2013
Available online xxx

Keywords:
Nanotoxicity
Nanomedicine
In vitro toxicology
C2C12 cell line
SWCNT
PAMAM dendrimer

ABSTRACT

Single-wall carbon nanotubes (SWCNTs) and polyamidoamine dendrimers (PAMAM) have been proposed for a variety of biomedical applications. The combination of both molecules makes this new composite nanomaterial highly functionalizable and versatile to theranostic and drug-delivery systems. However, recent toxicological studies have shown that nanomaterials such as SWCNTs and PAMAM may have high toxicity in biological environments. Aiming to elucidate such behavior, *in vitro* studies with different cultured cells have been conducted in the past few years. This study focuses on the effects of SWCNT–PAMAM nanomaterials and their individual components on the C2C12 murine cell line, which is a mixed population of stem and progenitor cells. The interactions between the cells and the nanomaterials were studied with different techniques usually employed in toxicological analyses. The results showed that SWCNT–PAMAM and PAMAM inhibited the proliferation and caused DNA damage of C2C12 cells. Data from flow cytometry revealed a less toxicity in C2C12 cells exposed to SWCNT compared to the other nanomaterials. The results indicated that the toxicity of SWCNT, SWCNT–PAMAM and PAMAM in C2C12 cells can be strongly correlated with the charge of the nanomaterials.

© 2013 Elsevier Ireland Ltd. All rights reserved.

1. Introduction

Nanotoxicology is a field that uses concepts from nanobiosciences to understand the potential toxic impacts of nanomaterials on biological systems. (Arora et al., 2012; Boulaiz et al., 2011; Love et al., 2012). Some properties of nanomaterials have been shown to change their biological or toxicological effects in biological systems. A comprehensive characterization of these systems is required for better understanding of how different nanomaterial properties affect their biological responses (Warheit, 2008). It is known that the interaction between nanomaterials is, in many cases, facilitated by the compatibility of their sizes and also by the charges of their surface modifications (Aillon et al., 2009; Ebbesen and Jensen, 2006). To promote the safe development of nanomedicine, especially in drug-delivery and theranostic (therapeutic and diagnostic) systems, it is essential to evaluate the potential adverse health consequences. This requires a systematic investigation of the influence of properties such as the composition and the size of nanomaterials using different methodologies for cytotoxicity studies.

Special attention has to be paid to the toxicity of carbon nanotubes (CNTs) because research in the areas of biomedical devices has focused on using this nanomaterial in biosensors and as drug and vaccine delivery vehicles (Monteiro-Riviere et al., 2005; Smart et al., 2006). The toxicity of CNTs is strongly correlated with their physicochemical properties, for example, their structure, length, surface area, metallic contamination and surface functionalization (Baughman et al., 2002; Pastorin, 2009). One of the major problems encountered in the investigation of CNT toxicity is the

* Corresponding author at: Laboratório de Nanomedicina e Nanotoxicologia, Grupo de Biofísica Molecular, Instituto de Física de São Carlos, Universidade de São Paulo, Avenida Sãocarlense, 400, CEP: 13560-970 São Carlos, São Paulo, Brazil. Tel.: +55 16 3373 9875; fax: +55 16 3371 5381.
E-mail addresses: jcancino@ursa.ifsc.usp.br, jucancino@yahoo.com.br (J. Cancino).

0378-4274/$ – see front matter © 2013 Elsevier Ireland Ltd. All rights reserved.
http://dx.doi.org/10.1016/j.toxlet.2013.02.009

tendency to aggregate (Smart et al., 2006). This tendency increases with the enlargement of the surface area, which gives the nanomaterial a greater contact area and thus a higher capacity for the absorption and transport of toxic substances, especially when long-term contact occurs, increasing the chances of damage to biological organisms (Kunzmann et al., 2011; Smart et al., 2006).

In the context of biomedical applications, the chemical functionalization of CNTs or the adsorption of biomolecules shows the most promise. Current studies have shown that upon changing some physical characteristics of CNT functionalized for drug or vaccine delivery, a lower toxicity is observed, compared to unmodified ones. In addition, it is also interesting to determine which functionalizations are most effective at enhancing the biocompatibility of CNTs in specific applications. One of the promising functionalized molecules that could decrease the toxicity of CNT is dendrimer molecules.

Dendrimers, first described in 1985, are well-defined, highly branched macromolecules in the nanoscale range with precisely controlled chemical structures. They are used extensively as carriers for drug delivery due to the high level of control over aspects of dendritic architecture such as size, branching density and surface functionality (Crespilho et al., 2007; Menjoge et al., 2010; Mintzer and Grinstaff, 2011). PAMAM dendrimers are one of the most intensively investigated members of this class from a technological and toxicological point of view. Some studies showed that cationic dendrimers could induce disruptions in cell membranes resembling pore structures (Cancino et al., 2013; Jones et al., 2012). Furthermore, cationic dendrimers were shown to induce apoptosis and negatively influence proliferation in a murine macrophage cell line (Sharifi et al., 2012).

Despite the intensive research efforts of various groups worldwide, information about cytotoxicity in biological systems exposed to nanomaterials is often inconsistent and even contradictory. Barktur et al. characterized the effects of exposure to SWCNTs on interleukin-8 (IL-8) expression in human alveolar epithelial cells (A549). When A549 cells were exposed to low concentrations of SWCNTs, IL-8 expression progressively increased; the induced IL-8 expression kept increasing even after the removal of SWCNTs from the medium (Baktur et al., 2011). Wörle-Knirsch et al. used the MTT assay to show that A549 cells incubated with carbon nanotubes exhibited a strong cytotoxic effect, reaching approximately 50% by 24 h (Worle-Knirsch et al., 2006). Chen et al. studied the exposure of a pancreatic cancer cell line (BXPC3) to single-walled carbon nanotubes modified with PAMAM dendrimers (SWCNT–PAMAM). The results showed that SWCNT–PAMAM complexes could be transfected into human pancreatic cancer cells by the process of cell pinocytosis and could be located in the cytoplasm, lysosomes and in the nuclei. Accordingly to the authors, although SWCNT–PAMAM were inside the cells, they did not exhibit toxicity to pancreatic cancer cells, which means that they can be applied in drug-delivery systems (Chen et al., 2010). Although a considerable number of nanotoxicological studies have been conducted using different cell lines, it is still important to investigate the effects in primary cell cultures because these model systems are more similar to the *in vivo* situation (Kunzmann et al., 2011).

Skeletal muscle satellite cells are a mixed population of stem and progenitor cells located under the muscle fiber sarcolemma (Martinello et al., 2011). They respond to damage induced by disease or exercise and become activated, proliferating and differentiating to form new or repair existing myotubes, in regeneration that strictly recapitulates the embryonic myogenic processes (Martinello et al., 2011; Taketo and Sonoshita, 2002). Their successful participation in this vital process is influenced by their immediate cellular microenvironment. To our knowledge, the interactions between this satellite cell line and SWCNT–PAMAM nanomaterials have not been studied.

This paper aims to explore the interactions between the C2C12 murine cell line and SWCNT–PAMAM nanomaterials or their individual components. The interactions between a cell line and the nanomaterials have been studied with different techniques following the methodologies and theoretical interpretations of previous research on similar compounds, including morphological analysis, a proliferation assay, an assay for the inhibition of cell adhesion, DNA damage and flow cytometry measurements.

2. Materials and methods

2.1. Chemicals

All experiments were performed in a sterile atmosphere to eliminate the chances of contamination that may interfere with the toxicity profiles of the nanomaterials. All chemicals used in the synthesis of the nanomaterials were purchased from Sigma–Aldrich (São Paulo, Brazil). Water for preparing the solutions was supplied by a water purification system (MilliQ-Plus®) and had a resistivity of 18.2 MΩ cm and pH of 5.5. DMEM, fetal bovine serum and antibiotics for the culture media were purchased from Sigma–Aldrich and Vitrocell (Campinas, Brazil). The second-generation polyamidoamine dendrimers (PAMAMs) and the single-wall carbon nanotubes (SWCNTs) functionalized with carboxylic groups were purchased from Sigma–Aldrich (São Paulo, Brazil). All other reagents were of analytical grade purity (pa).

2.2. SWCNT–PAMAM nanomaterial synthesis

The SWCNTs were further functionalized with second-generation polyamidoamine dendrimers (PAMAM-G2). Functionalization was performed based on previously reported methods (Cancino et al., 2013; Zeng et al., 2007). Briefly, SWCNTs were added to a 0.1 M PAMAM aqueous solution to produce a final concentration of 2.0 mg/mL of SWCNT. The resulting SWCNT–PAMAM solution was gently homogenized by stirring in an ultrasonic bath for 30 min. The pellet obtained from centrifugation was collected and resuspended for use in all the experiments. The effects of the nanomaterials on the C2C12 cell line were studied by exposing the cells to 10, 25, 50, 100 and 120 μg/mL concentrations in the proliferation assay and a fixed concentration of 50 μg/mL of SWCNT, SWCNT–PAMAM or PAMAM nanomaterials for all other assays (Cancino et al., 2013).

2.3. Cell culture

The C2C12 cell line was a supplied by Dr. Raquel Agnelli Mesquita Ferrari (UNINOVE, São Paulo, Brazil). The C2C12 murine myoblast cells were cultured in Dulbecco's modified Eagle medium (DMEM) supplemented with fetal bovine serum (Gibco, Grand Island, NY, USA) and antibiotics (100 units/mL penicillin and 100 μg/mL streptomycin (Sigma, Saint Louis, MO, USA). The cells were maintained in a 5% CO_2 incubator at 37 °C. Stock solutions of the nanomaterials (2 mg/mL) were prepared in sterile distilled water and diluted to the required concentrations using the cell culture medium. Appropriate concentrations of each nanomaterial stock solution were added and incubated for 12, 24, 36 or 48 h. The plates were observed under a light microscope (Olympus CK 40) to detect morphological changes and photographed using an Olympus C7070WZ camera.

2.4. Cytotoxicity assays

Cytotoxicity was assessed using the crystal violet assay. C2C12 cells were grown in 96-well plates from an initial plating of 1×10^5 cells per well, for 12, 24, 36 or 48 h, after which the growth medium was removed and replaced with 0.1 mL of fresh growth medium. Each nanomaterial was added to the cells at concentrations of 10, 25, 50, 100 and 120 μg/mL and incubated for 12, 24, 36 or 48 h. Next, 100 μL of ethanol solution (70%) was added to each well for 10 min. Sixty microlitters of crystal violet was added to each well. After the C2C12 cells were incubated for 30 min in the presence of 0.5% violet crystal, the wells were washed exhaustedly with phosphate buffered saline (PBS), and 100 μL of 1% SDS was added to each well for 30 min of incubation. Following solubilization of the crystal violet, the optical densities at 540 nm were measured with an ELISA reader (Dynex). Cell viability was expressed as the percentage relative to the untreated control cells.

2.5. Inhibition of the cell adhesion assay

For the inhibition of cell adhesion tests, fibronectin (10 μg/well) was immobilized on 96-well plates for 12 h at 4 °C. The wells were blocked with a bovine serum albumin solution (1% BSA solubilized in 200 mL/well of the buffer solution: HEPES 20 mM, NaCl 150 mM, $MgCl_2$ 5 mM and 0.25 mM $MnCl_2$, pH 7.4 200 mL/well) for 2 h. The blocking step was performed to assure that the cell adhesion proteins were immobilized only in the wells because BSA does not affect cell adhesion. The second step consisted of incubating the C2C12 cells (1×10^5 cells/well) with the nanomaterials for 30 min at 37 °C in Eppendorf tubes. These C2C12 cells were transferred to 96-well plates and incubated for 60 min at 37 °C. After washing the wells

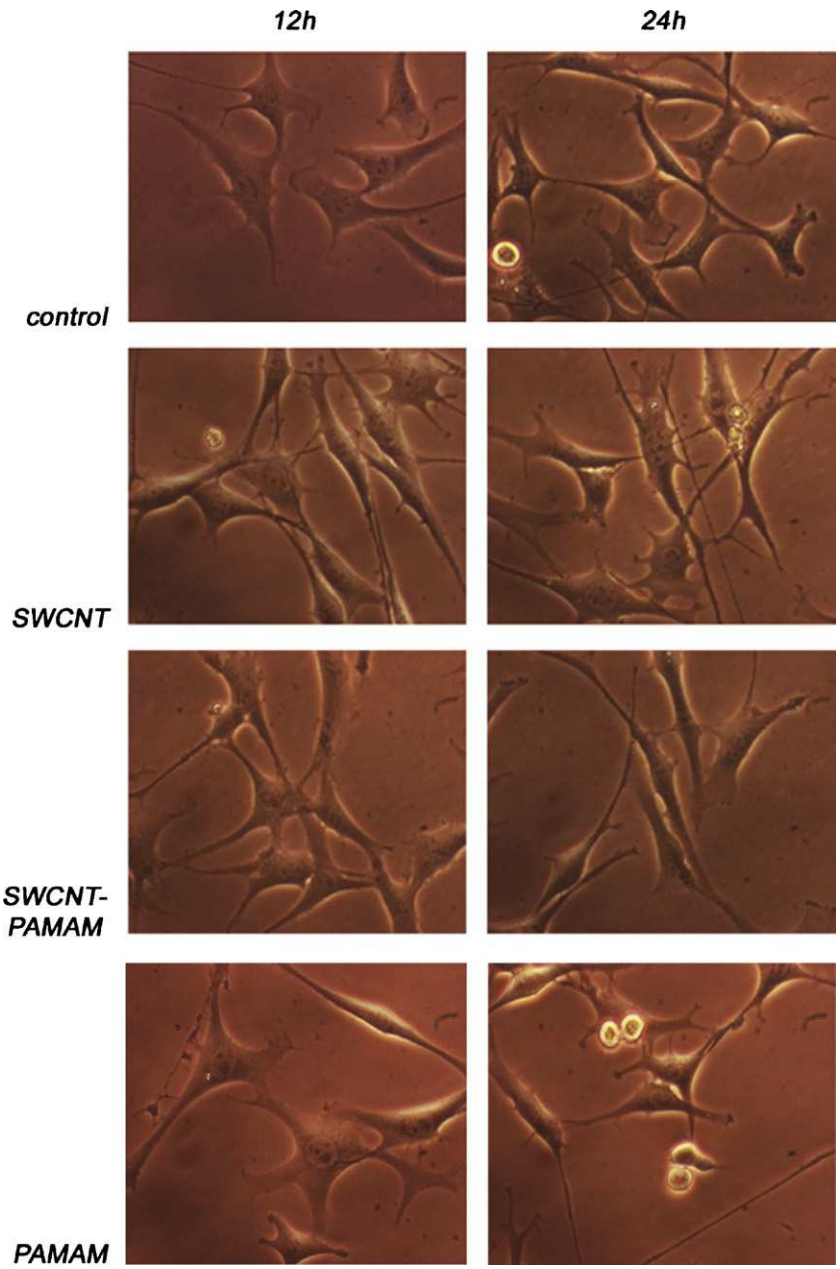

Fig. 1. Optical micrographs of untreated C2C12 cells and cells treated with 50 μg/mL of each nanomaterial, SWCNT, SWCNT–PAMAM or PAMAM. Incubation times: 12 and 24 h.

with adhesion buffer to remove the non-adherent cells, the remaining cells were fixed with 70% ethanol (100 mL) for 10 min. The adherent cells were stained with 0.5% crystal violet (60 μL for 20 min). Then, the wells were washed several times with PBS to remove the excess dye. Finally, the stained cells were solubilized in 1% SDS (100 mL) for 30 min. The optical densities at 540 nm were measured in an ELISA reader (Dynex). All experiments were performed in quadruplicate in three independent experiments.

2.6. Alkaline single-cell gel electroforesis (comet assay)

Alkaline comet assay or DNA damage was performed as described by Singh et al. (Singh et al., 1988) with slight modifications. The negative control was not exposed to nanomaterials under the same conditions. C2C12 cells were cultured in 12-well culture plates and tests were treated with the nanomaterials at 50 μg/mL concentration for 24 h (37 °C, humidified atmosphere with 5% CO_2). Microscope slides were prepared and coated with 1% normal melting point agarose (NMA) 12 h before the assay. After incubation, the cells were harvested, mixed with low-melting-point agarose, placed on these microscope slides, covered with coverslips and incubated at 4 °C for 10 min. After solidification of the suspension, the coverslips were removed. The slides were immersed (in the dark) in cold lysis solution (2.5 M NaCl, 100 mM EDTA, 10 mM Tris [pH 10], 1% Triton X-100 and 10% DMSO) at 4 °C overnight. The electrophoresis was performed for 20 min at 4 °C (25 V/300 mA) in fresh alkaline electrophoresis buffer (300 mM NaOH, 1 mM EDTA, pH > 13). Following electrophoresis, the samples were neutralized by incubation in 0.4 M Tris buffer solution, pH 7.5, for 15 min, dried at room temperature followed by dehydration in 100% ethanol for 5 min and stained with 20 μg/mL ethidium bromide in the dark. The DNA damage was immediately visualized under 20× objective magnification using a fluorescence microscope (Nikon Eclipse E200, Japan) equipped with an excitation filter of 515–560 nm and a barrier filter of 590 nm, connected to a digital camera (Nikon DS Qi1®, Japan). One hundred fifty nucleoids were analyzed per treatment (50 cells from each slide). Comets were classified visually as belonging to one of five classes according to tail size. Undamaged cells showed as intact nuclei without tails (score 0), whereas damaged cells showed the appearance of a comet (scores classes: 1–4; score 1 = low damage; 2 = medium damage; 3 = high damage; and 4 = almost all DNA in the tail or maximally damaged). The comet assay was analyzed by a single analyst by classical visual scoring. The DNA damage index was given by the formula: DNA damage index = (0 × n0) + (1 × n1) + (2 × n2) + (3 × n3) + (4 × n4), and it is based on the length of migration and on the amount of DNA in the tail.

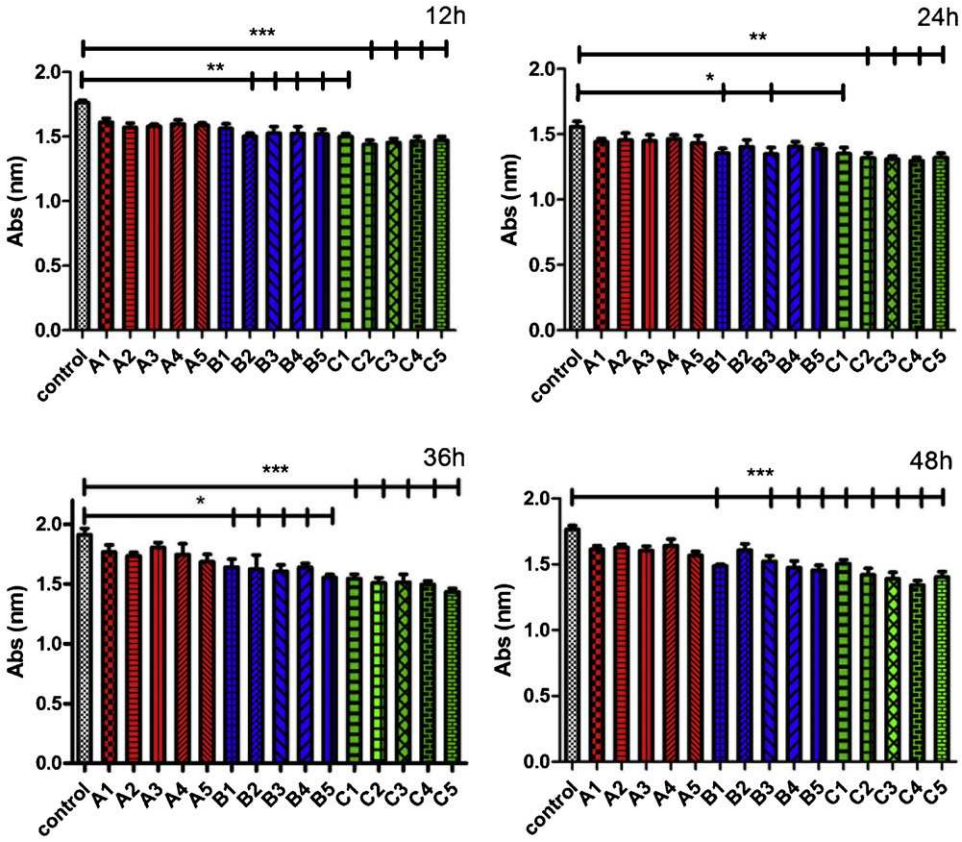

Fig. 2. Cytotoxicity assays of C2C12 cells after incubation with SWCNT, SWCNT–PAMAM or PAMAM nanomaterials for 12, 24, 36 or 48 h. The values were assigned with statistical significance at $P < 0.05$; indicated confidence values are 95% *, 99% ** or 99.9% *** (ANOVA one-way/Tukey). Nanomaterials at concentrations of 10, 20, 50, 100 and 120 μg/mL. The number of cells distributed per well was 1×10^5 cells/mL.

2.7. Flow cytometry – FITC annexin V and propidium iodide (PI)

After the C2C12 cells were incubated with the nanomaterials at 50 μg/mL concentration for 24 h, the treated cells were washed twice with cold PBS and resuspended in buffer at a concentration of 1×10^5 cells/mL. In a separate tube, 100 μL of C2C12 cells was added to 5 μL of FITC Annexin V and mixed. Next, 5 μL of PI staining was added. The tubes were incubated in a rotating shaker for 15 min, at room temperature, (25 °C) in the dark. After incubation, 400 μL of buffer was added to each tube. Analysis by flow cytometry was performed within 1 h. Apoptotic cells were defined as annexin V-FITC positive/PI negative cells and necrotic cells as Annexin V-FITC positive/PI positive cells. Live cells show no staining by either the PI solution or Annexin V-FITC conjugate. Data were acquired with a FACSCalibur® flow cytometer (Becton Dickinson, San Jose, CA), and the acquisition and analyses were performed using BD CellQuest Pro software.

2.8. Data analysis

The results were calculated as the mean ± standard deviation from three independent experiments conducted in quadruplicate. Statistical analysis was performed using Graph Pad Prism program software version 5.0 and using One-Way Analysis of Variance (ANOVA) followed by post hoc Tukey's Multiple Comparison Test. The statistical significance was set at $p < 0.05$.

3. Results

3.1. Effect on cell morphology

The first and most readily noticeable effect of exposure to toxic materials was the alteration of cell shape, or morphology, in the monolayer cultures. Fig. 1 shows optical micrographs of C2C12 cells treated with SWCNTs, SWCNT–PAMAM or PAMAM. The images revealed that C2C12 cells treated with SWCNTs or SWCNT–PAMAM had not undergone any distinct morphological changes during the time (12 and 24 h) of exposure to the nanomaterials compared to the control cells, indicating that the cells were as healthy as the controls.

Although C2C12 cells treated with PAMAMs showed a few floating cells over time, suggesting the possibility of widespread cell death due to necrosis or apoptosis, the morphologies of C2C12 cells exposed with PAMAM dendrimer did not modified as much as observed when C2C12 cells were in contact with SWCNT and SWCNT–PAMAM.

3.2. Cytotoxicity assay

Cytotoxicity assays are crucial to understand the cellular responses to a toxic agent. The cytotoxicity responses to 10, 25, 50, 100 and 120 μg/mL of SWCNT, SWCNT–PAMAM or PAMAM nanomaterials over time (12, 24, 36 and 48 h) are shown in Fig. 2. One may observe a short time-dependent decrease in the relative intensity of absorbance for the cells exposed to the nanomaterials compared to C2C12 control cells.

As observed in Fig. 2, PAMAM and SWCNT–PAMAM inhibited C2C12 cells more than SWCNTs, leaving more than 80% of the C2C12 cells alive. While SWCNT apparently induced the death of approximately 10% of C2C12 cells for any incubation time, the percentage of SWCNT-exposed C2C12 cells remained constant along the time and concentration studied, which suggested a low toxicity. SWCNT–PAMAM did not influence the proliferation of C2C12 cells by time and dose dependent, it was observed that the proliferation percentage reached a constant value, with approximately 85% of the cells alive even in high concentrations. After not observing any distinct behavior of the C2C12 upon varying time and dose of exposition, the following experiments were done with a fixed concentration of 50 μg/mL of each nanomaterial.

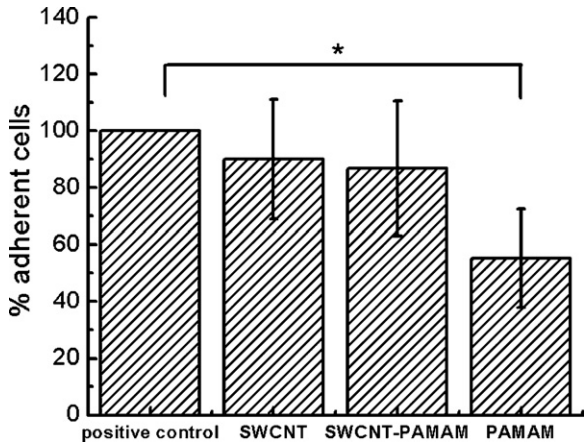

Fig. 3. Percentage of myoblasts adherent to fibronectin after incubation with SWCNT, SWCNT–PAMAM or PAMAM nanomaterials. The numbers of adherent cells were measured, and the values were normalized as a percentage relative to controls. Results were expressed as mean of three independent experiments conducted in quadruplicate. The nanomaterial concentration was 50 μg/mL. Values were assigned statistical significance at $P < 0.05$, with a confidence value of 95% * (one-way/Tukey ANOVA).

3.3. Inhibition of cell adhesion

The adhesive ability of C2C12 cells treated with SWCNT, SWCNT–PAMAM or PAMAM nanomaterials was evaluated as the ratio of adherent treated cells to the adherent control cells. The relative adhesion was tested with treated and untreated C2C12 cells growing on a fibronectin layer. Wells coated with BSA were used for the negative control of adhesion. The adhesion to fibronectin without nanomaterials was regarded as 100% (positive control). The results are shown in Fig. 3.

Treatment with SWCNT or SWCNT–PAMAM nanomaterials resulted in a slight inhibition of adhesion to fibronectin. The extent of observed inhibition was not statistically significant due to the high standard deviation. However, the adhesive ability of cells exposed to PAMAM decreased by 44%.

3.4. Analysis of apoptosis or necrosis by flow cytometry and DNA damage

To assess the extent of effects, FITC-Annexin V and PI staining, and DNA *damage* assays were performed. The data from the FITC-Annexin V and PI staining experiments indicated that exposure to 50 μg/mL of SWCNT, SWCNT–PAMAM or PAMAM nanomaterials did not increased the amount of cells undergoing apoptosis or necrosis, as shown in Fig. 4. Statistical data were extracted from the histogram plots obtained using CellQuest Pro software on the BD FACSCalibur data, based on the percentages of unstained cells (viable cells) and those labeled with FITC annexin-V (apoptotic cells) and PI (necrotic cells).

The statistical analysis from flow cytometry data depicted in Fig. 4B revealed a low percentage of positive, apoptotic cells among those exposed for 24 h to the nanomaterials at a concentration of 50 μg/mL. After exposure to SWCNT, 3.6% of the population of C2C12 cells was under apoptosis while 0.4% was under necrosis. After SWCNT–PAMAM treatment, 4.2% of the cells were in an apoptotic state and 0.6% in necrosis, an increase of only 0.6% of cells undergoing apoptosis compared to cells exposed to SWCNTs for 24 h. It was observed that almost 90% of the C2C12 cells exposed to SWCNT–PAMAM were alive, demonstrating the low toxicity to C2C12 cells upon exposure to SWCNT–PAMAM. Moreover, it was observed that 4.5% of the C2C12 cell populations exposed to PAMAMs undergone apoptosis compared to control cells and 0.7% in necrosis process. These values were similar to that observed for proliferation assay.

The DNA damage index for SWCNT–PAMAM and PAMAM at 50 μg/mL of each one in C2C12 cells were statistically significant ($p < 0.05$), compared to the negative control, whereas SWCNT at the same concentration did not show a significant effect. Comet assay analyses were conducted to study the DNA damage, as shown in Table 1.

4. Discussion

We evaluated the effects of SWCNTs, SWCNT–PAMAM and PAMAMs on the morphology, cytotoxicity and adhesion ability of C2C12 cells, as well as whether they caused cell death by an apoptotic or necrotic process, as assessed by flow cytometry and DNA damage. There is limited information about the possible impact of carbon nanotubes on human health or environment. Furthermore, there are no studies in the literature investigating the toxic effects of SWCNT–PAMAM or regarding the cyto or genotoxicity by comet assay of SWCNT to C2C12 cells. To our knowledge, this is the first study in which C2C12 murine myoblasts were used to evaluate the toxicological effects of SWCNTs, SWCNT–PAMAM and PAMAMs. Besides, in the present study, we advanced from this area to investigate the toxic effects of these nanomaterials in C2C12 cells.

PAMAM dendrimer was capable of inducing some changes in morphology of C2C12 cells. However, it was not observed any significant changes in cell morphology following exposure to SWCNTs or SWCNT–PAMAM, although we observed that SWCNT did not cause significant changes in the proliferation percentages of C2C12 cells. Our observations reveal that when PAMAM dendrimer was incubated with the cells, alone or combined with SWCNT, it changed cells characteristics, as observed via flow cytometry, DNA damage and especially in cell proliferation essays that were statistically significant ($p < 0.05$) compared with the control and SWCNT treated cells. SWCNT–PAMAM and PAMAM expressed a tendency to inhibit the proliferation of C2C12 cells, inducing cell apoptosis and decreasing cellular adhesive ability more strongly than did SWCNTs. SWCNT induced the death of approximately 10% of C2C12 cells independent of time and dose, suggesting reduced toxicity. SWCNT–PAMAM and PAMAM influenced the proliferation of C2C12 cells and more than 80% of the C2C12 cells were still alive; after 48 h. The latter is probably related to the highly positive charge density from dendrimer molecule surface (Chen et al., 2010; Jain et al., 2010; Jones et al., 2012). Interestingly, Baktur and co-workers observed no significant changes in cell proliferation from exposure to the same concentration of SWCNTs during 24 h, which they explained as the likely damages to the cellular components not preventing cell proliferation (Baktur et al., 2011). We also observed a significant difference in the cell adhesion properties when PAMAMs were incubated with C2C12 cells. According to Cui et al, cell adhesion to a substrate controls the behaviors of cells such as cell morphology, migration, growth, apoptosis and differentiation (Cui et al., 2005). Our data showed that the adhesion ability of C2C12 cells decreased with PAMAM exposure. Fig. 4 revealed that almost 44% of the C2C12 cells had damaged cell adhesion properties. These results showed that PAMAM had diminished cell adhesion in a different way than was observed for the same concentrations of SWCNTs and SWCNT–PAMAM. Cui et al. showed that the adhesion of HEK293 cells decreased with increased concentrations and times of exposure to SWCNTs (Cui et al., 2005). The authors observed the same behavior as that seen in our studies: that a 24 h exposure to 50 μg/mL of SWCNT did not affect cell adhesion.

Such behaviors can be explained by the biokinetic interactions of the nanomaterials and biomolecules often being dependent on

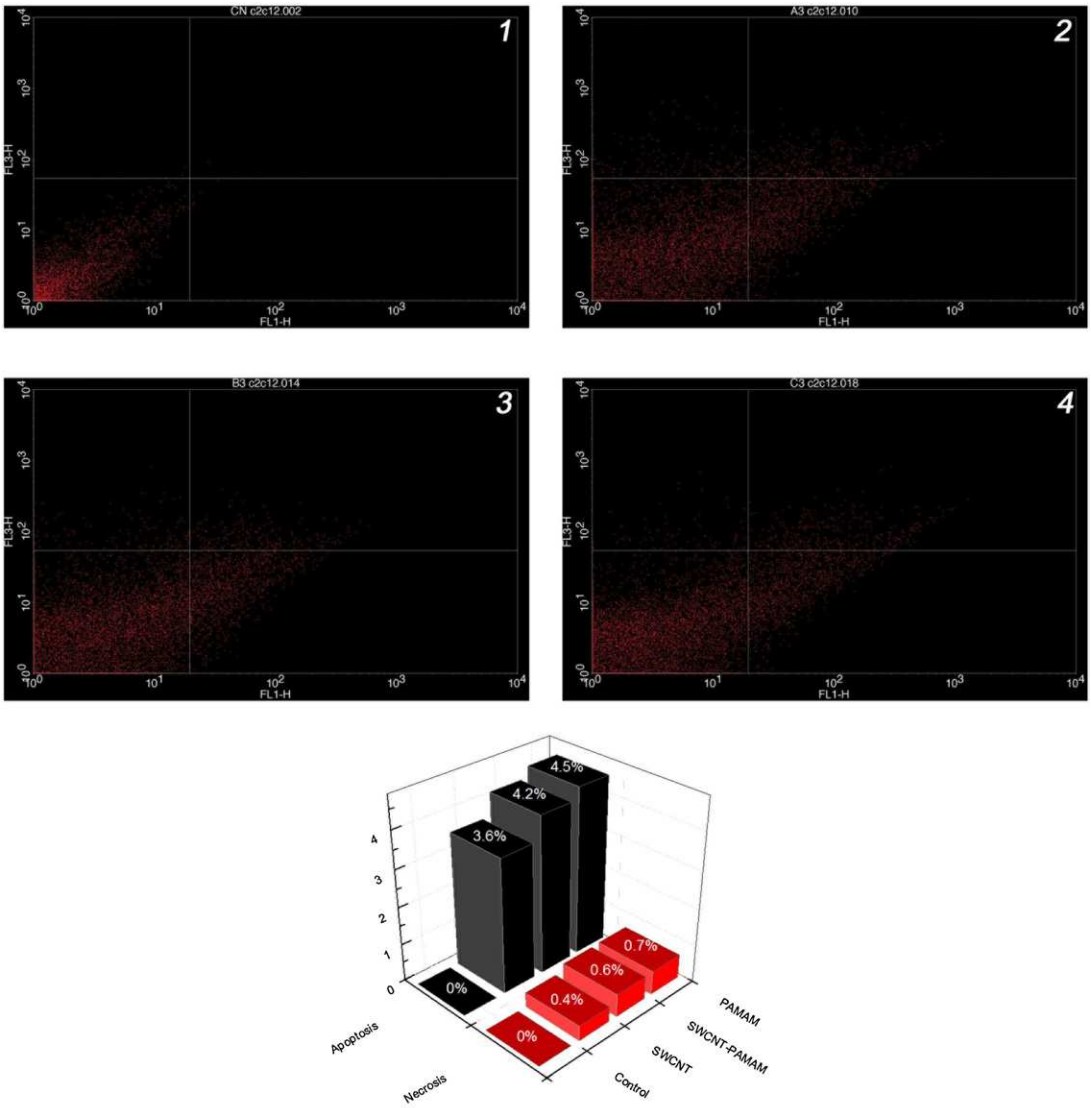

Fig. 4. Individual log fluorescence dot plot cyto-fluorometric analysis of FITC-Annexin V and PI stained of C2C12 control cells (1) and those present after 24 h exposure to 50 μg/mL of each nanomaterial: SWCNT (2), SWCNT–PAMAM (3) or PAMAM (4). Most of the cells are present in the lower left quadrant, exclude PI, are negative for annexin V, and can be considered healthy cells. Some apoptotic, annexin V Positive-PI negative, C2C12 cells can be observed. Low necrotic cells, PI positive (upper right quadrant), are present.

the physicochemical properties of the materials as well as the opportunity for increases in their uptake and their interactions with biological tissues (Johnston et al., 2010; Maynard et al., 2011; Oberdorster et al., 2005). According to Nel et al., the most important characteristics of nanomaterials is their size, and they fall in the transition zone between atoms and molecules and the corresponding bulk materials (Nel et al., 2006). The combination of these aspects can generate adverse biological effects on living cells, which would not occur were the same materials of a larger form, which is probably the case for the adhesion ability of C2C12 cells exposed to PAMAMs, which are densely positively charged. This difference in the C2C12 cell adhesion to fibronectin in the presence of PAMAMs may be related to the positive charges on the dendrimer surface. Fibronectin is one of a family of glycoproteins of high molecular weight, containing approximately 5% carbohydrate and protein components that bind to cell membrane receptors. In this case, the PAMAM dendrimer has a large number of amine groups on its surface that can minimize cell adhesion to fibronectin. Combining

Table 1
DNA damage index obtained by comet visual score in C2C12 cells pretreated with SWCNT, SWCNT–PAMAM and PAMAM at 50 μg/mL and the negative control.

Treatments	Comet	Classes				Damage index ± SD	Frequency (%)
	0	1	2	3	4		
Negative control	99	31	16	4	0	25.7 ± 3.0	34.0
SWCNT	71	53	19	6	1	37.7 ± 11.8	52.6
SWCNT–PAMAM	56	40	29	24	1	58.0 ± 7.9*	62.7
PAMAM	33	40	30	37	10	83.6 ± 14.5*	70.6

Data are reported as means ± standard deviation (SD) of triplicate experiments. One hundred fifty nucleoids were analyzed per treatment in C2C12 cells.
* Statistically significant from negative control (ANOVA, Tukey's Multiple Comparison Test, $p < 0.05$).

SWCNTs with PAMAMs neutralizes them sufficiently to inhibit the non-occurrence of adhesion.

The flow cytometry and DNA damage aimed at exploring the effects of SWCNTs, SWCNT–PAMAM and PAMAMs on C2C12 cells revealed some differences. When cells were exposure to 50 μg/mL of SWCNT–PAMAM or PAMAM, the DNA damage was statistically induced ($p < 0.05$), as an indicative of genotoxicity. Interestingly the DNA damage occurs when PAMAM molecules were presented and these findings may result from the positively charged PAMAM forming complexes. Our findings corroborate the results from Yamashita and colleagues (Yamashita et al., 2010), who studied DNA damage in the A549 cell line after exposure to 50 μg/mL of SWCNT or MWCNT for 24 h. The results showed that MWCNTs cause DNA damage and could increase the risk of cancer activity. This may be related to the length and thickness of MWCNTs. In contrast to it was observed for MWCNTs, the results indicate that SWCNTs did not cause DNA damage (Duke et al., 1986). Cui and collaborators also obtained the same result with respect to DNA damage in HEK293 cells exposed to SWCNTs (Cui et al., 2005). Therefore, from the results of the DNA damage assays, it is possible to state that SWCNT–PAMAM and PAMAM behaviors were related to the positive charge of the nanomaterias that easily undergo cell uptake through diffusion. The general mechanism of *in vitro* toxicity due to exposure to nanomaterials consists in the induction of reactive oxygen species (ROS), and ROS may cause the oxidation of DNA, DNA strand breaks or lipid peroxidation (Singh et al., 2009; Moller et al., 2010). But in some cases, the cell cycle arrest provides enough time to repair the DNA damage and it mechanism was reported by Mroz et al. (2007) for carbon black nanoparticles (Mroz et al., 2007). Naya et al. (2011) have reported that SWCNTs have no genotoxic potential in the battery of genotoxic assays (Naya et al., 2011). On the other hand, some investigators have reported genotoxic results obtained in comet assays or DNA damage induced by carbon nanutubes (Patlolla et al., 2010; Migliore et al., 2010; Di Giorgio et al., 2011). Lindberg et al. (2009) and Kisin et al. (2007) observed that carbon nanotubes induced DNA damage after 24 h treatment. Our results of SWCNT–PAMAM and PAMAM agree with the above mentioned studies regarding genotoxic effect by *in vitro* comet assay, for distinct carbon nanotubes and cell lines. *In vitro* and *in vivo* assays of genotoxic effects of SWCNTs and MWCNTs are available in the literature, but they are inconsistent and it is very difficult to confirm conclusions, especially on the physico-chemical features of nanomaterials that promote genotoxicity.

Flow cytometry using the marker FITC annexin-V and PI was used to determine quantitatively the percentage of cells within a population actively undergoing apoptosis and necrosis. This staining results from the loss of membrane asymmetry as the cell begins apoptosis (Koopman et al., 1994). In apoptotic cells, the phospholipid phosphatidylserine (PS) in the membrane is displaced from inside the plasma membrane to outside it, thereby exposing PS to the external environment (Kuypers et al., 1996). Some authors have been reported that apoptosis is a major mechanism of cell death in exposure to nanomaterials (Pan et al., 2007). Cells that are positive for FITC annexin-V are in an apoptotic state, and cells that are positive for PI are in necrosis state. The results shown in Fig. 4 could be interpreted as the cells having an increased resistance to death. In this case the apoptosis process was more evidenced than necrosis when C2C12 cells where incubated with SWCNT, SWCNT–PAMAM and PAMAM. Corroborating with our previous studies, C2C12 cells exposed to SWCNT–PAMAM and PAMAM increased the apoptosis and necrosis ability. Recent studies have identified apoptosis as a primary mechanism of cell death from exposure to SWCNT nanomaterials and their components (Mailaender and Landfester, 2009). Pulskamp et al. observed that the percentage of apoptotic human lung epithelial cells (A549) exposed to 50 μg/mL of SWCNT did not significantly exceed those of the control cells as indicated by the parameters assessed over time (Pulskamp et al., 2007).

Recent reports discussed whether SWCNTs are toxic *per se*; in most cases, the functionalization of SWCNT has been reported to increase their toxicity but, in some, to reduce it (Xia et al., 2010). These disparities in the toxic effects observed are due to differences in SWCNT functionalization and the degree of functionalization (Al-Jamal et al., 2012; Pichardo et al., 2012; Sharifi et al., 2012). Jones et al. demonstrated that PAMAM G7 dendrimers dramatically altered the morphology of platelets (Jones et al., 2012). According to the authors, these changes to platelet morphology altered platelet functions, such as increased aggregation and adherence to surfaces. The controversy comes from the variability of parameters, including cell lines used in toxicity assays, concentrations, surface charge and coatings (Martinez Paino et al., 2012). Our analyses provided evidence of the less toxic effect of SWCNT–PAMAM and PAMAM compared with SWCNT, indicating that surface charge may be a major determinant of how nanomaterials impact cellular processes.

5. Conclusion

We showed that PAMAM and SWCNT–PAMAM had different effects compared to SWCNT, in terms of citotoxicity and genotoxicity. It is possible that the combination of SWCNT and PAMAM increased toxicity to the cell cultures because of the positive charge from dendrimer molecules surface. The results indicate that the toxicity of SWCNTs, SWCNT–PAMAM and PAMAMs to C2C12 cells was strongly connected to the charge and the type of material. Controlling these properties is extremely important for the future design of theranostics and drug-delivery systems based on SWCNT and PAMAM dendrimers.

Conflict of interest

The authors report no conflict of interest. The authors are responsible for the content and writing of the paper.

Declaration of interest

This work was supported by Fundação de Amparo à Pesquisa do Estado de São Paulo (FAPESP) Project number 2008/00546-5 and 2012/03570-0.

References

Aillon, K.L., Xie, Y., El-Gendy, N., Berkland, C.J., Forrest, M.L., 2009. Effects of nanomaterial physicochemical properties on in vivo toxicity. Advanced Drug Delivery Reviews 61, 457–466.

Al-Jamal, K.T., Nunes, A., Methven, L., Ali-Boucetta, H., Li, S., Toma, F.M., Herrero, M.A., Al-Jamal, W.T., ten Eikelder, H.M.M., Foster, J., Mather, S., Prato, M., Bianco, A., Kostarelos, K., 2012. Degree of chemical functionalization of carbon nanotubes determines tissue distribution and excretion profile. Angewandte Chemie-International Edition 51, 6389–6393.

Arora, S., Rajwade, J.M., Paknikar, K.M., 2012. Nanotoxicology and in vitro studies: the need of the hour. Toxicology and Applied Pharmacology 258, 151–165.

Baktur, R., Patel, H., Kwon, S., 2011. Effect of exposure conditions on SWCNT-induced inflammatory response in human alveolar epithelial cells. Toxicology in Vitro 25, 1153–1160.

Baughman, R.H., Zakhidov, A.A., de Heer, W.A., 2002. Carbon nanotubes – the route toward applications. Science 297, 787–792.

Boulaiz, H., Alvarez, P.J., Ramirez, A., Marchal, J.A., Prados, J., Rodriguez-Serrano, F., Peran, M., Melguizo, C., Aranega, A., 2011. Nanomedicine: application areas and development prospects. International Journal of Molecular Sciences 12, 3303–3321.

Cancino, J., Nobre, T.M., Oliveira Jr., O.N., Machado, S.A.S., Zucolotto, V., 2013. A new strategy to investigate the toxicity of nanomaterials using Langmuir monolayers as membrane models. Nanotoxicology 7, 61–70.

Chen, D., Wu, X., Wang, J., Han, B., Zhu, P., Peng, C., 2010. Morphological observation of interaction between PAMAM dendrimer modified single walled carbon nanotubes and pancreatic cancer cells. Nano Biomedicine and Engineering 2.

Crespilho, F.N., Ghica, M.E., Zucolotto, V., Nart, F.C., Oliveira Jr., O.N., Brett, C.M.A., 2007. Electroactive nanostructured membranes (ENM): synthesis and electrochemical properties of redox mediator-modified gold nanoparticles using a dendrimer layer-by-layer approach. Electroanalysis 19, 805–812.
Cui, D.X., Tian, F.R., Ozkan, C.S., Wang, M., Gao, H.J., 2005. Effect of single wall carbon nanotubes on human HEK293 cells. Toxicology Letters 155, 73–85.
Di Giorgio, M.L., Di Bucchianico, S., Ragnelli, A.M., Aimola, P., Santucci, S., Poma, A., 2011. Effects of single and multi walled carbon nanotubes on macrophages: cyto and genotoxicity and electron microscopy. Mutation Research-Genetic Toxicology and Environmental Mutagenesis 722, 20–31.
Duke, R.C., Cohen, J.J., Chervenak, R., 1986. Differences in target-cell DNA fragmentation induced by mouse cytotoxic lymphocytes-T and natural killer cells. Journal of Immunology 137, 1442–1447.
Ebbesen, M., Jensen, T.G., 2006. Nanomedicine: techniques, potentials, and ethical implications. Journal of Biomedicine and Biotechnology 2006, 1–11.
Jain, K., Kesharwani, P., Gupta, U., Jain, N.K., 2010. Dendrimer toxicity: let's meet the challenge. International Journal of Pharmaceutics 394, 122–142.
Johnston, H.J., Hutchison, G., Christensen, F.M., Peters, S., Hankin, S., Stone, V., 2010. A review of the in vivo and in vitro toxicity of silver and gold particulates: particle attributes and biological mechanisms responsible for the observed toxicity. Critical Reviews in Toxicology 40, 328–346.
Jones, C.F., Campbell, R.A., Franks, Z., Gibson, C.C., Thiagarajan, G., Vieira-de-Abreu, A., Sukavaneshvar, S., Mohammad, S.F., Li, D.Y., Ghandehari, H., Weyrich, A.S., Brooks, B.D., Grainger, D.W., 2012. Cationic PAMAM dendrimers disrupt key platelet functions. Molecular Pharmaceutics 9, 1599–1611.
Kisin, E.R., Murray, A.R., Keane, M.J., Shi, X.-C., Schwegler-Berry, D., Gorelik, O., Arepalli, S., Castranova, V., Wallace, W.E., Kagan, V.E., Shvedova, A.A., 2007. Single-walled carbon nanotubes: Geno- and cytotoxic effects in lung fibroblast V79 cells. Journal of Toxicology and Environmental Health-Part a-Current Issues 70, 2071–2079.
Koopman, G., Reutelingsperger, C.P.M., Kuijten, G.A.M., Keehnen, R.M.J., Pals, S.T., Vanoers, M.H.J., 1994. Annexin-V for flow cytometric detection of phosphatidylserine expression on B-cells undergoing apoptosis. Blood 84, 1415–1420.
Kunzmann, A., Andersson, B., Thurnherr, T., Krug, H., Scheynius, A., Fadeel, B., 2011. Toxicology of engineered nanomaterials: focus on biocompatibility, biodistribution and biodegradation. Biochimica Et Biophysica Acta: General Subjects 1810, 361–373.
Kuypers, F.A., Lewis, R.A., Hua, M., Schott, M.A., Discher, D., Ernst, J.D., Lubin, B.H., 1996. Detection of altered membrane phospholipid asymmetry in subpopulations of human red blood cells using fluorescently labeled annexin V. Blood 87, 1179–1187.
Lindberg, H.K., Falck, G.C.M., Suhonen, S., Vippola, M., Vanhala, E., Catalan, J., Savolainen, K., Norppa, H., 2009. Genotoxicity of nanomaterials: DNA damage and micronuclei induced by carbon nanotubes and graphite nanofibres in human bronchial epithelial cells in vitro. Toxicology Letters 186, 166–173.
Love, S.A., Maurer-Jones, M.A., Thompson, J.W., Lin, Y.-S., Haynes, C.L., 2012. Assessing nanoparticle toxicity. Annual Review of Analytical Chemistry 5, 181–205.
Mailaender, V., Landfester, K., 2009. Interaction of nanoparticles with cells. Biomacromolecules 10, 2379–2400.
Martinello, T., Baldoin, M.C., Morbiato, L., Paganin, M., Tarricone, E., Schiavo, G., Bianchini, E., Sandona, D., Betto, R., 2011. Extracellular ATP signaling during differentiation of C2C12 skeletal muscle cells: role in proliferation. Molecular and Cellular Biochemistry 351, 183–196.
Martinez Paino, I.M., Marangoni, V.S., Silva de Oliveira, R., Greggi Antunes, d.C., Zucolotto, L.M.V., 2012. Cyto and genotoxicity of gold nanoparticles in human hepatocellular carcinoma and peripheral blood mononuclear cells. Toxicology Letters 215, 119–125.
Maynard, A.D., Warheit, D.B., Philbert, M.A., 2011. The new toxicology of sophisticated materials: nanotoxicology and beyond. Toxicological Sciences 120, S109–S129.
Menjoge, A.R., Kannan, R.M., Tomalia, D.A., 2010. Dendrimer-based drug and imaging conjugates: design considerations for nanomedical applications. Drug Discovery Today 15, 171–185.
Migliore, L., Saracino, D., Bonelli, A., Colognato, R., D'Errico, M.R., Magrini, A., Bergamaschi, A., Bergamaschi, E., 2010. Carbon nanotubes induce oxidative DNA damage in RAW 264.7 cells. Environmental and Molecular Mutagenesis 51, 294–303.
Mintzer, M.A., Grinstaff, M.W., 2011. Biomedical applications of dendrimers: a tutorial. Chemical Society Reviews 40, 173–190.
Moller, P., Jacobsen, N.R., Folkmann, J.K., Danielsen, P.H., Mikkelsen, L., Hemmingsen, J.G., Vesterdal, L.K., Forchhammer, L., Wallin, H., Loft, S., 2010. Role of oxidative damage in toxicity of particulates. Free Radical Research 44, 1–46.
Monteiro-Riviere, N.A., Nemanich, R.J., Inman, A.O., Wang, Y.Y.Y., Riviere, J.E., 2005. Multi-walled carbon nanotube interactions with human epidermal keratinocytes. Toxicology Letters 155, 377–384.
Mroz, R.M., Schins, R.P.F., Li, H., Drost, E.M., Macnee, W., Donaldson, K., 2007. Nanoparticle carbon black driven DNA damage induces growth arrest and AP-1 and NF kappa B DNA binding in lung epithelial A549 cell line. Journal of Physiology and Pharmacology 58, 461–470.
Naya, M., Kobayashi, N., Mizuno, K., Matsumoto, K., Erna, M., Nakanishi, J., 2011. Evaluation of the genotoxic potential of single-wall carbon nanotubes by using a battery of in vitro and in vivo genotoxicity assays. Regulatory Toxicology and Pharmacology 61, 192–198.
Nel, A., Xia, T., Madler, L., Li, N., 2006. Toxic potential of materials at the nanolevel. Science 311, 622–627.
Oberdorster, G., Oberdorster, E., Oberdorster, J., 2005. Nanotoxicology: an emerging discipline evolving from studies of ultrafine particles. Environmental Health Perspectives 113, 823–839.
Pan, Y., Neuss, S., Leifert, A., Fischler, M., Wen, F., Simon, U., Schmid, G., Brandau, W., Jahnen-Dechent, W., 2007. Size-dependent cytotoxicity of gold nanoparticles. Small 3, 1941–1949.
Pastorin, G., 2009. Crucial functionalizations of carbon nanotubes for improved drug delivery: a valuable option? Pharmaceutical Research 26, 746–769.
Patlolla, A., Knighten, B., Tchounwou, P., 2010. Multi-walled carbon nanotubes induce cytotoxicity, genotoxicity and apoptosis in normal human dermal fibroblast cells. Ethnicity & Disease 20, 65–72.
Pichardo, S., Gutierrez-Praena, D., Puerto, M., Sanchez, E., Grilo, A., Carnean, A.M., Jos, A., 2012. Oxidative stress responses to carboxylic acid functionalized single wall carbon nanotubes on the human intestinal cell line $Caco_2$. Toxicology in Vitro 26, 672–677.
Pulskamp, K., Woerle-Knirsch, J.M., Hennrich, F., Kern, K., Krug, H.F., 2007. Human lung epithelial cells show biphasic oxidative burst after single-walled carbon nanotube contact. Carbon 45, 2241–2249.
Sharifi, S., Behzadi, S., Laurent, S., Forrest, M.L., Stroeve, P., Mahmoudi, M., 2012. Toxicity of nanomaterials. Chemical Society Reviews 41, 2323–2343.
Singh, N., Manshian, B., Jenkins, G.J.S., Griffiths, S.M., Williams, P.M., Maffeis, T.G.G., Wright, C.J., Doak, S.H., 2009. NanoGenotoxicology: the DNA damaging potential of engineered nanomaterials. Biomaterials 30, 3891–3914.
Singh, N.P., McCoy, M.T., Tice, R.R., Schneider, E.L., 1988. A simple technique for quantitation of low-levels of DNA damage in individual cells. Experimental Cell Research 175, 184–191.
Smart, S.K., Cassady, A.I., Lu, G.Q., Martin, D.J., 2006. The biocompatibility of carbon nanotubes. Carbon 44, 1034–1047.
Taketo, M.M., Sonoshita, M., 2002. Phospolipase A(2) and apoptosis. Biochimica Et Biophysica Acta-Molecular and Cell Biology of Lipids 1585, 72–76.
Warheit, D.B., 2008. How meaningful are the results of nanotoxicity studies in the absence of adequate material characterization? Toxicological Sciences 101, 183–185.
Worle-Knirsch, J.M., Pulskamp, K., Krug, H.F., 2006. Oops they did it again! Carbon nanotubes hoax scientists in viability assays. Nano Letters 6, 1261–1268.
Xia, X.-R., Monteiro-Riviere, N.A., Riviere, J.E., 2010. An index for characterization of nanomaterials in biological systems. Nature Nanotechnology 5, 671–675.
Yamashita, K., Yoshioka, Y., Higashisaka, K., Morishita, Y., Yoshida, T., Fujimura, M., Kayamuro, H., Nabeshi, H., Yamashita, T., Nagano, K., Abe, Y., Kamada, H., Kawai, Y., Mayumi, T., Yoshikawa, T., Itoh, N., Tsunoda, S.-i., Tsutsumi, Y., 2010. Carbon nanotubes elicit dna damage and inflammatory response relative to their size and shape. Inflammation 33, 276–280.
Zeng, Y.-L., Huang, Y.-F., Jiang, J.-H., Zhang, X.-B., Tang, C.-R., Shen, G.-L., Yu, R.-Q., 2007. Functionalization of multi-walled carbon nanotubes with poly(amidoamine) dendrimer for mediator-free glucose biosensor. Electrochemistry Communications 9, 185–190.

6.3. MANUSCRITO V – Publicado como primeira autora em estágio no exterior

Carter RZ, ***Micocci KC****, Natoli A, Redvers RP, Paquet-Fifield S, Martin ACBM, Denoyer D, Ling X, Kim S-H, Tomasin R, Selistre-de-Araújo HS, Anderson RL, Pouliot N. Bone-metastatic breast tumours require αvβ3 integrin for early dissemination. The Journal of Pathology.* Fator de Impacto 7.330.

Accepted Article

Tumour but not stromal expression of β3 integrin is essential, and is required early, for spontaneous dissemination of bone-metastatic breast cancer

Rachel Zoe Carter[1#], Kelli Cristina Micocci[2#], Anthony Natoli[1], Richard Paul Redvers[1], Sophie Paquet-Fifield[3], Ana Carolina Baptista Moreno Martin[2], Delphine Denoyer[1], Xiawei Ling[1], Soo-Hyun Kim[1,4], Rebeka Tomasin[6], Heloisa Selistre-de-Araújo[2], Robin Lesley Anderson[1,4,5,7] and Normand Pouliot[1,4,5,7,‡]

[1]Metastasis Research Laboratory, Peter MacCallum Cancer Centre, Melbourne, Australia

[2]Department of Physiological Sciences, Federal University of São Carlos, São Carlos, Brazil

[3]Endothelial Regulation Laboratory, Peter MacCallum Cancer Centre, Melbourne, Australia

[4]Department of Pathology, University of Melbourne, VIC, Australia

[5]Sir Peter MacCallum Department of Oncology, University of Melbourne, VIC, Australia

[6]Laboratory of Nutrition and Cancer, Department of Functional and Structural Biology, Institute of Biology, State University of Campinas, São Paulo, Brazil

[7]Co-senior authors

[#]These authors made equal contribution

[‡]Corresponding author: Dr. Normand Pouliot

Mailing address: Peter MacCallum Cancer Centre, Locked Bag #1, A'Beckett St., Melbourne, VIC, 8006, AUSTRALIA. PH: 61396561285. FAX: 6139656 1411. E-mail: normand.pouliot@petermac.org

This article has been accepted for publication and undergone full peer review but has not been through the copyediting, typesetting, pagination and proofreading process, which may lead to differences between this version and the Version of Record. Please cite this article as doi: 10.1002/path.4490

This article is protected by copyright. All rights reserved

Accepted Article

Abbreviations: ECM, extracellular matrix; ER, estrogen receptor; LM, laminin; MMTV, mouse mammary tumour virus; PR, progesterone receptor.

Conflict of Interest: The authors declare no conflict of interest.

Abstract

Although many pre-clinical studies have implicated β3 integrin receptors (αvβ3 and αIIbβ3) in cancer progression, β3 inhibitors have shown only modest efficacy in patients with advanced solid tumours. The limited efficacy of β3 inhibitors in patients could arise from our incomplete understanding of the precise function of β3 integrin and, consequently, inappropriate clinical application. Data from animal studies are conflicting and indicate heterogeneity with respect to the relative contribution of β3-expressing tumour and stromal cell populations in different cancers. Here we aimed to clarify the function and relative contribution to metastasis of tumour versus stromal β3 integrin in clinically relevant models of spontaneous breast cancer metastasis, with particular emphasis on bone metastasis. We show that stable down-regulation of tumour β3 integrin dramatically impairs spontaneous (but not experimental) metastasis to bone and lung without affecting primary tumour growth in the mammary gland. Unexpectedly, and in contrast to subcutaneous tumours, orthotopic tumour vascularity, growth and spontaneous metastasis were not altered in mice null for β3 integrin. Tumour β3 integrin promoted migration, protease expression and trans-endothelial migration *in vitro* and increased vascular dissemination *in vivo,* but was not necessary for bone colonisation in experimental metastasis assays. We conclude that tumour rather than stromal β3 expression is essential and is required early for efficient spontaneous breast cancer metastasis to bone and soft tissues. Accordingly, differential gene expression analysis in

This article is protected by copyright. All rights reserved

cohorts of breast cancer patients showed a strong association between high β3 expression, early metastasis and shorter disease-free survival in patients with oestrogen receptor-negative tumours. We propose that β3 inhibitors may be more efficacious if used in a neoadjuvant setting rather than after metastases are established.

Key words: Breast cancer, β3 integrin, bone metastasis, syngeneic mouse model, vitronectin, DisBa-01

Accepted Article

This article is protected by copyright. All rights reserved

Accepted Article

Introduction

β3 integrins (αvβ3 and αIIbβ3) mediate cellular adhesion to extracellular matrix (ECM) substrates including vitronectin, bone sialoprotein, osteopontin and fibrinogen, and are attractive therapeutic targets for metastatic cancers [1]. Studies employing αv or β3 inhibitors demonstrate that αvβ3 integrin regulates multiple cellular responses required for metastasis including cell survival, migration, invasion through the ECM and angiogenesis [2]. However, while high β3 integrin expression is reported in several cancer types [3-8], its prognostic significance is still unclear. Tumour expression of αvβ3 integrin correlates inversely with invasive and metastatic behaviors in some melanoma and ovarian cancer lines [9,10] and is associated with better survival in ovarian cancer patients [10]. Enhanced αvβ3 levels in bone metastases compared to matched primary breast tumours have been reported in some [4,11] but not all [5] studies.

Preclinical studies evaluating the function of αvβ3 in breast cancer bone metastasis have been limited by lack of robust and clinically relevant animal models. High levels of αvβ3 in a bone metastatic subline of human MDA-MB-231 breast tumour cells (BO2) [12] or exogenous expression of β3 integrin in parental cells [5] correlates with increased adhesion to cortical bone and an increased number of osteolytic lesions in mice compared to parental cells, following tail vein injection. We showed previously that exogenous expression of β3 integrin in weakly metastatic 66cl4 mammary carcinoma cells that otherwise do not express αvβ3 or spread to bone from the mammary gland is sufficient to promote their spontaneous metastasis to bone without altering orthotopic tumour growth in immunocompetent mice [13]. While the above studies employing β3 overexpression showed that tumour αvβ3 integrin can "*contribute*" to bone metastasis, whether expression of αvβ3 is "*essential*" for spontaneous bone metastasis has yet to be demonstrated. Clinically, this distinction is

This article is protected by copyright. All rights reserved

Accepted Article

important since the effectiveness of therapies targeting tumour αvβ3 and their impact on bone metastasis and patient survival will be dictated by the dependency of tumours on αvβ3 integrin for successful metastasis. To our knowledge, the efficacy of αvβ3 integrin antagonists specifically against bone metastases has not been evaluated in patients.

Discrepancies also exist with regard to the precise contribution of β3 integrin expressed on stromal lineages to tumour growth and metastasis [14-20]. MMTV-c-neu transgenic mice null for either β3 or β3 and β5 integrins show no apparent changes in mammary tumour growth and vascularisation compared to normal MMTV-c-neu mice [20]. This contrasts with the anti-tumour/anti-angiogenic effects of αv or β3 inhibitors against subcutaneous melanoma and breast tumours [21-23] and with the enhanced growth and angiogenesis of transplanted melanoma, lung and colon tumours in β3-null mice [16,19]. Moreover, while experimental melanoma metastasis to bone is decreased in β3-null compared to wildtype mice [17], loss of β3 integrin has no impact on spontaneous metastasis of mammary tumours to lung in MMTV-c-neu mice null for β3 [20]. Importantly, since none of these models metastasise spontaneously to bone, the role of stromal β3 integrin in spontaneous metastasis to bone remains unknown. Collectively, these observations derived from various animal models of metastasis indicate that regulation of tumour growth, vascularisation and metastasis by tumour and stromal β3 integrin is likely to vary between tumour types and sites of tumour growth. These differences may account for the limited efficacy of integrin inhibitors in advanced cancer patients with solid tumours [2,24-34]. Accordingly, improvement in the efficacy of β3 integrin inhibitors in patients with metastatic cancer may require a reappraisal of the precise contribution of β3-type receptors to the growth and metastasis of each tumour type.

This article is protected by copyright. All rights reserved

Here, using clinically relevant mouse models of breast cancer metastasis to bone [35-37], a combination of *in vitro* assays, gene knockdown and β3 null mice, we demonstrate that β3 integrin in tumour cells but not in stromal cells is essential for spontaneous breast cancer metastasis and is required early for vascular dissemination to bone and other tissues. These findings have important implications for the design of therapies targeting β3 integrin in breast cancer patients.

This article is protected by copyright. All rights reserved

Accepted Article

Materials and methods

Cell culture

66cl4 mammary carcinoma cells stably expressing β3 integrin (66cl4pBabeβ3^{high}) and control empty pBabe-puro retroviral vector (66cl4pBabe) were described previously [13]. Bone-metastatic 4T1.2 with hygromycin-resistance and 4T1BM2 with mCherry expression were derived from 4T1 cells [35-38]. All lines were maintained for up to 4 weeks in αMEM/5% FCS/1% penicillin-streptomycin at 37°C, 5% CO_2. bEnd.3 murine microvascular endothelial cells, provided by Dr R Hallman (Jubileum Institute, Sweden), were cultured as described [13].

Knockdown of β3 integrin

Two oligonucleotides targeting β_3 integrin (NM-016780, sh1: AAGGATGATCTGTCCACGATC and sh2: AGCAAACAACCCGCTGTATAA start position 2387) were inserted into pRetroSuper (sh1) or pLMP (sh2) retroviral vectors using standard methodology [35]. A non-targeting sequence (AGTACTGCTTACGATACGG) was used as control. Viral supernatants from infection of PT67 packaging cells were used to infect 4T1.2 (sh1 hairpin) and 4T1BM2 (sh2 hairpin) cells. Cells expressing low levels of β3 integrin were isolated by flow cytometry, expanded in culture and frozen. Changes in integrin receptor expression were analysed by standard flow cytometry [13,39]. Primary antibodies used are described in the Supplementary Methods.

In vitro assays

Proliferation, adhesion and migration assays [13,35,36,39], zymography [40] and immunoblotting [41] are described in Supplementary Methods. For trans-endothelial migration, bEnd.3 cells (1×10^5) were seeded in triplicate Transwell inserts and incubated at

This article is protected by copyright. All rights reserved

Accepted Article

37°C for 24h to form a monolayer. Adherent cells were washed with PBS and calcein-labelled tumour cells (2×10^5) added to the insert in 200µl serum-free αMEM/glutamine (2mM)/BSA (0.05%)/sodium pyruvate (1mM) and antibiotics. Medium containing 10% FCS was added to the bottom chambers as chemoattractant. After 48h incubation at 37°C, migrated tumour cells on the underside [green (calcein) cytoplasm and red (propidium iodide) nucleus] (3 random 20× fields) were photographed on an Olympus BX-61 microscope and counted using Metamorph (Molecular Devices).

Tumour growth and metastasis

Procedures involving mice completed in accordance with National Health and Medical Research Council ethics guidelines and approved by the Peter MacCallum Animal Ethics Committee. Wildtype female Balb/c mice were purchased from the Walter and Eliza Hall Institute (Australia). β3-null mice [42] were backcrossed to Balb/c background (10 generations).

For spontaneous metastasis assays, 8-10 week old mice were inoculated with 10^5 cells into the 4th mammary fat pad. Tumour growth was measured with electronic calipers [13,35] and mice harvested as a group on day 30 or earlier if showing signs of distress due to metastatic disease. Analysis of tumour microvascular density [43] is described in Supplementary Methods. Lungs, femurs and spines were snap frozen in liquid nitrogen before processing for relative tumour burden (RTB) quantitation by real-time qPCR of the tumour-expressed reporter gene, as described previously [13,35,40]. For experimental bone metastasis assays, 5×10^4 (4T1.2 and 4T1BM2 cells) or 1×10^5 (66cl4) cells/100 µl PBS were injected into the left cardiac ventricle [44]. Mice were harvested as a group on day 15 or earlier if showing signs of distress. Specific primers and probes are detailed in Supplementary Methods. When

This article is protected by copyright. All rights reserved

comparing metastatic burden from two tumour lines, RTB values were adjusted for reporter gene copy number calculated from the level in genomic DNA in cultured cells.

Statistical analysis

Data were analysed using Prism 5.01 for Windows. For *in vitro* assays comparing multiple groups, a one-way ANOVA, Tukey's multiple comparisons test was completed. Proliferation assays were evaluated by two-way ANOVA with Bonferroni post-test. For *in vivo* assays, a Fisher's exact test was used for metastatic incidence and a Mann-Whitney test was completed for metastatic burden analysis. $p \leq 0.05$ was considered significant.

This article is protected by copyright. All rights reserved

Accepted Article

Results

Knockdown of β3 integrin in bone metastatic tumour cells

Exogenous expression of β3 in weakly lung-metastatic 66cl4 cells contributes to their spontaneous metastasis from the mammary gland to bone [13]. However, this approach does not reveal an essential requirement for bone metastasis, a critical consideration for anti-metastatic therapy. To address this, β3 integrin expression was reduced by stable expression of RNA interference vectors encoding separate hairpins in 4T1.2 (sh1) and 4T1BM2 (sh2) cells. These models were chosen for their clinical relevance, with both expressing αvβ3 integrin and, unlike xenograft models, metastasising spontaneously to bone with high incidence from mammary tumours in immunocompetent mice [36,37].

β3 expression was substantially reduced in 4T1BM2-β3lo compared to 4T1BM2β3-ctrl and parental 4T1BM2 cells and accompanied by down-regulation of αv integrin at the cell surface (Figures 1A-1B and Supplementary Figure 1A). Suppression of β3 transcript levels in 4T1BM2-β3lo cells was confirmed by qRT-PCR (Figure 1C). Despite reduced surface levels of αv integrin, αv mRNA expression was not decreased (Figure 1D). Moreover, western blot analysis of whole cell lysates showed that total αv protein levels in 4T1BM2-ctrl and 4T1BM2-β3lo cells were similar to parental cells (87% and 85% of parental cells respectively) and not significantly different from each other when normalised to tubulin (Figure 1E). Thus, surface localisation rather than expression of αv integrin is impaired by suppression of β3 integrin. Sustained coordinated downregulation of surface β3 and αv integrins was also observed using a different β3-targeting shRNA in 4T1.2 bone-metastatic cells (Supplementary Figure 1B). The overall expression pattern of other integrins was comparable between 4T1BM2 and 4T1.2 parental lines (Supplementary Figures 2A and 2B), with the exception that α2 was expressed at low levels in 4T1.2 but not in 4T1BM2 cells.

This article is protected by copyright. All rights reserved

Accepted Article

The expression of α2, α3, α5, α6, β1, β4, β5 and β6 integrin subunits was not significantly altered in 4T1BM2-β3lo cells compared to 4T1BM2-ctrl cells whereas 4T1.2 cells showed a small increase in α6 and β4 subunits following β3 downregulation.

Suppression of β3 integrin inhibits spontaneous metastasis to bone and soft tissues without altering primary tumour growth

Adhesion of all lines to uncoated plastic (30min) was negligible irrespective of β3 integrin levels (Figure 2A and Supplementary Figure 3A). As expected, adhesion of 4T1BM2-β3lo and 4T1.2-β3lo cells to vitronectin, the classical αvβ3 integrin ligand, was decreased (45-60% inhibition) compared to cells expressing a non-targeting shRNA. Adhesion to laminin (LM)-511 was unaffected by β3 suppression. Similarly, haptotactic migration towards vitronectin but not LM-511 was significantly inhibited by β3 suppression (Figure 2B and Supplementary Figure 3B) indicating that reduced adhesion and migration of cells with low β3 expression are substrate-specific. Proliferation of 4T1BM2 and 4T1.2 cells was unaffected by β3 integrin downregulation (Figure 2C and Supplementary Figure 3C).

In vivo, 4T1BM2-ctrl and 4T1BM2-β3lo tumours grew at the same rate (Figure 2D and 2E). However, visual examination of mice at harvest and quantitation of metastatic burden using a sensitive qPCR-based assay [35] revealed a dramatic effect of β3 downregulation on spontaneous metastasis. Semi-quantitative measurement (presence or absence) of metastasis indicated a significantly lower incidence of mice developing bone but not lung metastases in the 4T1BM2-β3lo group (Figure 2F). However, visual inspection of lungs at harvest showed fewer and smaller metastatic nodules in mice bearing 4T1BM2-β3lo tumours, indicating a lower overall lung metastatic burden (Figure 2F, right panels). These observations were confirmed and quantitated by qPCR, with 4T1BM2-β3lo metastatic burden in lung, femur,

This article is protected by copyright. All rights reserved

Accepted Article

spine and bone (combined femur and spine) (Figures 2G-2J) decreased significantly compared to 4T1BM2-ctrl bearing mice ($p<0.01$ in all organs). Suppression of β3 integrin similarly reduced metastatic burden in lung, femur, spine and bone but not tumour growth in the 4T1.2 model (Supplementary Figures 3D-3G). These results demonstrate conclusively that expression of β3 in mammary tumour cells is required for efficient spontaneous metastasis to multiple organs.

Loss of stromal β3 integrin expression does not alter orthotopic primary tumour growth or metastasis

Conflicting results exist regarding the contribution of stromal cell populations expressing β3 integrin to primary tumour growth [16,19-21] and metastasis [17,20]. Importantly, no study has investigated the role of stromal β3 integrin in spontaneous breast cancer metastasis to bone. Therefore, we compared the orthotopic growth and metastatic dissemination of 4T1BM2 (Figure 3) or 4T1.2 tumours (Supplementary Figure 4) in β3 null versus wildtype littermates. We found no difference in primary tumour growth (Figure 3A and Supplementary Figure 4A), final tumour weight (Figure 3B and Supplementary Figure 4B) or metastatic burden in lung, femur, spine or bone (combined femur and spine) (Figures 3C-3F and Supplementary Figures 4C-4F respectively) between integrin β3-null and wildtype mice.

The lack of effect of stromal β3 deletion on primary tumour growth contrasts with enhanced subcutaneous growth and vascularisation of melanoma, colon and lung carcinomas in β3 null mice [16,19] and could be due to differences in tumour type or to the site of tumour growth. To address this, we compared the growth of 4T1BM2 cells inoculated in the mammary fat pad or subcutaneously in wildtype and β3-null mice. Orthotopic 4T1BM2 tumours grew at the same rate in wild type and β3-null mice (Figures 3G-3I). Importantly, while subcutaneous

This article is protected by copyright. All rights reserved

Accepted Article

growth of 4T1BM2 tumours in wildtype or β3-null mice was visibly slower than in the orthotopic site (compare Figures 3G and 3J), it was significantly enhanced in β3-null mice compared to wildtype littermates (Figures 3J-3L). Moreover, quantitation of microvascular density revealed no difference in orthotopic tumours growing in wildtype and β3-null mice (Figure 3M) but a significant increase in microvascular density in subcutaneous tumours growing in β3-null compared to wildtype mice (Figure 3N). Collectively, these results indicate that, unlike subcutaneous tumours, orthotopic growth and vascularisation of mammary tumours are not affected by stromal β3 integrin deletion.

Tumour β3 integrin is required early to promote metastasis to bone

To assess the stage at which tumour β3 is required for metastasis to bone, we bypassed the formation of primary tumours by inoculating 4T1BM2 cells directly into the left cardiac ventricle of wildtype mice. In contrast to the strong reduction in spontaneous bone metastasis, suppression of tumour β3 integrin did not reduce experimental metastasis to femur, spine or bone (femur and spine combined) (Figures 4A-4C). We also compared the bone metastatic ability of 66cl4β3^{high} cells that overexpress β3 integrin and metastasise spontaneously to bone to that of non-expressing 66cl4pBabe cells that do not spread spontaneously to bone from the mammary gland [13]. Surprisingly, extensive metastasis to femur, spine or both (Figures 4D-4F) was observed regardless of β3 expression. Thus, tumour β3 integrin is not essential for homing, survival and colonisation of bone.

Next, we compared the ability of 4T1BM2-ctrl and 4T1BM2-β3lo or 4T1.2-ctrl and 4T1.2-β3lo cells to migrate towards a gradient of serum, a rich source of soluble vitronectin [45]. Integrin β3 suppression impaired migration towards serum by approximately 50% ($p<0.001$) (Supplementary Figures 5A and 5B). To further confirm that serum chemotaxis was

This article is protected by copyright. All rights reserved

Accepted Article

specifically dependent on β3 integrin we used DisBa-01, a potent snake venom-derived disintegrin that targets αvβ3 integrin [46]. DisBa-01 dose-dependently inhibited haptotatic migration of 4T1BM2 towards vitronectin but not towards collagen-IV, demonstrating its specificity towards αvβ3 integrin substrates (Supplementary Figure 5C). Importantly, chemotactic migration towards serum was also inhibited by DisBa-01 in a dose-dependent manner (Supplementary Figure 5D).

4T1-derived tumour lines secrete abundant MMP9 that contributes to their migration and invasion [13,36]. We found that 4T1BM2-β3lo and 4T1.2-β3lo cells secrete significantly less MMP9 than control cells (Supplementary Figures 6A and 6B). Moreover, migration across a monolayer of endothelial cells was enhanced significantly by elevated β3 expression in 66cl4 cells (Figure 5A) and was inhibited by suppression of β3 integrin in 4T1BM2 cells (Figure 5B). Reduced chemotaxis, protease secretion and trans-endothelial migration following β3 downregulation would be expected to prevent or delay tumour cell migration and intravasation. Indeed, qPCR signal for the mCherry tumour marker in blood on day 26 was near or below the limit of detection in the majority of 4T1BM2-β3lo tumour-bearing mice (mean value = 1.132) compared to control mice (mean value = 16.22) ($p = 0.01$) (Figure 5C).

In a second series of experiments, blood was collected by cardiac puncture when tumours were small (~0.5cm^3) and viable tumour cells scored by colony formation *in vitro*. Tumour weights were similar in both groups ($p = 0.944$) (Figure 5D) and while macro-metastases were not visible in either group at this early stage, qPCR quantitation revealed a higher lung ($p=0.05$) and spine ($p = 0.012$) tumour burden in control mice (Figure 5E). Importantly, only blood from 4T1BM2-ctrl-bearing mice gave rise to colonies ($p = 0.0006$) (Figure 5F)

This article is protected by copyright. All rights reserved

confirming that downregulation of tumour β3 significantly impairs the ability 4T1BM2-β3lo cells to enter the vasculature.

Since αvβ3 integrin controls an early step required for metastatic dissemination to multiple sites, high β3 expression in breast cancer patients would be expected to be associated with poor clinical outcome. To assess clinical relevance, we first ran a differential expression analysis for integrin β3 in Oncomine 4.4.4.3 [47], focusing on clinical outcome in breast cancer patients (fold-change ≥ 1.5, *p* value ≤ 0.05). In all, 10/13 analyses indicated that high β3 was associated with metastasis and recurrence (Supplementary Figures 7A-7B). The prognostic value of β3 integrin expression was further investigated in molecular subtypes of breast cancer using the BreastMark prognostic biomarker analysis tool [48]. High β3 integrin expression was correlated with shorter disease-free survival in patients with estrogen receptor negative (ER^-) tumours (Figures 6A and 6B) or with lymph node metastasis (LN^+) (Figure 6E and 6F). No significant association was found between β3 expression and progesterone receptor (PR) status (Figures 6C and 6D), high tumour grade (Gr3) (Figure 6G) or HER2 status [data not shown, $HER2^+$, p = 0.121; $HER2^-$, p = 0.282]. Multivariate analyses showed that high β3 expression is significantly associated with reduced survival in ER^-/PR^- (Figure 6H), ER^-/LN^+ (Figure 6I) and $ER^-/LN^+/Gr3^+$ tumours (Figure 6J). These observations in human breast tissues are consistent with the lack of ER and PR in 4T1BM2 primary tumours and the aggressive nature of this mouse model of metastasis (Supplementary Figure 7C).

Accepted Article

This article is protected by copyright. All rights reserved

Accepted Article

Discussion

The diversity of experimental approaches, animal models and tumour types used to investigate the contribution of β3 integrin to tumour growth and metastasis has made it difficult to reconcile some of the discrepancies between earlier studies. Unlike xenograft models, the 4T1BM2 and 4T1.2 models used herein have the unique ability to metastasise spontaneously and aggressively in immunocompetent mice [35-37]. Our data demonstrate conclusively that tumour-associated αvβ3 integrin is essential for efficient spontaneous metastasis to bone and lung but not for growth in the mammary gland. Integrin αvβ3 mediates tumour cell attachment to several bone-derived ECM proteins and is thought to be a critical for homing and colonisation of bone [13,49,50]. Unexpectedly, we found that β3 downregulation in 4T1BM2 and 4T1.2 decreased spontaneous but not experimental bone metastasis. Moreover, exogenous expression of β3 in 66cl4β3^{high} cells which promotes spontaneous metastasis to bone [13], did not enhance experimental bone metastatic burden compared to control cells. Clearly, 66cl4 cells do not require αvβ3 to home and colonise bone since they formed experimental bone metastases in 100% of animals (see Figure 4) even though they do not express this receptor [13]. These observations indicate that tumour αvβ3 is essential primarily during the early rather than late steps of breast cancer metastasis.

Suppression of tumour β3 reduced MMP9 secretion, serum chemotaxis and trans-endothelial migration. These responses are expected to contribute to the early dissemination of αvβ3-expressing breast tumours *in vivo* through interactions with its ligands, a conclusion further supported by decreased circulating tumour cells observed in 4T1BM2-β3lo tumour-bearing mice. Consistent with this, the expression of the αvβ3 ligand, vitronectin, is elevated in small vessel walls surrounding cancer cells in patients with early stage breast cancer and the concentration of vitronectin in serum is elevated in advanced breast cancer patients [51]. We

This article is protected by copyright. All rights reserved

Accepted Article

therefore conclude that the most critical role of tumour αvβ3 is to facilitate the early escape and intravasation of breast tumours, resulting in enhanced vascular dissemination and subsequent metastasis to multiple organs. The clinical relevance of our findings in mouse models is strongly supported by the correlation observed between high β3 expression, metastatic disease and poor clinical outcome in ER-negative breast cancer patients.

Our data appear at odds with earlier reports showing increased experimental bone metastasis in β3-overexpressing MDA-MB-231 variants [5,12]. However, it should be noted that while mice inoculated with these cells showed increased number of osteolytic lesions, the overall incidence of mice developing experimental bone metastases was, in agreement with our study, high in both control and β3-overexpressing groups. Tumour αvβ3 integrin does not directly stimulate metastatic growth in bone but promotes the recruitment of active osteoclasts in proximity of metastatic lesions [5,13]. Degradation of the bone matrix and the subsequent release of growth factors could provide a growth stimulus for breast tumour cells in bone. Consistent with this, β3 inhibitors reduce the formation of osteolytic lesions more potently when used as pretreatment [18] or as long-term daily treatments [5] at concentrations that also inhibit osteoclast activity. The extent to which αvβ3-expressing osteoclasts contribute to bone colonisation is likely to vary between tumours. MDA-MB-231 cells are aggressively osteolytic compared to 4T1 or 66cl4 cells, and presumably their growth in bone may be more dependent on the release of bone-derived growth factors. Collectively, data from the above studies and ours indicate that while there is heterogeneity amongst tumour lines in their dependency on osteoclasts to colonise bone, tumour αvβ3 is not essential for bone metastases to develop.

This article is protected by copyright. All rights reserved

Accepted Article

Most surprising was the lack of effect of stromal β3 ablation on tumour growth, vascularisation and spontaneous metastasis, given the numerous studies that have implicated endothelial cells or platelets in these processes [16,19,52-54]. Studies employing subcutaneous tumour transplantation models reported enhanced tumour growth and vascularisation following stromal β3 deletion [16,19]. While we could replicate these observations in mammary tumour cells implanted into the subcutis, stromal deletion of β3 integrin did not alter tumour growth in the mammary gland. These observations indicate that stromal β3 regulates tumour growth and angiogenesis in a tissue-specific manner and argue against a critical role for endothelial β3 in promoting the orthotopic growth and angiogenesis of breast tumours. Our data support those reported in the MMTV-c-neu/$\beta3^{-/-}$ transgenic model of breast cancer metastasis [20] and resolve the apparent conflicts with earlier tumour transplantation studies employing β3-null mice [55].

Most studies supporting the role of platelet αIIbβ3 in metastasis have made use of *in vitro* surrogate assays or *in vivo* experimental metastasis models in which tumour cells are injected directly into the vasculature [5,12,52,53,56]. In one study, pharmacological inhibition of platelet αIIbβ3 significantly reduced experimental melanoma metastasis to bone which was attributed to disruption of tumour cell-induced platelet aggregation [17]. Conceivably, injection of a large bolus of cells could enhance experimental metastasis by promoting excessive tumour cell clumping and/or exaggerating tumour-induced platelet aggregation, processes known to promote embolic arrest of tumour cells [53,57,58]. Interestingly, the well documented correlation between the ability of tumour cells to induce platelet aggregation and metastatic potential has not been observed consistently in breast cancer metastasis models [59]. To minimise tumour cell clumping and non-specific tumour-platelet interactions in our experimental metastasis assays, the number of cells injected (5×10^4 to 1×10^5) was

This article is protected by copyright. All rights reserved

significantly lower than that employed in most xenograft studies [5,12]. We do not interpret our results as evidence that tumour-platelet interactions are not required for spontaneous metastasis of breast tumours. Rather, we propose that platelet αIIbβ3 function is not essential for efficient breast cancer metastasis to bone and lung. Indeed, liposome-encapsulated Cilostazol, a platelet aggregation inhibitor, reduces spontaneous metastasis of 4T1 tumours to lung by 50% [60]. However, the effects of Cilostazol on bone metastasis and of αIIbβ3 integrin inhibition on spontaneous metastasis were not investigated in this study.

Current experimental and clinical evidence indicate that not all tumour types (or anatomical sites) could benefit from therapies employing αvβ3 integrin antagonists such as cilengitide [25,61]. Our study demonstrates for the first time that tumour rather stromal β3 integrin is a critical determinant of metastatic potential in breast cancer and is essential for efficient spontaneous metastasis to multiple sites, including bone. Regulation of early steps of metastasis to multiple organs by tumour β3 integrin is consistent with the association between high β3 expression and poor clinical outcome in ER-negative breast cancer patients. Our findings have important implications for the design of anti-metastatic therapies targeting β3 integrin in breast cancer and could explain in part the limited therapeutic response observed in clinical trials testing β3 inhibitors in patients with advanced metastatic disease [26-30]. We propose that to achieve optimal efficacy in breast cancer patients, β3 inhibitors should be used in a neo-adjuvant setting to target early steps of metastatic progression, rather than after metastases are established.

This article is protected by copyright. All rights reserved

Accepted Article

Acknowledgments

We thank Dr S.L. Teitelbaum for providing β3 integrin null mice and Ms. Rachel Walker for assistance with subcutaneous injections. We acknowledge the kind donation of pLMP retroviral vector by Dr. Ross Dickins (WEHI, Australia). This work was supported by a National Health and Medical Research Council Project grant to NP (#509131), a National Breast Cancer Foundation postgraduate scholarship to RZC and a National Breast Cancer Foundation Fellowship to RLA.

This article is protected by copyright. All rights reserved

Accepted Article

Author contribution statement

NP and RLA conceived and managed the study and wrote the manuscript. Experimental work was carried out by NP, RZC, KCM, AN, SP-F, ACBMM, DD, XL, S-HK and RT. HAS provided purified DisBa-01 and expert guidance. RPR completed the prognostic analyses. All authors revised and approved the final manuscript.

This article is protected by copyright. All rights reserved

Accepted Article

References

1. Switala-Jelen K, Dabrowska K, Opolski A*, et al.* The biological functions of beta3 integrins. *Folia biologica* 2004; **50**: 143-152.

2. Desgrosellier JS, Cheresh DA. Integrins in cancer: biological implications and therapeutic opportunities. *Nature reviews Cancer* 2010; **10**: 9-22.

3. Albelda SM, Mette SA, Elder DE*, et al.* Integrin distribution in malignant melanoma: association of the beta 3 subunit with tumor progression. *Cancer research* 1990; **50**: 6757-6764.

4. Liapis H, Flath A, Kitazawa S. Integrin alpha V beta 3 expression by bone-residing breast cancer metastases. *Diagnostic molecular pathology : the American journal of surgical pathology, part B* 1996; **5**: 127-135.

5. Zhao Y, Bachelier R, Treilleux I*, et al.* Tumor alphavbeta3 integrin is a therapeutic target for breast cancer bone metastases. *Cancer research* 2007; **67**: 5821-5830.

6. Cooper CR, Chay CH, Pienta KJ. The role of alpha(v)beta(3) in prostate cancer progression. *Neoplasia* 2002; **4**: 191-194.

7. Gruber G, Hess J, Stiefel C*, et al.* Correlation between the tumoral expression of beta3-integrin and outcome in cervical cancer patients who had undergone radiotherapy. *British journal of cancer* 2005; **92**: 41-46.

8. Vonlaufen A, Wiedle G, Borisch B*, et al.* Integrin alpha(v)beta(3) expression in colon carcinoma correlates with survival. *Modern pathology : an official journal of the United States and Canadian Academy of Pathology, Inc* 2001; **14**: 1126-1132.

9. Danen EH, Jansen KF, Van Kraats AA*, et al.* Alpha v-integrins in human melanoma: gain of alpha v beta 3 and loss of alpha v beta 5 are related to tumor progression in situ but not to metastatic capacity of cell lines in nude mice. *International journal of cancer Journal international du cancer* 1995; **61**: 491-496.

10. Kaur S, Kenny HA, Jagadeeswaran S*, et al.* {beta}3-integrin expression on tumor cells inhibits tumor progression, reduces metastasis, and is associated with a favorable prognosis in patients with ovarian cancer. *The American journal of pathology* 2009; **175**: 2184-2196.

11. Kitazawa S, Maeda S. Development of skeletal metastases. *Clinical orthopaedics and related research* 1995: 45-50.

12. Pecheur I, Peyruchaud O, Serre CM*, et al.* Integrin alpha(v)beta3 expression confers on tumor cells a greater propensity to metastasize to bone. *FASEB journal : official publication of the Federation of American Societies for Experimental Biology* 2002; **16**: 1266-1268.

This article is protected by copyright. All rights reserved

Accepted Article

13. Sloan EK, Pouliot N, Stanley KL, *et al.* Tumor-specific expression of alphavbeta3 integrin promotes spontaneous metastasis of breast cancer to bone. *Breast cancer research : BCR* 2006; **8**: R20.

14. Brooks PC, Clark RA, Cheresh DA. Requirement of vascular integrin alpha v beta 3 for angiogenesis. *Science* 1994; **264**: 569-571.

15. Brooks PC, Montgomery AM, Rosenfeld M, *et al.* Integrin alpha v beta 3 antagonists promote tumor regression by inducing apoptosis of angiogenic blood vessels. *Cell* 1994; **79**: 1157-1164.

16. Reynolds LE, Wyder L, Lively JC, *et al.* Enhanced pathological angiogenesis in mice lacking beta3 integrin or beta3 and beta5 integrins. *Nature medicine* 2002; **8**: 27-34.

17. Bakewell SJ, Nestor P, Prasad S, *et al.* Platelet and osteoclast beta3 integrins are critical for bone metastasis. *Proceedings of the National Academy of Sciences of the United States of America* 2003; **100**: 14205-14210.

18. Harms JF, Welch DR, Samant RS, *et al.* A small molecule antagonist of the alpha(v)beta3 integrin suppresses MDA-MB-435 skeletal metastasis. *Clinical & experimental metastasis* 2004; **21**: 119-128.

19. Taverna D, Moher H, Crowley D, *et al.* Increased primary tumor growth in mice null for beta3- or beta3/beta5-integrins or selectins. *Proceedings of the National Academy of Sciences of the United States of America* 2004; **101**: 763-768.

20. Taverna D, Crowley D, Connolly M, *et al.* A direct test of potential roles for beta3 and beta5 integrins in growth and metastasis of murine mammary carcinomas. *Cancer research* 2005; **65**: 10324-10329.

21. Brooks PC, Stromblad S, Klemke R, *et al.* Antiintegrin alpha v beta 3 blocks human breast cancer growth and angiogenesis in human skin. *The Journal of clinical investigation* 1995; **96**: 1815-1822.

22. Chen Q, Manning CD, Millar H, *et al.* CNTO 95, a fully human anti alphav integrin antibody, inhibits cell signaling, migration, invasion, and spontaneous metastasis of human breast cancer cells. *Clinical & experimental metastasis* 2008; **25**: 139-148.

23. Trikha M, Zhou Z, Nemeth JA, *et al.* CNTO 95, a fully human monoclonal antibody that inhibits alphav integrins, has antitumor and antiangiogenic activity in vivo. *International journal of cancer Journal international du cancer* 2004; **110**: 326-335.

24. Alva A, Slovin S, Daignault S, *et al.* Phase II study of cilengitide (EMD 121974, NSC 707544) in patients with non-metastatic castration resistant prostate cancer, NCI-6735. A study by the DOD/PCF prostate cancer clinical trials consortium. *Investigational new drugs* 2012; **30**: 749-757.

25. Millard M, Odde S, Neamati N. Integrin targeted therapeutics. *Theranostics* 2011; **1**: 154-188.

This article is protected by copyright. All rights reserved

Accepted Article

26. Delbaldo C, Raymond E, Vera K, *et al.* Phase I and pharmacokinetic study of etaracizumab (Abegrin), a humanized monoclonal antibody against alphavbeta3 integrin receptor, in patients with advanced solid tumors. *Investigational new drugs* 2008; **26**: 35-43.

27. Hersey P, Sosman J, O'Day S, *et al.* A randomized phase 2 study of etaracizumab, a monoclonal antibody against integrin alpha(v)beta(3), + or - dacarbazine in patients with stage IV metastatic melanoma. *Cancer* 2010; **116**: 1526-1534.

28. Kim KB, Prieto V, Joseph RW, *et al.* A randomized phase II study of cilengitide (EMD 121974) in patients with metastatic melanoma. *Melanoma research* 2012; **22**: 294-301.

29. Manegold C, Vansteenkiste J, Cardenal F, *et al.* Randomized phase II study of three doses of the integrin inhibitor cilengitide versus docetaxel as second-line treatment for patients with advanced non-small-cell lung cancer. *Investigational new drugs* 2013; **31**: 175-182.

30. O'Day SJ, Pavlick AC, Albertini MR, *et al.* Clinical and pharmacologic evaluation of two dose levels of intetumumab (CNTO 95) in patients with melanoma or angiosarcoma. *Investigational new drugs* 2012; **30**: 1074-1081.

31. Reardon DA, Fink KL, Mikkelsen T, *et al.* Randomized phase II study of cilengitide, an integrin-targeting arginine-glycine-aspartic acid peptide, in recurrent glioblastoma multiforme. *Journal of clinical oncology : official journal of the American Society of Clinical Oncology* 2008; **26**: 5610-5617.

32. Sawada K, Ohyagi-Hara C, Kimura T, *et al.* Integrin inhibitors as a therapeutic agent for ovarian cancer. *Journal of oncology* 2012; **2012**: 915140.

33. Patel SR, Jenkins J, Papadopolous N, *et al.* Pilot study of vitaxin--an angiogenesis inhibitor-in patients with advanced leiomyosarcomas. *Cancer* 2001; **92**: 1347-1348.

34. Friess H, Langrehr JM, Oettle H, *et al.* A randomized multi-center phase II trial of the angiogenesis inhibitor Cilengitide (EMD 121974) and gemcitabine compared with gemcitabine alone in advanced unresectable pancreatic cancer. *BMC cancer* 2006; **6**: 285.

35. Eckhardt BL, Parker BS, van Laar RK, *et al.* Genomic analysis of a spontaneous model of breast cancer metastasis to bone reveals a role for the extracellular matrix. *Molecular cancer research : MCR* 2005; **3**: 1-13.

36. Kusuma N, Denoyer D, Eble JA, *et al.* Integrin-dependent response to laminin-511 regulates breast tumor cell invasion and metastasis. *International journal of cancer Journal international du cancer* 2012; **130**: 555-566.

37. Lelekakis M, Moseley JM, Martin TJ, *et al.* A novel orthotopic model of breast cancer metastasis to bone. *Clinical & experimental metastasis* 1999; **17**: 163-170.

38. Denoyer D, Potdevin T, Roselt P, *et al.* Improved detection of regional melanoma metastasis using 18F-6-fluoro-N-[2-(diethylamino)ethyl] pyridine-3-carboxamide, a

This article is protected by copyright. All rights reserved

Accepted Article

melanin-specific PET probe, by perilesional administration. *Journal of nuclear medicine : official publication, Society of Nuclear Medicine* 2011; **52**: 115-122.

39. Chia J, Kusuma N, Anderson R, *et al.* Evidence for a role of tumor-derived laminin-511 in the metastatic progression of breast cancer. *The American journal of pathology* 2007; **170**: 2135-2148.

40. Denoyer D, Kusuma N, Burrows A, *et al.* Bone-derived soluble factors and laminin-511 cooperate to promote migration, invasion and survival of bone-metastatic breast tumor cells. *Growth Factors* 2014; **32**: 63-73.

41. Pouliot N, Nice EC, Burgess AW. Laminin-10 mediates basal and EGF-stimulated motility of human colon carcinoma cells via alpha(3)beta(1) and alpha(6)beta(4) integrins. *Experimental cell research* 2001; **266**: 1-10.

42. McHugh KP, Hodivala-Dilke K, Zheng MH, *et al.* Mice lacking beta3 integrins are osteosclerotic because of dysfunctional osteoclasts. *The Journal of clinical investigation* 2000; **105**: 433-440.

43. Paquet-Fifield S, Levy SM, Sato T, *et al.* Vascular endothelial growth factor-d modulates caliber and function of initial lymphatics in the dermis. *The Journal of investigative dermatology* 2013; **133**: 2074-2084.

44. Arguello F, Baggs RB, Frantz CN. A murine model of experimental metastasis to bone and bone marrow. *Cancer research* 1988; **48**: 6876-6881.

45. Shaffer MC, Foley TP, Barnes DW. Quantitation of spreading factor in human biologic fluids. *The Journal of laboratory and clinical medicine* 1984; **103**: 783-791.

46. Ramos OH, Kauskot A, Cominetti MR, *et al.* A novel alpha(v)beta (3)-blocking disintegrin containing the RGD motive, DisBa-01, inhibits bFGF-induced angiogenesis and melanoma metastasis. *Clinical & experimental metastasis* 2008; **25**: 53-64.

47. Rhodes DR, Kalyana-Sundaram S, Mahavisno V, *et al.* Oncomine 3.0: genes, pathways, and networks in a collection of 18,000 cancer gene expression profiles. *Neoplasia* 2007; **9**: 166-180.

48. Madden SF, Clarke C, Gaule P, *et al.* BreastMark: An Integrated Approach to Mining Publicly Available Transcriptomic Datasets Relating to Breast Cancer Outcome. *Breast cancer research : BCR* 2013; **15**: R52.

49. van der P, Vloedgraven H, Papapoulos S, *et al.* Attachment characteristics and involvement of integrins in adhesion of breast cancer cell lines to extracellular bone matrix components. *Laboratory investigation; a journal of technical methods and pathology* 1997; **77**: 665-675.

50. Schneider JG, Amend SR, Weilbaecher KN. Integrins and bone metastasis: integrating tumor cell and stromal cell interactions. *Bone* 2011; **48**: 54-65.

This article is protected by copyright. All rights reserved

51. Kadowaki M, Sangai T, Nagashima T*, et al.* Identification of vitronectin as a novel serum marker for early breast cancer detection using a new proteomic approach. *Journal of cancer research and clinical oncology* 2011; **137**: 1105-1115.

52. Bambace NM, Holmes CE. The platelet contribution to cancer progression. *Journal of thrombosis and haemostasis : JTH* 2011; **9**: 237-249.

53. Honn KV, Tang DG, Crissman JD. Platelets and cancer metastasis: a causal relationship? *Cancer metastasis reviews* 1992; **11**: 325-351.

54. Lal I, Dittus K, Holmes CE. Platelets, coagulation and fibrinolysis in breast cancer progression. *Breast cancer research : BCR* 2013; **15**: 207.

55. Tucker GC. Inhibitors of integrins. *Current opinion in pharmacology* 2002; **2**: 394-402.

56. Gay LJ, Felding-Habermann B. Contribution of platelets to tumour metastasis. *Nature reviews Cancer* 2011; **11**: 123-134.

57. Liotta LA, Saidel MG, Kleinerman J. The significance of hematogenous tumor cell clumps in the metastatic process. *Cancer research* 1976; **36**: 889-894.

58. Updyke TV, Nicolson GL. Malignant melanoma cell lines selected in vitro for increased homotypic adhesion properties have increased experimental metastatic potential. *Clinical & experimental metastasis* 1986; **4**: 273-284.

59. Estrada J, Nicolson GL. Tumor-cell-platelet aggregation does not correlate with metastatic potential of rat 13762NF mammary adenocarcinoma tumor cell clones. *International journal of cancer Journal international du cancer* 1984; **34**: 101-105.

60. Wenzel J, Zeisig R, Fichtner I. Inhibition of metastasis in a murine 4T1 breast cancer model by liposomes preventing tumor cell-platelet interactions. *Clinical & experimental metastasis* 2010; **27**: 25-34.

61. MacDonald TJ, Taga T, Shimada H*, et al.* Preferential susceptibility of brain tumors to the antiangiogenic effects of an alpha(v) integrin antagonist. *Neurosurgery* 2001; **48**: 151-157.

This article is protected by copyright. All rights reserved

Accepted Article

Figure legends

Figure 1. Stable suppression of β3 integrin expression induces coordinated downregulation of αv integrin subunits at the cell surface. Parental 4T1BM2 cells (Parent) and cells expressing a non-targeting (Control) or a β3-targeting shRNA (β3lo) were analysed for the expression of β3 (A) and αv (B) integrin by standard flow cytometry. Solid grey = isotype control antibody. β3 (C) and αv (D) mRNA transcripts were analysed by qRT-PCR. Graph shows mean transcript abundance relative to GAPDH ± SEM of 9 independent replicates. *$p<0.05$, one-way ANOVA, Tukey's multiple comparison test. (E) Representative western blot analysis of total integrin αv and tubulin (loading control) detected in whole cell lysates (left panel) and quantitation of triplicate samples of 4T1BM2-ctrl versus 4T1BM2-β3lo (right panel) by densitometry are shown. n/s, not significant, $p = 0.700$.

This article is protected by copyright. All rights reserved

Accepted Article

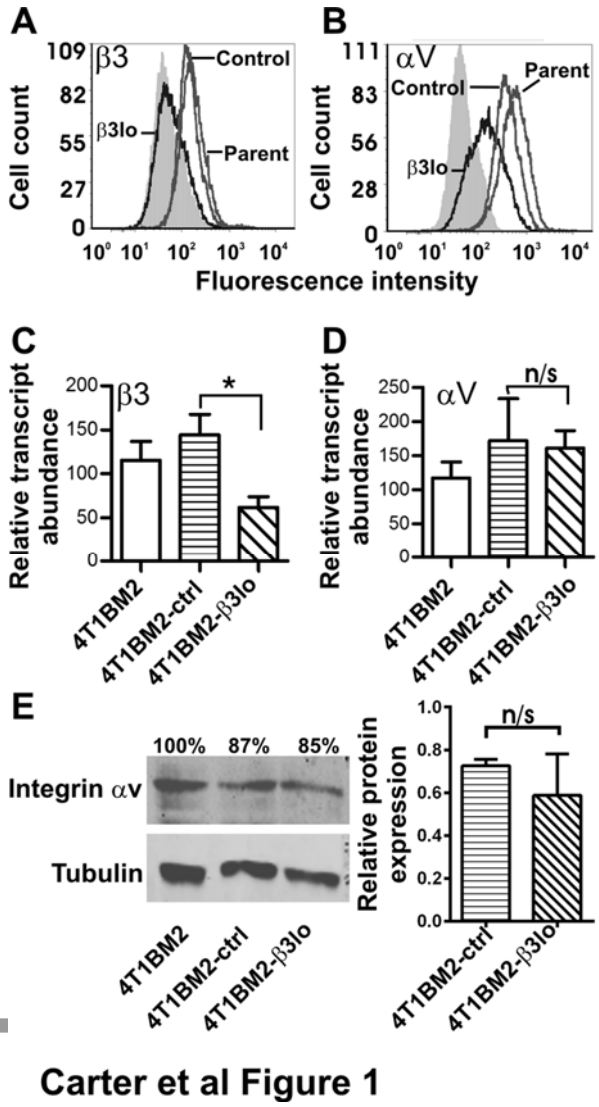

Carter et al Figure 1

Figure 2. Downregulation of αvβ3 integrin impairs vitronectin-mediated adhesion and migration and inhibits 4T1BM2 spontaneous metastasis to bone and lung. (A) Short term adhesion (30 min) was measured in uncoated (plastic) or vitronectin- or LM-511-coated 96-well plates as indicated. Data show % of total cell input ± SD of representative experiments (n = 3), each completed in triplicate (***p < 0.001, one-way ANOVA Tukey's multiple comparison test). (B) Haptotactic migration towards vitronectin or LM-511 was measured in Transwell chambers after 4 hours at 37°C in the absence of serum. Data show mean number of migrated cells ± SEM of 9 replicate images (3 random fields of view per Transwell

This article is protected by copyright. All rights reserved

Accepted Article

membrane x 3 membranes) (*** < p 0.001, one-way ANOVA Tukey's multiple comparison test). (C) Proliferation was measured in 96-well plates in the presence of 5% serum and quantitated every 24 hours using a sulforhodamine B colorimetric assay. Data are presented as means ± SEM of 6 replicate wells/condition and are representative of 3 independent experiments (n/s = not significant, p = 0.634). (D) 4T1BM2-ctrl and 4T1BM2-β3lo orthotopic tumour growth was monitored thrice weekly by caliper measurements (p = 0.254, 2-way ANOVA). (E) Tumour weight at harvest (day 26, p = 0.782, Mann Whitney test). Data in (D) and (E) show means ± SD of 15 mice/group. (F) The incidence of mice developing metastases in lung, femur, spine or bone (combined femur + spine) was assessed by visual inspection and confirmed by qPCR detection of a marker gene (mCherry) relative to vimentin. Organs with a qPCR amplification signal above background compared to a naïve mouse were considered positive (n/s in lung, p = 1.00, *p < 0.05, **p < 0.01, Fisher's exact test). Right panels show representative images of lungs from 4T1BM2-ctrl and 4T1BM2-β3lo tumour-bearing mice (arrows; metastases). Metastatic burden in lung (G), femur (H), spine (I) and combined bone score (J) was determined by genomic qPCR detection of mCherry DNA relative to vimentin DNA. Data show one point for each mouse (n = 15/group) and mean burdens (horizontal bar) ± SEM (**p < 0.01, Mann Whitney test).

This article is protected by copyright. All rights reserved

Accepted Article

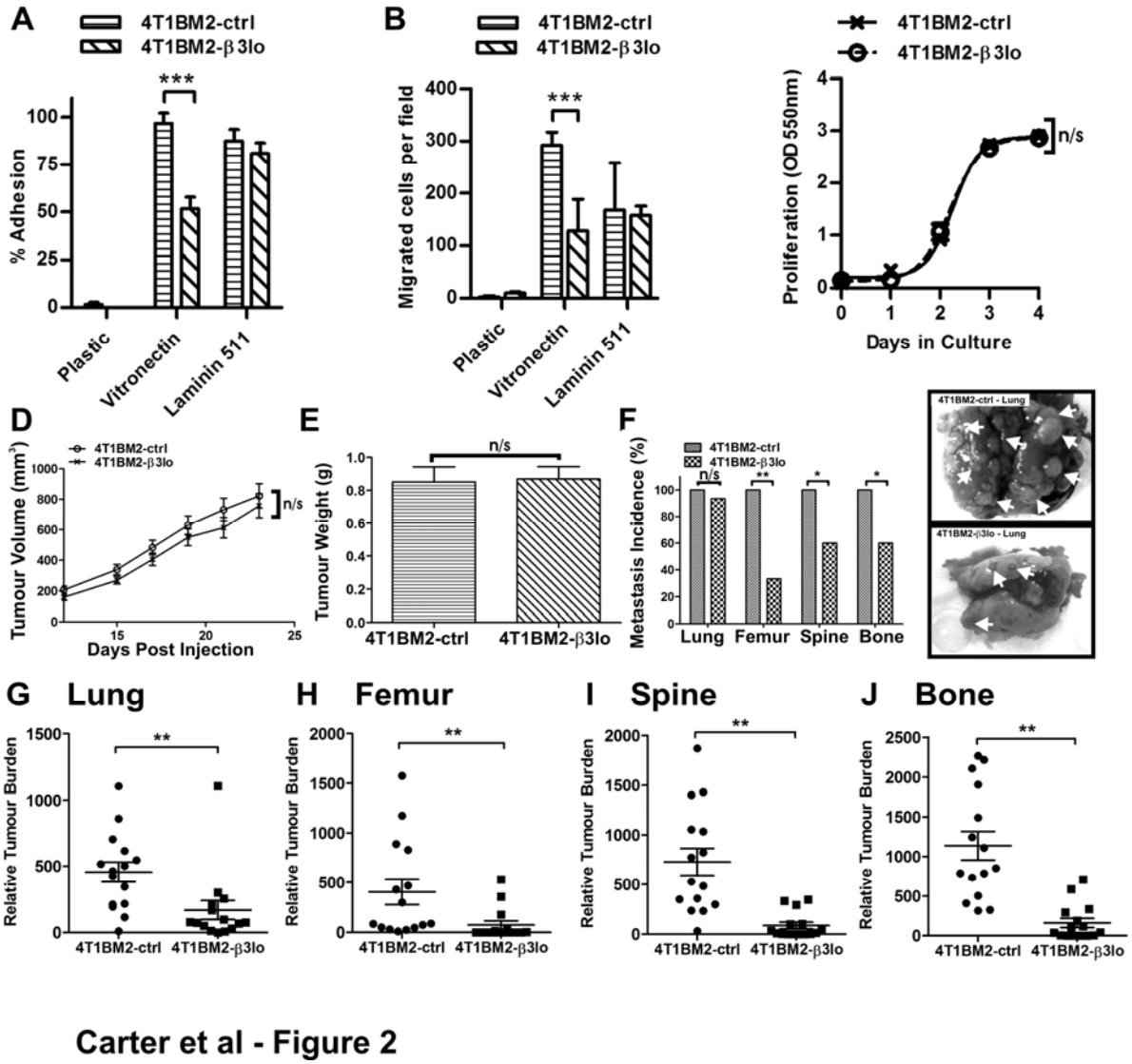

Carter et al - Figure 2

Figure 3. Stromal deletion of β3 integrin does not alter 4T1BM2 orthotopic tumour growth and spontaneous metastasis but enhances subcutaneous tumour growth and vascularisation. Parental 4T1BM2 cells (1×10^5) were inoculated orthotopically into wildtype (n = 20) or littermate β3 knockout (n = 18) syngeneic Balb/c mice. Tumour growth rate (A), tumour weight at harvest (day 27) (B) and metastatic burden in lung (C), femur (D), spine (E) and bone (F) were measured as described in the legend of Figure 2. Data show one point for each mouse and mean burdens (horizontal bar) ± SEM. No statistical differences (n/s) in tumour growth rate (p = 0.848, 2-way ANOVA), tumour end weight (p = 0.895, Mann Whitney test)

This article is protected by copyright. All rights reserved

or metastatic burden between WT and KO mice were observed in lung ($p = 0.056$), femur ($p = 0.578$), spine (0.793) or bone ($p = 0.530$), Mann Whitney test. Parental 4T1BM2 cells (1×10^5) were inoculated orthotopically (IMFP) (G-I) or subcutaneously (SC) (J-L) into wildtype or β3 knockout mice (5 mice/group) as indicated. (G, J) Tumour growth was monitored over 19 days and differences in growth rate analysed by 2-way ANOVA, Bonferroni post-test (n/s = not significant, $p = 0.590$; **$p < 0.01$,). (H, K) Tumour weight at harvest (Mann Whitney test; n/s, $p = 0.854$; **$p < 0.01$,). Data in (G, H, J, K) show means ± SD of 5 replicates/group. (I, L) Images showing size comparison between orthotopic (I) or subcutaneous tumours (L) growing in wildtype and β3 knockout mice. Scale bar = 1cm. Microvascular density in orthotopic (M) and subcutaneous tumours (N) was analysed by IHC detection of CD31. Data show mean pixels ± SEM from 15 replicates (3 fields/section ± 5 section/tumour) (n = 5 mice/group; n/s, $p = 0.444$, *$p < 0.05$, Mann Whitney test). Representative CD31 staining in wildtype and β3 knockout mice are shown in the right panels. Scale bar, 100μm.

This article is protected by copyright. All rights reserved

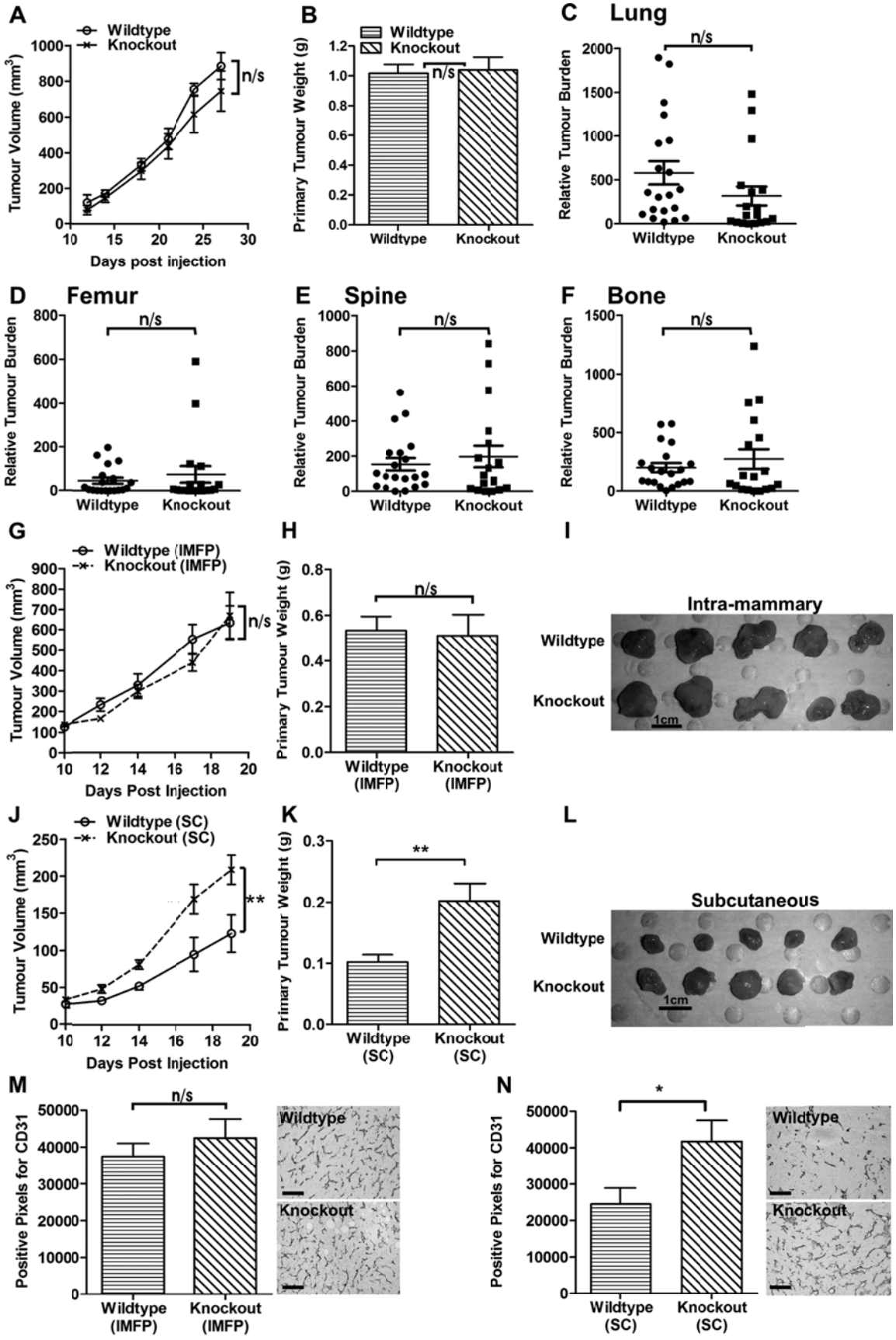

Carter et al - Figure 3

Accepted Article

Figure 4. Experimental bone metastasis is not affected by changes in tumour β3 integrin expression. Balb/c mice were inoculated into the left ventricle of the heart with 4T1BM2-ctrl versus 4T1BM2-β3lo cells (5×10^4/mouse, n = 11 and 13 mice/group respectively) (A-C) or 66cl4pBabe versus 66cl4β3^{high} cells (10^5/mouse, n = 13 mice/group) (D-F). Mice were sacrificed after 14 days and metastatic burden in femurs (A, D), spine (B, E) or bone (C, F) analysed by genomic qPCR detection of mCherry or puromycin resistance gene relative to vimentin. Data show one point for each mouse and mean burdens (horizontal bar) ± SEM. No statistical differences (n/s) in metastatic burden were found between 4T1BM2-ctrl and 4T1BM2-β3lo femur (p = 0.368), spine (p = 0.495) or bone (p = 0.511) and between 66cl4pBabe and 66cl4β3high femur (p = 0.140), spine (p = 0.964) or bone (p = 0.315) (Mann Whitney test).

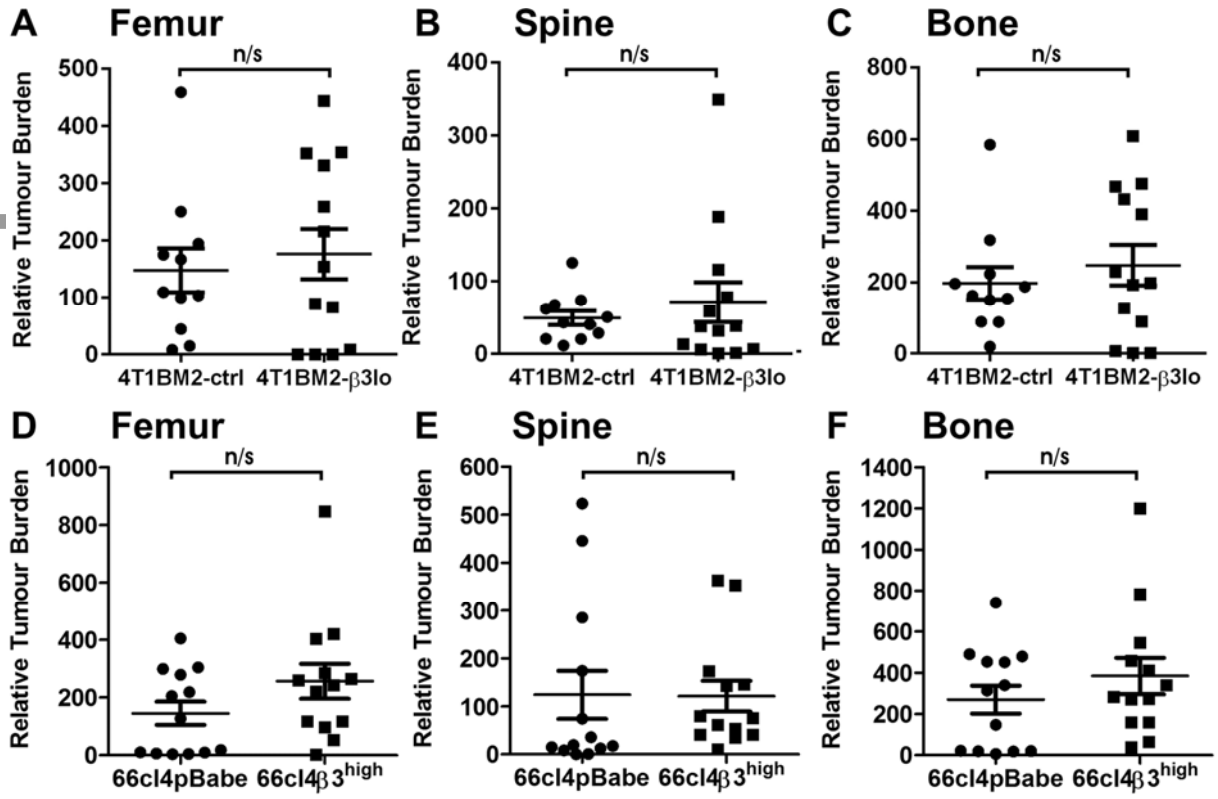

Carter et al - Figure 4

This article is protected by copyright. All rights reserved

Accepted Article

Figure 5. Integrin αvβ3 promotes trans-endothelial migration and intravasation of tumour cells. (A) β3 integrin overexpression enhances trans-endothelial migration *in vitro*. (B) β3 integrin suppression inhibits trans-endothelial migration *in vitro*. Migration of tumour cells (1×10^5 cell/well) through a monolayer of bEnd.3 endothelial cells was measured after 48 hours. Data in (A) and (B) show mean number of migrated cells ± SD of 9 replicate images (3 random fields of view per Tanswell membrane x 3 membranes) from a representative experiment (n = 3; *** < p 0.001, Mann Whitney test). (C) β3 integrin suppression inhibits intravasation *in vivo*. 4T1BM2-ctrl and 4T1BM2-β3lo tumour cells (1×10^5) were inoculated orthotopically into syngeneic Balb/c mice and blood collected by cardiac puncture after 26 days. Relative number of circulating tumour cells was quantitated by genomic qPCR detection of mCherry gene relative to vimentin. Data show one point for each mouse and mean (horizontal bar) ± SEM, n = 13 mice/group. **p = 0.01, Mann Whitney test. (D-F) β3 integrin suppression delays vascular dissemination. Mice were inoculated with 4T1BM2-ctrl (n = 7) and 4T1BM2-β3lo cells (n = 6) as above. Blood was collected by cardiac puncture when mammary tumours reached ~0.5cm^3 and viable circulating tumour cells scored by colony formation in culture (0.5ml/dish). (D) Tumour weight at harvest. (E) Metastatic burden in lung and spine was determined by genomic qPCR. (F) Colony formation assay. The number of colonies after 10 days (>50 cells) was counted and the data expressed as the number circulating tumour cells/ml of blood. Data in (D-F) show one point per mouse and mean values (horizontal bar) ± SEM (n/s = not significant, p = 0.944, *p<0.05, **p <0.01, ***p < 0.001, Mann Whitney test).

This article is protected by copyright. All rights reserved

Accepted Article

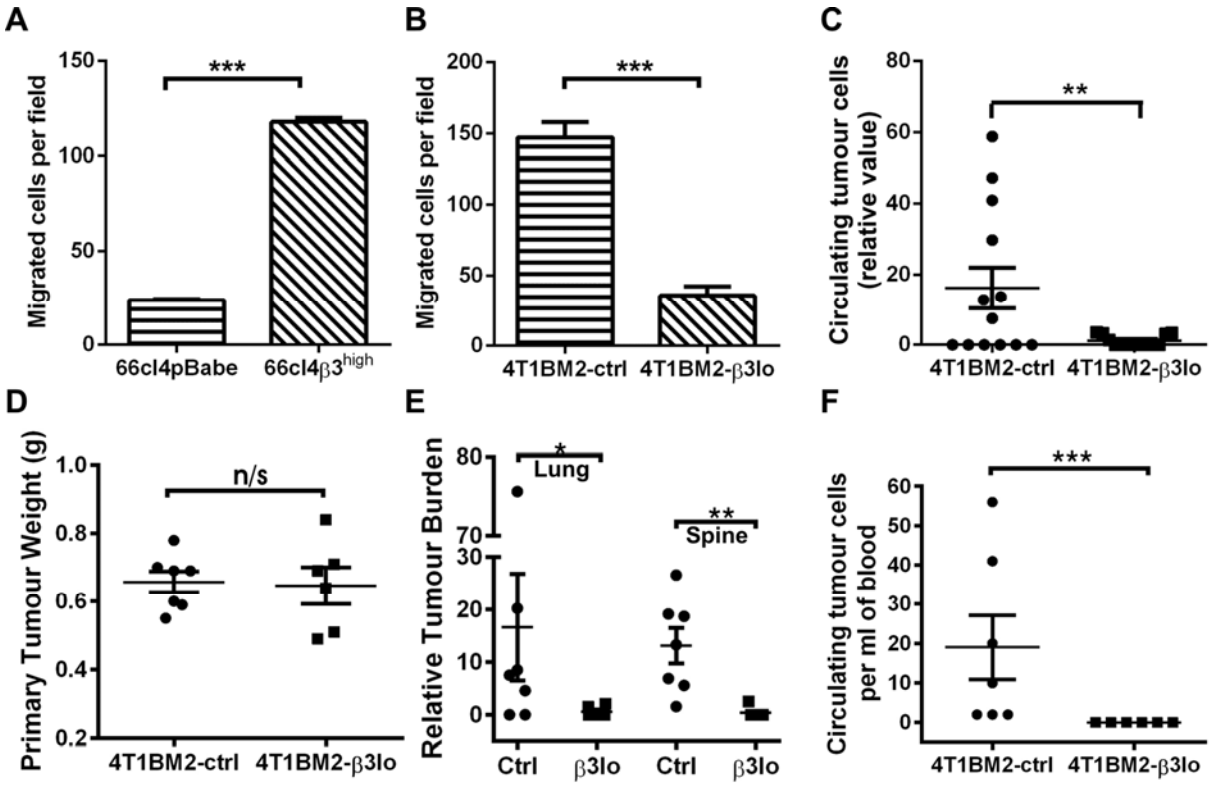

Carter et al - Figure 5

Figure 6. Association between β3 integrin expression and disease-free survival. The association between β3 expression and disease free survival (DFS) in human breast tumour samples was interrogated in public databases using BreastMark prognostic biomarker analysis tool [48]. $\beta3^{high}$ and $\beta3^{low}$ (median cut-off) are shown in blue and red respectively. Dotted lines show confidence intervals. (A) Estrogen receptor-positive (ER+) tumours. (B) Estrogen receptor-negative (ER-) tumours. (C) Progesterone receptor-positive (PR+) tumours. (D) Progesterone receptor-negative (PR-) tumours. (E) Lymph node-positive (LN+) tumours. (F) Lymph node-negative (LN-) tumours. (G) Grade 3 (Gr3) tumours. (H) Estrogen receptor-negative/progesterone receptor-negative (ER-/PR-) tumours. (I) Estrogen receptor-negative/lymph node-positive (ER-/LN+) tumours. (J) Estrogen receptor-negative/lymph node-positive/grade 3 (ER-/LN+/Gr3) tumours.

This article is protected by copyright. All rights reserved

Accepted Article

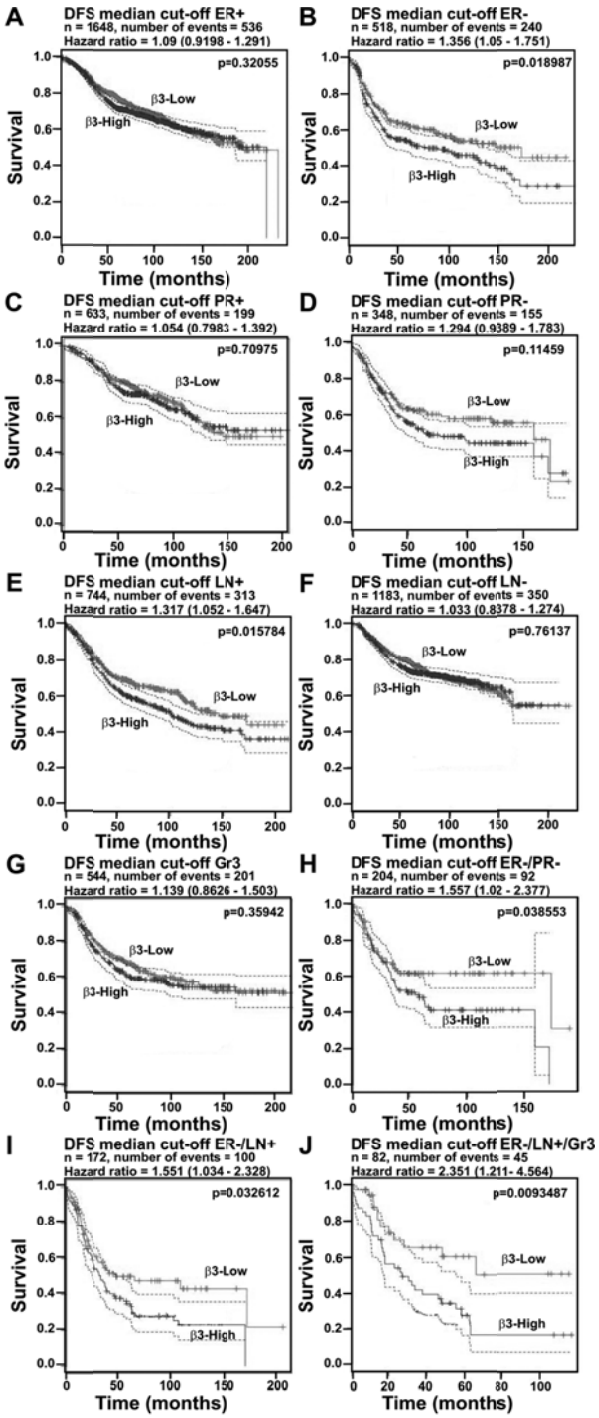

Carter et al - Figure 6

This article is protected by copyright. All rights reserved